Membrane trafficking of ATP-sensitive potassium channels

Andrew James Smith

Thesis submitted in accordance with the requirements for the degree of Doctor of philosophy

The University of Leeds
School of Biomedical Sciences

April 2005

The candidate confirms that the work submitted is his own and the appropriate credit has been given where reference has been made to the work of others

Acknowledgements

I would like to thank everybody who has helped me during my time in the lab. Special thanks go to the guys and girls in the lab (Edd, Tim, Dave, Jamel, Chris C, Tarvinder, Lindsey, Qad, Jim) for making my working life all the more enjoyable. Particular thanks go to Chris P and most of all Rao for teaching me everything that I now know. I would also like to thank Vas for providing many fantastic antibodies and labelling solutions, Malcolm for his patch-clamp skills and good advice and Aruna for the Northern blotting. To the rest of the guys, thanks for the many great Friday night pub trips and afternoon tea drinking expeditions.

Finally, special thanks go to my family for all of their help, love and support (both mental and financial) throughout my time at University. Cheers guys.

I was supported throughout my studies by the Emma and Leslie Reid scholarship.

Abstract

ATP-sensitive potassium (K_{ATP}) channels are known to play a vital role in the regulation of insulin secretion from pancreatic β-cells. Changes in the ratio of [ATP] / [ADP] within the cell are known to regulate the activity of channels, but very little is known how the number of channels at the cell surface is regulated. The number of channels in the plasma membrane could be regulated in two ways; firstly by regulating the overall population of channels within the cells by increasing / decreasing the rates of channel synthesis or degradation, and secondly by regulating the insertion and removal of channels from the plasma membrane. The aim of the current study is to investigate the involvement of both of these mechanisms in regulating the cell surface density of K_{ATP} channels.

It is shown that a sudden decrease in glucose concentration causes a rapid stimulation of K_{ATP} channel synthesis as shown by both immunocytochemistry and protein chemistry in both INS-1e and isolated mouse pancreatic β-cells. The intensity of fluorescence associated with Kir6.2 and SUR1 was ~ 2.5 fold greater in cells incubated with 3 mM compared to 25 mM glucose. This sudden increase in channel numbers is due to an increase in the rate of translation of pre-existing mRNA and may be mediated by the activation of AMP-activated protein kinase. Despite the ~ 2.5 fold increase in channel numbers only a small, but non-significant, difference in cell surface density was observed as determined by patch-clamp. The internalisation of K_{ATP} channels with an extracellular HA-epitope was also investigated in stably transfected HEK293 cells. Channels were seen to internalise rapidly from the cell surface into a perinuclear compartment. The trafficking itinerary of these channels has been found to include the sorting endosome, late endosome and elements of the *trans*-Golgi network. Upon inhibition of protein kinase-C activity the internalised channels are redirected into a pathway which allows rapid recycling of the channels. Trafficking and function of K_{ATP} channels has also been shown to be disrupted by mutations of Kir6.2 known to cause congenital hyperinsulinism.

In summary, it has been demonstrated that both regulated expression and trafficking are likely to be involved in determining the cell surface density of pancreatic K_{ATP} channels.

Table of contents

List of figures

List of tables

Abbreviations

ABC	ATP-binding cassette
ADP	Adenosine diphosphate
AMP	Adenosine monophosphate
AMPK	AMP-activated protein kinase
AP	Adaptor protein
ATP	Adenosine triphosphate
BSA	Bovine serum albumin
CCV	Clathrin coated vesicle
cDNA	Complementary DNA
CFTR	Cystic fibrosis transmembrane regulator
CHI	Congenital hyperinsulinism
CI-M6PR	Cation-independent mannose-6-receptor
Cy3	Cyanine-3
ENaC	Epithelial sodium channel
ER	Endoplasmic reticulum
ERC	Endocytic recycling compartment
FCS	Fetal calf serum
FITC	Fluorescein isothiocyanate
GRN	Glucose responsive neurones
GSIS	Glucose stimulated insulin secretion
K_{ATP}	ATP-sensitive potassium channel
KCO	Potassium channel opening drug
KDa	Kilodalton
Kir	Inwardly rectifying potassium channel
LDL	Low density lipoprotein
LE	Late endosome
MRP	Multi-drug resistance protein
MVB	Multi-vesicular body
MW	Molecular weight
N	Number of channels

NA	Numerical aperture
NBF	Nucleotide binding fold
N-terminus	Amino-terminus
PCR	Polymerase chain reaction
PKA	Protein kinase-A
PKC	Protein kinase-C
PM	Plasma membrane
PNDM	Permanent neonatal diabetes mellitus
P_o	Open probability
RT	Room temperature
SDS-PAGE	SDS-polyacrylamide gel electrophoresis
SE	Sorting endosome
SNARE	Soluble NSF attachment protein receptor
SNr	Substantia nigra reticulate
SUR	Sulphonylurea receptor
t½	Half-life
TfR	Transferrin receptor
TGN	*Trans*-Golgi network
TM (1 or 2)	Transmembrane helix (1 or 2)
TMD	Transmembrane domain
TNDM	Transient neonatal diabetes mellitus
UTR	Untranslated region
V	Voltage
VDCC	Voltage dependent calcium channel

Amino acids

	Three letter code	*Single letter code*
Alanine	Ala	A
Arginine	Arg	R
Asparigine	Asn	N
Aspartic acid	Asp	D
Cysteine	Cys	C
Glutamine	Gln	Q
Glutamic acid	Glu	E
Glycine	Gly	G
Histidine	His	H
Isoleucine	Ile	I
Leucine	Leu	L
Lysine	Lys	K
Methionine	Met	M
Phenylalanine	Phe	F
Proline	Pro	P
Serine	Ser	S
Threonine	Thr	T
Tryptophan	Trp	W
Tyrosine	Tyr	Y
Valine	Val	V

Chapter 1

Introduction

1.1 - ATP-sensitive potassium (K_{ATP}) channels

1.1.1 - Identification and cloning of K_{ATP} channels

ATP-sensitive potassium (K_{ATP}) currents were first described by Noma (1983) as K^+ selective channels inhibited by application of ATP to the intracellular face of cardiac cell membranes. K_{ATP} channels have since been found to be expressed in numerous other tissues including many regions of the brain (Ashford *et al.* 1990a,b, Ohno-Shosaku & Yamamoto 1992, Roper & Ashcroft 1995, Zawar *et al.* 1999), pancreas (Cook & Hayles 1984), skeletal muscle (Spruce *et al.* 1985) and vascular smooth muscle (Masuzawa *et al.* 1990). Since the cloning of the channel (Inagaki *et al.* 1995) it has become apparent that K_{ATP} channels are a hetero-octameric complex composed of two distinct subunits (see Aguilar-Bryan & Bryan (1999) for review). The channel pore is composed of four Kir6.X subunits, members of the inwardly rectifying potassium channel family. In addition to the central pore, four sulphonylurea receptor subunits (SUR) act as regulators of channel gating, providing much, but not all, of the nucleotide and drug sensitivity. The role of each of these subunits is discussed in more detail below.

1.1.2 - The channel pore

The Kir channel family

Early analysis of ATP-sensitive currents in both cardiac myocytes and pancreatic β-cells revealed them to be both K^+ selective and inwardly rectifying (Noma *et al.* 1984, Ashcroft *et al.* 1984) suggesting the presence of members of the inwardly rectifying potassium (Kir) channel family. Kir channels are characterised by their ability to pass inward current more effectively than outward current. At membrane potentials greater than E_K (the reversal potential of K^+) potassium ions will be driven along their electrochemical gradient out of the cell (Hille 2001). Other positively charged ions (particularly Mg^{2+}) and small molecules such as polyamines (e.g. spermine) may also be driven into the Kir channel conduction pathway from the cytoplasm where it is thought they block the channel pore disrupting the outward flux of K^+ (Horie *et al.* 1987, Kurata *et al.* 2004). This gives rise to inward rectification. At membrane potentials lower than E_K potassium ions are driven into the cell (Hille 2001).

Individual Kir channel subunits comprise two membrane spanning helices (TM1 and TM2), either side of a re-entrant pore-forming loop (P-loop) which contains the K^+ selectivity filter. The short amino- and longer carboxyl- termini are both intracellular. Further insights into the structural features of these channels have been made possible by the crystallisation of the archetypal bacterial potassium channels KcsA (Doyle *et al.* 1998) and MthK (Jiang *et al.* 2002) and more recently the bacterial Kir channel homologue Kirbac1.1 (Kuo *et al.* 2003) as depicted in figure 1.1. The crystal structure by Doyle *et al.* (1998) elucidated the structure of KcsA to a 3.2 angstrom resolution and revealed the key principles behind potassium selectivity and the architecture of the potassium ion conduction pathway. The channels were composed of four identical subunits, forming an 'inverted teepee' which contained the selectivity filter at its outer end. The narrow selectivity filter itself was lined by the carbonyl oxygen atoms of the (-GYG-) motif which was held open by structural constraints allowing correct coordination with K^+ ions but not with Na^+ ions. Below the selectivity filter is a large water-filled cavity and K^+ ions within this cavity are stabilized by pore helix dipoles. The selectivity filter contained two K^+ ions 7.5 angstroms apart which was sufficiently close to exploit the repulsive forces between the two K^+ to force ion conduction. The innermost membrane spanning helix (TM2) forms the permeation pathway with the signature K^+ channel sequence (-GYG-) positioned at the narrow opening near the extracellular face of the protein. From investigations into the gating mechanics of these channels, particularly in KcsA (which was crystallised in the closed conformation) (Doyle *et al.* 1998) and MthK (which was crystallized in the open conformation) (Jiang *et al.* 2002), it is thought that the channel gate lies at the cytoplasmic ends of TM2, with twisting or lateral motions of these portions of the protein responsible for allowing access of ions into a water filled vestibule immediately below the K^+ selectivity filter as first proposed for KcsA (Doyle *et al.* 1998). A second gate has recently been suggested to reside at the K^+ selectivity filter itself (Claydon *et al.* 2003). To date 15 Kir channel genes have been cloned and have been subdivided into 7 distinct groups as summarised in table 1.1.

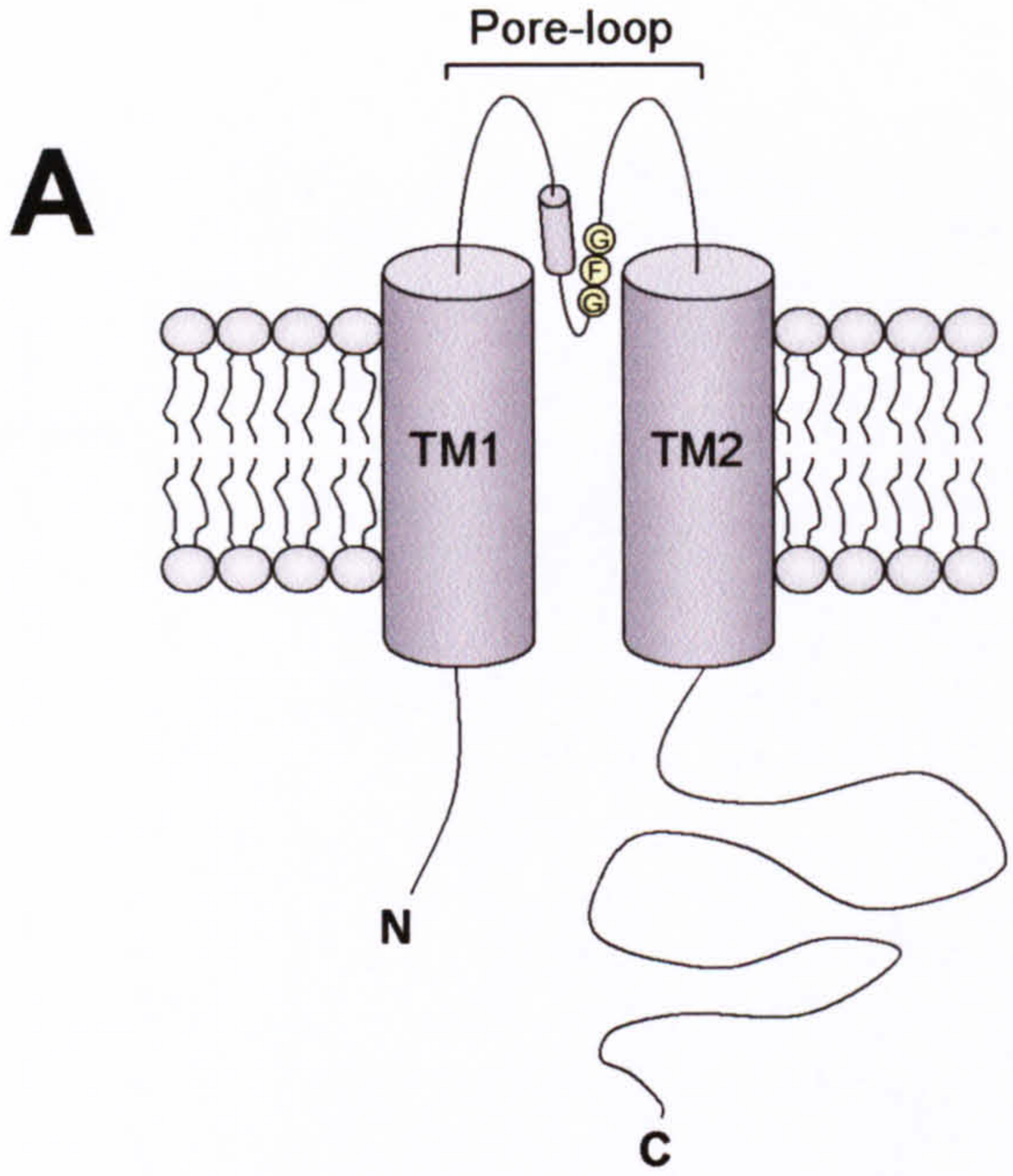

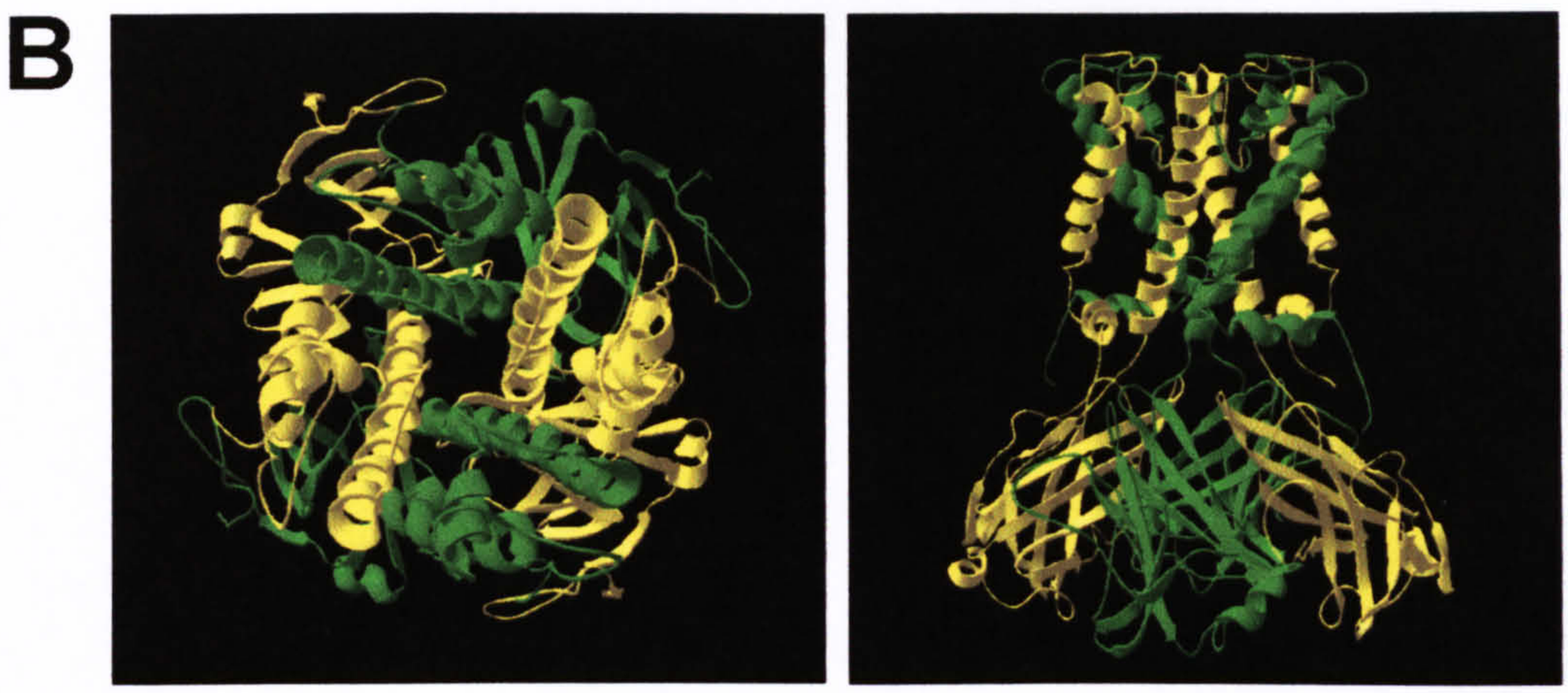

Figure 1.1 - *Predicted structure of Kir channels.* **A** - Predicted topology of a single Kir6.2 channel subunit showing intracellular N- and C-termini and the two membrane spanning helices (TM1 & TM2) flanking the pore loop which contains the potassium selectivity filter consensus sequence GFG (normally GYG in other Kir isoforms). **B** - Three dimensional structure of the bacterial Kir channel homologue Kirbac1.1. The top down view (*left hand panel*) looks down into the conduction pathway through the K^+ selectivity filter. The side view (*right hand* panel) shows the transmembrane helices forming the upper half of the channel and the N-and C-terminal domains at the cytoplasmic side. The three dimensional images were generated using the coordinates, 1P7B, obtained from the protein data bank using Deepview / Swiss-PdbViewer software.

Family	Subunits	Gene	Tissue Distribution	Roles	Associated Diseases	References
Kir1.X	Kir1.1 (ROMK1)	*KCNJ1*	Kidney	Maintenance of K^+ homeostasis, renal K^+ secretion	Barters syndrome	Ho *et al.* (1993)
Kir2.X	Kir2.1 (IRK1) Kir2.2 Kir2.3 (HIR) Kir2.4 (IRK4)	*KCNJ2* *KCNJ12* *KCNJ4* *KCNJ14*	Forebrain, heart, skeletal muscle	Maintenance of resting membrane potential, modulation of action potential waveforms	Andersons syndrome	Kubo *et al.* (1993), Takahashi *et al.* (1994), Lesage *et al.* (1994), Topert et al. (1998)
Kir3.X	Kir3.1 (GIRK1) Kir3.2 (GIRK2) Kir3.3 (GIRK3) Kir3.4 (GIRK4)	*KCNJ3* *KCNJ6* *KCNJ9* *KCNJ5*	Heart	Modulation of heart rate and neuronal excitability	Weaver phenotype (mouse) - Kir3.2	Lesage *et al.* (1994)
Kir4.X	Kir4.1 Kir4.2 (Kir1.3)	*KCNJ10* *KCNJ15*	Kidney, brain	Maintenance of K^+ homeostasis in kidney and glia	N/A	Shuck *et al.* (1997), Gosset et al. (1997)
Kir5.X	Kir5.1	*KCNJ16*	Kidney, pancreas	Does not form functional channel. May modulate activity of other Kir channels	N/A	Liu *et al.* (2000)
Kir6.X	Kir6.1 (uKATP-1) Kir6.2 (BIR)	*KCNJ8* *KCNJ11*	Pancreas, brain, vascular and skeletal muscle	Links metabolic state to membrane excitability. Roles in insulin secretion, cytoprotection, maintenance of vascular tone.	PHHI - Kir6.2, Diabetes (type 2, Permanent neonatal diabetes mellitus; PNDM) - Kir6.2	Inagaki *et al.* (1995), Tokuyama *et al.* (1996)
Kir7.X	Kir7.1 (Kir1.4)	*KCNJ13*	Brain, kidney, intestine	Maintenance of resting membrane potential	N/A	Krapivinsky *et al.* (1998)

Table 1.1 - *The Kir channel family.* Shown is a summary of the nomenclature, tissue distribution, roles and physiological states associated with members of the inwardly rectifying potassium (Kir) channel family.

Cloning of the Kir6.X family

Kir6.1 was first cloned by Inagaki *et al.* (1995) using a fragment of Kir3.1 (GIRK) cDNA as a probe with a rat DNA library and was found to have a very broad tissue distribution, hence the designation uK_{ATP} (u representing the ubiquitous expression). It was however absent in pancreatic β-cell lines so using Kir6.1 cDNA as a probe, Kir6.2 was cloned (originally designated as BIR for β-cell Kir channel). Kir6.2 was found to be relatively abundant in pancreatic islets, particularly β-cells, as well as in the brain, heart and in skeletal muscle. Kir6.1 and Kir6.2 have a relatively high degree of sequence homology, ~ 70 % overall, but significantly higher in the transmembrane domains, the pore-region and in the cytoplasmic domains nearest the plasma membrane (Tokuyama *et al.* 1996).

1.1.3 - The K_{ATP} channel β-subunit

The sulphonylurea receptor

A number of studies described a high affinity sulphonylurea receptor in membranes isolated from β-cells (Kaubisch *et al.* 1982, Gaines *et al.* 1988), β-cell lines such as HIT T15 (Santerre *et al.* 1981) and RINm5F (Ronner *et al.* 1993), the heart (Fosset *et al.* 1988) and the brain (Lupo & Battalie 1987). The first report of a purified high affinity sulphonylurea receptor by Bernardi *et al.* (1988) described a 150 KDa protein isolated from brain. The involvement of the high affinity sulphonylurea receptor in K_{ATP} channels was suggested by Rajan *et al.* (1993) and Ronner *et al.* (1993) who characterised sulphonylurea sensitive K_{ATP} channel currents, measured by Rb^+ efflux and single channel recordings, concluding that they were the same as those of the pancreatic β-cell K_{ATP} channel.

Cloning of the sulphonylurea receptors

Using the N-terminal protein sequence, Aguilar-Bryan *et al.* (1996) designed a set of oligonucleotide primers for amplification of a small segment of the sulphonylurea receptor cDNA. This cDNA fragment was then used to screen cDNA libraries of hamster, rat, mouse and human leading to the isolation of full length clones of SUR1. These clones comprised 1581 amino acids in the rodent and 1582 amino acids in the human. A second SUR isoform was cloned by Inagaki *et al.* (1996) using SUR1 cDNA fragments as probes and was designated SUR2. It has since become apparent

that two alternatively spliced forms of SUR2 exist, SUR2A and SUR2B, and that these two are differentially expressed (SUR2A - cardiac, SUR2B - smooth muscle).

The structure and topology of SUR1

Blast searches of SUR1 sequences revealed that it shared many similarities to proteins of the ATP-binding cassette (ABC) family which includes multi-drug resistance proteins (MRP) (Fojo *et al.* 1985) and cystic fibrosis transmembrane conductance regulator (CFTR) (Riordan *et al.* 1989). According to the guidelines for ABC protein classification (Tusnady *et al.* 1997) SUR1 belongs to the same family as the MRP proteins, based on its predicted membrane topology, its two nucleotide binding folds and its hydrophobic N-terminal domains. The highest degree of homology between SUR1 and the other ABC proteins occurs at the nucleotide binding folds (NBF). These are characterised by the two Walker motifs (Walker *et al.* 1982) (Walker A - GlyXXGlyXGlyLysSer/Thr; where X is any amino acid, Walker B - YYYYAsp; where Y is any hydrophobic amino acid) and the conserved linker region between the two Walker motifs (LeuSerGlyGlyGlu). A predicted transmembrane topology of SUR1 was proposed by Aguilar-Bryan *et al.* (1995) based on hydropathy plots and several structural determinants. N-linked glycosylation sites found near the N-terminus (position N10) suggested that the N-terminus was extracellular and the two NBF regions were intracellular. Recent work by Raab-Graham *et al.* (1999) and Conti *et al.* (2001) has further refined these models, and it is now generally accepted that SUR1 has 17 transmembrane helices grouped into three transmembrane domains (TMD0, TMD1 and TMD2) containing 5 TM - 6 TM - 6 TM respectively. The N-terminus is extracellular whereas the C-terminus is intracellular. The first NBF (NBF1) is thought to be located in the cytoplasm between TMD1 and TMD2 and the second NBF is though to be located in the cytoplasm in the proximal C-terminus. Figure 1.2 summarises this model. More recently the crystal structure of MSBA, a MRP homologue from *Vibrio* cholera containing only two TMD regions corresponding to TMD1 and TMD2 of SUR1, confirmed much of the above model (Chang 2003). Two N-linked glycosylation sites in SUR1, one at position N10 and the other at N1050, have been confirmed by site-directed mutagenesis to be required for channel export from the ER (Conti *et al.* 2002).

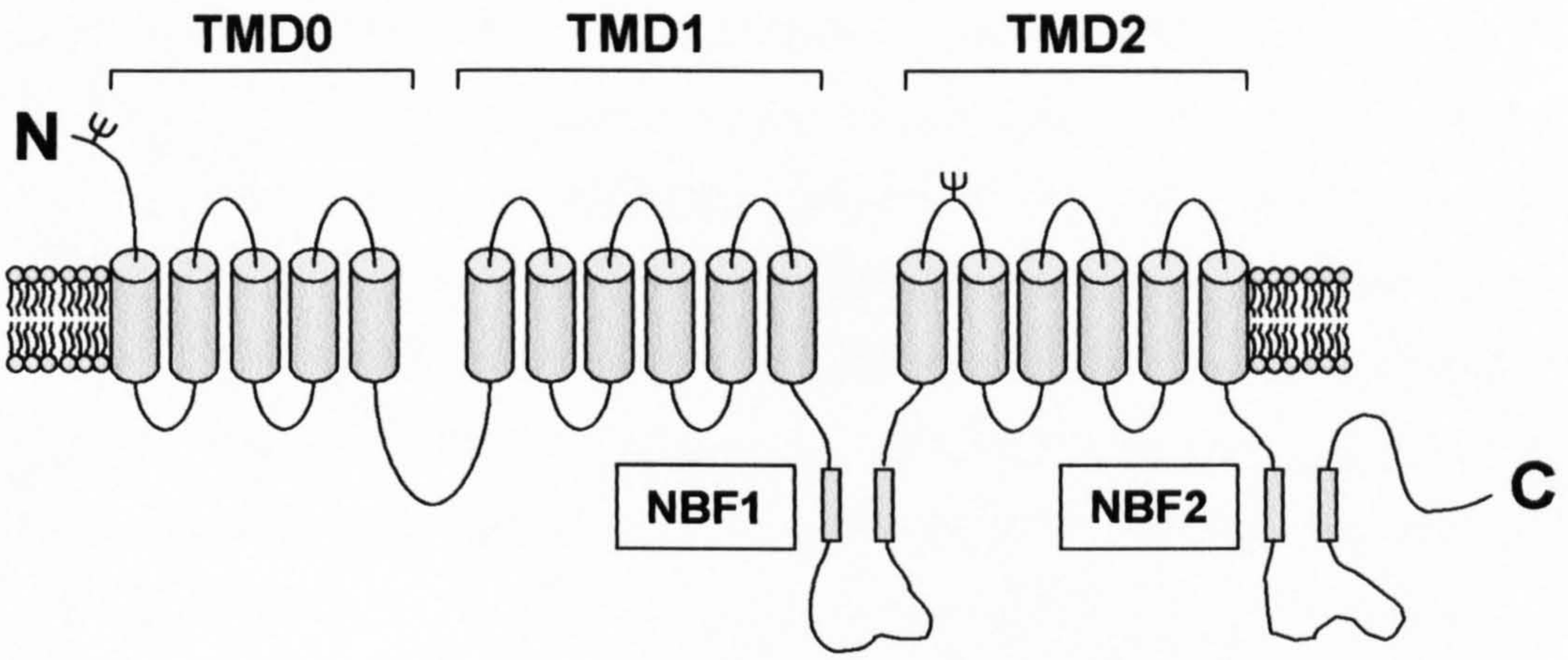

Figure 1.2 - *Predicted transmembrane topology of SUR1.* SUR1 is thought to consist of 17 transmembrane helices grouped into three transmembrane domains, TMD0, TMD1 and TMD2. Two nucleotide binding folds (NBF1 and NBF2) are found between TMD1 and TMD2 and in the C-terminus, both of which are cytoplasmic. The N-terminus is extracellular and contains an N-linked glycosylation site (Ψ). A second N-linked glycosylation site is located on an extracellular loop in TMD2.

1.1.4 - K_{ATP} channel structure

Both Kir and SUR subunits are required for functional expression

Following the cloning of the subunits, it was noticed that both the Kir and SUR subunits were required for expression of active K_{ATP} channels. Expression of SUR1 in the absence of Kir6.2 yielded no K_{ATP} channel currents and it displayed an apparent mass of ~ 140 KDa when examined by SDS-PAGE. When both SUR1 and Kir6.2 were co-expressed K_{ATP} channel currents were elicited. In this case, an examination of SUR1 by SDS-PAGE showed additional species with an apparent mass corresponding to ~ 150 - 190 KDa in addition to the previous ~ 140 KDa species (Clement *et al.* 1997). It has since been shown that these species with an apparent higher molecular weight correspond to the glycosylated forms of SUR1. Interestingly the glycosylated forms of SUR1 are only present when the Kir subunit is co-expressed, suggesting that the presence of the Kir subunit is a requirement for SUR1 maturation (Clement *et al.* 1997). Expression of Kir6.2 alone was also seen to be insufficient to form functional channels (Inagaki *et al.* 1995, Clement *et al.* 1997).

Kir forms the channel pore

The roles that Kir and SUR played in the channels were also the subject of intense investigation following cloning of the channel subunits. It was soon confirmed that Kir formed the channel pore independently of SUR1. Firstly it was shown by Clement *et al.* (1997) and Shyng *et al.* (1997) that mutations in TM2 of Kir6.2 affected the degree of rectification displayed by the channels. This suggested the involvement of Kir6.2 in ion conduction, but it did not rule out a role for SUR1 in forming the pore itself. This question was answered when Tucker *et al.* (1997) showed that truncation of the C-terminal 26 amino acids (Kir6.2Δ26) allowed Kir6.2 to form functional inwardly rectifying, potassium selective channels in the absence of SUR1. This demonstrated that SUR1 was not required for formation of the ion conduction pathway.

K_{ATP} channel stoichiometry

The findings suggesting that Kir expression was required for SUR1 maturation suggested that the two subunits were forming into complexes in order to form the functional channel. Indeed the mass of the channel multimer, as estimated from sucrose density gradients (Clement *et al.* 1997), was ~ 950 KDa suggesting a large

complex composed of four SUR1 subunits (each of ~ 170 KDa not including glycosylation) and four Kir6.2 subunits (each of ~45 KDa). This stoichiometry was simultaneously confirmed by a number of groups (Inagaki *et al.* 1997, Shyng & Nichols 1997). Figure 1.3 shows a representation of how it is thought the K_{ATP} channel octomer may appear. At the centre of the complex are the four Kir subunits forming the ion conduction pathway. Associated with each Kir subunit is a single SUR subunit, surrounding the channel pore.

K_{ATP} channel assembly and ER export

From the early studies it was apparent that neither Kir6.2 nor SUR1 could traffic to the cell surface in the absence of the other (Inagaki *et al.* 1995, Aguilar-Bryan *et al.* 1996, Inagaki *et al.* 1996). This implied that the two subunits would have to associate with each other and assemble into channel complexes for trafficking to occur. The direct physical association between the Kir subunit and the SUR subunit of K_{ATP} channels has been shown by co-immunoprecipitation studies (Lorenz *et al.* 1998, Lorenz & Terzic 1999). The nature of these interactions are not yet fully understood but it is thought that they may involve association of the outer helix of Kir subunit (TM1) with the first domain of SUR1 (TMD0) (Babenko & Bryan 2003). Recent data also suggest that the proximal C-terminus of SUR2A is required for the assembly of functional channels containing Kir6.2 (Rainbow *et al.* 2004), although previously published data found that the C-terminus of SUR1 was not required for assembly with Kir6.2 to form heteromultimers (Gilbin *et al.* 2002). A key element in the process of channel assembly and maturation appears to be the glycosylation of SUR at two N-linked glycosylation sites (Asn10 + Asn1050 in SUR1). It has been reported that glycosylation of these sites is required for efficient exit from the endoplasmic reticulum (ER), and that removal of either glycosylation site significantly impairs ER export (Conti *et al.* 2002). Another determinant of channel trafficking through the biosynthetic pathway is the ER-retention motif contained within the distal C-terminus of Kir subunits and within an intracellular domain of SUR (Zerangue *et al.* 1999). This motif consisting of -RKR- is thought to act as an ER-retention signal. The exact mechanism is unknown, although it may involve interactions with the epsilon and zeta forms of 14-3-3 (Yuan *et al.* 2003). During channel assembly the retention signals of both subunits are masked allowing exit from the ER. Indeed, the existence of this retention motif explains why the Δ26 truncated form of Kir6.2 described by Tucker *et*

al. (1997) is able to traffic to the cell surface in the absence of SUR1, since the -RKR- motif is contained within the excised fragment.

The lifespan of K_{ATP} channels

Studies by Crane & Aguilar-Bryan (2004) examined the turnover of both fully assembled channels and individual K_{ATP} channel subunits using pulse-chase methods in COS7 cells. It was found that when Kir6.2 was expressed alone, ~ 60 % was degraded very rapidly (t½ = 36 min) and the remaining 40 % was longer lived (t½ = 1.2 hours). When SUR1 was expressed alone it appeared very stable with a t½ of approximately 25.5 hours. When expressed together, both subunits appeared to assemble into channels very rapidly, and the rapid loss of Kir6.2 did not occur. Fully assembled channels were shown to have a t½ of approximately 7.3 hours.

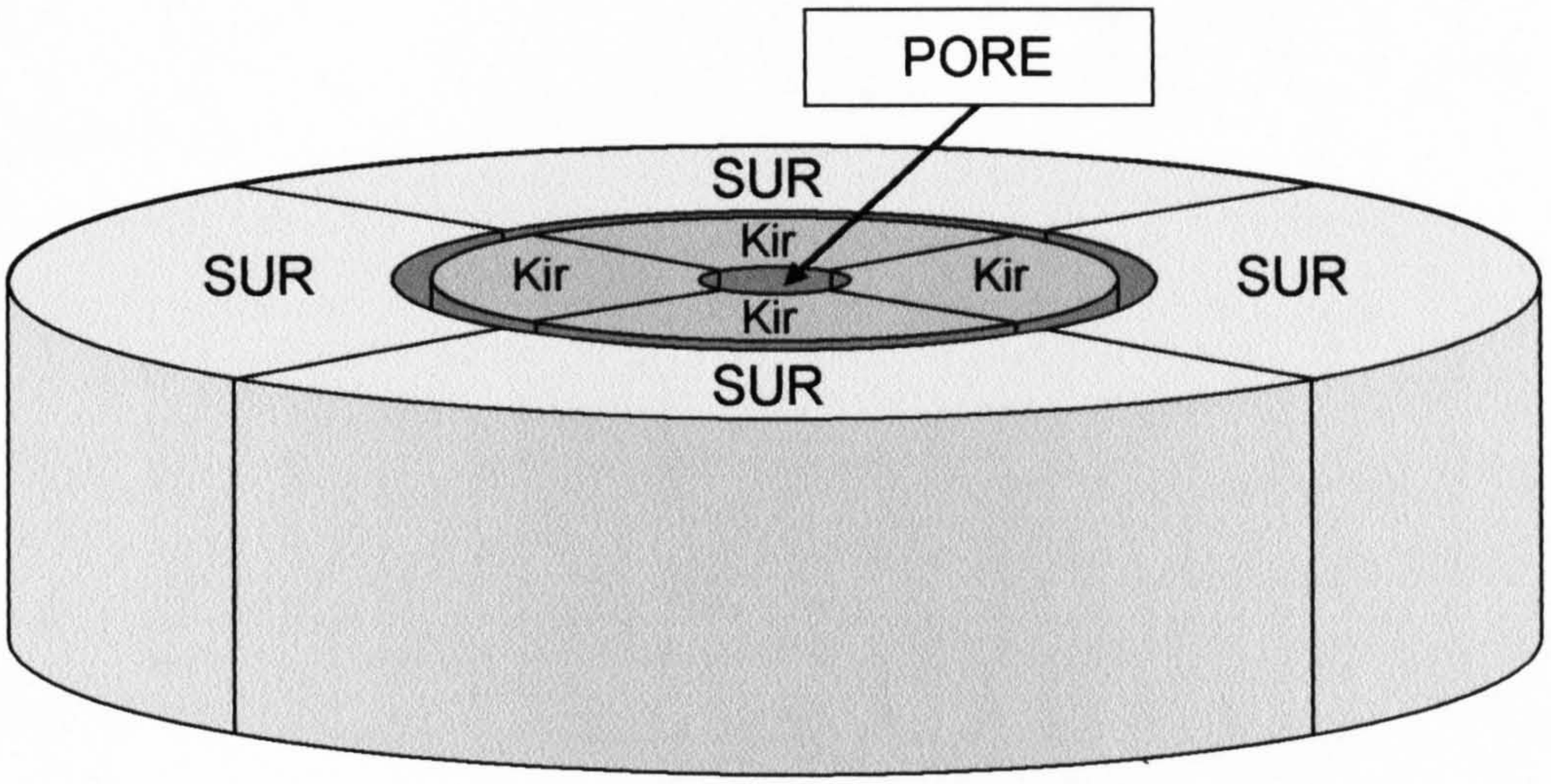

Figure 1.3 - *Proposed arrangement of the K_{ATP} channel subunits.* The K_{ATP} channel is thought to comprise four Kir subunits which assemble to form the ion conduction pathway with a central pore which is selective for the conduction of potassium ions. Each Kir subunit is thought to associate with a SUR subunit which surrounds the Kir channel forming the periphery of the channel.

1.2 - Channel regulation

1.2.1 - Physiological regulation

The activity of K_{ATP} channels is regulated by a number of factors. These factors primarily include nucleotides and membrane phospholipids (particularly PIP_2) although several other proteins have been implicated in modulating channel activity such as protein kinase A and C and, in the case of SUR1, certain elements of vesicle trafficking machinery as described below in more detail.

Channel regulation by nucleotides

K_{ATP} channels were first identified as potassium selective channels which were inhibited by application of ATP to their cytoplasmic face (Cook & Hayles 1984). It has since become apparent the K_{ATP} channels are regulated by cytoplasmic nucleotides, more particularly, the ratio of ATP concentration compared to ADP concentration ([ATP] / [ADP] ratio). When ATP levels rise, for example due to an increase in glucose metabolism resulting in an increase in the [ATP] / [ADP], channel activity is inhibited. When ATP levels drop, for example due to a decrease in glucose metabolism, the [ATP] / [ADP] ratio is decreased due to the increased hydrolysis of ATP to produce ADP. This decrease in the [ATP] / [ADP] ratio stimulated channel activation (see Aguilar-Bryan & Bryan 1999, Campbell *et al.* 2003 for reviews).

Recent evidence suggests that channel inhibition by ATP is mediated through a direct interaction with the cytoplasmic domains of Kir6.2. In the absence of SUR1, channels composed of Kir6.2 (truncated forms which traffic to the surface) show brief openings without long bursts and channel activity is inhibited by both ATP and ADP (Tucker *et al.* 1997, John *et al.* 1998). The ATP binding site, which is contained within the cytoplasmic domain of Kir6.2, has been located and its architecture is beginning to become clearer. It appears that positively charged residues in both the N- (R50) and C-terminus (K185) of Kir6.2 interact directly with ATP (Trapp *et al.* 2003). A second study also highlighted K185 along with R201 as important residues in ATP binding, suggesting that ATP binding to these residues could cause a conformational change in the architecture of the surrounding region thus closing the channel (John *et al.* 2003). In these schemes it is proposed that R50, K185 and R201 interact with the γ-phosphate, β-phosphate and α-phosphate of ATP respectively (John

et al. 2003, Trapp *et al.* 2003). More recent modelling of the ATP-binding site by Antcliffe *et al.* (2005) supports these observations and also suggests interactions between E179 and R301 with the N6 atom of the adenosine ring.

When Kir6.2 is expressed alongside SUR1, channel openings become longer and occur in bursts. Electrophysiological studies showed that the inhibition associated with ATP application can be overcome by the addition of Mg-ADP, which can also activate bursting behaviour in channels in the absence of ATP (Findlay *et al.* 1988, Terzic *et al.* 1994). It is now clear that this stimulation of channel activity is mediated by the interaction of nucleotides with the NBFs of SUR1. Both of the NBFs, NBF1 and NBF2, bind ATP although NBF2 hydrolyses ATP at a much higher rate than NBF1 (Ueda *et al.* 1999, Bienegraeber *et al.* 2000). Although the exact nature of the mechanisms leading from nucleotide binding to SUR1 to channel activation is not fully understood many models have been proposed which share many common features. In essence it is thought that channel activation relies on a functional coupling between NBF1 and a positively charged region of the C-terminus of Kir6.2 which contains the residues R176 and R177 (John *et al.* 2001). For NBF1 to interact with Kir6.2 it appears that it must first have ATP bound, a process which is stabilised by Mg-ADP binding to NBF2 (Ueda *et al.* 1999, John *et al.* 2001).

Another class of molecules which have been shown to modulate K_{ATP} channel activity are the dinucleoside polyphosphates, such as diadenosine tetraphosphate (AP4A) and diadenosine tetraphosphate (AP3A) (Jovanovic *et al.* 1997, Jovanovic & Jovanovic 2001). The action of these molecules has been shown to be functionally significant in both cardiac myocytes (Sumiyoshi *et al.* 1998, Flores *et al.* 1999, Ahmet *et al.* 2000) and in pancreatic β-cells (Ripoll *et al.* 1996, Courtois *et al.* 2000). The binding of dinucleoside polyphosphates has been shown to inhibit K_{ATP} channel openings (Jovanovic *et al.* 1997).

Channel activation by membrane phospholipids

It has been demonstrated that negatively-charged phospholipids, particularly phosphatidylinositol-4,5-bisphosphate (PIP_2) activate many Kir channels, including K_{ATP} channels, by stabilizing the open conformation (Hilgemann & Ball 1996; Fan & Makielski 1997, Huang *et al.* 1998). In the case of K_{ATP} channels, as well as an

increase in channel open probability a parallel decrease in ATP sensitivity is also observed when exposed to PIP_2.(Baukrowitz *et al.* 1998, Shyng & Nichols 1998, Fan & Makielski 1997). This suggests that ATP and PIP_2 may compete for the same or an overlapping binding site. In support of this, mapping of the residues which influence PIP_2 binding shows a number of similarities to those found to be involved in ATP binding. Two residues of particular interest are R201 in the C-terminus, which is thought to directly interact with ATP as well as PIP_2, and R54 which is very close to another residue implicated in ATP binding (R50) (Shyng *et al.* 2000, Schulze *et al.* 2003).

Channel regulation by other proteins

The roles that protein kinases, particularly protein kinase A (PKA) and protein kinase C (PKC), play in regulating the activity of K_{ATP} channels have been extensively investigated. A number of groups have shown a stimulatory effect of PKA on K_{ATP} channel activity. In channels composed of Kir6.2 and SUR1, Beguin *et al.* (1999) found that PKA phosphorylation of S372 in Kir6.2 led to an increase in channel activity whereas phosphorylation of S1571 in SUR1 would lead to an alteration to the channel properties (e.g. a shortening of the bust duration) and also led to an increase in the cell surface channel density. Another study by Lin *et al.* (2000) showed that the increase in open probability of channels containing Kir6.2 associated with elevated PKA activity was as a result of phosphorylation of S224, resulting in a decrease in channel ATP sensitivity. The smooth muscle K_{ATP} channel composed of Kir6.1 and SUR2B is also activated by PKA, due to phosphorylation of S385 in Kir6.1 and T633 and S1465 in SUR2B (Quinn *et al.* 2004). It has also been demonstrated that angiotensin II-stimulated vasoconstriction is mediated by inhibition of PKA, which in turn inhibits K_{ATP} channels (Hayabuchi *et al.* 2001). The regulation of K_{ATP} channels by PKC is somewhat more unclear. A number of groups have reported that PKC activation mediates channel inhibition. For example, both Kubo *et al.* (1997) and Hayabuchi *et al.* (2001) reported that angiotensin II stimulated vasoconstriction was mediated by smooth muscle K_{ATP} channel inhibition by activation of PKC. Inhibition of K_{ATP} channels by PKC has also been reported in colonic myocytes and arterial smooth muscle (Bonev & Nelson 1996, Jun *et al.* 2001). In contrast, both Dunne (1994) and Light *et al.* (2000) have reported K_{ATP} channel activation by PKC. According to Dunne (1994) pancreatic K_{ATP} channels, which have since been shown

to be composed of Kir6.2 and SUR1, were initially inhibited by PKC activation with PMA but recovered with prolonged exposure to the drug, eventually leading to an increase in channel activity compared to basal levels. Light *et al.* (2000) demonstrated that PKC activation was associated with an increase in the open probability of channels containing Kir6.2 due to the phosphorylation of T180, resulting in a decrease in ATP binding. The examples given above where PKC is associated with channel inhibition all involve channels thought to contain Kir6.1 as the pore forming subunit, whereas all examples where PKC mediates channel activation all contain Kir6.2. It may be that the effect of PKC on channel activity depends on the composition of the channel. In support of this, Thorneloe *et al.* (2002) have shown that PKC causes a decrease in the open probability of channels composed of Kir6.1 / SUR2B whereas it increases the open probability of channels composed of Kir6.2 / SUR2B, so it may be that channels containing Kir6.1 are inhibited by the action of PKC whereas channels containing Kir6.2 are stimulated.

It was recently suggested that the binding of the SNARE (soluble NSF attachment protein receptor) protein syntaxin1A to K_{ATP} channels could inhibit channel activity in both pancreatic β-cells and cardiac myocytes (Kang *et al.* 2004, Pasyk *et al.* 2004). It was subsequently shown that the action of syntaxin1A in inhibiting K_{ATP} channels was due to an interaction of syntaxin 1A with the NBFs of the channels thus reducing channel open probability (Cui *et al.* 2004). A similar mechanism of regulation has been described for other ion channels including CFTR (Naren *et al.* 1998) and ENaC (Condliffe *et al.* 2003). A number of other proteins have been shown to interact directly with K_{ATP} channels in various tissues and cell types, for example the cardiac K_{ATP} channel has been shown to interact with both creatine kinase (Crawford *et al.* 2002) and the actin cytoskeketon (Furukawa *et al.* 1996).

1.2.2 - Pharmacological regulation

K^+ channel opening drugs

The potassium channel opening (KCO) drugs are a diverse family of agents which activate K_{ATP} channels. KCO drugs have been used to treat excessive insulin secretion (diazoxide) and also for hair restoration (minoxidil). The most commonly studied KCO drugs are diazoxide, minoxidil, pinacidil, nicorandil and cromakalim (see Ashcroft & Gribble 2000, Mannhold 2004 for reviews).

An interesting property of the KCO drugs is that certain agents appear to be specific for certain isoforms of K_{ATP} channels. For example, the β-cell channel, composed of Kir6.2 and SUR1, is activated by diazoxide but not by cromakalim or nicorandil (Ashcroft & Rorsman 1989). In contrast, the cardiac channel, composed of Kir6.2 and SUR2A, is activated by pinacidil, cromakalim and nicorandil but not by diazoxide (Terzic *et al.* 1995, Isomoto & Kurachi 1997). Channels containing SUR2B are sensitive to all of the above drugs, albeit with differing affinities (Quayle *et al.* 1997). It appears that the responsiveness of each channel to individual KCO drugs depends largely on the SUR isoforms contained within the channel. The binding sites for some of these compounds have been identified. The binding site for pinacidil was isolated to 2 key domains contained within TM 16-17 and part of the cytoplasmic loop between TM 13-14 of the SUR2 isoforms by performing binding assays on chimeras containing regions of SUR1 (which does not bind pinacidil) (Uhde *et al.* 1999). The binding site for cromakalim has also been isolated to the same regions (Babenko *et al.* 1999, D'hanan *et al.* 1999). The binding site of diazoxide is less well known. Sensitivity to diazoxide can be conferred on SUR2A by substituting TM 6-11 and NBD1 from SUR1 (Babenko *et al.* 1999). It appears that the action of diazoxide is nucleotide dependent. Diazoxide is only effective in opening channels when Mg-nucleotides are present at the intracellular face of the cell membrane (Gribble *et al.* 1997, Shyng *et al.* 1997, Trapp *et al.* 1997) and when either of the NBFs of SUR1 are made less able to bind nucleotides by mutation the effect of diazoxide is lessened (Trapp *et al.* 1997, Reimann *et al.* 2000). This suggests that, in the case of diazoxide at least, correct nucleotide binding is required for KCO binding.

Sulphonylureas

The sulphonylurea compounds were first used in the Second World War as antibiotic agents, where it was noticed that hypoglycaemia was a common side effect. It has since become apparent that this hypoglycaemia is due to the inhibition of K_{ATP} channels by these compounds, and as such they are now commonly used to treat type-2 diabetes (see Proks *et al.* 2002 for review).

The sulphonylurea compounds are known to bind with a high affinity to the SUR subunit of K_{ATP} channels (Sturgess *et al.* 1985, Belles *et al.* 1987) and at a lower affinity to the Kir subunit (Gribble *et al.* 1997). The binding of sulphonylureas to

SUR is isoform dependent; the β-cell isoform, SUR1, is the only SUR type to bind tolbutamide and gliclazide whereas other SUR isoforms (SUR2A and 2B) bind all other types of sulphonylureas (Gribble *et al.* 1997, Gribble & Ashcroft 1999, Reimann *et al.* 2001, Sunaga *et al.* 2001). This is thought to be due to the existence of two types of sulphonylurea binding sites. The first binding site is thought to bind sulphonylureas similar in structure to tolbutamide and the second is thought to bind only the benzamido sulphonylurea compounds such as meglitinide. SUR1 is thought to contain both binding sites whereas the SUR2 isoforms are thought to contain only the benzamido binding site (Gribble *et al.* 1998, Song & Ashcroft 2001). A residue thought to be vital in the binding of sulphonylureas to the tolbutamide binding site is S1237 in SUR1. Mutation of this residue has been shown to affect the binding of tolbutamide (Ashfield *et al.* 1999), mitiglinide (Reimann *et al.* 2001) and nateglinide (Hansen *et al.* 2002) and also alter the binding properties of glibenclamide, which normally binds to both sites, allowing glibenclamide blockade of the channels to be more easily reversible (Ashfield *et al.* 1999). The blockade of K_{ATP} channels by the sulphonylureas can also be modulated by other factors which affect the open probability of the channels. For example, blockade of the channel is lessened when PIP_2 levels are elevated leading to an increase in open probability (Krauter *et al.* 2001). In contrast to this, elevated levels of Mg-nucleotides have been shown to increase the level of block mediated by sulphonylureas (Schwanstecher *et al.* 1992).

1.3 - Tissue distribution and roles

K_{ATP} channels have been shown to be expressed in numerous tissues where they are thought to play a wide range of roles. They are found in abundance in specific regions of the brain, in cardiovascular tissues, skeletal muscle and in the pancreas. Investigation of their roles in each of these tissues has been facilitated by the generation of K_{ATP} null mice deficient in Kir6.1 (Miki *et al.* 2002), Kir6.2 (Miki *et al.* 1998), SUR1 (Seghers *et al.* 2000) or SUR2 (Chutkow *et al.* 2001). Transgenic mice expressing dominant negative Kir6.2 (Miki *et al.* 1997, Koster *et al.* 2000) or expressing overactive Kir6.2 (Koster *et al.* 2000 - pancreas, Koster *et al.* 2001 - heart) or overexpression of SUR1 in the forebrain (Hernandez-Sanchez *et al.* 2001) have also been used in an attempt to elucidate the physiological roles of these channels.

1.3.1 - K_{ATP} channels in the brain

K_{ATP} channels have been shown to be expressed in several regions of the brain including the neocortex (Ohno-Shosaku & Yamamoto 1992), hippocampus (Zawar *et al.* 1999), Substantia nigra (SNr) (Roper & Ashcroft 1995, Stanford & Lacey 1996) and in the hypothalamus (Ashford *et al.* 1990).

K_{ATP} in the hypothalamus

K_{ATP} channels have been shown to be particularly abundant in the hypothalamus and their role here has been reasonably well studied. It is known that the hypothalamus is important in regulating the secretion of a number of counter-regulatory hormones involved in glucose homeostasis, including glucagon, via the autonomic nervous system (Taborsky *et al.* 1998). Indeed, transgenic mice lacking Kir6.2 ($Kir6.2^{-/-}$ mice) have been shown to have impaired glucagon secretion compared to wild-type mice. However, glucagon secretion from isolated islets from the same $Kir6.2^{-/-}$ mice was comparable to islets isolated from wild-type mice suggesting that the defect in the regulation of glucagon secretion lies upstream of the pancreatic α-cell (Miki *et al.* 2001). It has been known for some time that glucagon secretion from pancreatic α-cells can be increased by inducing hypoglycaemia in the hypothalamus (neuroglycopenia) (Borg *et al.* 1995, 1999). This effect has been attributed to a population of glucose sensitive neurones in the ventromedial hypothalamus (VMH) known as glucose-responsive neurones (GRNs) (Oomura *et al.* 1969, Minami *et al.*

1986). Dialysis of isolated GRNs with ATP-free pipette solution activated tolbutamide sensitive K^+ currents in the wild-type cells but not in the Kir6.2$^{-/-}$ cells indicating that Kir6.2 containing K_{ATP} channels are present. The composition of this population of K_{ATP} channels was confirmed by single-cell RT-PCR which showed that GRNs contain K_{ATP} channels composed of Kir6.2 and SUR1, the same composition as the pancreatic β-cell. The role of K_{ATP} channels in the hypothalamus is summarised in a model proposed by Miki *et al.* (2001) suggesting that "the pancreatic β-cell and the hypothalamus are functionally interactive: the insulin secretion system and the glucagon secretion system are integrated into the maintenance of glucose homeostasis through a common K_{ATP} channel". They propose that as blood glucose levels rise, K_{ATP} channels of the pancreatic β-cell are inhibited leading to insulin secretion and a corresponding lowering of blood glucose. As the blood glucose level falls, activation of K_{ATP} channels in the GRNs of the hypothalamus stimulates glucagon release by the pancreatic α-cells via the autonomic nervous system, which in turn raises the blood glucose level again. In this way blood glucose levels can be maintained at an appropriate level.

K_{ATP} channels in the substantia nigra (SNr)

K_{ATP} channels were first localised to the substantia nigra reticulate by Mourre *et al.* (1989) by [^{3}H] glibenclamide binding studies. The presence of a high affinity glibenclamide binding site suggests the presence of the pancreatic β-cell type K_{ATP} channel. The presence of Kir6.2 and SUR1 containing channels was confirmed by RT-PCR (Liss *et al.* 1999). Due to the proposed role of the substantia nigra as a central gating system for propagation of seizures (Iadarola & Gale 1982, De Sarro *et al.* 1984, Depaulis *et al.* 1994), and that such seizures are commonly associated with metabolic stresses such as hypoxia or hypoglycaemia, it was proposed that K_{ATP} channels may play a role in the supression of seizures in ATP-depleted conditions. Studies into the role of K_{ATP} channels in hypoxia induced seizures using Kir6.2$^{-/-}$ mice showed that tolerance to brief hypoxia was impaired in the Kir6.2 null mouse. Whereas wild-type animals remained sedated throughout the hypoxic challenge, making a complete recovery, Kir6.2$^{-/-}$ mice responded to the same challenge with a myoclonic jerk followed by severe tonic-chronic convulsions and death. The resting membrane potential of hypoxia challenged neurones was observed to be depolarised in Kir6.2$^{-/-}$ mice in comparison to wild-type neurones which displayed a tolbutamide

reversible hyperpolarization. It has therefore been suggested that K_{ATP} channels in the substantia nigra reticulate acts as a metabolic sensor which prevents seizure propagation during hypoxic stress.

K_{ATP} channels in the forebrain

Transgenic mice overexpressing SUR1 in the forebrain (Hernandez-Sanchez *et al.* 2001) have been shown to be resistant to kainic acid-induced seizures. Whereas wild-type mice showed significant loss of hyppocampal pyramidal neurones following kainic acid treatment, SUR1 overexpressing mice showed no change. This suggests that SUR1 containing K_{ATP} channels play a protective role from seizures and neuronal damage bought about by acute or chronic stress such as focal or global ischaemia (Heurteaux *et al.* 1993).

1.3.2 – K_{ATP} channels in the cardiovascular system

K_{ATP} channels have been identified in both vascular smooth muscle and in cardiomyocytes, but appear to behave very differently to each other. In vascular smooth muscle Kajioka *et al.* (1991) described channels with single channel conductance of ~ 30 pS which required both the removal of ATP and the addition of nucleoside diphosphates for activation. This is in contrast with cardiomyocytes where single channel conductance is ~ 70 - 90 pS (Ashcroft & Ashcroft 1990) with only removal of ATP required for channel activation. These differences have been attributed to varying constituent subunits being present in the channels. Reconstituted K_{ATP} channels containing Kir6.2 and SUR2A behave similarly to those found in cardiomyocytes (Inagaki *et al.* 1996), whereas channels reconstituted from Kir6.1 and SUR2A behave similarly to those found in vascular smooth muscle (Yamada *et al.* 1997). That the cardiomyocyte K_{ATP} channel contains Kir6.2 is supported by the observation that Kir6.2$^{-/-}$ mice lack K_{ATP} currents whereas Kir6.1$^{-/-}$ mice retain K_{ATP} activity (Miki *et al.* 2002). It was recently reported that K_{ATP} channels of human coronary artery endothelial cells may consist of Kir6.1 and Kir6.2 heteromultimeric pores as well as SUR2B (Yoshida *et al.* 2004).

K_{ATP} channels of the cardiovascular system have been principally implicated in the regulation of both vascular tone (Chrissobolis & Sobey 2003 for review) and the contractility of cardiomyocytes (Gross & Peart 2003 for review). In vascular smooth

muscle, K_{ATP} channel activity results in vasodilation, a process which is utilised by a number of vasodilatory drugs e.g. pinacidil, minoxidil and cromakalim. Stimulation of K_{ATP} channels by numerous endogenous substances also contributes to the resting tone of vascular smooth muscle. These substances include certain neuropeptides (Nelson *et al.* 1990, Miyoshi & Nakaya 1995) and adenosine (Daut *et al.* 1990, Belloni & Hintze 1991) and may also include nitric oxide (Murphy & Brayden 1995) and are thought to act via PKA dependent mechanisms (Kleppisch & Nelson 1995). Vasoconstriction may also be mediated by inhibition of K_{ATP} channel activity by substances which include angiotensin II (Miyoshi *et al.* 1991) and vasopressin (Wakatsuki *et al.* 1992) via PKC mediated pathways (Hayabuchi *et al.* 2001). K_{ATP} channels of cardiac tissues are activated by ischemia and hypoxic shock and the resulting K^+ efflux results in a shortening of the cardiac action potential. This has the effect of helping to prevent damage to the cardiac tissue under periods of ischemia or hypoxia suggesting a cardioprotective role for these channels. This protective role of these channels may involve trafficking of channels to the cell surface as well as changes in their functional characteristics (Budas *et al.* 2004). It has also been suggested that chronic mild hypoxia can increase the expression SUR2A in the heart derived H9c2 cell line, which may in turn lead to an increase in functional K_{ATP} channels (Crawford *et al.* 2003). The cardioprotective role of these channels may also be dependent on both gender and age, with K_{ATP} channel numbers decreasing with age although this is thought only to occur in females (Ranki *et al.* 2002).

1.3.3 – K_{ATP} channels in skeletal muscle

K_{ATP} channels in skeletal muscle were first described by Spruce *et al.* (1985). The subunit composition of these channels remains somewhat unclear to this day, although the characteristics of the endogenous channels are similar to those of recombinant channels reconstituted from Kir6.2 and SUR2B (Inagaki *et al.* 1996). The main function of K_{ATP} channels in skeletal muscle appears to be to protect the muscle cells during periods of fatigue due to over-contraction. During contractions of the muscle cell, metabolism and ATP usage is greatly increased. Due to depletion of ATP, channels are activated allowing an outward flux of K^+ ions. The effect of the outward flux is thought to be two-fold. Firstly the duration of action potential and thus the contraction is shortened (Gramolini & Renaud 1997). Secondly hyperpolarization of

the cell membrane limits Ca^{2+} influx into the cell and so prevents Ca^{2+} overload which could otherwise be damaging (Burton & Smith 1997).

It has also been proposed that K_{ATP} channels play a role in the uptake of glucose by skeletal muscle, although this idea remains somewhat controversial. It has long been known that certain sulphonylurea drugs can help maintain correct glucose homeostasis in patients with type-2 diabetes (Wang *et al.* 1989). It is thought that this effect is due to the sulphonylureas acting on peripheral tissues to improve glucose uptake whilst lowering insulin resistance, although no direct evidence to implicate the skeletal muscle K_{ATP} channel in this has yet been presented. Interestingly, the glucose lowering effect of insulin appears to be attenuated in Kir6.2$^{-/-}$ mice (Miki *et al.* 1998) and the rate of glucose uptake into the gastronemius muscle of the same mice also appears to be increased (Miki *et al.* 2002). Similarly, SUR2$^{-/-}$ mice (Chutkow et al. 2001) show lowered fasting and fed serum glucose levels and show improved glucose tolerance to a glucose tolerance test. It appears clear that K_{ATP} channels play some role in glucose uptake into skeletal muscle, but the exact mechanisms remain unclear.

1.3.4 - K_{ATP} channels of the pancreas

K_{ATP} channels are contained in each of the three main types of secretory cell in pancreatic islets, namely the α-cell, β-cell and δ-cell. The secretion of glucagon from α-cells (Gopel *et al.* 2000a) and the secretion of somatostatin from δ-cells (Gopel *et al.* 2000b) are thought to be regulated by K_{ATP} channels. It has been shown that K_{ATP} channels from α-cells contain the Kir6.2 and SUR1 subunits (Bokvist *et al.* 1999). The β-cell K_{ATP} channel and its role in the regulation insulin secretion has been very well characterised and will be discussed in greater detail in section 1.4 below.

1.4 - The role of K_{ATP} channels in insulin secretion

1.4.1 - Glucose homeostasis

The importance of maintaining the correct blood glucose levels cannot be overstated. The ultimate purpose of glucose homeostasis is to provide neuronal cells with adequate supplies of glucose to be utilised as fuel (Unger 1981, Cryer & Gerich 1985). One reason for this is because neuronal cells lack the ability to utilize alternative fuel supplies for themselves; for example through the production of ketone bodies or through the metabolism of amino acids and fatty acids, without inducing damaging structural and functional changes (Auer 1986). Hypoglycaemia, lowered blood glucose, may lead to altered states of consciousness and eventually death whereas prolonged hyperglycaemia, elevated blood glucose, may lead to damage to cellular proteins due to excessive glycosylation, affecting the structure and function of all proteins in all parts of the body. These effects have been well characterised in sufferers of diabetes, where, if not correctly controlled, blood glucose may fluctuate wildly. As an example of this, the effects of hypoglycaemia can lead to severe retinopathy in only a few years in diabetic patients (Cerami *et al.* 1979, Pettitt *et al.* 1980).

The balance of blood glucose is maintained principally by the contrasting actions of two hormones: insulin and glucagon (see Tirone & Brunicardi 2001 for review). In simple terms, insulin is released form the pancreatic β-cell when blood glucose is elevated, leading to increased glucose uptake into peripheral tissues such as the liver, adipose tissue and skeletal muscle where it is converted into the storage compound glycogen by the action of the enzyme glycogen synthetase (Rhodes & White 2002, Ferrer *et al.* 2003). When blood glucose levels are decreased the conversion of glycogen back into free glucose is stimulated by the action of the hormone glucagon on the peripheral tissues following its secretion from the pancreatic α-cell (Jiang & Zhang 2003). Of course the secretion of both of these hormones must be tightly regulated if glucose homeostasis is to prove effective. The mechanisms which ensure that the level of insulin secretion is appropriate to the level of blood glucose are now fairly well characterised and it is understood that one of the principal players in this process are the K_{ATP} channels of the pancreatic β-cell.

1.4.2 - The role of K_{ATP} channels in insulin secretion at the pancreatic β-cell

K_{ATP} channels are vital to correct glucose stimulated insulin secretion (GSIS). This is exemplified where disruption or loss of K_{ATP} channel activity leads to an inappropriate elevation in insulin secretion (as with congenital hyperinsulinism) or where K_{ATP} channel activity is heightened leading to inappropriately low insulin secretion (as may be the case with type-2-diabetes). Put simply, the K_{ATP} channel of the pancreatic β-cell can be seen as a switch which turns on or off insulin secretion as demanded by blood glucose levels, a process referred to as stimulus secretion coupling.

Figure 1.4 outlines the role of K_{ATP} channels in the regulation of normal GSIS in the pancreatic β-cell (see Nichols & Koster 2002 for review). In the scheme outlined in figure 1.4, a meal has just been eaten leading to an increase in blood glucose levels. The increased availability of extracellular glucose allows an increased rate of glucose uptake through specialized glucose transporters at the pancreatic β-cell surface. This glucose transporter has been shown to be GLUT2 in rodents, and it is likely that this is also true of humans although this has yet to be conclusively confirmed (Waeber *et al.* 1994, Heimberg *et al.* 1995, Guillam *et al.* 2000). The increased uptake of glucose into the cell leads to an increase in the cytosolic glucose concentration which translates to an increase in the rate of glucose metabolism. The first rate-limiting step in glucose metabolism, the conversion of glucose to glucose-6-phosphate, is catalysed by the hexokinase enzymes. This process in pancreatic β-cells differs from that in almost all other cell types because it involves a particular hexokinase isoform called glucokinase (hexokinase IV). Compared to the other three hexokinase isoforms, glucokinase has a much lower affinity for glucose and has a Km value of ~ 6 mM glucose which lies within upper end of the normal blood glucose range (Matschinsky 1990). These properties mean that the activity of glucokinase will increase or decrease in response to only very small fluctuations in the cytosolic glucose concentration, meaning that it is ideally suited to act as a glucose sensor (see Postic *et al.* 2001 for review). The increased rate of glucose metabolism leads to an increase in the rate at which ADP is converted into ATP. This increased rate of conversion has the effect of increasing the ratio between the amounts of cytosolic ATP and ADP ([ATP] / [ADP] ratio). The increase in [ATP] / [ADP] ratio in turn inhibits the K_{ATP} channels found at the cell membrane, as described in chapter 1.2.

When open, K_{ATP} channels would pass an outward flux of K^+, thus hyperpolarising the plasma membrane. In the scheme shown in figure 1.4, due to the elevated ATP / ADP ratio the K_{ATP} channels will be closed and the outward flux of K^+ will be halted, allowing the plasma membrane to depolarise freely. This depolarisation of the plasma membrane allows the opening of voltage dependent Ca^{2+} channels with a resultant influx of Ca^{2+}. The increase in cytosolic Ca^{2+} stimulates the movement to and fusion with the membrane of dense-core insulin containing granules via pathways which are still largely unclear.

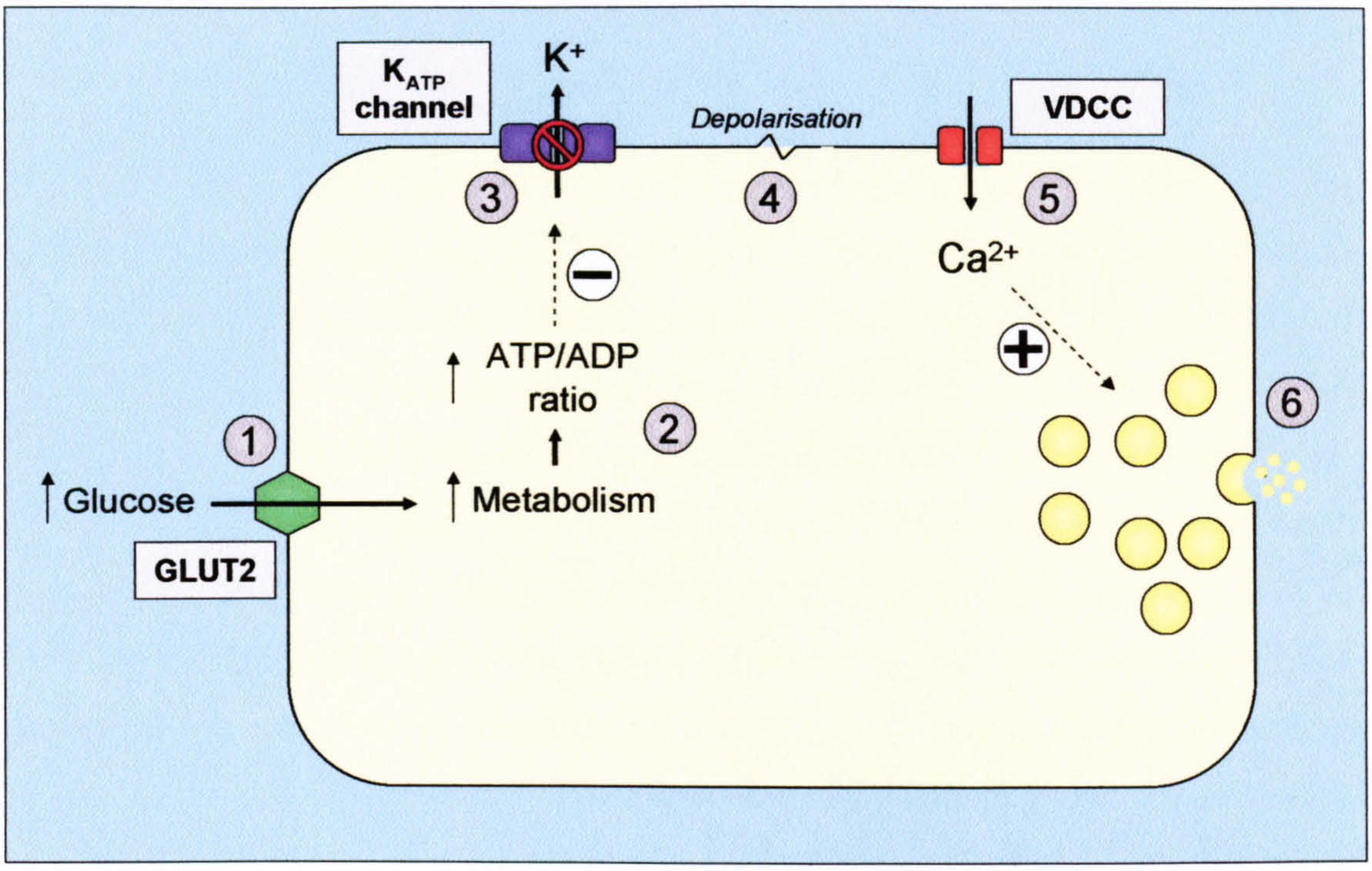

Figure 1.4 - *Regulation of glucose stimulated insulin secretion (GSIS) in the pancreatic β-cell.* Shown is a schematic outlining the role of K_{ATP} channels in the stimulus secretion coupling of GSIS. An increase in the extracellular glucose concentration is accompanied by an increase in the rate of uptake of glucose into the cell via glucose transporters, most likely GLUT2 (1). The increase in intracellular glucose results in an increase in the rate of metabolism which in turn causes the ATP/ADP ratio to rise due to the increased conversion of ADP to ATP (2). The increase in the ATP/ADP ratio results in inhibition of K_{ATP} channels halting the hyperpolarising outward flux of K^+ (3). The plasma membrane can therefore depolarise much more freely (4) resulting in the opening of voltage-dependent calcium channels (VDCC) and an inward flux of Ca^{2+} (5). This in turn stimulates the movement and fusion of insulin containing granules with the plasma membrane (6).

1.5 - Pathophysiology of K_{ATP} channels

Defects in K_{ATP} channels have been implicated in the onset of two disorders of glucose homeostasis, namely congenital hyperinsulinism and diabetes.

1.5.1 - Congenital hyperinsulinism

Congenital hyperinsulinism (CHI) is a disorder characterised by inappropriately elevated insulin secretion which is independent of blood glucose levels, leading to often profound hypoglycaemia. Mutations in Kir6.2 and particularly in SUR1 have been shown to be responsible for the majority of cases of CHI with an identified cause (see Dunne *et al.* 2004 for review). Over 100 mutations have been identified in either SUR1 or Kir6.2 which cause CHI (Fournet & Junien 2003). These mutations have been shown to reduce or abolish K_{ATP} channel function, allowing insulin secretion to occur without the requirement of the correct metabolic signals. These mutations have been shown to affect K_{ATP} channels in a number of ways including disrupting transport to the cell surface or defects associated with channel function. For example, trafficking defects have been reported for the R1394H and L1544P SUR1 mutations (Partridge *et al.* 2001, Taschenberger *et al.* 2002) whereas a number of other mutations associated with NBF of SUR1 (e.g. R1420C and E1506K) may lead to functional defects (Huopio *et al.* 2000, Matsuo *et al.* 2000).

For a more thorough and comprehensive introduction to CHI, see chapter 6, which describes the characterisation of two CHI causing mutations of Kir6.2.

1.5.2 - Diabetes

Type-2 diabetes

Type-2 diabetes is characterised by elevated blood glucose levels due to impairments in both the secretion and action of insulin. The exact causes of type-2 diabetes are still unclear but recent advances have begun highlighting a number of genetic determinants which are thought to predispose individuals to the disease at a later date (see Ashcroft & Rorsman 2004 a,b for reviews). Since the action of K_{ATP} channels are central to the correct secretion of insulin, gain-of-function mutations within either of the two channel subunits would be expected to produce diabetes like symptoms due to the suppression of insulin secretion, and it appears that this is the case. It is now

well established, following an initial period of controversy, that the E23K polymorphism of Kir6.2 is linked to the onset of type-2 diabetes (Hani *et al.* 1998, Gloyn *et al.* 2001, Schwanstecher *et al.* 2002a, Schwanstecher & Schwanstecher 2002, Gloyn *et al.* 2003, Love-Gregory *et al.* 2003, Nielsen *et al.* 2003). When heterologously expressed in mammalian cells, it has been shown to reduce ATP-sensitivity of Kir6.2 two-fold, and it is thought that this is a sufficient reduction to vastly attenuate insulin secretion *in vivo* (Schwanstecher *et al.* 2002b). It has also been suggested that SUR1 polymorphisms may play a role in the onset of type-2 diabetes (Hani *et al.* 1997). The E1506K polymorphism first found in a family of Finnish origin has been shown to first lead to congenital hyperinsulinism in infancy, then to loss of insulin secretory capacity in early adulthood and then finally to diabetes in middle age (Huopio *et al.* 2003). It remains unclear why this form of diabetes develops in this manner.

Other forms of diabetes

Mutations associated with either channel subunit, particularly Kir6.2, have been implicated in the onset of other rarer forms of diabetes. Neonatal diabetes is characterized as an insulin-requiring hyperglycaemia which presents in infants within the first three months of life (Shield 2000, Polak & Shield 2004). Two distinct forms of neonatal diabetes are known, transient neonatal diabetes mellitus (TNDM) and permanent neonatal diabetes mellitus (PNDM), and in each case mutations of Kir6.2 have been identified as the cause in the majority of cases where causes are known (Gloyn *et al.* 2004a,b, Vaxillaire *et al.* 2004, Gloyn *et al.* 2005, Massa *et al.* 2005).

1.6 - Trafficking pathways

The regulation of K_{ATP} channel trafficking is poorly understood. The export of newly synthesized channels from the ER is governed by the presence of -RKR- retention motifs contained within the cytoplasmic domains of both Kir6.2 and SUR1 (Zerangue *et al.* 1999). The act of channel assembly is thought to mask these motifs allowing the release of fully formed channels but not individual subunits. It also appears that glycosylation of SUR1 is required for the efficient transport of newly synthesized channels through the biosynthetic pathway (Conti *et al.* 2002). The mechanisms regulating the endocytic trafficking of K_{ATP} channels is even less well understood. Recent data (Hu *et al.* 2003) suggests that the endocytosis of K_{ATP} channels is regulated by the action of PKC, however, the fate of the internalized channels was not investigated in any detail. For this reason the endocytic trafficking of K_{ATP} channels will be investigated.

1.6.1 - Overview of endocytic trafficking

When proteins are internalised from the cell surface they are directed to different destinations within the cell, usually via well defined and tightly regulated pathways. Many proteins like the epidermal growth factor receptor (EGFR) are targeted for degradation by proteolysis. Some proteins like the transferrin receptor are rapidly recycled back to the surface. Others, as in the case of the glucose transporter GLUT4, are sequestered into a storage compartment to be released only by application of the correct stimulus. The targeting of each protein along its own specific pathway is determined by the recognition of specific amino acid motifs by other accessory proteins situated in and around each of the organelles of the endocytic pathways.

Endocytic compartments

Figure 1.5 shows an overview of the known endocytic trafficking pathways. Proteins at the cell surface are internalised by numerous means including clathrin coated pits and caveolae, depending on which sub-domain of the membrane the protein is being retrieved. Following internalisation proteins enter the endocytic trafficking pathways via the sorting endosomes. Here proteins are recognised and concentrated into specific domains of the endosome membrane. Some of these domains containing a specific complement of accessory and cargo proteins will develop into a population of

tubular endosomes, called the endocytic recycling compartment (ERC), which allow rapid recycling back to the cell surface. The remainder of the early endosome is thought to aggregate into multi-vesicular bodies (MVB) which in turn mature into the late endosome. A great deal of material which enters the late endosome will remain within as it acidifies and matures into the lysosome, the main site of proteolysis within the cell. Some cargo proteins in the late endosome, however, are able to escape this degradative pathway and are targeted to the *trans*-Golgi network (TGN). Transport to the TGN is also achieved by a number of proteins which traverse the ERC. Once at the TGN proteins may be released into the biosynthetic pathway, enter into a futile cycle of trafficking through the endocytic compartments or be routed into a specialised storage compartment. The role of each of the endocytic compartments mentioned above as well as some details of proteins which traffic through them is discussed in more detail below (See Pfeffer 2003 for review covering the above general trafficking pathways).

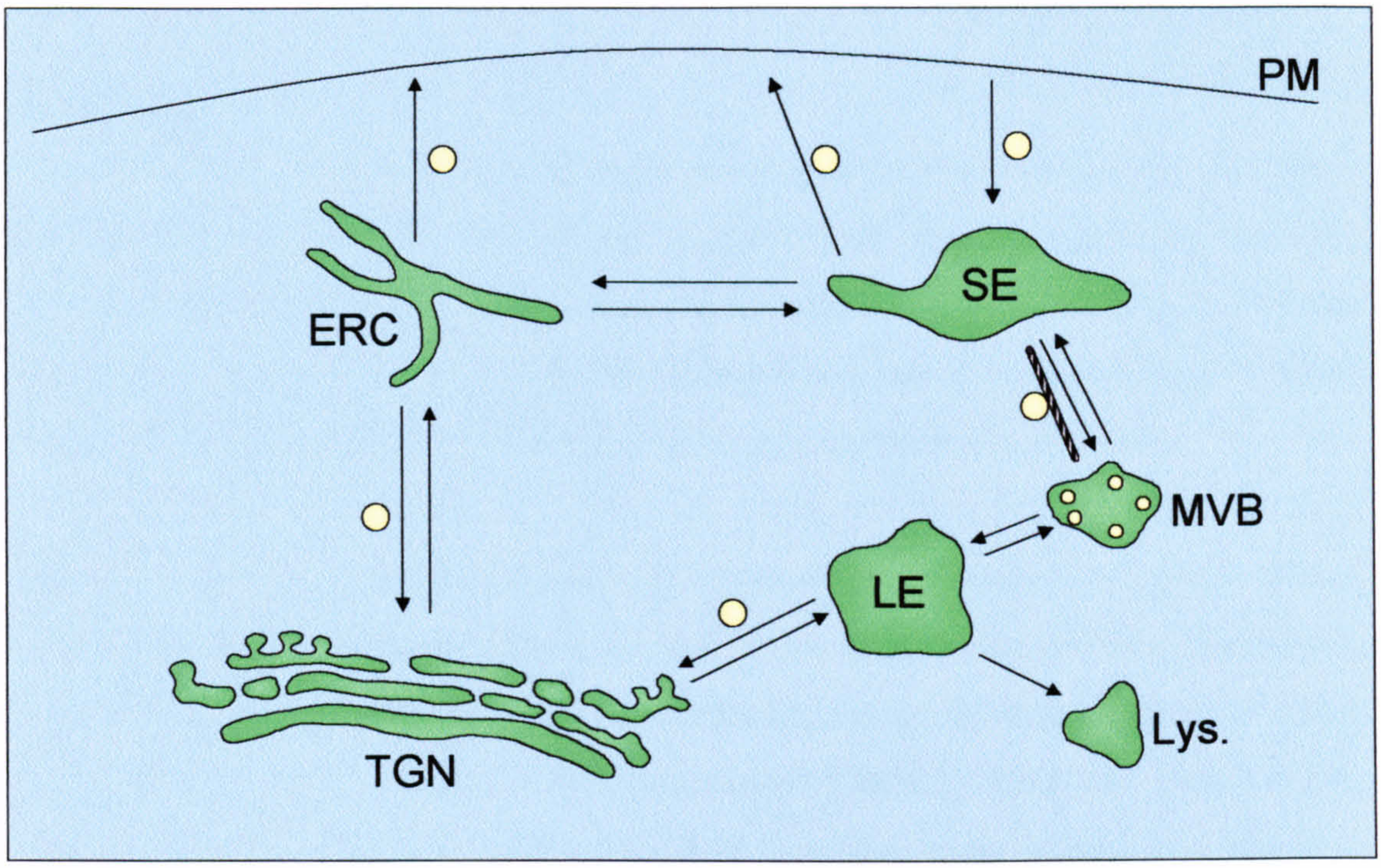

Figure 1.5 - *An overview of the endocytic trafficking pathways of mammalian cells.* Endocytosed proteins are first delivered from the plasma membrane (PM) to the sorting endosomes (SE) in transport vesicles. From the SE cargo proteins are routed toward the endocytic recycling compartment (ERC) to the multi-vesicular bodies (MVB), via microtubules (black and white striated bar), or returned directly back to the cell surface. Proteins directed towards the ERC may then be returned to the cell surface or be trafficked to the *trans*-Golgi network (TGN). Proteins directed to the MVB will continue through to the late endosome (LE) where they will be directed to either the lysosome (Lys.) or the TGN.

1.6.2 - Regulators of trafficking

Two classes of proteins which have been identified as being important in regulating endocytic protein transport are the Rab GTPase and the syntaxin families. Each compartment has its own distinct collections of each of these proteins and this can be used to characterise and distinguish each of the endocytic organelles from one another.

Rab proteins

Rab proteins are monomeric small-GTPase proteins of the Ras superfamily; they have been suggested to play a role in the regulation of vesicle trafficking in both endocytosis and exocytosis, where they have been chiefly implicated in vesicle docking and fusion. Of the ~ 60 Rab isoforms which have been identified 12 have been localised to the endosomal system (For review see Seabra *et al.* 2002).

The Rab proteins are thought to principally be involved in vesicle docking and fusion to target membranes (Schimmoller *et al.* 1998, Gonzalez & Scheller 1999, Mohrmann & van der Slujis 1999) although they have been implicated in other steps of vesicular transport as discussed below. In the active, GTP-bound, form Rab proteins are recruited to specific membrane domains where they selectively interact and recruit a wide range of effector proteins which facilitate discrete steps of membrane transport. These effector proteins include protein kinases, SNARE proteins and certain cytoskeletal proteins (Stenmark *et al.* 1995, Ren *et al.* 1996, Echard *et al.* 1998, Christoforidis *et al.* 1999). As well as vesicle docking and fusion, Rab proteins have been implicated in the regulation of the process of vesicle budding (Riederer *et al.* 1994, Jedd *et al.* 1997, McLauchlan *et al.* 1998, Jones *et al.* 1999) and in facilitating transport of vesicles along the cytoskeleton (Echard *et al.* 1998, Nielsen *et al.* 1999).

Each compartment has its own complement of Rab proteins which also appear to be segregated to specific domains within the membranes of each organelle. For example, both Rab5 and Rab4 are present in the sorting endosomes but it appears that they occupy distinct, non-overlapping regions of the endosomal compartments (Sonnichsen *et al.* 2000). As such, Rab proteins could prove useful as selective markers for endosomal compartments in cell biological studies. The distribution of

each Rab protein known to interact with specific endosomal compartments are shown in figures 1.8 - 1.10.

Syntaxin proteins

The syntaxin proteins are members of the SNARE (soluble NSF attachment protein receptor) family of trafficking regulators which function to ensure that vesicles fuse to the correct membrane domains. There are 15 syntaxins in mammals, each of which is localised to specific membranes within the cell (see Teng *et al.* 2001 for review)

The syntaxins are all anchored to the cell membrane (except for syntaxin 11) via the C-terminus, with the N-terminus extending into the cytoplasm of the cell. They all contain several hydrophobic regions which are thought to form coiled-coil α-helical structures. One of these domains of ~ 60 amino acids is the SNARE domain, characteristic of all of the SNARE proteins (Weimbs *et al.* 1997). The SNARE domains of the syntaxins interact with SNARE domains of other SNARE proteins on target membranes, so called t-SNAREs (usually other syntaxins or SNAP-25 family proteins). This complex can then interact with SNARE proteins found of the vesicle membranes, the v-SNAREs, commonly members of the vesicle associated membrane protein (VAMP) family of proteins to form a core fusion complex (Sutton *et al.* 1998) as shown in figure 1.6. This tethers the vesicle close to the target membrane so that vesicle fusion can occur. The N-terminus of some syntaxin proteins has a bundle of 3 α-helices which is thought to act as an auto-inhibitory domain. This function has been best studied in syntaxin 1 (Lerman *et al.* 2000). The auto-inhibitory domain can fold back onto the SNARE domain when the protein is in its "closed" state so it is unable to interact functionally with other SNARE proteins. Specific chaperone proteins bind to syntaxin in this conformation in order to keep it in the closed conformation. In the case of syntaxin 1 the chaperone protein is munc18. Specific Rab-GTPases can cause the chaperone protein to dissociate, allowing the syntaxin to enter the open conformation, facilitating SNARE binding.

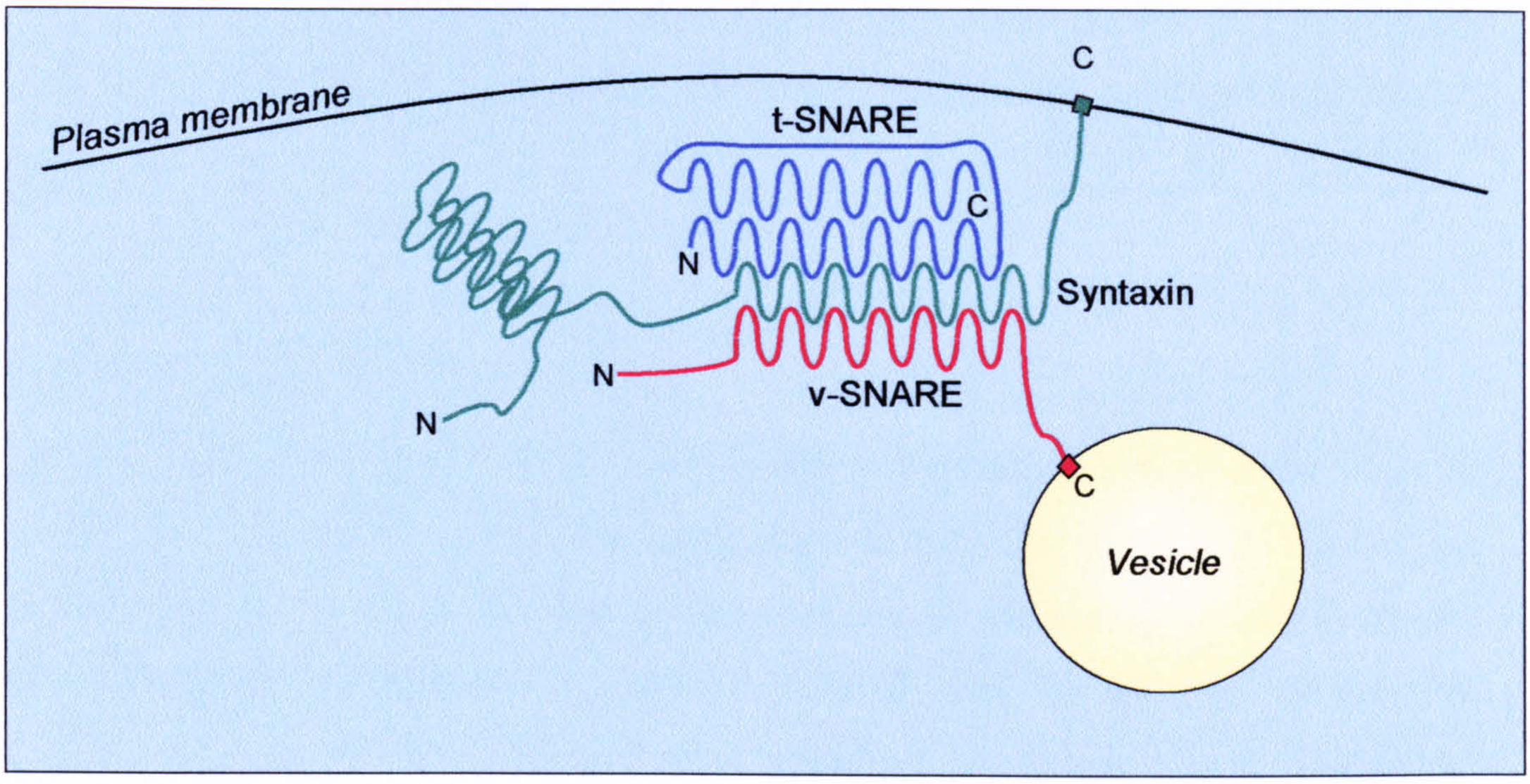

Figure 1.6 - *The role of syntaxins in vesicle fusion.* Shown is a schematic representation of the four helical coil structure of the core fusion complex formed by the t-SNARE (usually SNAP-25 family) (BLUE), the VAMP (RED) and a member of the syntaxin family (GREEN). The t-SNARE interacts with syntaxin and this complex then in turn interacts with v-SNARE on the vesicle membrane. N - amino terminus, C - carboxyl terminus.

Since each syntaxin protein is expressed at very specific locations within the cell and each syntaxin will bind to only a few other specific SNARE proteins they provide a mechanism whereby vesicles can bind selectively to certain membrane domains. Because of this limited localisation, they can also be used to identify compartments. For example, the *trans*-Golgi network exclusively expresses syntaxin 6 and 16 and syntaxin 12/13 is only found in the early endosomal compartments. The distribution of each of the syntaxins in each of the endocytic compartments is shown in figures 1.8 - 1.10.

1.6.3 - Endocytosis

Clathrin mediated endocytosis

Clathrin mediated endocytosis is the most widely studied and best understood of all the endocytic processes, and is known to occur in all cells where it is vital to the uptake of numerous nutrients and to the turnover of most cell surface receptors, transporters and channels (See Conner & Schmid 2003 for review). Material is internalised from the cell surface by the formation of clathrin coated pits, which eventually separate from the membrane to form clathrin coated vesicles (CCV). The formation of CCV's relies on the recruitment of coat proteins to the cell surface to form a lattice of clathrin molecules. Central to this recruitment are the adaptor protein complexes of which four isoforms have been isolated (termed AP1-4). Each adaptor protein complex has a distinct subcellular distribution and the isoform responsible for endocytic CCV formation is AP2. AP2 is a heterotetrameric complex which is targeted to the plasma membrane by the α-adaptin subunit, whereas the β2-subunit mediates clathrin assembly, and interaction with sorting motifs on cargo molecules occurs through the μ2 subunits. The sorting motifs which are recognized by the μ2 subunit commonly consist of two leucine residues, so called di-leucine motifs (-LL-) and are common in membrane bound proteins. Once AP-2 has been recruited to the cell surface by interaction with cargo proteins, clathrin molecules begin to be recruited by interactions with AP-2. Clathrin is composed of two proteins, the clathrin light chain (CLC) and the clathrin heavy chain (CHC). Each clathrin complex is composed of three each of CLC and CHC arranged at 120° angles from each other to form complexes termed clathrin triskelions. When the clathrin triskelions are recruited to the cell surface in sufficient numbers, they polymerise to form a polygonal lattice which deforms the cell membrane, beginning the

invagination which will eventually form the CCV. The final scission which will result in the separation of the clathrin coated pit from the membrane to form the final CCV is dependent on the action of dynamin, a multi-domain GTPase which is recruited to the neck of clathrin coated pits where it forms a spiral collar which is thought to regulate the membrane fission although the exact mechanisms are still not fully understood.

Caveolin mediated endocytosis

Caveolae were first described over fifty years ago as flask shaped invaginations of the plasma membrane which were abundant in epithelial cells. They are now known to be present in most cell types and to occur only in microdomains of the plasma membrane which are enriched in cholesterol and sphingolipids into which certain proteins are concentrated (reviewed in Anderson *et al.* 1998).

The presence of caveolae is dependent on the expression of the protein caveolin. Caveolin is a dimeric protein which binds to cholesterol in the inner leaflet of the plasma membrane. When bound to cholesterol in the membrane caveolin self assembles to form a striated coat which covers the surface of the caveolae. The importance of caveolin in the formation of caveolae has been reinforced by the establishment of caveolin null mice in which no caveolae were detectable (Drab *et al.* 2001). These null mice have no overt phenotype and appear to develop normally, suggesting that either caveolae do not play a very important role or that other mechanisms can compensate for their loss. Closer examination of caveolin deficient cells revealed that their ability to endocytose serum albumin was impaired, suggesting a role in transcellular transport (Razani *et al.* 2002). The rate of internalisation of caveolae is very slow compared to other modes ($t_{1/2} > 20$ minutes) and the size of the final vesicles are also small (50 - 60 nm in diameter compared to ~ 120 nm for clathrin coated vesicles). As such it is thought that caveolae constitute only a very small proportion of total uptake into cells. Indeed, caveolae are often immobile in the membrane, requiring tyrosine-phosphorylation of constituent proteins for initiation of internalisation (Pelkmans & Helenius *et al.* 2002).

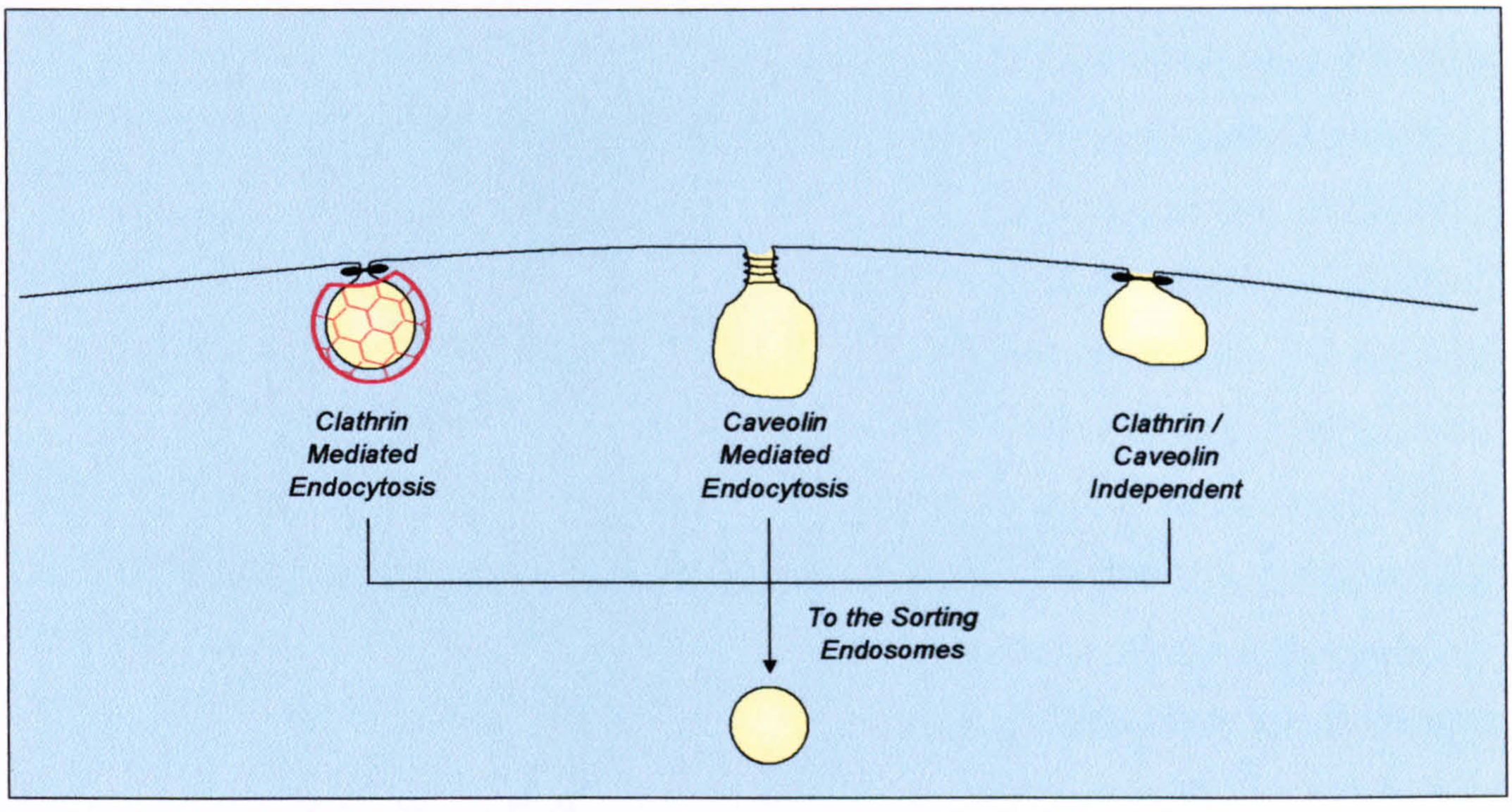

Figure 1.7 - *Mechanisms of endocytosis.* The main mechanisms of endocytosis are depicted. Clathrin mediated endocytosis relies on the recruitment of adaptor proteins e.g. AP-2, by cargo proteins at the cell surface. This in turn allows the formation of the clathrin coat. Scission of the vesicle relies on the action of dynamin (⬬). Caveolin mediated endocytosis relies on the action of caveolin for the final vesicle scission and does not involve clathrin. Clathrin / caveolin independent endocytosis covers all other mechanisms of endocytosis which are independent of the action of either clathrin or caveolin. See chapter 1.6.3 for further details.

Clathrin / caveolin independent endocytosis

A number of alternative pathways for the endocytosis of membrane proteins from cholesterol-rich lipid rafts are thought to exist, which are independent of the function of either clathrin or caveolin. The unique lipid composition of these lipid rafts provides a physical basis for the specific sorting of membrane proteins into small membrane domains of ~ 40-50 nm diameter (Edinin *et al.* 2001). The internalisation of the interleukin 2 (IL-2) receptor in lymphocytes is a known example of such a clathrin / caveolin independent mechanism. The IL-2 receptor is associated with lipid rafts, but is internalised in a clathrin and caveolin independent manner. This is in contrast to a number of other lipid raft associated proteins e.g the shiga- and cholera-toxins which are known to bind to raft associated glycolipids and are internalised along with clathrin coated vesicles (Sandvig *et al.* 2002, Thomsen *et al.* 2002). The internalisation of the IL-2 receptor is not affected by dominant-negative forms of Eps-15 (an important AP-2 complex binding partner which is involved in clathrin mediated endocytosis), but it is inhibited by dominant-negative forms of dynamin. It has been shown that it is possible to follow these events using GFP-labelled GPI-anchored proteins but even with these tools the mechanisms are still poorly understood (Nichols & Lippincott Schwartz 2001).

1.6.4 - Early endosomes

The early endosomal system is the first destination for the majority of material endocytosed from the cell surface. It is thought to comprise two distinct types of endosomal compartment, termed here the sorting endosome and the endocytic recycling compartment. The main distinction between the two compartments is their complement of regulatory proteins. Shown in figure 1.8 is a representation of the early endosome compartments and trafficking pathways.

Sorting endosomes

The sorting endosomes are the first main branch point in the endosomal trafficking system. Endocytosed material is transported from the cell surface in vesicles which fuse with the sorting endosomes where cargo proteins are recognised and distributed along the correct sorting pathways as shown in figure 1.8. Destinations to which proteins are targeted from the sorting endosome are the endocytic recycling compartment, the late endosome / multi-vesicular body and the cell surface.

The sorting endosomes are short lived, peripheral located, tubular-vesicular structures that have a luminal pH of ~ 6.0 (Johnson *et al.* 1993, Presley *et al.* 1997). They only accept endocytosed material for ~ 5 - 10 minutes, after which they move along microtubules becoming more acidic and taking on the characteristics of late endosomes. Because of the slightly acidic pH in the sorting endosome lumen, most ligands dissociate from receptors, remaining in the lumen whilst the endosome matures into a late endosome. This allows the removal of many ligands to the lysosome without the need for any specialised targeting mechanisms. Most receptors and other cell surface proteins are concentrated into narrow-diameter tubules which are excised from the sorting endosome, either returning immediately to the cell surface in a direct recycling pathway or becoming part of the endocytic recycling compartment (Dunn *et al.* 1989, Mayor *et al.* 1993). These narrow-diameter tubules have a very high surface area to volume ratio, meaning that whilst a large proportion of membrane proteins can be efficiently removed the soluble components in the lumen are largely excluded. It is thought that the vast majority of proteins not containing any specialised late endosome targeting motifs are removed from the sorting endosome in this manner. Those proteins which are not destined for rapid recycling remain in the sorting endosome as it matures into a late endosome.

Proteins which are characteristic of the sorting endosome are early-endosome antigen 1 (EEA1) and Rab5 which are involved in endocytic vesicle fusion and Rab4 which is involved in directing cargo recycling via the endocytic recycling compartment.

Endocytic Recycling Compartment (ERC)

The endocytic recycling compartment (ERC) was initially characterised by its involvement in the rapid recycling of the transferrin receptor (TfR) (Hopkins *et al.* 1983, Yamashiro *et al.* 1984). Endocytosed membrane proteins are translocated to the ERC from the early sorting endosomes. These proteins are then directed either towards the cell membrane or the *trans*-Golgi network (TGN) as depicted in figure 1.8.

The ERC is a collection of tubular organelles associated with microtubules with an internal diameter of ~ 60 nm and a luminal pH of ~ 6.5 (Hopkins *et al.* 1983,

Yamashiro *et al.* 1984, McGraw *et al.* 1993). The ERC is a relatively long-lived compartment which suggests that both entry and exit of material is dependent on the formation of transport intermediates. The machinery responsible for the sorting of cargo proteins in the ERC is only poorly understood, although indications suggest that it is likely to be fairly similar to that of other compartments. A number of studies suggest that clathrin and its various associated adaptor complexes are present in the ERC (Pagano *et al.* 2004), and indeed perturbation of these mechanisms appears to alter the recycling kinetics from this compartment. Two proteins which have been shown to be important for correct function of the ERC are Rme1, an Eps15-homology-domain protein (Lin *et al.* 2001), and Rab11 (Chen *et al.* 1998, Ren *et al.* 1998). Disruption of the function of either of these proteins has been shown to be sufficient to interfere with trafficking from the ERC to either the cell surface or the TGN. In addition to Rme1 and Rab11 it appears the Rab6a is also involved in transport to the TGN (Mallard *et al.* 2002).

Proteins which are characteristic of the ERC include Rab4 and Rab11, although these are also present to some extent in sorting endosomes and the TGN respectively. Rme1 serves as a much more selective marker as its expression is limited to the ERC. Fluorophore-conjugated transferrin is also commonly used to fluorescently label the compartments of the rapid recycling pathway which includes the ERC, although other compartments such as the sorting endosome will also be labelled.

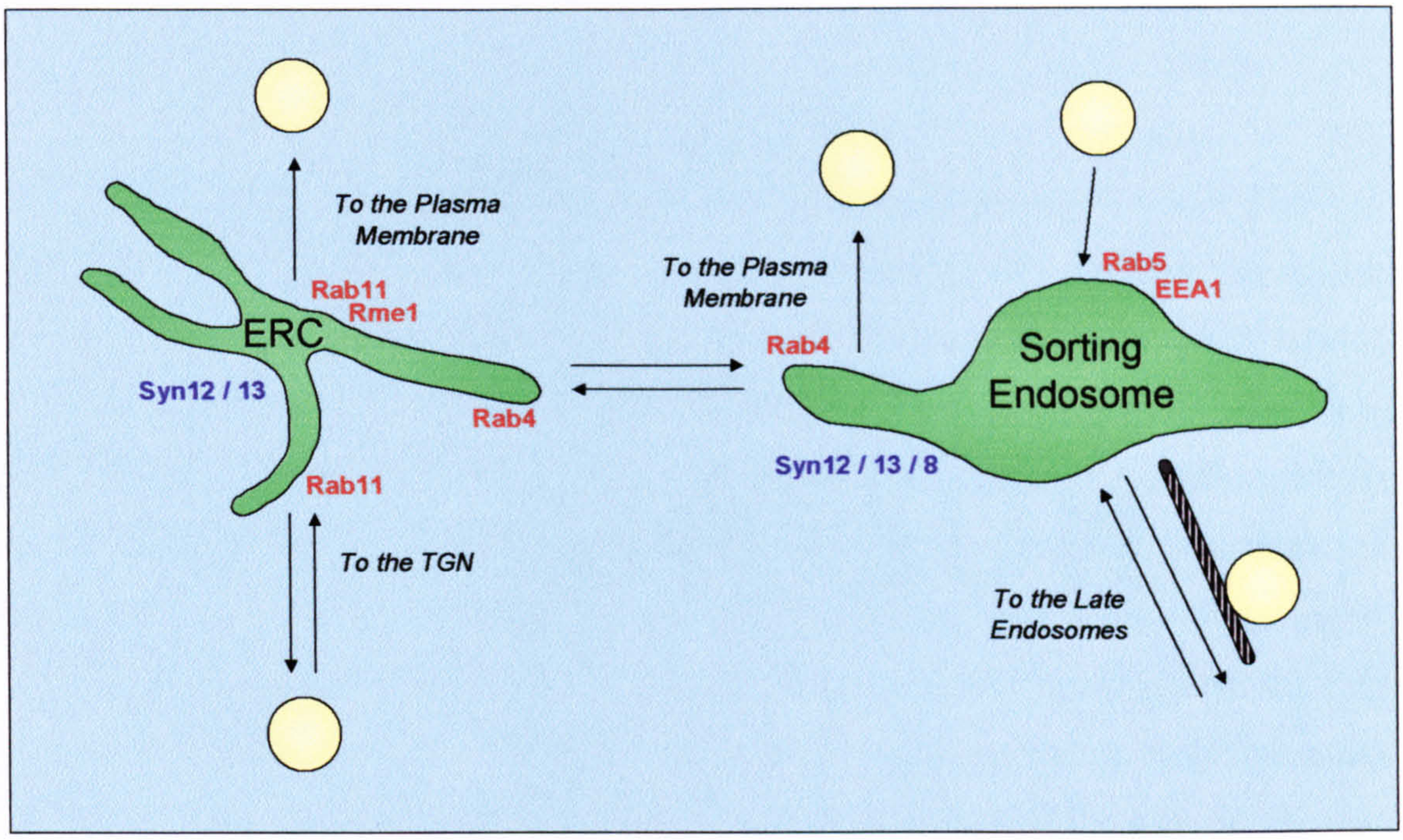

Figure 1.8 - *The early endocytic trafficking pathways.* The trafficking pathways of the early endosomal compartment are depicted. The key regulatory proteins involved in trafficking are shown in red and the syntaxin isoforms associated with each compartment are shown in purple. The function of each compartment is described in more detail in section 1.6.4. ERC - Endocytic recycling compartment.

1.6.5 - Late Endosomes / Lysosomes

Proteins and ligands which are destined for degradation are targeted to late endosomes during sorting at the early endosome. These compartments have a significantly lower pH than the early endosomal compartments and are enriched in proteolytic enzymes. Shown in figure 1.9 is a representation of trafficking pathways within the late endosomal system.

Multi-Vesicular Compartments

Multi-vesicular compartments were first described over 50 years ago by the pioneers of electron microscopy who observed organelles consisting of a limiting membrane containing a large number, often several hundred, of smaller vesicles each with a diameter or ~ 40-90 nm (see Gruenberg & Stenmark 2004 for review). It has since been shown that these multi-vesicular compartments represent an intermediate compartment of trafficking between the early and late endosomal compartments (Bomsel *et al.* 1990, Aniento *et al.* 1993). Since they are formed from early endosomes they contain a lot of material which has been endocytosed from the cell surface but they also receive material from the TGN including a number of lysosomal enzyme precursors. In most cases the multi-vesicular compartments mature into or fuse with the late endosomal compartment which ultimately leads to lysosomes (see Luzio *et al.* 2003 for review).

The purpose of the two topologically distinct membrane domains, the limiting membrane and the intraluminal vesicles, is not fully understood but several possibilities exist. Firstly, transmembrane proteins in the intraluminal membranes would likely be susceptible to degradation by lysosomal hydrolases whereas transmembrane proteins in the limiting membrane may be more resistant to a similar degradation because their exposed regions would most likely contain glycosyl-residues and so be resistant to the effect of the proteolytic enzymes (Felder *et al.* 1990). Secondly, it has been proposed that the intraluminal vesicles may act as a storage compartment for transmembrane proteins which would be released back to the cell surface in a controlled manner. Thirdly, it is theoretically possible for the proteins in the limiting membrane to participate in receptor signalling events whereas those proteins in the intraluminal membranes would be precluded from participation. These hypotheses demonstrate how the sorting of endocytosed proteins into the

distinct membrane domains provided by the intraluminal and limiting membranes could allow both the selective delivery to either the lysosome or the extracellular space and also to allow the ability of endocytosed receptors to mediate signalling events.

Late Endosomes

The late endosomes are morphologically similar to the MVB, indeed some controversy exists as to whether the MVB represent a separate compartment from the late endosome. However, significant differences exist between the composition of late endosomes and MVB. Late endosomes are highly pleiomorphic, consisting of regions of cisternal, tubular and multivesicular domains. The lipid and protein composition of late endosomes is also very distinct from other organelles, containing large amounts of so-called lysosomal glycoproteins e.g. Lamp 1 and Lamp 2 (Griffiths *et al.* 1988). The late endosomes are also rich in lysobisphosphatidic acid (LBPA) which is not found in any other organelle (Kobayashi *et al.* 1998, Matsuo *et al.* 2004). Finally the late endosomes act as a major sorting station within the endosomal system (Goda & Pfeffer 1988), a process which is discussed in more detail below. The luminal pH of late endosomes varies between 5.5 - 6.0. Proteins are delivered to the late endosome primarily from the early endosome although some proteins are also transported to the late endosome via specialised pathways from the TGN.

Materials destined for degradation by the lysosome are passed through the late endosome. Indeed lysosome biogenesis is thought to rely on the maturation of late endosomes into lysosomes in a process dependent on both Rab7 and syntaxin7 (Bucci *et al.* 2000). However, all proteins translocated into the late endosome are not targeted towards the lysosome. The late endosome acts as a sorting station for a number of proteins with direct trafficking to the TGN. One of the best characterised of these proteins is the cation independent mannose-6-phosphate receptor (CI-M6PR) which chaperones lysosomal enzymes from the biosynthetic pathway at the TGN to the late endosome. CI-M6PR contains an acidic motif in its cytoplasmic domains which is known to mediate trafficking to the TGN from the late endosome (Schafer *et al.* 1995, Voorhees *et al.* 1995, Alconada *et al.* 1996, Mauxion *et al.* 1996, Dittie *et al.* 1997). Also associated with the acidic motif is a casein kinase II (CKII)

phosphorylation site (Meresse *et al.* 1990). When this CKII site is phosphorylated the acidic motif is able to interact with a similar acidic motif contained in a chaperone protein called PACS-1 (Wan *et al.* 1998). It is this interaction which allows trafficking to the TGN to occur via AP-1 or AP-3 binding to PACS-1 which allows clathrin coat formation (Crump *et al.* 2001). Another adaptor protein known to be involved in transport between the late endosome and TGN is Tip47, although little is known about its mechanism of action (Diaz & Pfeffer 1998).

Proteins which are characteristic of the late endosome are CI-M6PR and Rab7 since these are enriched in these compartments. Other markers such as Lamp1 will label late endosomes, but will also label lysosomal compartments to a larger extent.

Lysosomes

Lysosomes have long been regarded as the terminal degradative compartment of the endocytic pathway. They are membrane bound organelles of ~ 0.5 μm diameter containing a variety of acid hydrolases associated with its internal limiting membranes. These glycoproteins are grouped into three distinct classes; the limps (lysosomal integral membrane proteins), the lamps (lysosomal associated membrane proteins) and the lgps (lysosomal glycoproteins) (see Luizio *et al.* 2003 for comprehensive review). Lysosomes are distinguished from late endosomes by the absence of CI-M6PR and recycling membrane proteins which are abundant in late endosomes but absent in lysosomes (Kornfeld & Mellmann 1989, Luzio *et al.* 2000, Mullins & Bonifacino 2001). When examined by electron microscopy lysosomes are morphologically heterogenous and more electron dense than the surrounding cytoplasm. They also appear to contain numerous smaller vesicles of membrane 'whirls'. Lysosomes are thought to constitute ~ 0.5 - 5 % of the total cell volume and are always located near the microtubule organising centre (Matteoni & Kreis 1987)

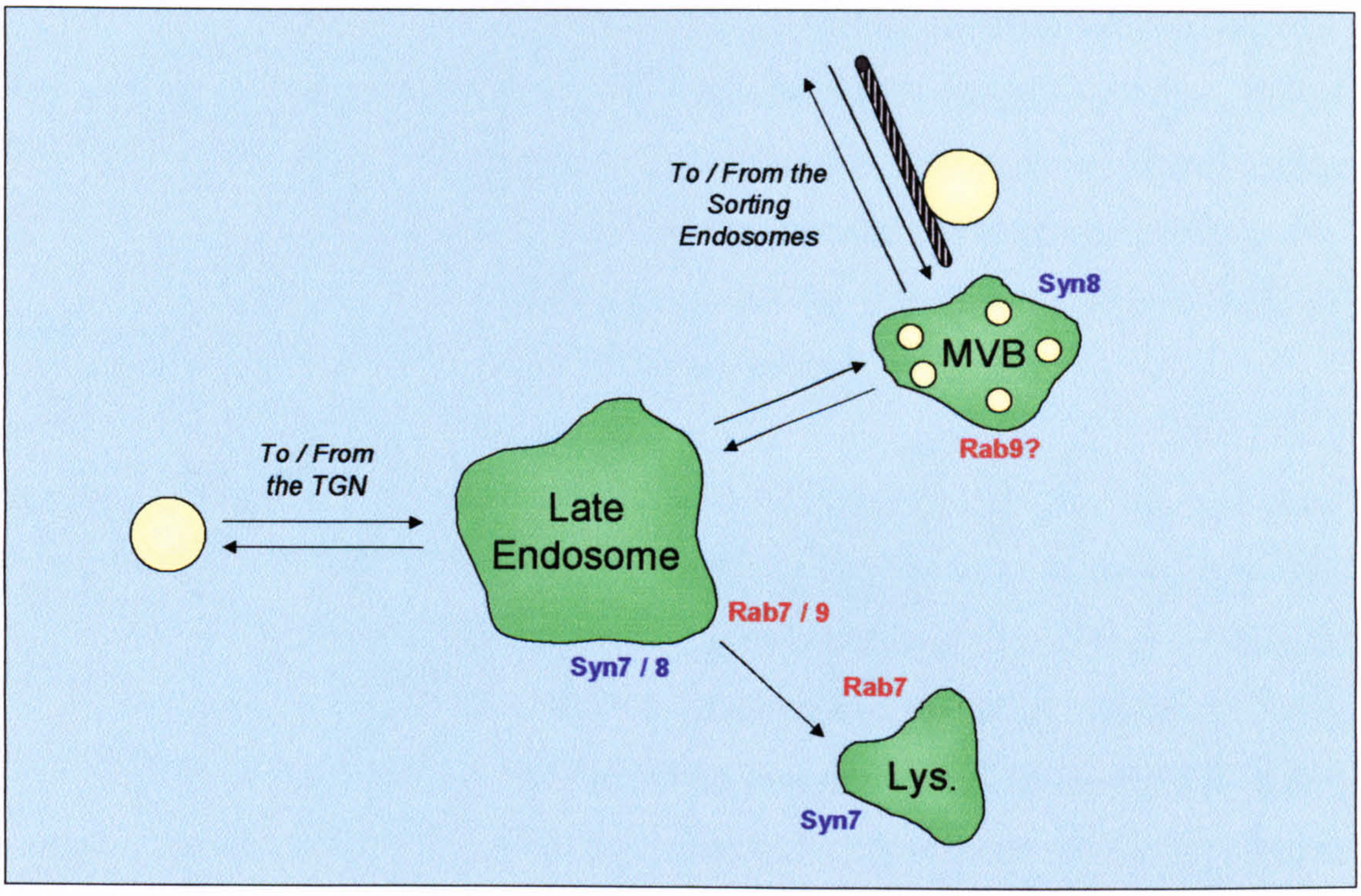

Figure 1.9 - *The late endosomal compartments.* The trafficking pathways of the late endosomal compartments are shown. The key regulatory proteins involved in trafficking are shown in red and the syntaxin isoforms associated with each compartment are shown in purple. The function of each compartment is described in more detail in section 1.6.5. MVB - Multi-vesicular body, Lys. - Lysosome.

1.6.6 - *Trans*-Golgi Network (TGN)

The *trans*-Golgi network (TGN) is the terminal compartment of the Golgi stack and as well as being a major site of protein processing in the biosynthetic pathway it also acts a major sorting station of the cell. It co-ordinates the regulated export of proteins, lipids and membrane domains (see Gleeson *et al.* 2004 for review). The TGN gives rise to a multitude of membrane carriers which mediate both anterograde and retrograde trafficking pathways to the cell surface and to other organelles. It has also been shown that the TGN plays an important role in the endocytic trafficking pathways of many proteins e.g. furin and GLUT4 (Ralston & Ploug 1996, Farquhar & Palade 1998, Ramm *et al.* 2000, Shewan *et al.* 2003). A schematic representation of trafficking pathways to and from the TGN is shown in figure 1.10.

In order to fulfil its many varied roles it appears that the TGN has developed multiple domains arranged in numerous cisternae and so-called vesicle budding domains. Electron microscopy has revealed that these vesicle budding domains give rise to a number of different membrane trafficking intermediates including distinctly coated vesicles (e.g clathrin coated vesicles), uncoated vesicles and tubular extensions. Each vesicle budding domain appears to give rise to specific forms of each of these trafficking intermediates (Ladinsky *et al.* 1994, Marsh *et al.* 2001). The use of GFP-tagged Golgi proteins in live cell imaging studies have shown that the TGN membrane domains are very dynamic in nature, forming tubules which extend and retract continuously (Lippincott-Schwartz *et al.* 1998, Lippincott-Schwartz *et al.* 2000) as well as forming membrane carriers, vesicles and tubules which vary greatly in size and shape. These vesicles range from spherical structures which have diameters of ~ 200 nm right up to tubules which extend along microtubules for 100 μm or more (Hirschberg *et al.* 1998, Toomre *et al.* 1999) which are continuously leaving and rejoining the TGN.

Ultrastructural studies of the TGN membranes have revealed 'hot spots' of cargo export, termed cargo domains from which cargo-laden transport intermediates leave the TGN (White *et al.* 2001, Ladinsky *et al.* 2002). In these domains cargo proteins are segregated from resident proteins (Hirschberg *et al.* 1998) and basolaterally destined and apically destined proteins are also separated from each other (Keller *et al.* 2001, Jacob & Naim 2001, Rustom *et al.* 2002). The developing picture of TGN

protein sorting involves subdomains of the TGN in which cargo proteins are segregated and concentrated depending on the trafficking pathways into which it will be entered. These specific subdomains of the membrane would allow the recruitment of specific coat proteins to facilitate such specialised release processes.

Apart from the proteins from the biosynthetic pathway, proteins are known to enter the TGN from the endocytic trafficking compartments, specifically the endocytic recycling compartment (ERC), as in the case of TGN38 and GLUT4 or the late endosome, as in the case of CI-M6PR and furin (see section 1.6.7 below). These pathways have been fairly well characterised and are discussed in more detail above in the relevant sections.

Proteins which are characteristic for the TGN are the TGN resident proteins such as TGN46. Unfortunately as described above the majority of these resident proteins are excluded from some regions of the TGN, especially some of the more peripheral domains which may be more involved in endocytic protein trafficking. For these reasons, syntaxin6 may be used as a marker as it is thought to be universally distributed in the TGN, but especially present in the more peripheral TGN-derived endosomal trafficking compartments.

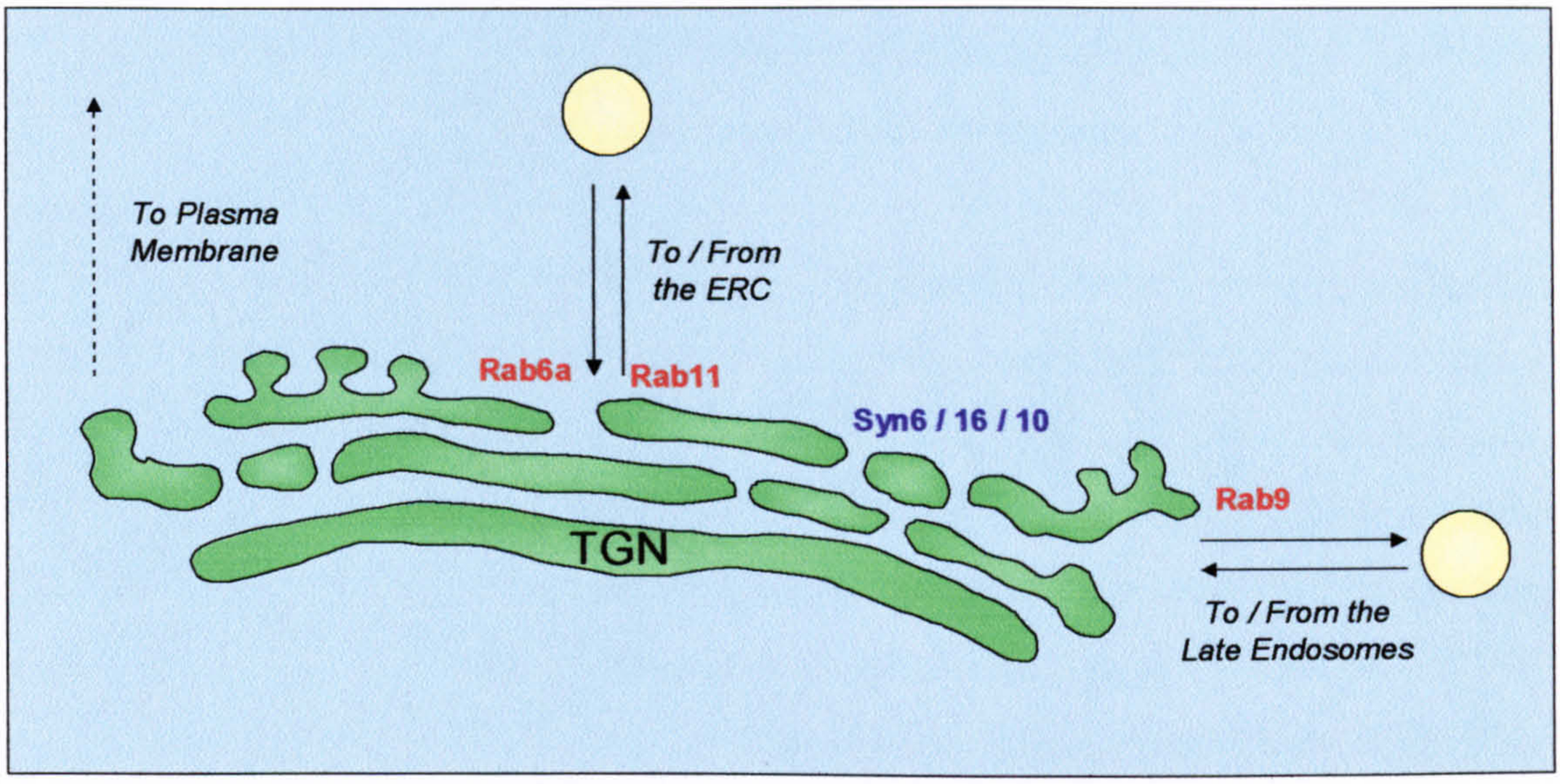

Figure 1.10 - *The trans-Golgi network.* The trafficking pathways to and from the TGN are depicted. The key regulatory proteins involved in trafficking are shown in red and the syntaxin isoforms associated with each compartment are shown in purple. The function of each compartment is described in more detail in section 1.6.6.

1.6.7 - Known endocytic trafficking itineraries

Figure 1.11 shows the trafficking pathways of a number of proteins and ligands whose endocytic itineraries are fairly well characterised. These are the iron transporter transferrin receptor (TfR), a *trans*-Golgi network resident protein TGN38, the low-density lipoprotein receptor (LDLR), the serine protease furin, the glucose transporter GLUT4 and the lysosomal protein chaperone the cation-independent mannose-6-phosphate receptor (CI-M6PR). Comparison of these endocytic trafficking pathways shows what diversity exists with the endocytic trafficking itineraries of endocytosed cell surface proteins (see Maxfield & McGraw 2004 for review).

At the cell surface, the transferrin receptor, LDLR and CI-M6PR bind their ligands, diferric transferrin, LDL and lysosomal enzymes respectively. They are then concentrated in the membrane and internalised via clathrin coated pits, the mechanism by which TGN38, furin and GLUT4 are also internalised. The internalised vesicles are first delivered to the sorting endosomes where the slightly acidic pH causes the majority of ligands to dissociate from their receptor, although in the case of TfR the Fe^{2+} dissociates from transferrin, but transferrin itself remains bound to the TfR. The majority of proteins including TfR, TGN38, LDLR, CI-M6PR and GLUT4 which lack certain targeting motifs are quickly removed from the sorting endosome and are either transported directly back to the cell surface or to the endocytic recycling compartment. Furin on the other hand, remains in the sorting endosome along with the dissociated ligands as the compartment matures into multi-vesicular bodies and late endosomes. From the late endosome furin is transported to the trans-golgi network (TGN) whereas the majority of ligands are transported to the lysosome. Those proteins which had been transported to the endocytic recycling compartment are also sorted to different destinations. The TfR and LDLR are returned back to the cell surface, whereas CI-M6PR, TGN38 and GLUT4 are transported to the TGN. Further sorting occurs once these proteins reach the TGN. CI-M6PR, which still has lysosomal enzymes bound, is translocated to the late endosome where, because of the acidic pH, lysosomal enzymes dissociate allowing the unbound CI-M6PR to recycle back to the TGN. GLUT4 is known to be translocated into a specialised insulin-responsive storage compartment. The exact nature of this compartment remains controversial, although it is thought that it consists of elements of both the TGN and

the early endosomal system. TGN38 is thought to largely remain in the TGN, except for a small proportion which is transported back to the cell membrane.

1.7 - Aims of the study

The overall magnitude of the current carried by K_{ATP} channels in any given cell is determined by both the open probability of the channel (P_o) and by the number of channels at the cell surface. The regulation of P_o has been fairly well characterised, but the factors responsible for regulating the cell surface density of the channel are, by comparison, poorly understood. The overall aim of the current study is to investigate the mechanism(s) that control the overall density of channels at the cell surface using cell biological and functional approaches and how these mechanisms are perturbed by genetic mutations that lead to congenital hyperinsulinism (CHI). Specific questions to be addressed include: (i) how glucose, the primary stimulant of insulin secretion, influences the channel density in pancreatic β-cells, (ii) how are the channels internalised from, and recycled back into, the plasma membrane, (iii) what is the pathway via which the channels move during the process of internalisation and recycling and finally, (iv) how genetic mutations that cause CHI affect the trafficking and / or function of the channel.

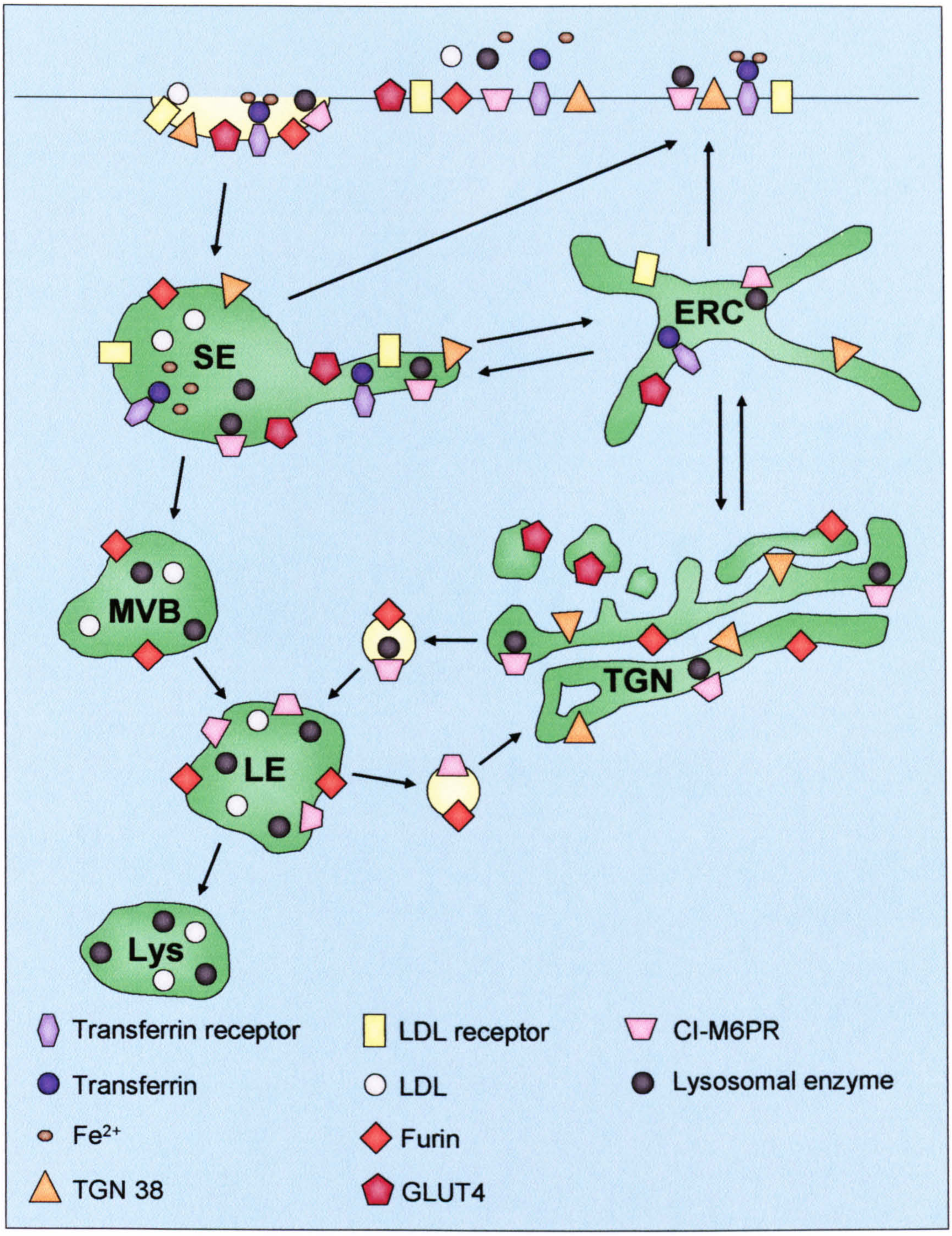

Figure 1.11 - *Endocytic trafficking pathways of well characterised cargo proteins and ligands.* The trafficking itineraries of several molecules are shown. See chapter 1.6.7 for further details. SE - Sorting Endosome, ERC - Endocytic Recycling Compartment, MVB - Multi Vesicular Body, LE - Late Endosome, Lys. - Lysosome, TGN - *trans*-Golgi Network.

Chapter 2

General methods

2.1 – Materials

Sterile deionised Milli-Q water (18 MΩ, Milli Pore), sterile tips, tubes and solutions were used whilst handling DNA and RNA. Plastics, glassware and heat stable solutions were sterilised by autoclaving. Heat labile solutions were filter sterilised using 0.2 μm Acrodisc PF filters (Gelman Science).

2.1.1 – Tissues

6-8 week old male BALB/c and C57bl6 mice for the isolation of pancreatic β-cells were obtained from Central Biomedical Services, University of Leeds. Female *Xenopus laevis* South African clawed frogs for the isolation of oocytes were also obtained from Central Biomedical Services, University of Leeds.

2.1.2 – Cell lines

Rin-m (rat insulinoma), COS7 (simian kidney epithelial), HEK (human kidney epithelial) cells were obtained from the European Cell Culture Collection (ECACC, Cambridge, UK). INS1 (rat insulinoma) cells were supplied as a kind gift from Dr G. Hardie (Dundee University, UK). Early and late passage INS1-e (rat insulinoma) cells were a kind gift from Dr C. Wollheim (University of Geneva, CH). HEK293-MSRII cells were a kind gift from Glaxo-SmithKline, UK. The HEK293-MSRII cells are a modified form of the HEK293 cell line which stably expresses the membrane bound macrophage scavenger receptor I. This allows these cells to adhere much more strongly to the growth surface which in turn allows more rigorous protocols to be carried out in these cells compared to standard HEK293 or tsA cells.

2.1.3 – Chemicals and solutions

General laboratory reagents and chemicals were purchased from Sigma, BDH and the Anachem Chemicals company unless otherwise stated. Isopropanol and ethanol were purchased from BDH. Radio-chemicals were purchased from ICN.

2.1.4 – Growth media

Bacto-tryptone and yeast extract were purchased from Amersham and Difco laboratories. Bacterial agar was purchased from Oxoid. Electrophoresis grade agarose was purchased from Life Technologies.

2.1.5 – DNA restriction and modification enzymes

Restriction endonucleases were purchased from, Promega, Boehringer Mannheim, New England Biolabs (NEB), Pharmacia or MBI Fermenters. *Pfu* DNA polymerase was purchased from Stratagene and *Taq* DNA polymerase from Promega. Calf intestine phosphatase (CIP) was purchased from Boehringer Mannheim. T4 DNA ligase and T4 DNA polymerase were purchased from NEB.

2.1.6 – Plasmid vectors

The mammalian expression vectors pcDNA3.1(+), pcDNA6/V5-HisA and pSport2 were obtained from Invitrogen / Life Technologies. The pKSglobin vector was constructed in the laboratory in order to allow expression of constructs in *Xenopus laevis* oocyte expression systems. This vector was contructed by inserting 5' and 3' untranslated regions (UTR) of the Xenopus β-globin gene either side of the multiple cloning site of pBluescriptKS. It has previously been shown the presence of the UTR sequences either side of the gene of interest can increase expression efficiency by ~300 fold in Xenopus oocytes. Plasmid maps are included as an appendix at the end of the thesis.

2.1.7 – cDNA clones

Hamster SUR1 (Genbank accession number L40624) was obtained from Dr J. Bryan (Baylor College of Medicine) and was subcloned into pcDNA6/V5-HisA (Hough 2000). Mouse Kir6.2 (Genbank accession number D50581) was obtained from Prof. S. Seino (Osaka, JP) (Baylor College of Medicine) and was subcloned into pcDNA3.1. The Human pEGFP-C2-TGN46 clone was provided by Dr S. Ponnambalam (University of Leeds). Mouse pEGFP-C2-EEA1 was kindly provided by Dr. H. Stenmark (Norwegian Radium Hospital, Oslo, Norway). Dog pEGFP-C1-Rab7 clones were obtained form Dr B. van Deurs (Copenhagen, DK) and Rat pEGFP-C1-Rme1 clones were obtained from Dr B. Grant (Reutgers University, NY, USA). Rat pEGFP-C2-Lamp1 clones were obtained from Dr P. Boquet (Institut National de la Sante et la Recherche Medicale, Nice, France). Rat pEGFP-C2-Rab4A clones were obtained from Dr M. Skidmore (Cornell University, NY, USA).

2.1.8 – Oligonucleotides

Oligonucleotide primers for the purposes of polymerase chain reaction (PCR), site-directed mutagenesis or DNA sequencing were made to order by Sigma-Genosys or

Invitrogen / Life Technologies. Primers were reconstituted in sterile Mili-Q to the concentration of 1nmol μl^{-1} for long term storage at -20°C.

The sequences of all oligonucleotides used in the current studies are shown in table 2.1.

Primer name	Primer sequence (5' - 3')
Rat SUR1 probe1 For	AGAAGACACGCAGGAAGGAA
Rat SUR1 probe1 Rev	CTGGAAGGCTGTTCCAGAAG
Rat SUR1 probe2 For	GCCTTCGCTGTCTACACCTC
Rat SUR1 probe2 Rev	CTGGAAGGCTGTTCCAGAAG
Kir6.2HAinsert For	TACCAGATTACGCTGGAGAGGGCACCAATGTGCCCT
Kir6.2HAinsert Rev	CGTCGTATGGGTAGGGGGCCAGGTCACCGTG
Kir6.2+11aa-insert For	TGGAGAAAGGCATCACGGACCTGGCCCCCTACCC
Kir6.2+11aa-insert Rev	TGTAAGCATAGATGTCACCGTGGGCGAAGGCGATG
Kir6.2deltaHF FOR	GATTCCTTGTCCTGAGCATCCGTTGAA
Kir6.2deltaHF REV	TTCAACGGATGCTCAGGACAAGGAATC
Kir6.2-W91R FOR	CCATGGTCTGGCGTCTCATCGCCTTCGC
Kir6.2-W91R REV	GCGAAGGCGATGAGACGCCAGACCATGG
Kir6.2-L147P FOR	ATGTCCCCTGGCCATCCCCATTCTCATTGTGCAGA
Kir6.2-L147P REV	TCTGCACAATGAGAATGGGGATGGCCAGGGGCAAT

Table 2.1 - *Sequences of oligonucleotides used during the current study.*

2.1.9 – Bacterial strains

For general procedures the XL-Blue (Stratagene) and DH-5α (Gibco BRL) *E.coli* strains were used. Strains were used for growth and propagation of plasmid DNA.

When grown in liquid media, *E.coli* cells were incubated in an orbital shaking-incubator at 200-250 rpm.

2.1.10 – Antibodies and labelling solutions

Anti-Kir6.2 antibodies were custom made by Sigma-Genosys. For Kir6.2, antibodies were raised in rabbits against an antigen peptide of the sequence EDPAEPRYRARQRRARFVSKK, corresponding to the intra-cellular N-terminal region between residues 19-39 of mouse Kir6.2 (Genbank accession number D50581). Anti-

SUR1 antibodies raised in rabbits against an antigen peptide of the sequence EEAAESEEDDNLSSVLHQRAK were custom made by Sigma-Genosys. This epitope corresponds to a region of the first intracellular loop between the first and second transmembrane domains (TMD0-TMD1) between residues 975-995 of hamster SUR1 (Genbank accession number L40624). Rat anti-HA antibodies (clone 3F10) were purchased from Roche Diagnostics. Mouse anti-HA alexafluor593-conjugated antibodies and FITC-conjugated transferrin were purchased from Molecular Probes. Other FITC and Cy3-conjugated secondary antibodies were purchased from Jackson ImmunoResearch. Sheep anti-TGN48 antibodies were provided by Dr S. Ponnambalam (University of Leeds). Mouse anti-cathepsin-D antibodies were purchased from DakoCytomation. Mouse anti-EEA1 antibodies and mouse anti-syntaxin6 antibodies were purchased from BD Pharmingen. Mouse anti-CI-M6PR antibodies were purchased from Abcam. FITC-conjugated Wheat-germ agglutinin and FITC-conjugated dextran were obtained from Sigma Drugs Company.

2.1.11 - Pharmaceutical agents

The translation inhibitor cycloheximide was purchased from ICN biomedicals and was stored as 25 mg ml^{-1} stocks in ethanol at -20°C. The transcription inhibitor actinomycin-D was purchased from Sigma and was stored as 5 mg ml^{-1} in ethanol at 4°C. The transcription inhibitor α-amanitin was purchased from Calbiochem and was stored as 10 mg ml^{-1} stocks in DMSO at -20°C. The PKC activator phorbol-12-myristate-13-acetate (PMA) was obtained from Calbiochem and was stored as 1.62 mM stocks (10 mg ml^{-1}) in DMSO at -20°C. The PKC antagonist chelerythrine chloride was purchased from Sigma and was stored as 26 mM stocks (10 mg ml^{-1}) in DMSO at -20°C. G418 (geneticin) was purchased from Sigma Drugs Company and was stored as 400 mg ml^{-1} stocks in water at -20°C. Blasticidin was obtained from Invitrogen Lifetechnologies and was stored as 5 mg ml^{-1} stocks in DMSO at -20°C. The K_{ATP} channel opener diazoxide was obtained from Sigma and was stored as 200 mM stocks in DMSO. The sulphonylurea glibenclamide was obtained from ICN biomedicals and was stored as 1 mM stocks in DMSO. The metabolic poison sodium azide was obtained from Sigma and was stored as 3M stocks in water. The translational inhibitor cycloheximide was purchased from ICN biomedicals and was stored as 25 mg ml^{-1} stocks. All stocks were stored as small aliquots at -20°C.

2.2 – General solutions

2.2.1 – Antibiotic solutions

Antibiotic solutions were used to supplement bacterial growth media in order to maintain the growth of plasmid and to enable the selection of antibiotic-resistant bacteria.

Ampicillin

A stock solution of ampicillin was made to 50 $mg.ml^{-1}$ in Milli-Q, filter-sterilised (0.2 µm filter, Acrodisc), aliquoted into Eppendorf tubes and stored at -20°C.

Kanamycin

A stock solution of kanamycin was made to 25 $mg.ml^{-1}$ in Milli-Q, filter-sterilised (0.2 µm filter, Acrodisc), aliquoted into Eppendorf tubes and stored at -20°C.

2.2.2 – Bacterial growth media

Bacteria can be maintained with either solid or liquid media, depending on the application

Solid media

Solid media are used when the growth of bacterial colonies is required.

2YT-agar selection plates

Agar (1%) was suspended in 2YT (2X yeast-tryptone) and the suspension was sterilised by autoclaving at 115 °C for 20 minutes. The medium was cooled to approximately 55°C, the appropriate antibiotic added to the desired concentration (see table 2.2) then poured into sterile Petri dishes and allowed to set. The plates were then stored for up to one month at 4°C. Before use, the plates were pre-warmed to 37°C for optimal growth of bacterial colonies.

Antibiotic	**Final concentration (µg ml^{-1})**
Ampicillin	50
Kanamycin	30

Table 2.2 - *Selection antibiotics for 2YT-agar plates.*

Liquid media

Liquid media are used when bacterial cultures are required for DNA isolation protocols.

LB medium (Luria-Bertani medium), pH 7.0

Bactotryptone	10 g
Bacto yeast extract	5 g
NaCl	10 g

The reagents above were added to 950 ml of distilled water, or Milli-Q, and the pH was adjusted by the addition of 10 M NaOH. The volume was then made up to 1 L with distilled water and autoclaved at 115°C for 20 min. The media was stored at room temperature.

2YT medium

Bacto-tryptone	16 g
Bacto yeast extract	10 g
NaCl	5 g

The components above were dissolved in 900 ml water and the solution was adjusted to pH 7.0 with NaOH. The volume was made up to 1 L with water and was then sterilised and stored as described above. Alternatively, 2YT medium was made by dissolving 31g of 2YT powder (Difco) in 1L of distilled water followed by sterilisation and storage as described above.

Bacterial storage medium

For long-term storage of bacterial cultures, 0.15 ml of sterilised glycerol was added to 0.85 ml of an overnight bacterial culture. Cultures were stored at -80°C. In order to recover the bacteria, the vial was removed from storage and a sample streaked across the top of a 2YT-agar plate containing the necessary antibiotics and grown at 37°C overnight.

2.2.3 – Mammalian cell culture medium

Media for COS7and HEK293 cells

COS7 and HEK293 cells were cultured in DMEM media supplemented with L-glutamine (conc), $NaHCO_3$ (conc), 10 % heat inactivated fetal bovine serum, 100 U ml^{-1} penicillin and 100 µg ml^{-1} streptomycin.

Media for INS, INS-1e, RIN and primary β- cell lines

INS and INS1e cells were cultured in RPMI 1640 media supplemented with 10 % heat inactivated fetal bovine serum, 10 mM HEPES, 2 mM glutamine, 1 mM sodium pyruvate, 50 µM β-mercaptoethanol, 1nM glucagon-like peptide 1 (GLP-1), 100 U ml^{-1} penicillin and 100 µg ml^{-1} streptomycin.

Media for HEK293-MSRII cells

HEK293-MSRII cells were cultured in DMEM / F-12 media supplemented with 10 % fetal bovine serum, 2.56 mM glutamax, 15 mM HEPES and 400 µg ml^{-1} G418.

2.2.4 – Solutions for DNA preparation

For mini-plasmid preparations (mini-prep)

All solutions below are sufficient for 12 preparations. All stock solutions are prepared as described by Sambrook and Russell (2001).

Solution A (Prepare immediately before use)

H_2O	2.8 ml
Tris-EDTA (100x)	75 µl
Glucose (2M)	75 µl
Lysosome	50 µl

Solution B (prepare immediately before use)

H_2O	4.5 ml
SDS (10%)	0.5 ml
NaOH (10M)	100 µl

Solution C (prepare immediately before use)

Ammonium Acetate (7.5M)	5 ml
RNase (10mg/ml)	25 µl

For large-scale plasmid preparations

Where possible, the stock solutions used should be sterile. All stock solutions have been made as described in Sambrook and Russell (2001).

Solution 1

Glucose	9 g
Tris; pH 8.0 (1M)	12.5 ml
EDTA (0.5M)	10 ml
H_2O	475 ml

Solution 2 (prepare fresh)

NaOH (10M)	1.6 ml
SDS (10%)	8.0 ml
H_2O	70.4 ml

Solution 3 (3M potassium acetate pH 5.2)

Potassium acetate	147 g
Acetic Acid	58 ml

2.2.5 – Electrophoresis solutions

Solutions for agarose gel electophoresis

The following solutions are used to examine DNA samples by agarose gel electrophoresis.

Tris-acetate-EDTA (TAE) gel running buffer (50 X stock)

Tris-base	242 g
Glacial acetic acid	57.1 g
0.5 M EDTA (pH 8.0)	100 ml
Distilled water to 1L	

This stock solution is diluted 50 X (to make 1 X buffer) in distilled water before use and is used to make and run all agarose gels

6X DNA gel-loading buffer (pH 8.0)

0.25% bromophenol blue

1 mM EDTA (pH 8.0)

30% glycerol in water

0.25% xylene cyanol FF

Polyacrylamide gel electrophoresis (SDS-PAGE)

The following solutions are used to examine protein samples via SDS-polyacrylamide electrophoresis.

Resolving gels

The constituents of SDS-polyacrylamide gels vary depending on the required percentage, typically between 5 – 15 %. The resolving gels used to separate K_{ATP} channels subunits were prepared as 5 - 15 % gradient gels and were poured using a peristaltic pump attached to a gradient maker (home-made). The volumes shown below are sufficient to pour one gel using the Amersham Hoeffer gel casting kit.

Resolving gel	*5 %*	*15 %*
Water	1.15 ml	0 ml
30 % acrylamide	0.38 ml	1.15 ml
75 % glycerol	0.15 ml	0.52 ml
1.5 M Tris (pH8.8)	0.58 ml	0.58 ml
10 % SDS	23 µl	23 µl
10 % ammonium persulphate	23 µl	23 µl
TEMED	2 µl	2 µl

5 % Stacking gel

Water	1.4 ml
30 % acrylamide + N.N'methylenebisacrylamide (BDH)	330 µl
1.5 M Tris-CI (pH 6.8)	250 µl
10 % SDS	20 µl
10 % Ammonium persulphate	20 µl
TEMED	2 µl

SDS-PAGE running buffer

25 mM Tris-Cl (pH 8.3)

250 mM glycine

0.1 % SDS

2X alkaline SDS sample buffer (β-mercaptoethanol free)

25 mM sodium bicarbonate (pH 10.4)

4 % SDS

0.2 % bromophenol blue

20 % glycerol

Coomassie blue stain

0.25 % Coomassie Brilliant Blue R250

45 % methanol

10 % acetic acid

De-stain solution

30 % methanol

10 % acetic acid

Salicylic acid solution

1M salicylic acid in water

2.2.6 – Reagents for making competent cells

Transformation buffer (pH 6.7)

PIPES	10 mM
$MnCl_2$	55 mM
$CaCl_2$	15 mM
KCl	250 mM

This was prepared in Milli-Q.

2.2.7 – Other commonly used molecular biology buffers

10 X Phosphate buffered saline (PBS)

PBS was made by dissolving PBS tablets (Gibco BRL) in Mili-Q water, as per manufacturers' instructions.

Tris-Cl EDTA, pH 7.5 ($TE^{7.5}$)

10 mM Tris-Cl (pH 7.5)

1 mM EDTA

Tris-Cl EDTA pH 8.0 ($TE^{8.0}$)

10 mM Tris-Cl (pH 8.0)

1 mM EDTA

GENECLEAN™ NEW Wash buffer

10 mM Tris-Cl, pH 8.0

2.5 mM EDTA

100 mM NaCl

50 % ethanol

2.2.8 – Solutions for immunocytochemistry

2% Paraformaldehyde (PFA)

Dissolve 0.5 g of paraformaldehyde in 1 ml of 0.05M NaOH at 60°C. When dissolved add 50 µl of 1M HCl, 0.5 ml of 10 X PBS and 3.45 ml of Mili-Q water.

2.3 – General molecular biology methods

2.3.1 – Competent cell preparation

E. coli cells have the capacity to take up foreign DNA. Competent cells are chemically treated bacterial cells capable of taking up plasmid DNA when 'shocked' with an appropriate stimulus such as heat. Competent cells were prepared in the laboratory using the protocol by Inoue *et al* (1991). A glycerol stock (80 % culture, 20 % glycerol) of DH5α or XL blue cells (GibcoBRL, Life Technologies) was streaked on a LB plate and

incubated overnight at 37°C. One colony from this plate was then streaked onto another plate and incubated overnight at 37°C. 200 ml SOB medium was inoculated with 10-12 colonies from this second plate. The cells were incubated (room temperature, 200 rpm) until the A_{600} (absorbance at 600 nm) reached 0.6. The cells were chilled for 10 min on ice prior to being centrifuged (Beckman JA10 rotor, 4000 rpm, 4°C for 10 min) and allowed to come to rest without the use of the brake. 16 ml of ice-cold TB was added to the pellet and the cells were chilled on ice for a further 10 min before being re-centrifuged as above. The supernatant was decanted and the cell pellet resuspended in 16 ml TB, 1.2 ml DMSO (final concentration of 7 %) was then added dropwise and the cells kept on ice for a further 10 min. Cells were frozen in dry ice and then stored in 1 ml aliquots at –80°C. Cells with a competency of $>10^7$ colonies / µg DNA were used in subsequent procedures. The competency of the cells was tested by transforming 1 pg of control DNA template (as described in 2.3.2) into 100 µl of *E.coli* cells and is calculated, by describing the number of colonies per microgram of transformed DNA (cfu μg^{-1}). Typical cell competency is 1 X 10^7 cfu μg^{-1}.

2.3.2 – Transformation of *E.coli* with plasmid DNA

For each transformation 100 µl of competent cells were slowly thawed on ice. 1 - 10 µl of DNA (25 – 50 ng) was added and gently mixed and incubated on ice for 30 minutes. The cells were then 'heat-shocked' at 42°C in a water bath for 40 seconds and then placed on ice for a further 2 minutes. 900 µl of LB medium was then added to the cells and they were placed in a 37°C shaking incubator for 1 hour. The cells were then pelleted by centrifugation at 7K rpm and 900 µl of the supernatant discarded. The pellet was then resuspended into the remaining media and plated onto pre-warmed 2YT-agar plates (containing appropriate selection antibiotics) with a sterile glass spreader. The inoculated plates were then placed in a 37°C incubator overnight to allow growth.

2.3.3 – Preparation of plasmid DNA

The alkaline-lysis method was employed for isolating plasmid DNA from bacterial cells. The method is a modification of the technique described by Birnboin and Doly (1979); Ish-Horoweiz and Burke (1991).

Mini-preparation of DNA

5 ml of 2YT or LB medium supplemented with appropriate selection antibiotics was inoculated with a single bacterial colony transformed with the plasmid DNA to be purified and incubated overnight at 37°C in a shaking incubator. 1.5 ml of the culture was centrifuged (bench top microfuge, 4400 g, RT, 1 min) and the supernatant discarded. The pellet was resuspended in 200 µl of miniprep solution A and incubated at RT for 5 min. Cells were lysed by addition of 400 µl of miniprep solution B, gently mixed and incubated at room temperature for a further 5 min. Next, 300 µl of miniprep solution C was added and the preparation incubated on ice for 10 min before centrifugation (bench top microfuge, 16000 g, RT, 15 min). The supernatant was decanted into a fresh tube, 600 µl isopropanol added and the mixture incubated at RT for 10 min prior to re-centrifugation (as above). The supernatant was discarded, the pellet washed with 70 % ethanol, dried and resuspended in 40 µl TE 8.0. 1 µl of the resulting isolated DNA was then examined by agarose gel electrophoresis.

Large-scale preparation of DNA

5 ml of 2YT or LB media supplemented with appropriate antibiotics was inoculated with a single bacterial colony from a plate transformed with the plasmid DNA to be isolated. This starter culture was grown for 16 hrs at 37°C in a shaking incubator. This start culture was added to 400 ml 2YT containing appropriate selection antibiotics and grown at 37°C in a shaking incubator for a further 16-24 hrs. The cell suspension was centrifuged (Beckman JA10 rotor, 4400 g, 4°C, 15 min). The supernatant was decanted and the cell pellet resuspended in 10 ml of solution 1. The cells were lysed by addition of 20 ml of solution 2, gently mixed for approximately one minute and incubated on ice for a further 10 min. 10 ml of solution 3 (4°C) was added and the preparation incubated on ice for 5 min prior to centrifugation (as above). The supernatant was filtered through a clean filter paper, then 50 ml of isopropanol was added and the mixture re-spun (as above). The supernatant was decanted and the pellet dried. The pellet was resuspended in 2 ml TE 8.0, 50 µl RNAse A (10 mg ml^{-1} stock) added and the solution incubated at 37°C for 30 min. Plasmid DNA was purified by organic extraction, once each with phenol then phenol-chloroform and twice with chloroform and precipitated by addition of 0.5 ml 20 % PEG 8000 and 25 µl 1 M $MgCl_2$. The DNA was pelleted by centrifugation (bench top microfuge, 16000 g, RT, 15 min), washed twice with 70 % ethanol, air-dried, and

dissolved in TE 8.0. The DNA concentration was estimated by agarose gel electrophoresis

2.3.4 – Purification of DNA

GENECLEAN™ protocol

In order to isolate a particular DNA fragment from a mixture, samples were first separated by agarose gel electrophoresis. The separated DNA fragments were visualised on a UV transilluminator and the band corresponding to the fragment of interest was carefully excised using a clean scalpel blade. The gel fragment, containing the DNA of interest, was then dissolved in 3 X volumes of 6M NaI by heating in a 55°C water bath. Once dissolved 10 µl of EZ GLASSMILK™ was added and incubated at room temperature with thorough mixing by rotation. The EZ GLASSMILK™ was then pelleted by brief centrifugation (16000 g, RT) and the supernatant discarded. The EZ GLASSMILK™ pellet was then washed twice in 200 µl volumes of ice-cold New-wash buffer by resuspension and brief centrifugation (as above). Following the second wash in New-wash buffer the EZ GLASSMILK™ pellet was washed twice in ice-cold 70 % ethanol as above. Following the second ethanol wash the EZ GLASSMILK™ pellet was dried and resuspended in 10 µl of Mili-Q. DNA was eluted from the EZ GLASSMILK™ by incubation for 15 minutes in a 55°C water bath. Following centrifugation the supernatant (containing DNA) was transferred into a fresh tube and centrifuged again as above to remove any remaining traces of EZ GLASSMILK™. An aliquot of the DNA was examined by agarose gel electrophoresis.

Phenol-chloroform extraction of DNA

Phenol-chloroform extraction of DNA can be used to remove protein contamination from DNA samples, which might interfere with DNA modification or transfection experiments.

The DNA sample to be cleaned was made up to a volume of 200 µl and then thoroughly mixed with an equal volume of phenol. This was then centrifuged (16000 g, RT, 5 min). The upper, aqueous layer was carefully transferred, avoiding the protein interface, to a fresh tube and an equal volume of phenol-chloroform-isoamyl alcohol (50:48:2 v/v) was added. Following centrifugation, as above, the upper layer was again carefully transferred to a fresh tube and an equal volume of chloroform-isoamyl alcohol (48:2 v/v)

was added. Following centrifugation, the upper layer was again carefully removed and treated for a second time with chloroform-isoamyl alcohol (48:2 v/v) as above. Following the final centrifugation, the aqueous layer was transferred to a fresh tube and 30 µl of 3M sodium acetate (pH 5.2) were added, followed by 2.5 volumes of ethanol. The mixture was then incubated at -20°C for 30 minutes, and the DNA was then pelleted by centrifugation, washed with ice-cold 70% ethanol and dried. The DNA pellet was then redissolved in 10 µl of Milli-Q and an aliquot examined by agarose gel electrophoresis.

Purification of DNA in aqueous solution by guanidium thiocyanate

To the DNA sample, to be purified, five volumes of denaturation solution (see below) and 10µl of GLASSMILK™ was mixed and incubated at room temperature for 10 min. The rest of the protocol was as the GENECLEAN™ protocol (section 2.3.4).

Denaturation solution contains 6 M guanidium thiocyanate, which was made in DMSO containing 0.7% of 2-mercaptoethanol and stored in 1 ml aliquots at -20°C. This method is particularly good for purification of linearised DNA templates for RNA synthesis, as an alternative to phenol/chloroform extraction.

DNA precipitation

Isopropanol or ethanol can be used for precipitating DNA (and RNA) in solution. To the solution containing the DNA, 2.5 volumes of ethanol (or 0.6 volumes of isopropanol) and 0.1 volume of 3 M NaOAc (pH 5.2) were added, vortexed and incubated for at least 1 h at -20°C. The DNA was then pelleted by centrifuging at 16000 g for 15 min and the supernatant discarded. 0.5 ml of 70% ethanol (-20°C) was then added to the wet pellet and centrifuged as above. The supernatant was discarded and the pellet dried at room temperature or 37°C. The pellet was then dissolved in the appropriate volume of $TE^{8.0}$ or Milli-Q. A sample of the DNA was then examined by agarose gel electrophoresis.

2.3.5 – In vitro transcription

cRNA was transcribed from linearised DNA under the T7 promoter. Linearised DNA was obtained either by restriction endonuclease digestion at the 3' end of the insert to be transcribed or by PCR based isolation of the insert and promoter sequences where no suitable restriction sites are available. The DNA template was cleaned by the guanidium

thiocyanate method (2.3.4.3) followed by isolation by the GENECLEAN™ protocol (2.3.4). DNA was eluted from the EZ GLASSMILK™ into RNase free water. Capped cRNA was transcribed in vitro using the T7 MEGAscript kit (Ambion) along with $m^7G(5')ppp(5')G$ cap analog (Ambion) according to manufacturers instructions. An aliquot of the finished cRNA was examined by agarose gel electrophoresis.

2.3.6 – Agarose gel electrophoresis of DNA

Gel preparation

For most purposes 1 % agarose gels proved sufficient. For this, 100ml of 1 X TAE buffer is added to 1g of electrophoresis grade agarose and heated until dissolved. The molten gel was allowed to cool to ~ 60°C and 5µl of 10mg ml^{-1} ethidium bromide was added and mixed by swirling. The gel was then poured into a mould and allowed to set.

Sample preparation and electrophoresis

6 X loading buffer was added to the DNA sample(s) to be examined to a final concentration of 1 X and the samples mixed by resuspension. The pre-cast agarose gel was placed into the gel electrophoresis tank and barely covered in 1 X TAE buffer. The DNA samples were loaded into individual wells and electrophoresed at 90 V for ~ 50 minutes. For estimation of sample DNA size marker DNA fragments were run alongside. Following electrophoresis, DNA fragments were visualised on either a UV-transilluminator or a Bio-Rad gel documentation system.

2.3.7 – Subcloning of DNA

It is sometimes necessary to take a gene of interest from one plasmid expression vector and insert it into another in order to allow expression of the gene in different expression systems. This process, termed subcloning, is a multi-stage process. Firstly the gene of interest is isolated from the parent plasmid vector by restriction endonuclease digestion and purified by the GENECLEAN protocol. Secondly the recipient plasmid vector is restricted by endonuclease digestion, ideally so it is left with 5' and 3' ends complementary to those of the gene of interest. Its ends are then dephosphorylated and finally the recipient vector is purified.

Restriction of DNA

DNA to be restricted was digested with the appropriate enzyme using conditions recommended by the manufacturer. For analytical digestions, approximately 1-2 µg of DNA was digested for 3 hours in a total volume of 30 µl with 5-10 U of restriction enzyme at 37°C. For preparative digestions, 5-10 µg of DNA was digested in a 30-50 µl final volume with 10-20 U of restriction enzyme overnight at 37°C.

Dephosphorylation of plasmid vector DNA

Dephosphorylation prevents self-ligation and recircularisation of the restricted vector DNA, thereby improving ligation efficiency. Prior to dephoshporylation, DNA restrictions were performed in a volume of 30 µl. To this, 5 µl of 10X calf intestinal phosphatase (CIP) buffer, 10 µl of Milli-Q water and 5 µl (5U) of CIP were added, mixed and incubated at 45°C for 2 hours. CIP was inactivated by addition of 0.5 M EDTA and incubation at 45°C for 10 min. Dephosphorylated DNA was then subjected to the guanidium thiocyanate purification.

Ligation of DNA fragments

Estimations of the quantity of vector and insert DNAs were made from the intensity of bands upon agarose gel electrophoresis. Typical ligation reactions comprised a 3:1 molar ratio of vector: insert DNA, 1 µl of 10x ligation buffer and 1 µl (1U) of T4 DNA ligase in a 10 µl reaction. The reaction was performed at room temperature for 2 hours and immediately transformed into competent *E.coli*. Control ligations included vector and insert alone.

Subcloning of Kir6.2 constructs

Kir6.2-HA+11aa-HMKFLAG was subcloned into the BamHI / EcoRI sites of each plasmid vector as shown in figure 2.1.

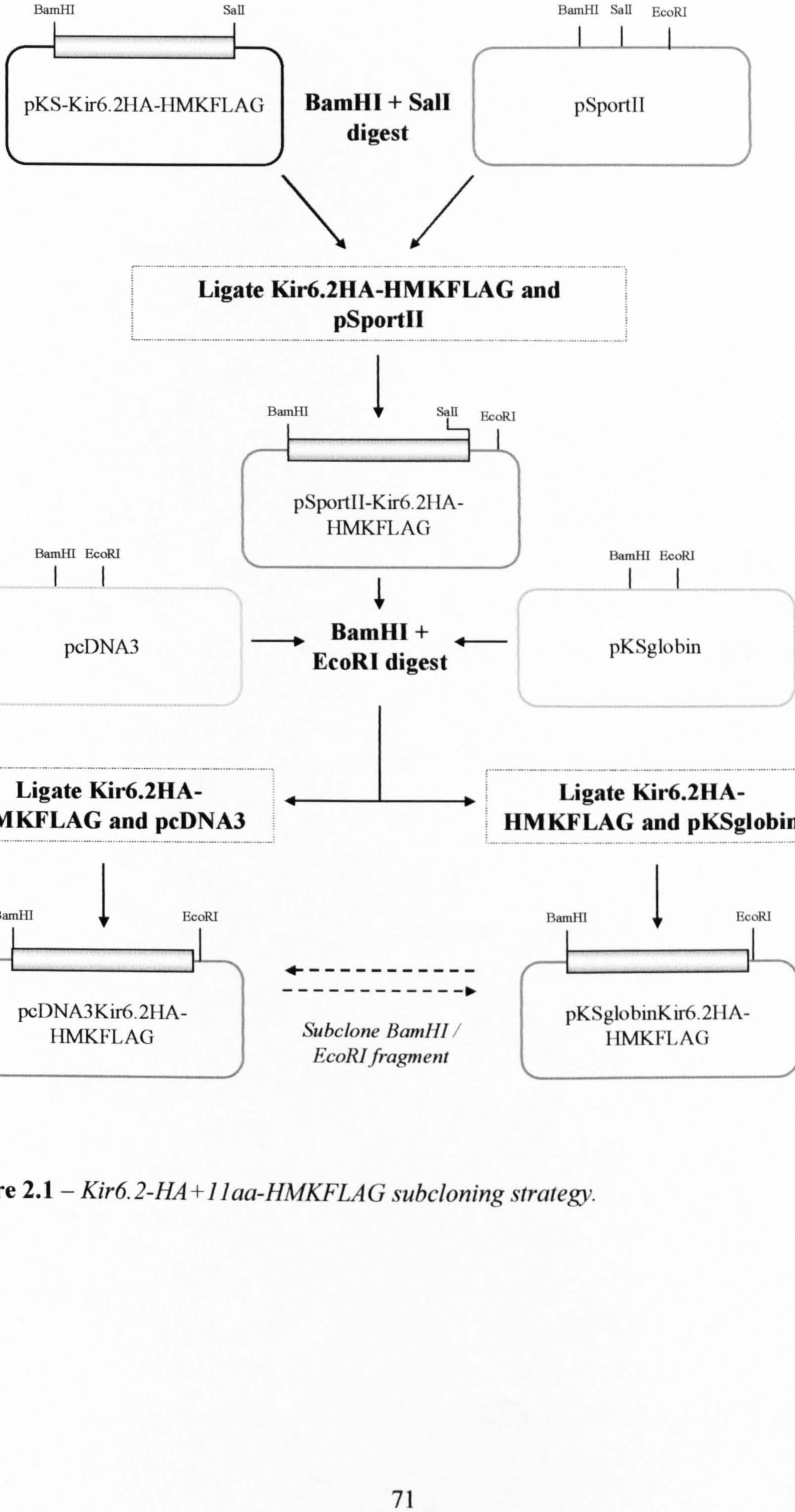

Figure 2.1 – *Kir6.2-HA+11aa-HMKFLAG subcloning strategy.*

2.3.8 – Polymerase chain reaction (PCR)

PCR has many diverse applications that can be applied to numerous tasks in the laboratory. The following protocol can be used in analytical investigations such as checking the orientation of DNA inserts following ligation, or as a preparative tool as in the isolation of linearised templates for in vitro cRNA transcription, the generation of gene fragments or gene specific probes to be used in further studies.

PCR reactions were performed in 0.5 ml PCR tubes at a total volume of 50 µl per reaction. For each reaction 1 – 50 ng of template DNA was required. Together with the template DNA, each reaction consisted of 10 pmol each of the forward and reverse primer, 200 µM dNTP's mixture, 1 X cloned *pfu* Turbo DNA polymerase buffer (Stratagene) and 1 µl (2.5U) cloned *pfu* Turbo DNA polymerase (Stratagene). Each reaction was then overlaid with 40 µl mineral oil. We have used *pfu* Turbo DNA polymerase in preference to *Taq* DNA polymerase because it has a 3' – 5' "proof-reading" activity which results in the high-fidelity replication of DNA. Typically, PCR reactions were pre-heated to 95°C prior to addition of the DNA polymerase (hot-start). Annealing temperatures for this type of PCR is calculated from the following formula:

69.3 + (0.41 X %GC base content) – 650/L (where L = length of primer in bases)

All PCR reactions were performed using either a Perkin-Elmer DNA thermal cycler or a Hybaid Omn-E PCR block

Insertion of the HA epitope into pKS-Kir6.2-HMKFLAG

The HA antibody epitope was inserted into Kir6.2 by an insertion PCR based protocol as is shown in figure 2.2. The DNA template used for HA insertion was pKS-Kir6.2-HMKFLAG. Prior to the insertion PCR reaction the oligonucleotide primers (Kir6.2HAinsert For and Kir6.2HAinsert Rev) were kinased. The PCR reaction comprised 25pmol kinased oligonucleotides, 1 x *pfu* DNA polymerase reaction buffer, 200 µM dNTP's mixture, 10 % glycerol, 25 ng template DNA and 2.5 U *pfu* DNA polymerase. Each reaction was overlaid with mineral oil and subjected to the following reaction parameters: 95°C for 40 seconds, 58°C for 1 minute and 72°C for 10 minutes. Following 30 cycles of these parameters, the DNA was finally extended for 7 minutes at 72°C. Following completion of the reaction, the PCR product was treated with DpnI restriction endonuclease (1 hour, 37°C), and then the main product isolated by the GENECLEAN™ method. Following isolation the product was transformed into *E.coli*

and DNA prepared by the mini-prep protocol and checked by restriction with BamHI and HindIII. Samples showing the correct digestion pattern were examined for correct insertion by DNA sequencing with T7 primers.

Production of pcDNA3-Kir6.2-HA+11aa-HMKFLAG

The 11 amino acid linker region (+11aa) was inserted into Kir6.2-HA by an insertion PCR based protocol and is shown in figure 4.2. The DNA template used for +11aa insertion was pcDNA3-Kir6.2-HA-HMKFLAG. Prior to the PCR reaction the oligonucleotide primers (Kir6.2+11aa-insert For and Kir6.2+11aa-insert Rev) were kinased. The PCR reaction comprised 25pmol kinased oligonucleotides, 1 x *pfu* DNA polymerase reaction buffer, 200 μM dNTP's mixture, 10 % glycerol, 25 ng template DNA and 2.5 U *pfu* DNA polymerase. Due to problems associated with a large amount of non-specific oligonucleotide binding, a touchdown PCR method was employed in an attempt to improve oligonucleotide binding specificity. Each reaction was overlaid with mineral oil and subjected to the following reaction parameters: 95°C for 40 sec, 65°C for 1 min and 72°C for 10 min for 2 cycles; 95°C for 40 sec, 63°C for 1 min and 72°C for 10 min for 2 cycles; 95°C for 40 sec, 61°C for 1 min and 72°C for 10 min for 2 cycles; 95°C for 40 sec, 59°C for 1 min and 72°C for 10 min for 16 cycles. The reactions were finally extended for 7 min at 72°C followed by treatment with DpnI restriction endonuclease (1 hour, 37°C), and then the main product isolated by the GENECLEAN™ method. Correct insertion of the +11aa linker sequence was confirmed by DNA sequencing using T7 primers.

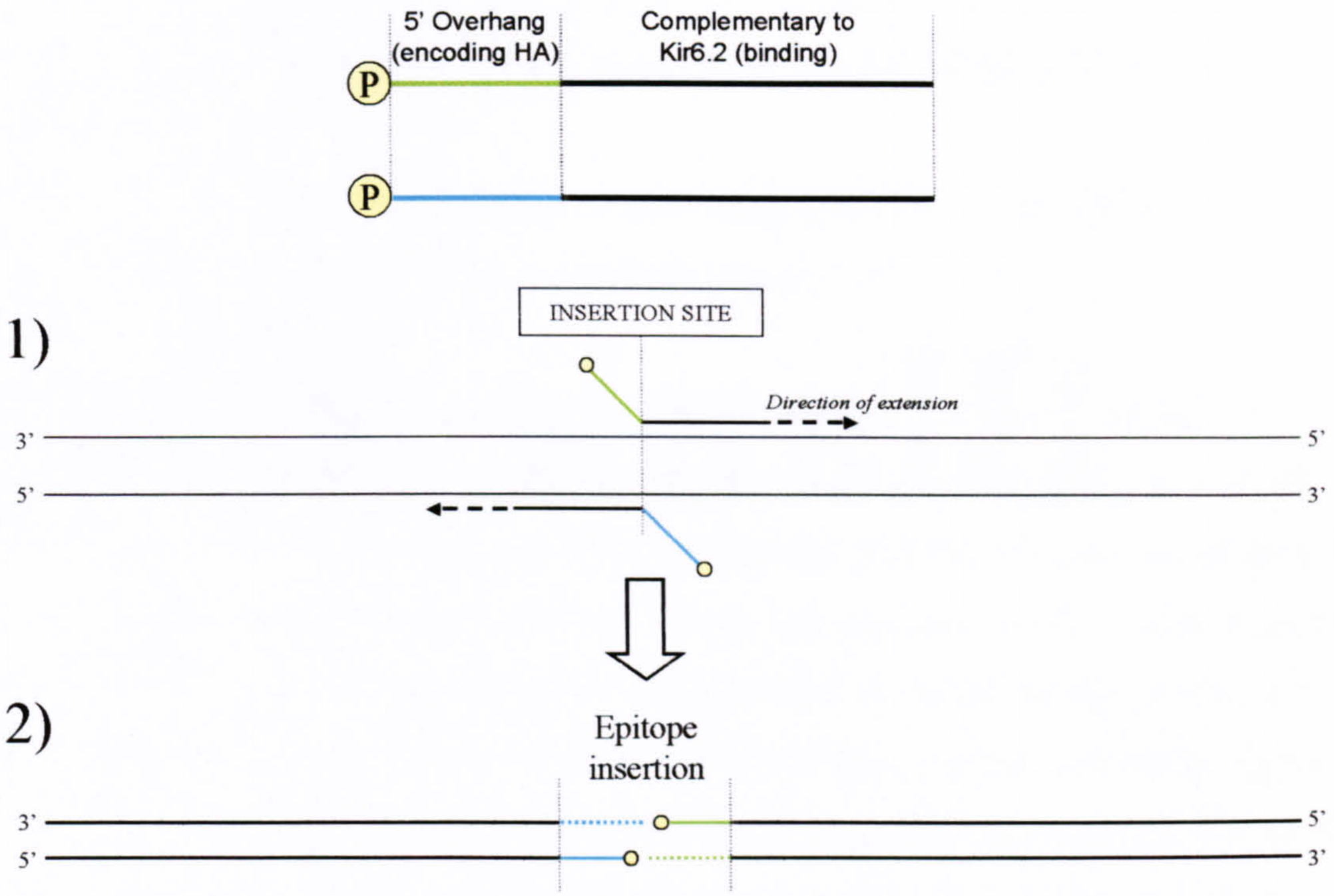

Figure 2.2 – *Epitope insertion strategy.* Insertion PCR primers with 5' overhanging ends encoding for half each of the inserted sequence were designed to bind directly either side of the insertion site. Prior to PCR primers were 5' phoshorylated (yellow circles). Binding of primers (1) would, following several rounds of PCR, eventually lead to insertion of the full epitope (2).

2.3.9 - QuikChange™ mutagenesis

Site directed mutagenesis was performed using the QuikChange™ method developed by Stratagene and primers were designed accordingly. Primers were required to be between 25-40 bases in length and have a melting temperature of ~ 10°C above the standard extension temperature of 68°C. Melting temperatures were calculated using the formula:

$$T_m = 81.5 + 0.41(\%GC) - 675/N - \%\ mismatch$$

Where *N* is the primer length in base pairs, %GC is the overall guanine and cytosine content.

Finally, the desired mutation (deletion or insertion) should be in the middle of the primer with ~10-15 bases of correct sequence on both sides.

Each reaction contained 1µl of DNA template (150 ng/µl^{-1}) with 1µl of forward primer (10 pmol/µl^{-1}), 1µl reverse primer (10 mol/µl^{-1}), 5 µl of 2 mM dNTP's, 5µl of 10X *Pfu* reaction buffer, and 1µl of *Pfu* Turbo DNA polymerase (2.5 U/µl^{-1}) and was made up to a final volume of 50 µl with sterile Mili-Q. Each reaction was overlaid with mineral oil (Fluka), placed in a DNA thermal cycler and subjected to the following parameters: 95°C for 30 seconds (denaturation stage) followed by 55°C for 1 minute (annealing stage), and 68°C (elongation stage). The duration of the elongation stage depended on the length of the template, with each 1000 base pairs of template requiring 2 minutes of extension time. Following 16 cycles of these parameters, the DNA was finally extended for 7 minutes at 72°C. Following the end of the PCR each sample was treated with 1 µl of DpnI restriction endonuclease (20U) for 1 hour at 37°C in order to digest the parental supercoiled DNA. The PCR products were then transformed into competent XL blue cells.

Construction of Kir6.2-HA+11aa-ΔHMKFLAG

For the construction of Kir6.2-HA+11aa-ΔHMKFLAG a stop codon was inserted into the sequence of pcDNA3.1(+)-Kir6.2-HA+11aa-HMKFLAG directly following the final codon of Kir6.2 via Quikchange site-directed mutagenesis. This resulted in the loss of HMKFLAG from the C-terminus of the Kir6.2 subunit. The mutagenesis reaction comprised: 1µl of DNA template (150 ng µl^{-1}) with 1µl of forward primer (10 pmol µl^{-1}), 1µl reverse primer (10 mol µl^{-1}), 200 µM dNTP's, 1X *Pfu* reaction buffer, and 2.5U of *Pfu* Turbo polymerase and was made up to a final volume of 50 µl with sterile Mili-Q.

Each reaction was overlaid with mineral oil (Fluka), placed in a DNA thermal cycler and subjected to the following parameters: 95°C for 30 seconds (denaturation stage) followed by 55°C for 1 minute (annealing stage), and 68°C (elongation stage). Following completion of the reaction the product was treated with *DpnI* restriction endonuclease for 1 hour at 37°C before transformation into XL-blue competent cells. Plasmid DNA was then amplified from transformed colonies and isolated by the mini-preparation protocol. Correct insertion of the stop codon was confirmed by DNA sequencing.

2.3.10 – DNA sequencing

DNA sequencing was performed by Lark technologies or by the Department of Biochemistry, Oxford University. The sequences of the primers used for DNA sequencing are shown in table 2.2.

Primer name	Primer sequence (5' - 3')
M13F	CCCAGTCACGACGTTGTAAAACG
T7F	TAATACGACTCACTATAGGG
Kir6.2 C-terminus seq.	GTGCAGAATATCGTCGGGCTG
Kir6.2 C-terminus seq 2	CGCTTTGTCCCCATTGTGGCC

Table 2.3 - *Sequences of primers used for DNA sequencing.*

2.3.11 – Northern blotting

Probe preparation

Total RNA was extracted from INS1e cells using Tri-reagent (Sigma) as per manufacturer's instructions. The extracted total RNA was then reverse transcribed to produce cDNA as follows. First, RNA and oligo dT were incubated at 70°C for 5 min followed by incubation on ice for a further 5 min. This was used as a basis for a reverse transcription-PCR reaction comprising 1 X RT buffer, 1 X dNTPs, 1 X RNase inhibitor and 1.5 U RTase (NEB – RT kit). This was then incubated at 37°C-42°C for 1 hour followed by 5 min at 95°C before storing on ice. The cDNA produced was used as a template for a PCR reaction to produce the short northern blot probes. β-actin probes were constructed as described by Misty *et al.* (1983).

Construction of SUR1 northern blot probes form cDNA by PCR

SUR1 northern blot probes were produced by a PCR based method using the cDNA produced from the reverse transcription as a template. 2 µl of the cDNA was added to a 50 µl PCR reaction mixture containing 1 X Taq polymerase buffer, 200 µM dNTPs mixture, 2.5 U Taq DNA polymerase and 20 pmol each of forward and reverse oligonucleotides primer. Each reaction was overlaid with mineral oil and subjected to the following reaction parameters: 95°C for 40 sec, 56°C for 1 min and 72°C for 1.5 min. Following 35 cycles of these parameters the products were finally extended at 72°C for 7 min. Following completion of the reaction the products were separated by agarose gel electrophoresis and the main product isolated by GENECLEAN™ (2.3.4).

Northern blot protocol

Northern blot analysis was performed by Dr A. Asipu (St James' University Hospital, Leeds)

Prior to northern blot analysis, INS-1e cells were incubated for 2 hours in media containing either 3 mM or 25 mM glucose at 37°C. Total RNA was extracted from the cells using tri-reagent and the abundance of specific RNAs examined by northern blot analysis. Northern blotting analysis was performed as described in Sambrook & Russell (1999).

2.4 – Immunocytochemical methods

All reagents used were purchased as cell culture grade where possible, or were prepared and sterilised by autoclaving or passing through a 0.2 µm filter as appropriate.

2.4.1 – Maintenance of immortal cell lines

Routine culture of HEK293 and COS7 cells

Cells were grown in 25 cm^2 or 75 cm^2 culture flasks (Sarstedt) at 37°C in a humidified atmosphere of 5 % CO_2 / 95 % air. When ~ 70-75 % confluent the cells were passaged as described below. The cells were first detached from the growth surface using either Ca^{2+} / Mg^{2+}-free PBS or Trypsin-EDTA solution [0.05 % (w/v) and 0.02 % (w/v) respectively] (both from Sigma chemical company). The detached cells were then resuspended in 5 volumes of pre-warmed media and an aliquot transferred to a fresh culture flask containing 10 volumes of pre-warmed media. The cells were then returned to the incubator.

INS1e and RIN-m cell culture

INS1e and RIN-m cells were grown at 37°C in a humidified atmosphere of air / 5 % CO_2. Cells were re-fed with fresh culture medium on the third and fifth days of culture and split on the seventh day having reached 60-70 % confluency. The cells were split as follows. The culture medium was decanted and the residual medium removed by rinsing with PBS. Sufficient ice-cold trypsin-EDTA solution [0.05 % (w/v) and 0.02 % (w/v) respectively] to just cover the cells was added and the cells were returned to the incubator. The cells were inspected regularly until detached (typically 2-3 minutes) then culture media equivalent to 5 volumes of the trypsin-EDTA used was added. This cell suspension was split 1:3 into fresh culture flasks and supplemented with sufficient culture media.

Long-term liquid N_2 storage

For long-term storage cells were stored under liquid nitrogen (N_2). Cells in suspension in growth media were centrifuged at low speed until a pellet had formed. The media was removed and the pellet was resuspended in cell freezing medium. The cell freezing media typically consisted of the standard growth media (DMEM or RPMI1640 depending on the cell type) supplemented with 20 % FCS and 8 % DMSO. The resulting suspension of cells in freezing medium was aliquoted in 1 ml volumes into freezing vials and stored at -80°C for 48 hours before being transferred into a liquid nitrogen storage container. When required, cells were thawed quickly by immersion of the freezing vial in a 37°C water bath with gentle agitation. Once thawed, cells were diluted in 20 volumes of culture media and placed in culture flask for growth as described above.

Isolation and maintenance of primary β-cell cultures

BALB/C and C57bl6/J mice were killed by cervical dislocation in full accordance with Home Office schedule 1 guidelines. The pancreas was immediately removed via a midline incision, and rinsed twice in Hanks solution (mM: 137 NaCl, 1.2 NaH_2PO_4, 4.2 $NaHCO_3$, 5.6 KCl, 1.2 $MgCl_2$, 2.6 $CaCl_2$, 10 HEPES, pH to 7.4 with NaOH) supplemented with 2.8 mM D-glucose and 5 mg ml^{-1} bovine serum albumin (BSA). Using a 28-gauge needle, the pancreas was then perfused with Hanks solution supplemented with 2.8 mM D-glucose, 5 mg ml^{-1} BSA and 1.5 mg ml^{-1} type-V collagenase and incubated at 37°C for 20 minutes in a further 5 ml of collagenase solution of the same composition. Following the incubation the tissue was agitated vigorously to

provide a suspension of cells. This suspension was then centrifuged gently until all cells had formed a pellet, and the collagenase solution was then transferred into a fresh tube. The cell pellet was resuspended in Hanks solution supplemented with 2.8 mM D-glucose and 5 mg ml^{-1} BSA and placed in a dish under a well-lit dissection microscope and viewed against a black background. Any large pieces of tissue remaining were returned to the collagenase solution for further enzymatic disruption. The remaining tissue debris was then examined under the microscope for intact isolated islets, which appear as white opaque oval or spherical structures against the finer, pink coloured more dispersed exocrine tissue. The islets were then picked by pipette and transferred into fresh Hanks solution supplemented with 2.8 mM D-glucose and 5 mg ml^{-1} BSA. If dispersal of the islets into individual cells was required, they were incubated at 37°C in Ca^{2+} free Hanks (mM: 137 NaCl, 1.2 NaH_2PO_4, 4.2 $NaHCO_3$, 10 HEPES, 1 EGTA, pH to 7.4 with NaOH) supplemented with 2.8 mM D-glucose and 0.01% trypsin for five min followed by gentle agitation with a pipette. Cells were plated straight onto the growth surface required for experimentation and were cultured for no more than 5 days in standard INS1 culture media (as defined in 3.2.2).

2.4.2 – Preparation of adherent cells for immunocytochemistry

Preparation of poly-L-lysine coated coverslips

Borosilicate glass coverslips were first rinsed in 70% ethanol before being overlaid with a 100 µg ml^{-1} of poly-L-lysine (MW: 70000-120000) for 2 hours at room temperature. The poly-L-lysine solution was then removed and the coverslips rinsed with 1X PBS.

Immunofluorescent staining of isolated pancreatic β-cells

It was noticed that individual cells from dispersed isolated islets attached poorly to either untreated or poly-L-lysine coated glass coverslips. For the purpose of fluorescent staining, cells from dispersed isolated islets were plated onto microscope slides made from permanox plastic (Nunc) which appeared to aid attachment. For identification of β-cells amongst other islet cell types (α and δ cells) in addition to remaining exocrine tissue, cells were counterstained using mouse anti-insulin antibodies (Sigma Drugs company).

2.4.3 – Transfection methods

Transfection with anionic lipid transfection reagents

Mammalian cells were typically transfected with plasmid DNA using Fugene6 transfection reagent (Roche diagnostics) as per manufacturers' instructions. Briefly, cells were plated onto glass coverslips in individual wells of a 24 well culture plate and incubated overnight for the cells to adhere. Prior to transfection the growth media in each well was removed and replaced with 0.5 ml of fresh pre-warmed growth media. For each well, 0.6 µl of Fugene6 transfection reagent was added to 20 µl of optimem serum free media and lightly mixed by gentle agitation. To the Fugene6 / optimem mixture, 0.2 µg of DNA per well was added and again lightly mixed by gentle agitation. This mixture was left at room temperature for 30 minutes before transferring to each well of the 24-well plate.

Calcium phosphate method

Calcium phosphate transfection of adherent cells was performed using a calcium phosphate transfection kit (Stratagene). Briefly, cells were plated into wells of a 6-well plate to reach ~ 50 - 60 % confluency. 2 hours prior to transfection the medium was removed and replaced with 1.2 ml of fresh pre-warmed media. The calcium phosphate transfection mixture was prepared by mixing 1.7 µg DNA and 10.4 µl 2M $CaCl_2$ and water up to 85 µl (per well) and adding this mixture to 2X HBS dropwise whilst gently mixing. This final mixture was allowed to sit for 25 minutes at room temperature before resuspending and adding dropwise to the media covering the cells in the 6 well plate. Following 16-24 hours the media was changed for fresh pre-warmed media. Expression was assessed following a further 24-48 hours.

2.4.4 – Establishment / maintenance of a HEK293 cell line stably expressing K_{ATP}-HA

HEK293 cells stably expressing K_{ATP}-HA were established by Miss L. Mair (University of Leeds).

HEK-293 cells were cultured in DMEM media supplemented with 10 % fetal bovine serum and 100 U ml^{-1} penicillin and 100 µg ml^{-1} streptomycin at 37°C in a humidified atmosphere of air / 5 % CO_2. HEK293 cells were transfected with pcDNA3.1-Kir6.2-HA+11aa-HMKFLAG and pcDNA6-His6-SUR1 using fugene6 transfection reagent. Following 48 hours the culture media was supplemented with 800 µg ml^{-1} G418 and 10

μg ml^{-1} blasticidin to select for those cells expressing both plasmids. Following continued treatment with G418 and blasticidin for several days the remaining cells were re-plated at a low density and allowed to grow to form colonies. Individual colonies were then cultured and assayed for expression of K_{ATP} channels. The clone displaying the most optimal expression of K_{ATP} channels was then maintained in culture media supplemented with 200 μg ml^{-1} G418 and 2 μg ml^{-1} blasticidin.

2.4.5 – Immunocytochemical methods

Staining of permeabilised cells

Cells were plated onto glass coverslips and transfected as required 48 hours prior to labelling with antibodies. Following any treatments which may be required cells were fixed by addition of methanol (chilled to -20°C) for 10 minutes and the cell membranes subsequently permeabilised by the addition of acetone / methanol (1:1) (chilled to -20°C) for 5 minutes. As an alternative to methanol to fix the cells 2 % PFA has been used. Following permeabilisation the cells were blocked with 5 % goat serum in 1X PBS for 30 minutes to block any non-specific binding of antibodies at a later stage. Following the blocking stage the cells were incubated with primary antibodies diluted in 5 % goat serum in 1X PBS for 2 hours at room temperature. Following the primary antibody incubation the cells were washed 8X with 1X PBS followed by incubation with appropriate fluorescently labelled secondary antibodies diluted in 5 % goat serum in 1X PBS for 1 hour at room temperature. Following the secondary antibody incubation the coverslips were again washed 8X with 1X PBS before being removed from the 24 well plate to air dry. Once dry, the coverslips were mounted cell-side down onto VECTASHIELD™ hard-set mounting media on a microscope slide. Slides were stored at 4°C until viewed by laser-scanning confocal microscopy.

Staining of unpermeabilised cells

Some applications required that the membranes of the labelled cells remained intact throughout the antibody labelling process. This allows the selective staining of cell surface channels as opposed to all channels within cells.

Cells were plated onto glass coverslips and transfected as required 48 hours prior to labelling with antibodies. Following any treatments which may be required cells were fixed by addition of 2 % PFA for 10 minutes at room temperature. The cells were not

permeabilised. Following fixation the cells were blocked with 5 % goat serum in 1X PBS for 30 minutes to block any non-specific binding of antibodies at a later stage. Following the blocking stage the cells were incubated with primary antibodies targeted against an extracellular epitope diluted in 5 % goat serum in 1X PBS for 2 hours at room temperature. Following the primary antibody incubation the cells were washed 8X with 1X PBS followed by incubation with appropriate fluorescently labelled secondary antibodies diluted in 5 % goat serum in 1X PBS for 1 hour at room temperature. Following the secondary antibody incubation the coverslips were again washed 8X with 1X PBS before being removed from the 24 well plate to air dry. Once dry, the coverslips were mounted cell-side down onto VECTASHIELD™ hard-set mounting media on a microscope slide. Slides were stored at 4°C until viewed by laser-scanning confocal microscopy.

Staining sectioned Xenopus laevis oocytes

Oocytes were injected with cRNA as required and allowed to express for 48-72 hours. The oocytes were then fixed by immersion in methanol (-20°C) for > 4 hours and cryopreserved in PBS containing 30 % sucrose at 4°C overnight. Intact oocytes were then embedded in octyl transferase (BDH) and cut into 20 µm sections using a cryostat (Bright, UK). The sections were mounted onto microscope slides coated with either poly-D-lysine or VECTABOND and subsequently blocked with 5 % goat serum in 1X PBS for 30 minutes. Following blocking the cells were incubated with primary antibodies diluted in 5 % goat serum in 1X PBS for 2 hours at room temperature. Following the primary antibody incubation the sections were washed 8X with 1X PBS followed by incubation with appropriate fluorescently labelled secondary antibodies diluted in 5 % goat serum in 1X PBS for 1 hour at room temperature. Following the secondary antibody incubation the sections were washed 8X with 1X PBS and left to air dry. Once dry the sections were overlaid with VECTASHIELD mounting medium and covered with a glass coverslip. Slides were stored at 4°C until viewed by laser-scanning confocal microscopy.

Internalisation staining protocol

Cells were grown on poly-D-lysine coated coverslips for 48 hours prior to staining so that they reached a confluency of ~ 65 - 70 %. For the purposes of labelling the cells the medium used was glucose-free DMEM supplemented with 5 % goat serum and 1 mM

glucose. Culture medium was removed and the cells were rinsed with labelling medium and pre-treated with drugs as required. Following any pre-incubation steps, cells were incubated in labelling medium supplemented with 0.2 μg ml^{-1} rat anti-HA antibodies and requisite drugs at 37°C for the desired duration to allow internalisation. Unless otherwise stated in the figure legend the duration of this internalisation step was 2 hours. Following incubation for the desired duration, labelling medium was removed and cells were briefly rinsed with 1X PBS before fixing with methanol (-20°C) for 10 minutes. Following fixation, methanol was removed and replaced with acetone / methanol (1:1) (-20°C) for 4 - 5 minutes for permeabilisation. If no permeabilisation was required this step was omitted. Following these steps, cells were blocked with 5 % goat serum in 1X PBS for 30 minutes at room temperature before labelling with anti-rat FITC or Cy3 conjugated antibodies in 5 % goat serum in 1X PBS for 1 hour at room temperature. Coverslips were then mounted onto microscope slides using VECTASHIELD mounting medium and cells were then examined by confocal microscopy.

Recycling staining protocol

The protocol used to examine channel recycling by immunofluorescence is summarised in figure 2.3. Cells were grown on poly-D-lysine coverslips for 48 hours prior to commencement of the experiment. For the purposes of labelling the cells the medium used was glucose-free DMEM supplemented with 5 % goat serum and 1 mM glucose. Culture medium was removed and the cells were rinsed with labelling medium and pre-treated with drugs as required. Typically, cells were pre-treated with drugs for 20 minutes at 37°C prior to commencement of the experiment. Following drug pre-treatments cells were incubated with labelling medium supplemented with 0.2 μg ml^{-1} rat anti-HA antibodies and requisite drugs at 37°C for 2 hours to allow internalisation and for antibody labelled channels to reach a steady state distribution through the endocytic compartments. Following this internalisation step the cells were rinsed in chilled 1X PBS then incubated in chilled acidic stripping buffer (0.5 % acetic acid + 0.5 M NaCl; pH 3.0) for 30 minutes to remove any surface bound anti-HA antibodies. Cells were then rinsed twice with chilled 1X PBS and twice with chilled labelling medium. Following the washes cells were incubated in pre-warmed labelling medium supplemented with 1.25 μg ml^{-1} anti rat-FITC conjugated antibodies at 37°C for the desired length of time. Following this incubation, medium was removed and cells were fixed with methanol (-20°C) for 10 minutes before permeabilisation with acetone / methanol (1:1) (-20°C) for 4-

5 minutes. Remaining HA bound channels were then labelled with anti-rat Cy3 conjugated antibodies diluted in 5 % goat serum in 1X PBS for 1 hour at room temperature. Coverslips were then mounted onto microscope slides with VECTASHIELD™ mounting medium and examined by confocal microscopy.

Live-cell imaging

Cells were grown in poly-D-lysine coated glass-bottomed culture dishes for 48 hours prior to commencement of imaging. Culture media was removed and replaced with CO_2-independent media and the dish was placed into a heated chamber at 37°C mounted onto a DeltaVision™ wide-field fluorescence microscope for 30 minutes to allow equilibration. Following equilibration the media was supplemented with 2 μg ml^{-1} mouse anti-HA Alexafluor595-conjugated antibodies and incubated for 15 minutes to allow antibody binding to cell surface channels. Following antibody binding the media was replaced with fresh pre-warmed CO_2-independent media and imaging of labelled cells began.

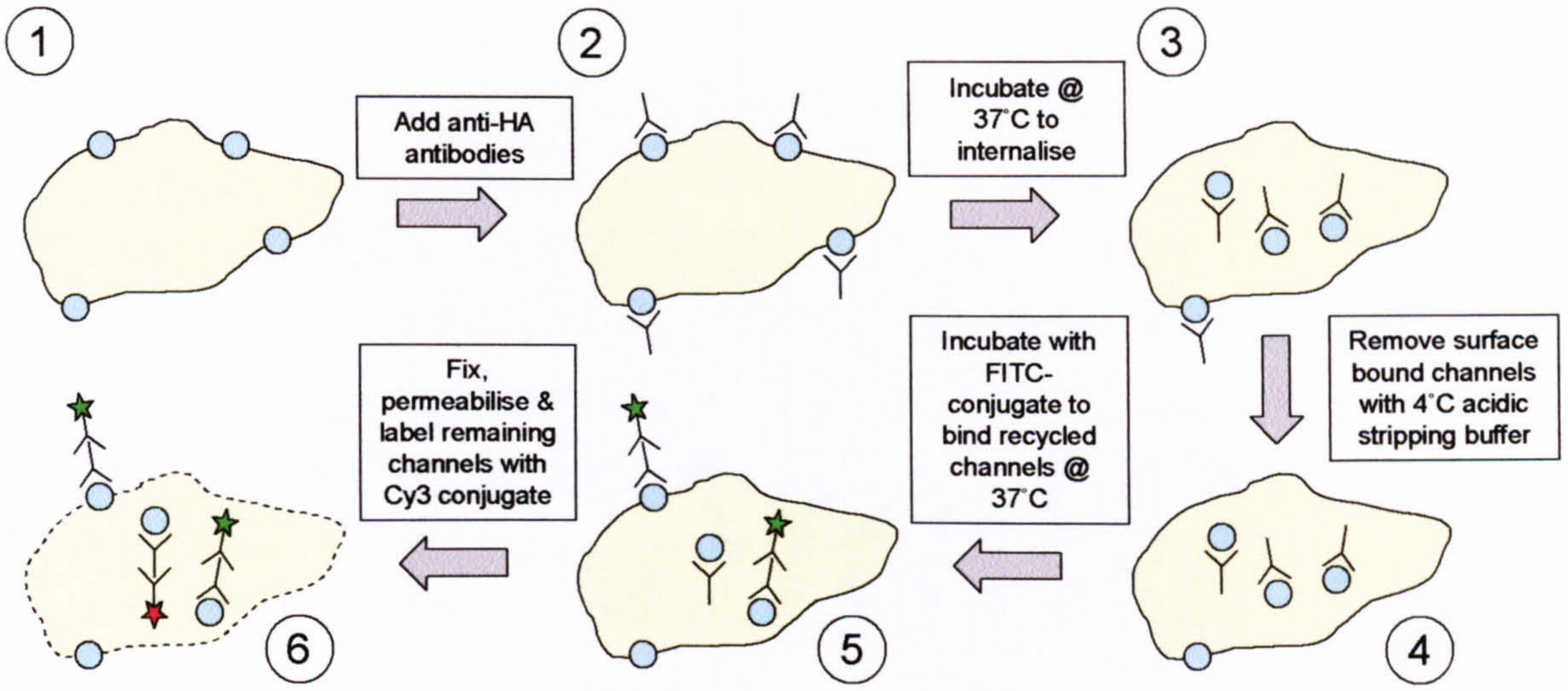

Figure 2.3 - *Schematic of the recycling staining assay protocol.* Shown is an outline of the protocol used to examine the recycling of K_{ATP}-HA channels by immunocytochemistry. First, cells expressing K_{ATP}-HA are plated onto poly-L-lysine coated coverslips (1). The cells are then incubated with rat anti-HA antibodies (2) so that surface channels become labelled. The labelled channels are then allowed to internalise for 2 hours so that the endocytic trafficking pathways become filled with labelled channels (3). The cells are then chilled to 4°C to halt trafficking and anti-HA antibodies at the cell surface are stripped using an acidic stripping buffer (4). Channel trafficking is reinitiated by incubating the cells at 37°C in media supplemented with anti-rat FITC-conjugated antibodies to label any recycled channels (5). Depending on the duration of this stage labelled channels may be reinternalised into the cells. Following the recycling step the cells are fixed, permeabilised and the remaining anti-HA bound channels are labelled with anti rat Cy3-conjugated antibodies (6). This population of channels represents those channels which did not recycle to the cell surface.

2.4.6 – Imaging fluorescently labelled cells

Confocal microscopy

The main advantage which confocal microscopy offers over conventional fluorescence microscopy is that it is capable of imaging with a very high resolution the light emitted from a single plane through a specimen as opposed to the specimen as a whole. In the case of laser scanning confocal microscopy this is achieved by exciting fluorophore compounds bound to structures within the cell and collecting the emitted light through the use of a laser beam which scans through the sample line by line. The emitted light is collected by the objective lens of the microscope and is focused through a small pinhole which blocks any light which originated from above or below the plane of focus. The light which passes through the pinhole is then collected by detectors and the image corresponding to the plane of focus through the sample is reconstructed. This is summarised in figure 2.4. By sequentially imaging several planes of focus in the sample it is possible to reconstruct 3-dimensional images of cells.

Imaging fixed cells via confocal microscopy

Labelled cells were viewed using either a Leica TCS NT or a Zeiss 510-META laser scanning confocal microscope (LSCM) under an oil-immersed 63× objective lens (NA = 1.40). FITC (494 nm excitation: 519 nm emission) was excited using an argon laser fitted with 488 nm filters and Cy3 (550 nm excitation: 570 nm emission) was excited using a helium / neon laser fitted with 543 nm filters.

2.4.7 – Quantification of fluorescence intensity

Quantification of fluorescence intensity was attempted by measuring the mean pixel intensity of individual cells using the ImageJ software package (NIH). Individual cells in representative confocal images were outlined by hand and the mean pixel intensity calculated. All values for each population were collated and means and standard errors for each population were calculated and expressed as a percentage of the maximum value. For these studies all cells were imaged using identical confocal microscope settings. The settings were tailored so that the intensity of each pixel was within the range of sensitivity of the fluorescence detectors, i.e no pixel showed saturation of fluorescence.

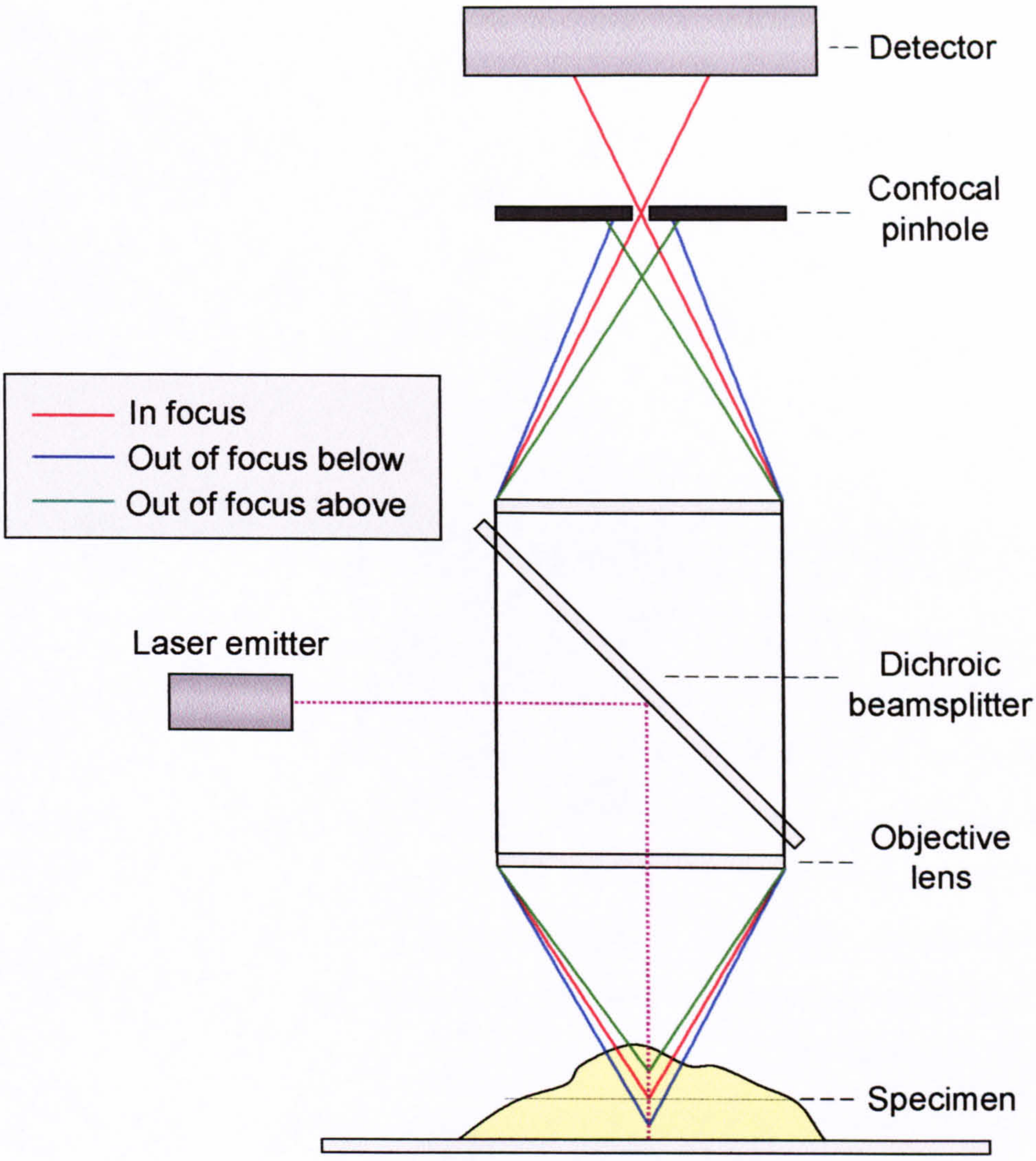

Figure 2.4 - *Beam path in a laser scanning confocal microscope.* A laser beam of a particular wavelength (purple dotted line) is targeted via a dichroic beamsplitter so that it illuminates the sample exciting fluorophore molecules that it encounters resulting in the emission of light of a different wavelength. This light travels up through the objective lens, through the dichroic beamsplitter and up through a second lens which refocuses the light. Light originating from the plane of focus (red line) is refocused so that it may pass through the narrow opening of the confocal pinhole where it is recorded by the detector. Light coming from focal planes above (green line) and below (blue line) the plane of focus are not focused through the pinhole and so are largely blocked from reaching the detectors. The resulting image will therefore be composed almost entirely of light emitted from a very narrow focal plane.

2.5 – Protein chemistry

2.5.1 – SDS-polyacrylamide gel electrophoresis (SDS-PAGE) methods

SDS-PAGE gels were produced as described in section 2.2.5 above. Gels were mounted into the gel running apparatus as per manufacturers' instructions (BioRad or Hoeffer) and sufficient SDS-PAGE running buffer was added to both the central reservoir and the surrounding tank. 20 µl of each sample was then added to each individual well as required along with 10 µl of marker proteins. Gels were then run at 200V until sufficient separation of prestained marker proteins had occurred.

2.5.2 – Detection of radiolabelled proteins

For the detection of radiolabelled proteins separated by SDS-PAGE the gels were first prepared and run as described above. The gels were stopped once sufficient separation of the pre-stained protein markers had occurred and the gels were removed from the gel running apparatus. The gels were then rinsed in water before incubation in Coomassie brilliant blue stain for 30 minutes at room temperature with gentle agitation. Following coomassie blue treatment the gel was washed in destain solution at room temperature with gentle agitation with frequent changes of the destain solution until protein bands within the gel became distinct. The gel was then rinsed several times with water and subsequently incubated with 1M salicylic acid for 30 minutes. The gel was then transferred onto a piece of card, covered in saran wrap and placed in a gel drier for 1 hour. The radiolabelled proteins in the dried gel were then visualised by exposing the gel to either photographic film for 48 hours of by exposing to a phosphorimaging plate overnight.

2.5.3 - Pulse labelling

Sample preparation

INS1e cells were grown in 6-well plates in INS1e cell culture media (as defined in 3.2.2) at 37°C in an atmosphere of 5% CO_2 / air until ~ 80 % confluency. The medium was removed and replaced with sufficient prewarmed cysteine / methionine deficient media and the cells were incubated for 30 min at 37°C. The medium was then removed and replaced with 1 ml of cysteine / methionine deficient media supplemented with 200 µCi of Tran-^{35}S-label radiolabelled methionine (ICN biomedicals) and incubated at 37°C. Following the desired period of incubation in the presence of ^{35}S labelled methionine (the pulse period) radiolabel incorporation was halted by the addition of 10 mM cysteine and

4 mM methionine. Medium was then removed and the cells were lysed on ice by addition of 1 ml of RIPA buffer (20 mM Tris-HCl, 150 mM NaCl, 2 mM EDTA, 1 % Nonidet-P40, 1 % Na-deoxycholate, 0.1 % SDS) supplemented with protease inhibitor cocktail (Sigma drugs company). Debris was removed from the cell lysates by high speed centrifugation at 4°C for 30 minutes.

Isolation of K_{ATP} channel subunits by immunoprecipitation

Cell lysates were pre-cleared by incubation with fresh protein-G-sepharose for 1 hr at 4°C with rotation, and then separated by centrifugation. The pre-cleared supernatant was removed and added to protein-G-sepharose which had previously been bound with rabbit anti-SUR1 antibodies and incubated for 16 hr at 4°C with rotation. The beads were then washed twice with ice-cold RIPA buffer then twice in ice cold high salt buffer (0.5 M LiCl, 0.1 M Tris-HCl in RIPA buffer). The washed beads were then resuspended in alkaline SDS-sample buffer (as described in 2.2.5) supplemented with 10 mM 1,4-Dithio-DL-threitol (DTT) and boiled for 5 minutes.

Separation and visualisation of radiolabelled proteins

Immunoprecipitated protein samples were separated by SDS-PAGE on a 5 - 15 % gradient gel prepared as described in chapter 2.2.3. 20 µl of each sample were loaded into individual wells alongside 10 µl of marker protein samples. The marker proteins used were Biorad precision plus protein standards [(Size in KDa): 250, 150, 100, 75, 50, 37, 25, 20, 15, 10] and New England Biolabs prestained protein marker [(size in KDa): 175, 83, 62, 47, 32, 25, 16, 6]. Once the gels had run they were rinsed in water and incubated in 1 M sodium salicylate solution before being dried. Once dry the gels were exposed either to photographic film or to a phosphorimaging plate overnight to visualise the separated radiolabelled proteins.

2.5.4 – Insulin assays

Sample preparation

INS1e or RIN-m cells were plated into wells of a 24 well plate and cultured until reaching 60-70 % confluency. Cells were then incubated in KRB-HEPES supplemented with either 3 mM or 25 mM glucose for 1 hour at 37°C. Following 1 hour supernatants were removed for insulin assay. The cells were retained for protein assay.

Insulin assay

Insulin content of supernatants was determined using an insulin radioimmunoassay kit (ICN-biomedicals) as per manufacturer's instructions. Insulin content of the samples was normalized to total protein of the corresponding cells. Insulin secretion was expressed as insulin units per μg cellular protein per hour (IU/μg protein/hr).

Protein content determination

Following removal of supernatants for insulin assay, cells were solubilised in lysis buffer (0.5 % Triton-X100 / 0.1 % SDS) and assayed for protein by bicinchoninic acid (BCA) assay. Several dilutions of cell lysate samples were added to individual wells of a flat-bottomed 96-well plate and made up to a final volume of 10 μl with sterile water. To each sample 200 μl of BCA reagent was added and incubated at 37°C for 20-30 min. BCA reagent was prepared by mixing bicinchoninic acid solution and 4 % $CuSO_4$ (50:1 ratio). Concurrently, several samples containing a known amount of BSA (ranging between 0-10 μg) were also subjected to BCA assay in order to construct a standard curve. Following the 37°C incubation the absorbance at 550 nm of each sample and standard was read and protein content of each sample was calculated from the standard curve.

2.6 – Electrophysiological methods

2.6.1 – Two electrode-voltage clamp

Removal and preparation of Xenopus laevis *oocytes*

Female *Xenopus laevis* frogs were anaesthetised by immersion in 2% 3-aminobenzoic acid (pH 7.2 with TRIS and HCl) for 45 min. The frogs were then killed by cervical dislocation and pithing, in full accordance to Home-office schedule 1 guidelines. Ovarian lobes were then removed via a mid-line incision (Stuhmer & Parekh 1995).

The ovarian lobes were torn into small clumps and further fragmented by two 45 minute incubations with type-I-collagenase (1 mg ml^{-1}) dissolved in OR-Mg solution (mM: NaCl 82, $MgCl_2$ 2, HEPES 0.5, KCl 0.2; pH 7.4) . The cell suspension was thoroughly washed between and following collagenase treatments with OR-Mg solution with the resultant single cell suspension finally transferred into ND-96 solution (mM: NaCl 9.6, $MgCl_2$ 0.1, HEPES 0.5, $CaCl_2$ 0.18, KCl 0.2; pH 7.4) from where Dumont stage V and VI oocytes were selected for injection.

cRNA microinjection of Xenopus laevis *oocytes*

Prior to injection, glass capillaries were sterilised by baking at 200°C for at least 4 hours. Sterile glass capillaries were pulled into very fine tipped pipettes and then broken to the correct diameter with a pair of flame-sterilised forceps. 50 nl of cRNA was injected into the light hemisphere of each oocyte using a Pneumatic PicoPump pressure injection system (WPI). The oocytes were returned to ND-96 solution and incubated at 18°C for 2-4 days.

Electrophysiological recordings from Xenopus laevis *oocytes*

A schematic representation of the two-electrode voltage clamp setup is shown in figure 2.5.

The GeneClamp 500 amplifier (Axon Instruments) was used for electrophysiological recordings. Both current and voltage outputs from the voltage clamp amplifier were shown on a Takronix 5113 dual beam storage oscilloscope (using D.C. coupled 5A22N and 5A21N amplifiers). The signals were fed via a CED 1401 analogue interface to a computer running the CED on-line analysis software (version 6). The current signal was low pass filtered at 1 kHz by the amplifier and sampled at 4 kHz.

The oocytes to be examined were placed in an oocyte chamber which was perfused with bath solution as described below at a rate of ~ 2 ml min^{-1}. The solution was continuously removed from the oocyte chamber by a suction tube connected to a peristaltic pump. The electrode holders containing the current and voltage electrodes were mounted onto headstages and were placed at either side of the oocyte chamber. The bath electrode was placed so that it was submerged in the bath solution. Finally, to minimize the interference between the current and voltage electrodes a copper shield was placed between the two electrodes once the oocyte had been impaled. To further minimize interference from external sources the whole apparatus were assembled inside a Faraday cabinet which was placed on an anti-vibration table, both of which were earthed to the circuit ground.

Before the electrodes were used to impale the oocyte the resistances were checked and if necessary adjusted by gently touching the tip with a pair of fine forceps. The current electrode resistance was adjusted between 0.3 and 1 MΩ and the voltage electrode between 0.3 and 2 MΩ. Both electrodes were then offset to 0 mV and the electrodes

advanced so that they bareley impaled the oocyte. Healthy oocytes typically had membrane potentials of ~ - 30 to - 70 mV. Following impalement of both electrodes, the oocyte was left until the membrane potential had stabilised, normally between 1 and 10 min. The amplifier was then set to clamp and the gain and stability controls on the amplifier were adjusted to maximise the clamp. An ideal clamp results in a square pulse for the voltage trace with small capacitance transients for the current trace. Once set, the clamp stability was monitored using the online display on the computer screen during recordings.

TEVC protocol

Whole-cell currents were recorded in high potassium Ringers solution containing: (mM) 90 KCl, 1 $MgCl_2$, 1.8 $CaCl_2$, 5 HEPES (pH 7.4) at room temperature. A ramp voltage protocol from -150 to +50 mV was used with the cells being held at -30 mV. Currents were elicited by perfusion of the oocyte in Ringers solution supplemented with 3mM sodium azide, a metabolic inhibitor and 200 μM diazoxide, a selective K_{ATP} channel opener. Currents elicited in this manner were then inhibited by perfusion in Ringers solution supplemented with 1 μM glibenclamide.

Data analysis

The current / voltage relationships obtained from the TEVC protocol were analysed using EPC version 6.42 software (Cambridge electronic design). The current passing at -120 mV was recorded from sequential ramp protocols and plotted against time to allow the construction of current versus time plots.

2.6.2 – Whole-cell patch clamp recordings

Whole cell patch clamp recordings were performed by Dr M. Hunter (University of Leeds)

The pipette solution for whole cell recordings comprised (mM): 140 KCl, 0.6 $MgCl_2$, 1.03 $CaCl_2$, 10 EGTA, 10 HEPES, 0.1 MgATP, and 0.1 ADP (adjusted to pH 7.2). The bath solution for whole cell recording comprised (mM): 122.5 NaCl, 5.0 KCl, 1.0 $MgCl_2$, 1.0 $CaCl_2$, 10 HEPES (adjusted to pH 7.4). This bath solution was supplemented with 25 mM D-glucose or 3 mM D-glucose + 22mM D-sorbitol as required.

Currents were recorded in the whole cell configuration. The currents were measured during a voltage ramp (-100 mV to +100 mV) from a holding potential of 0 mV and normalised to the membrane capacitance. Diazoxide (200 μM) was perfused to activate the channel, and tolbutamide (100 μM) to block the activated currents.

2.7 - Data and statistical analysis

When relating to immunocytochemistry, pulse labelling, two-electrode voltage clamp or insulin assay based experiments, 'n' numbers relate to the number of separate occasions on which the experiment was performed. For fluorescence quantification experiments the 'n' numbers relate to the number of individual cells examined for fluorescence intensity. Where required the statistical significance of data was determined by performing the student t-test.

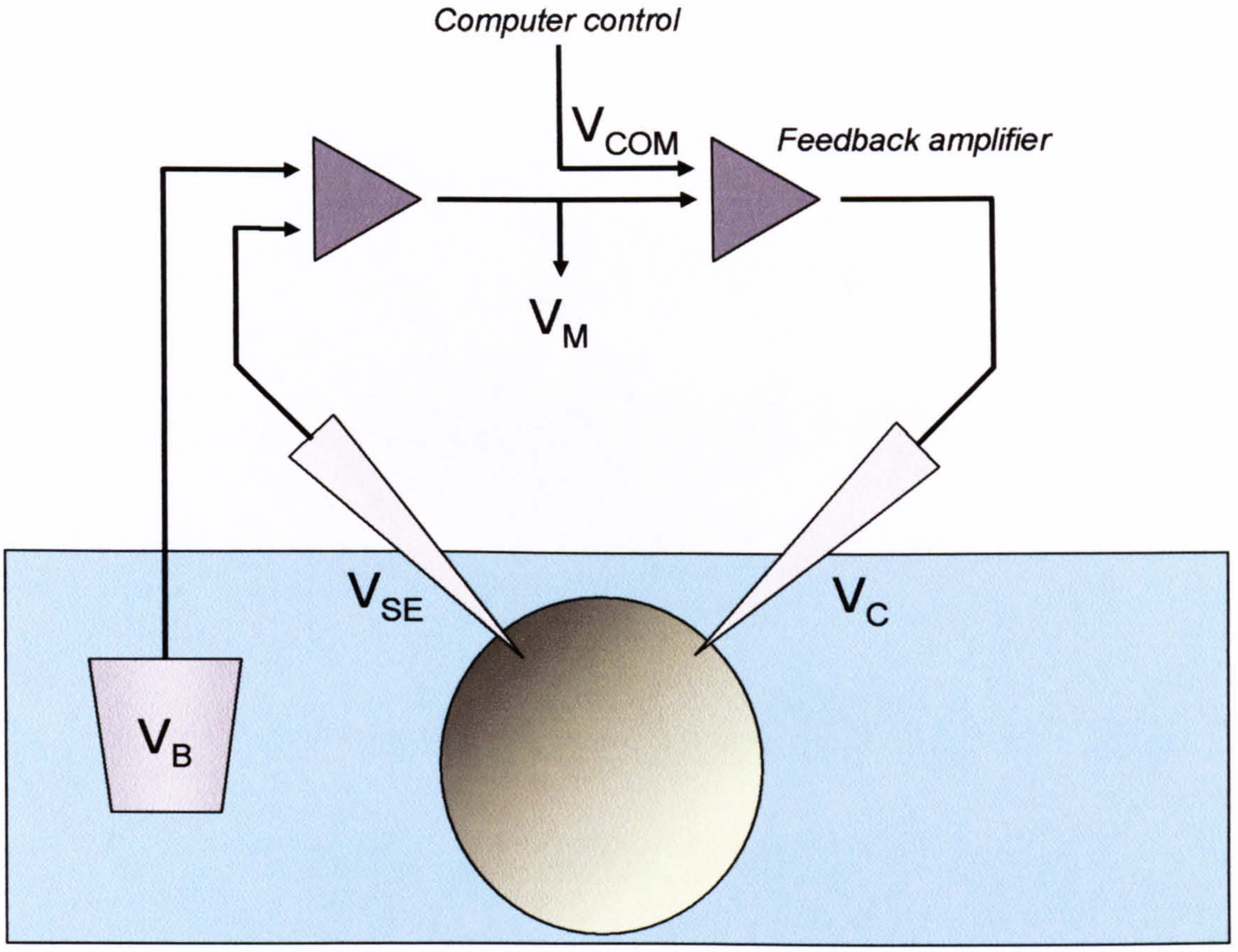

Figure 2.5 - *Schematic of the main components of the two-electrode voltage clamp configuration.* All electrophysiological recordings were made on *Xenopus* oocytes using conventional two-electrode voltage clamp. This technique allows the membrane potential to be clamped at a specified value while simultaneously recording whole cell currents. By comparing the voltages measured by the bath electrode (V_B) and the voltage sensing electrode (V_{SE}) a measure of membrane potential is calculated. The desired membrane potential (V_{COM}) is maintained by an injection of current by the current-passing electrode (V_C) through a negative feedback loop. The whole cell current being passed is equivalent to the ionic flow across the membrane at the clamped membrane potential.

Chapter 3

Regulation of K_{ATP} channel expression by glucose in pancreatic β-cells

3.1 – Introduction

It has been established that the overall activity of K_{ATP} channels in a pancreatic β-cell membrane correlates very closely with the overall level of insulin secretion. The overall activity of a given ion channel at the cell surface is determined by its open probability (P_o) and the number of channels (N) present (Hille 2001). Although a great deal of research has focused on the regulation of the P_o of these channels by changes in glucose concentrations (See Aguilar-Bryan & Bryan 1999 for review), the effect of these same changes in glucose on the number of channels (N) has not yet been extensively investigated. The importance of understanding exactly how channel numbers are regulated and how this may impact on the overall level of K_{ATP} channel currents and thus regulation of insulin secretion should not be underestimated. This importance has been reinforced in recent times by the discovery of a number of K_{ATP} channel mutants which have been shown to cause hyperinsulinaemia by disrupting normal channel trafficking and thus cell surface density of the channels (Cartier *et al.* 2001, Partridge *et al.* 2001, Taschenberger *et al.* 2002, Reimann *et al.* 2003).

Nutrient regulation of gene expression has long been known to be a very important adaptation allowing survival of an organism on intermittent food supplies (Johnston *et al.* 1999). Since glucose is the most abundant and commonly used fuel by almost all organisms it is hardly surprising that mechanisms exist whereby changing glucose availability cause changes in the expression of certain genes. In yeast, these mechanisms are fairly well understood (see Johnston *et al.* 1999 for review). An increase in glucose availability will cause an increase in the expression of a number of metabolic genes and the suppression of many genes involved in the utilisation of alternative energy sources. The role of glucose in the regulation of gene expression in mammalian cells is less clear. This is largely due to the added complication of hormonal control of systemic glucose concentrations in addition to any cell specific responses to fluctuations in local glucose levels. Despite this, the importance of glucose regulated gene expression has begun to be revealed in numerous tissues, particularly the pancreas and liver. In the pancreas elevated glucose has been shown to induce the expression of the pre-proinsulin gene (Permutt *et al.* 1972) as well as a number of glycolytic enzymes (Marie *et al.* 1993, Roche *et al.* 1997) and suppress the expression of other genes, e.g. peroxisome proliferator-activated receptor-α (PPARα)

(Roduit *et al.* 2000). In the liver, elevated glucose has been shown to induce the expression of the glucose transporter GLUT2 (Asano *et al.* 1992, Rencurel *et al.* 1996) and a number of glycolytic enzymes, e.g. L-type pyruvate kinase (Vaulont *et al.* 1986, Thompson *et al.* 1991) and acetyl-CoA carboxylase (Pape *et al.* 1988) as well as some lipogenic enzymes such as fatty acid synthase (Paulauskis & Sul 1989, Katsurada *et al.* 1990). It is perhaps worth noting however, that although glucose has been shown to regulate the expression of a number of genes, these reports describe changes in the level of expression only at the transcriptional level, and to my knowledge, no report has yet described an associated change in protein levels.

More recently it has begun to become apparent that specific protein kinases play important roles in the regulation of the expression of these glucose responsive genes. One of the most important and currently best understood of these protein kinases is AMP-activated protein kinase (AMPK). AMPK is a serine / threonine kinase which has been described to act as a metabolic "master switch" by phosphorylating target proteins involved in carbohydrate and fat metabolism in response to changes in cellular energy charge (see Leclerc *et al.* 2002, Rutter *et al.* 2003 for reviews). It has been shown that in pancreatic β-cells, glucose concentrations above ~8 mM inhibit the activity of AMPK (Salt *et al.* 1998, da Silva Xavier *et al.* 2000b). This inhibition of AMPK by high glucose, or pharmacological activation of the protein kinase by the addition of 5-amino-4-imidazolecarboxamide riboside (AICAR) have been shown to be sufficient to alter the expression level of most of the more common glucose responsive genes (da Silva Xavier *et al.* 2000a,b, Woods *et al.* 2000, da Silva Xavier *et al.* 2003). Since the activity of AMPK in pancreatic β-cells has been recently shown (Leclerc *et al.* 2004) to also be very closely linked to overall level of insulin secretion, this may implicate a possible link between blood glucose levels, AMPK activity and overall K_{ATP} channel activity.

Since all of the genes identified to date which display glucose regulated expression are involved in some way with glucose homeostasis, it is conceivable that any gene involved with the regulation of glucose levels might be similarly regulated. Since the function of K_{ATP} channels in the pancreatic β-cell is to sense changes in blood glucose concentrations and to regulate the secretion of insulin accordingly, the possibility that

expression of these channels might be regulated by glucose warrants further examination.

INS1e cells were used for the majority of this study as a model for the pancreatic β-cell in preference to a number of other similar cell lines such as MIN6, RIN-m and HIT-15. Whereas most other pancreatic β-cell lines have a tendency to lose their ability to secrete insulin correctly following prolonged culture, INS1e cells have previously been shown to be able to maintain this ability for much longer periods of time (Poitout *et al.* 1996, Salt *et al.* 1998). In addition, INS1e cells have also been shown to respond to glucose in the normal physiological range and the combination of these properties means that they represent the best available model cell line for this type of study. Since these cells do resemble native β-cells so closely it is hoped that any findings will have direct implications with respect to physiological regulation of K_{ATP} channel regulation and ultimately insulin secretion.

Using both INS1e and pancreatic β-cells isolated from mouse islets the effect of acute changes in glucose concentrations on the expression levels of K_{ATP} channels were investigated.

3.2 – Results

3.2.1 – Anti-SUR1 and anti-Kir6.2 antibodies are specific

Labelling proteins using specific antibodies coupled with fluorescent conjugates provides a quick and easy way of visualizing proteins in cells. In addition, by examining the intensity of fluorescent staining it is possible to compare the amounts protein of interest present within two or more populations of labelled cells. This approach has been used here to examine the effect of varying glucose concentrations on the expression of both Kir6.2 and SUR1 in the INS1e pancreatic β-cell derived cell line and also in primary cultures of β-cells freshly isolated from pancreas. The validity of data obtained from such experiments however relies on the antibodies to have a high specificity for the target protein. It has previously been shown (Hough 2000, Partridge *et al.* 2001) that the antibodies used in this study show a very high degree of specificity for the intended target proteins as demonstrated by clear fluorescence in cells transfected with both Kir6.2 and SUR1 and an absence of staining in cells which had not been transfected.

3.2.2 – Glucose regulates the expression of Kir6.2 and SUR1 in INS1e cells

The effect of glucose concentration of the extracellular medium on the expression level of K_{ATP} channels was investigated using INS1e cells as a pancreatic β-cell model. INS1e cells grown on poly-L-lysine coated coverslips were incubated for 2 hr in glucose free media supplemented with varying concentrations of glucose, ranging from 0 mM to 25 mM. Following this incubation Kir6.2 or SUR1 protein within these cells were labelled using either anti-Kir6.2 or anti-SUR1 antibodies, followed by FITC-conjugated secondary antibodies. The intensity of fluorescent staining of the cells was then examined by confocal microscopy, during which all microscope settings were kept identical to allow direct comparison between each set of images. It was observed that cells incubated in low glucose concentrations showed significantly greater levels of fluorescence than cells incubated in higher glucose concentrations, indicating greater levels of protein in cells incubated low glucose (figure 3.1). Indeed, measurement of the mean pixel intensity of each cell showed that the fluorescence observed in cells incubated in 0.5 mM glucose was 2 - 2.5 fold higher than in cells incubated in 25 mM glucose (figure 3.2). This was true of cells stained for both Kir6.2 and SUR1. Interestingly the distribution of K_{ATP} channel subunits was not uniform

throughout the cell, and this was particularly true of cells incubated in high glucose and stained with anti-SUR1 antibodies. As the overall intensity of fluorescence decreased within cells with the increase in glucose concentration, the staining towards the periphery of the cell appeared to be more prominent whereas the staining in the peri-nuclear regions appeared to be much more greatly reduced by comparison. Cells incubated in low glucose conditions showed much more even staining throughout the cytoplasm often in vesicular structures. For the purposes of further experimentation two glucose concentrations were chosen, 3 mM and 25 mM, with which to proceed. These two glucose concentrations have been widely used previously and represent the lower limits of normal blood glucose and a profoundly hyperglycemic blood glucose level respectively. The possibility that altered osmolarity of the incubation medium was responsible for the effect was also tested. INS1e cells incubated in media supplemented with 3 mM glucose and 22 mM mannitol, a non-metabolisable glucose derivative, showed a comparable difference in fluorescence intensity relative to cells incubated in 25 mM glucose to cells incubated with 3 mM glucose alone (figure 3.3).

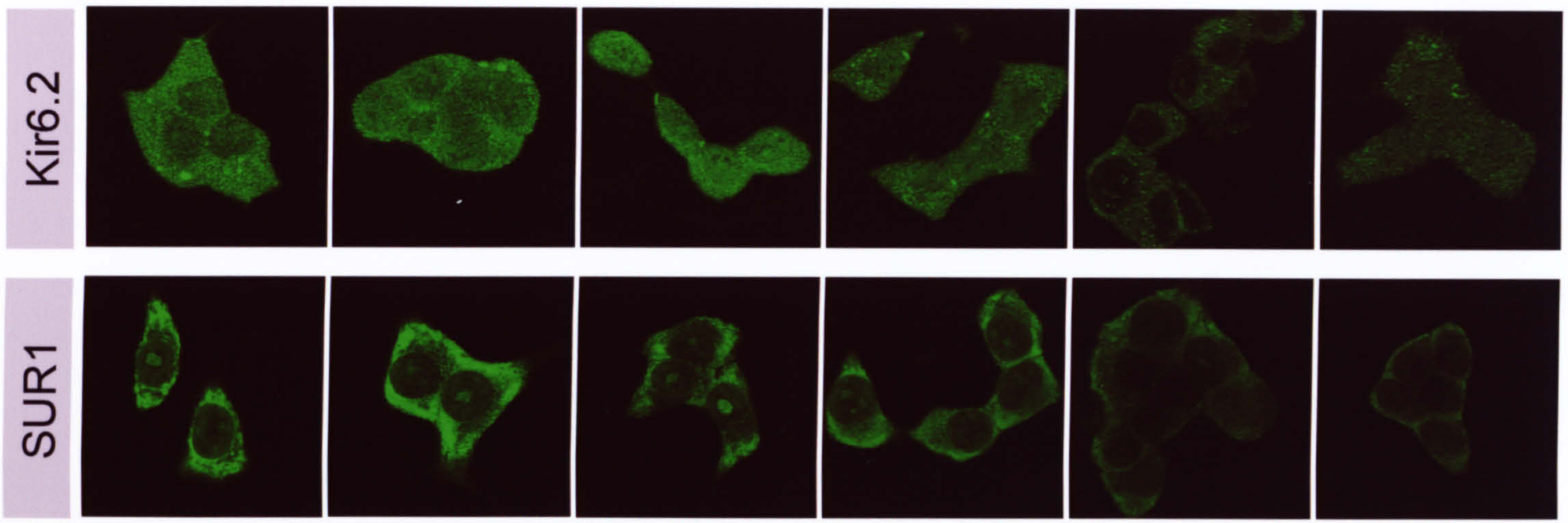

Figure 3.1 - *Glucose affects the expression of K_{ATP} channel in INS1e cells.* INS1e cells were incubated for 2 hours in media containing the stated glucose concentration then K_{ATP} channel subunits were visualised using either anti-SUR1 or anti-Kir6.2 antibodies followed by FITC-conjugated secondary antibodies. Labelled cells were examined by LSCM using identical settings for each image. (n = 3).

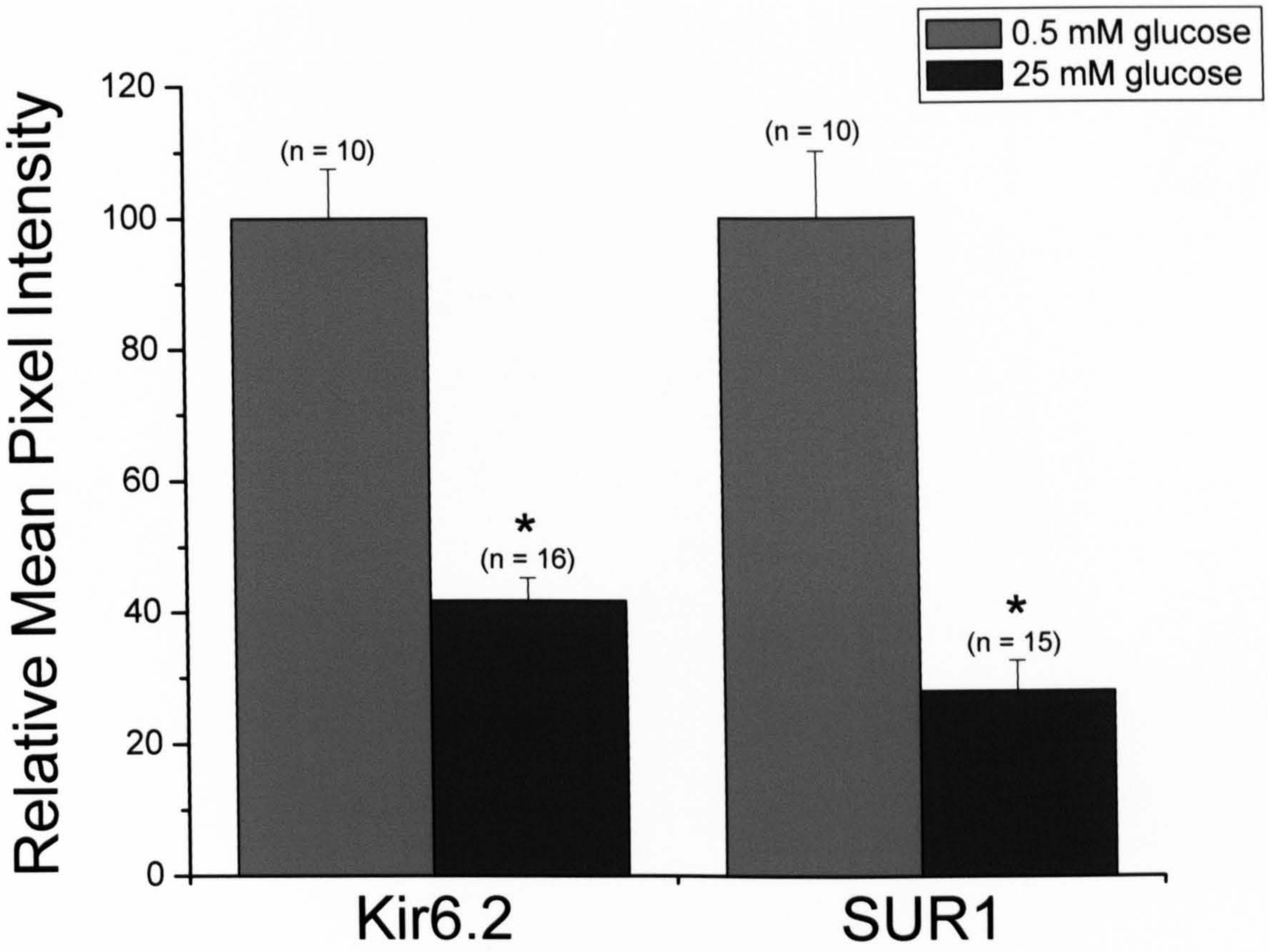

Figure 3.2 - *Mean pixel intensities of INS1e cells incubated in either 0.5 mM or 25 mM glucose for 2 hours.* Mean pixel intensities of cells were measured using ImageJ software (NIH) as described in the methods. (n = number of cells analysed). * = P < 0.01 (unpaired students t-test) - fluorescence intensity of cells incubated in 25 mM compared to those incubated in 3 mM.

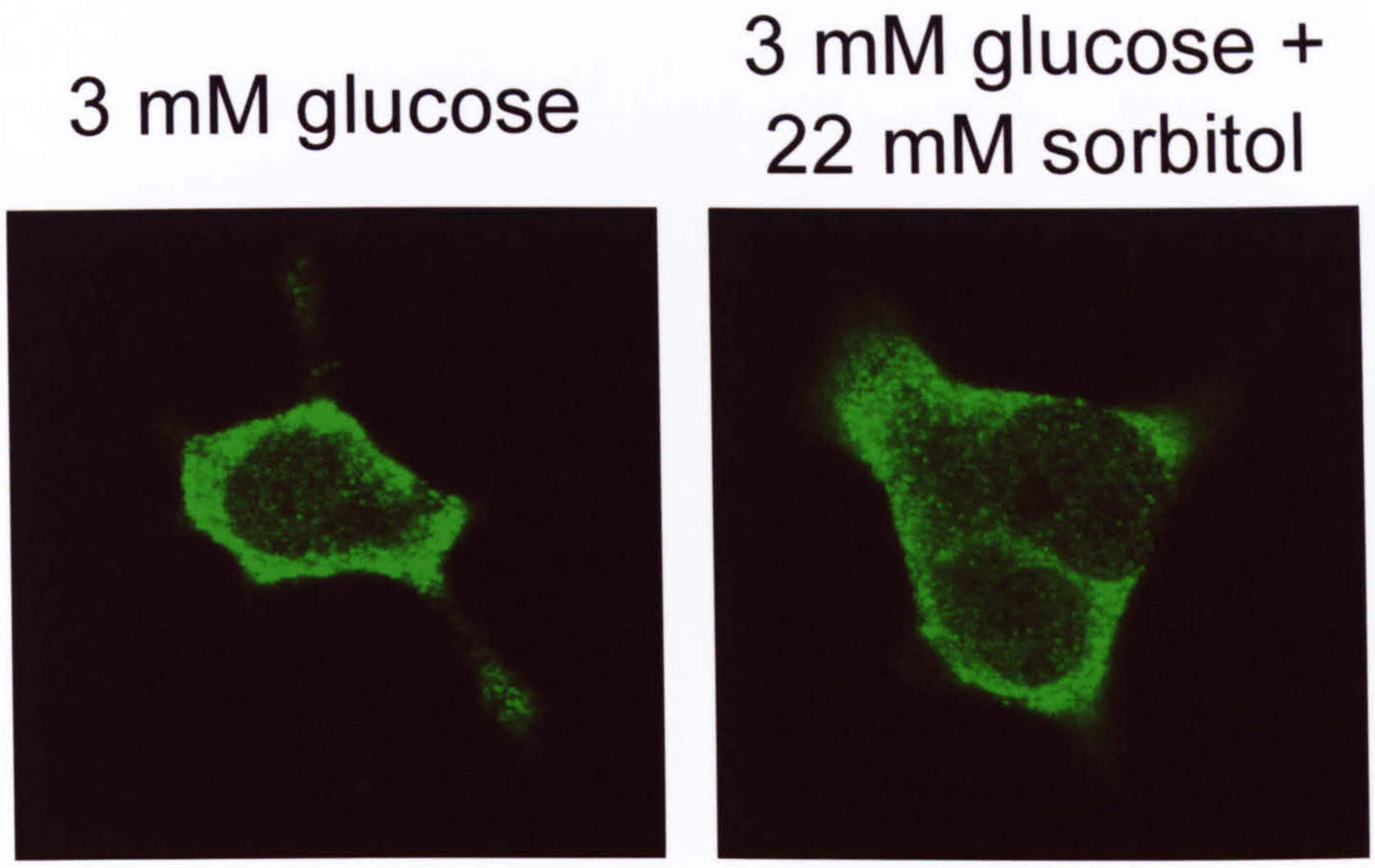

Figure 3.3 - *Altered osmolarity of the medium does not affect K_{ATP} channel expression.* INS1e cells were incubated for 2 hours in media containing either 3 mM glucose of 3mM glucose + 22 mM mannitol. Cells were then stained using anti-SUR1 antibodies followed by FITC-conjugated secondary antibodies. Labelled cells were then examined by LSCM using identical settings for each image. (n = 3)

3.2.3 – Altered K_{ATP} channel expression is specific to glucose responsive pancreatic β-cells

The possibility that glucose regulation of K_{ATP} channel expression is specific to pancreatic β-cells was next investigated. HEK293 cells stably expressing both Kir6.2 and SUR1 which were similarly treated with 3 mM or 25 mM glucose did not show the difference in the intensity of staining seen with INS1e cells (figure 3.4). Also investigated was the possibility that in order to show the differences in K_{ATP} channel expression in response to glucose, the β-cell must also show a responsiveness to glucose with respect to correct glucose stimulated insulin secretion (GSIS). This was made possible by the fact that many, if not all pancreatic β-cell derived cell lines such as RINm, MIN6 and indeed INS1e lose the ability for normal GSIS with prolonged culture and passage (Poitout *et al.* 1996). The glucose responsiveness, measured by the ability for GSIS, of late passage RINm cells were compared to early passage INS1e and the effect of varied glucose concentrations on the expression of K_{ATP} channels examined. Early passage INS1e cells showed robust insulin secretion in response to high glucose. Cells exposed 25 mM glucose secreted ~11 fold more insulin compared to cells exposed 3 mM glucose ($p < 0.01$) (figure 3.5A). Staining of corresponding INS1e cells confirmed that levels of SUR1 were greater in cells incubated with 3 mM glucose compared to those incubated in 25 mM glucose. In contrast, late passage RINm cells showed no significant difference in the levels of insulin secreted between cells incubated in 3 mM and 25 mM glucose ($p > 0.05$). Examination of K_{ATP} channel expression in these RINm cells lacking normal GSIS showed that there appeared to be no difference in the levels of staining when cells incubated in 3 mM glucose were compared to those incubated with 25 mM glucose (figure 3.5).

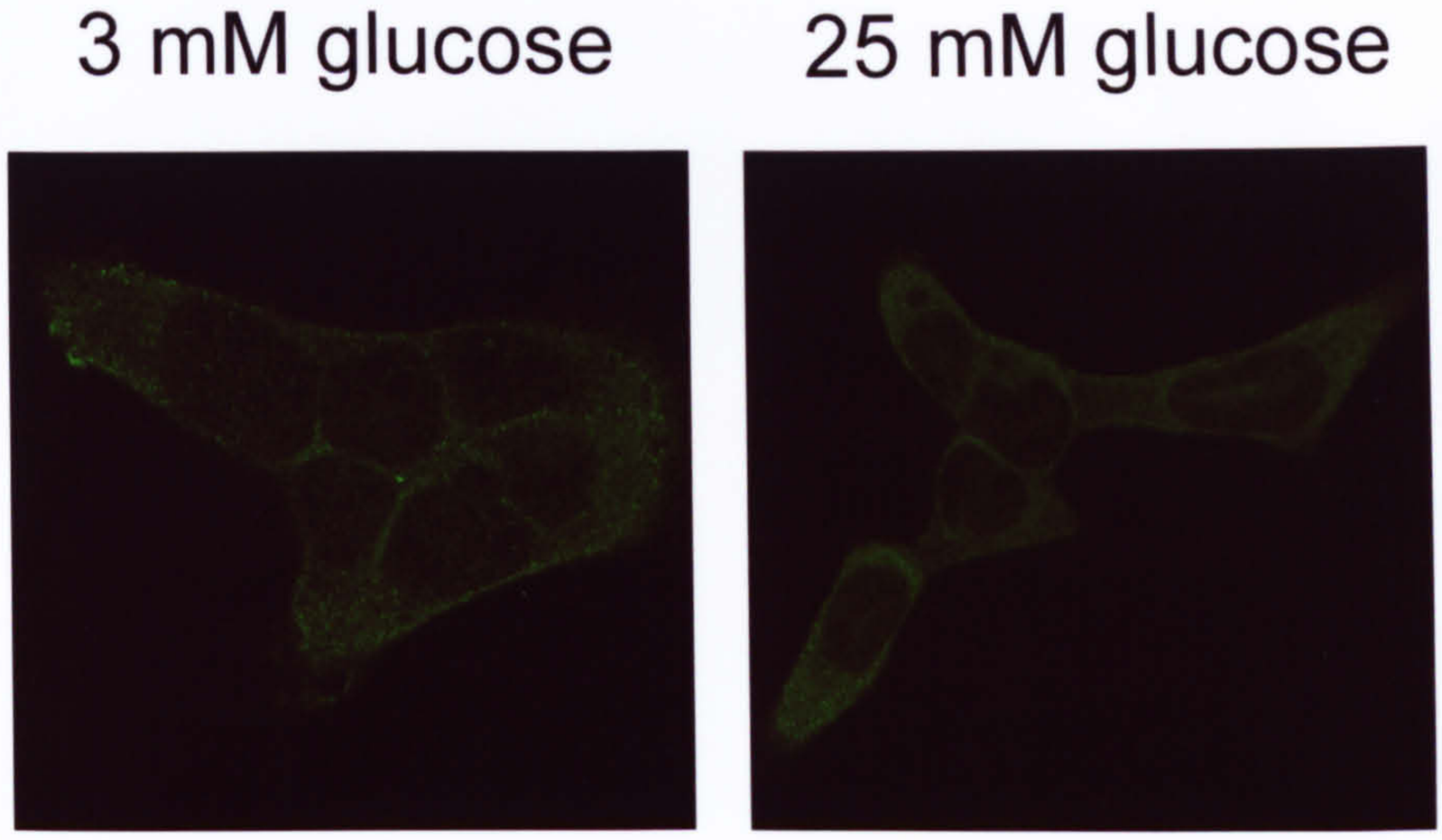

Figure 3.4 - *Expression of K_{ATP} channels in HEK293 cells stably expressing Kir6.2 and SUR1 is not glucose dependent.* Stably expressing HEK293 cells were incubated for 2 hours in media containing either 3 mM glucose or 25 mM glucose. Cells were then stained using anti-SUR1 antibodies followed by FITC-conjugated secondary antibodies. Labelled cells were then examined by LSCM using identical settings for each image. (n = 3)

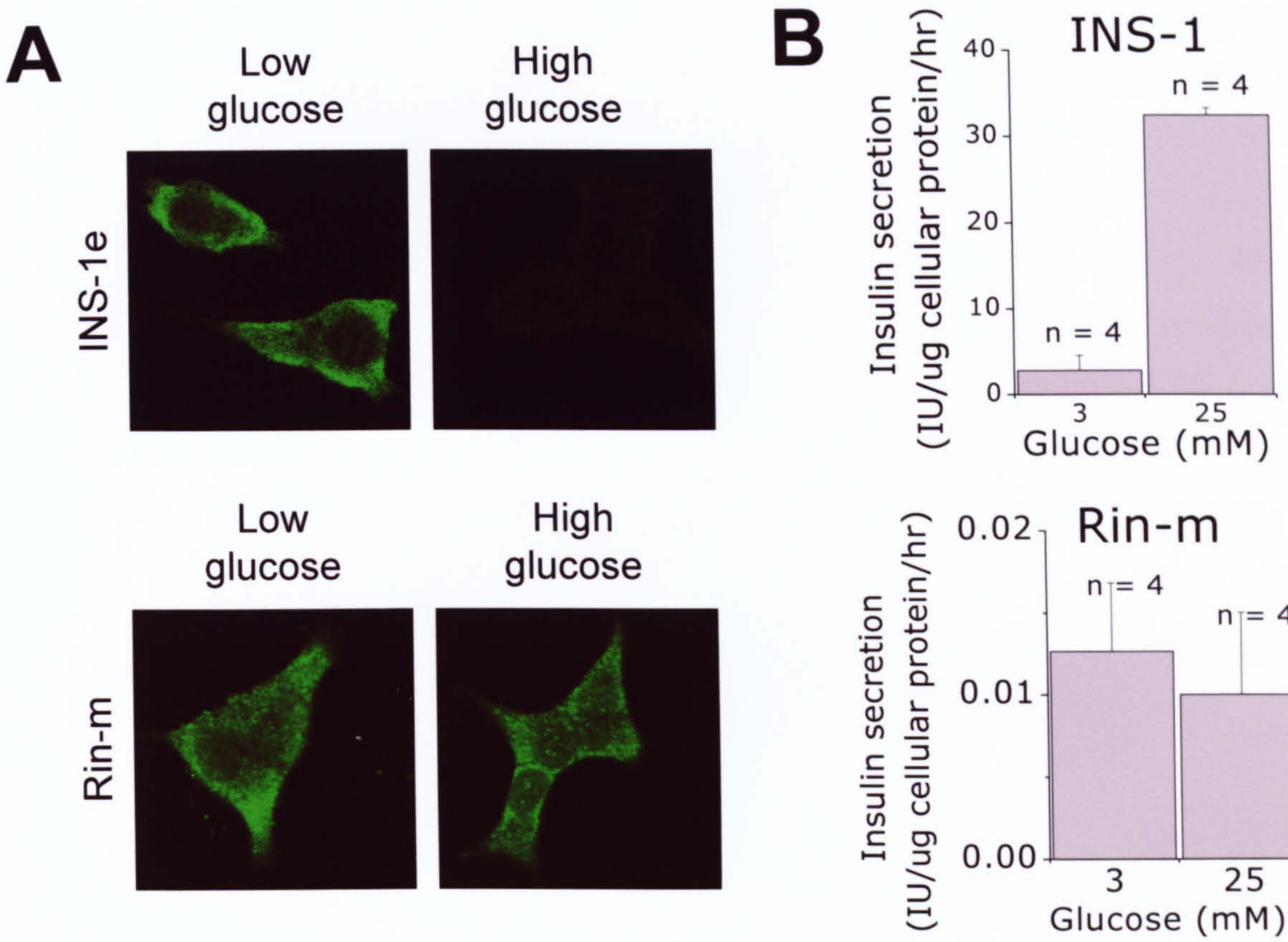

Figure 3.5 - *Glucose mediated regulation of the density of K_{ATP} channels is dependent on the ability of β-cells for GSIS.* **(A)** INS1e and Rin-m cells were incubated in low (0.5 mM) and high (25 mM) glucose for 2 hrs before immunostaining for SUR1. Representative images are shown. **(B)** Glucose induced insulin secretion from INS-1 and Rin-m cells. Cells were incubated in 3 mM or 25 mM glucose for 2 hr and the amount of insulin secreted into the medium was assayed. The data represent the mean ± s.e.m of three independent experiments. (n = 3).

3.2.4 – Time-course of K_{ATP} appearance and disappearance in response to changes in ambient glucose concentration

Next to be investigated was whether the increased levels of K_{ATP} channels in cells incubated in low glucose was due to either an increase in the rate of channel synthesis or due to a decrease in the rate of channel degradation. To achieve this INS1e cells were first cultured overnight in either 3 mM or 25 mM glucose in order to achieve a steady state level of channel expression. The culture medium bathing the cells was then switched for media containing the opposite glucose concentration, i.e. cells previously incubated in 25 mM glucose were switched to media containing 3 mM glucose, and vice-versa. Following incubations of the desired duration in media containing the second glucose concentration the cells were fixed and stained as described previously. Cells incubated in 25 mM glucose overnight showed very low levels of expression prior to incubation with 3 mM glucose (figure 3.6). Following switch to 3 mM glucose levels of fluorescence increased very rapidly, with cells incubated for only 15 minutes showing noticeably increased fluorescence. The intensity of fluorescence continued to increase for the duration of the experiment.

Cells incubated in 3 mM glucose overnight showed high levels of fluorescence. Following the switch to 25 mM glucose however the levels of fluorescence decreased, albeit relatively slowly (figure 3.7).

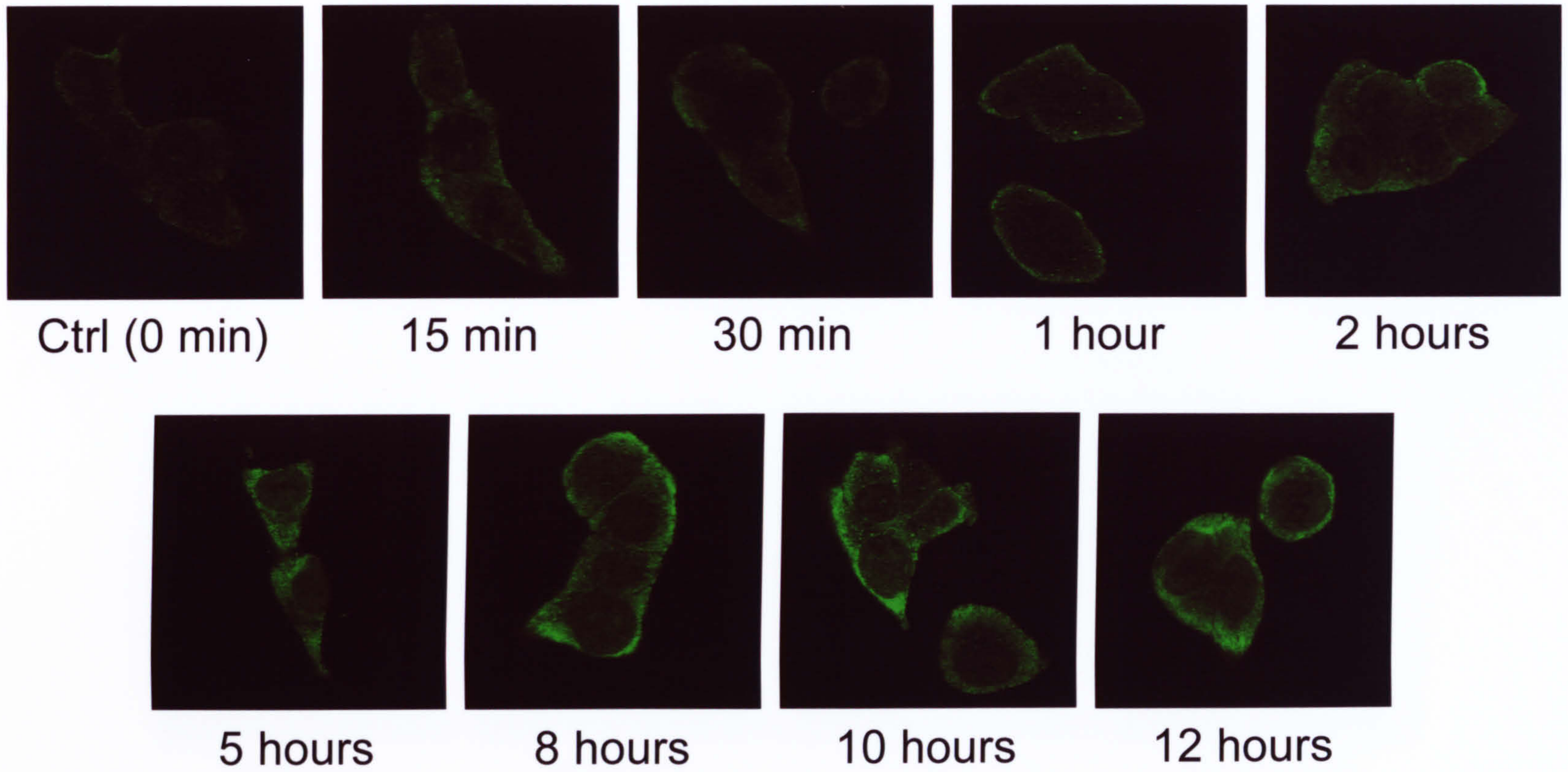

Figure 3.6 - *K_{ATP} channel expression increases rapidly following a switch from high to low glucose concentrations.* INS1e cells were incubated overnight in media containing 25 mM glucose before incubation with 3 mM glucose for the stated length of time. K_{ATP} channel subunits were then visualised using anti-SUR1 antibodies followed by FITC-conjugated secondary antibodies. Labelled cells were examined by LSCM using identical settings for each image. (n = 3).

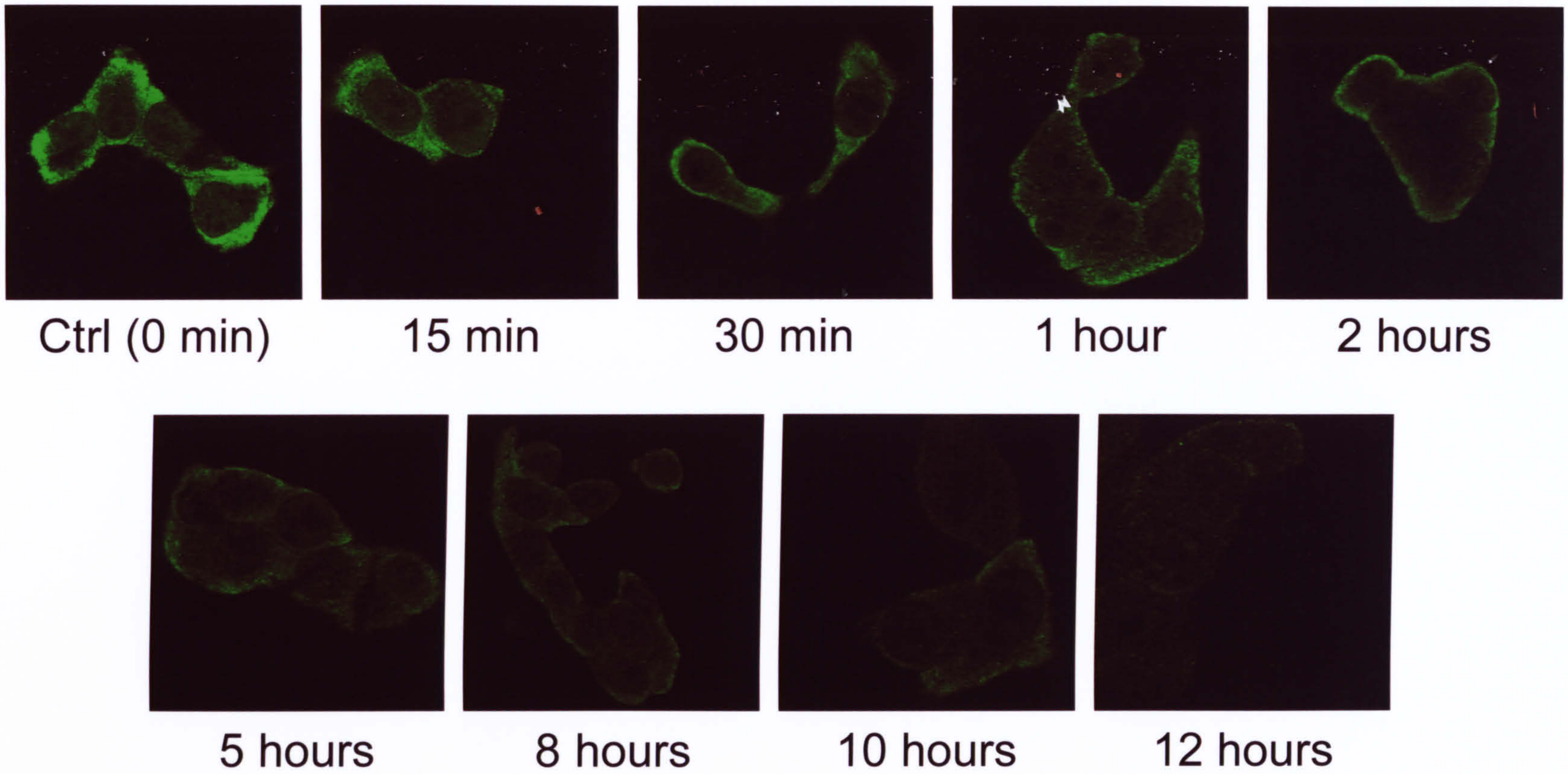

Figure 3.7 - *K_{ATP} channel expression decreases relatively slowly following a switch from low to high glucose concentrations.* INS1e cells were incubated overnight in media containing 3 mM glucose before incubation with 25 mM glucose for the stated length of time. K_{ATP} channel subunits were then visualised using anti-SUR1 antibodies followed by FITC-conjugated secondary antibodies. Labelled cells were examined by LSCM using identical settings for each image. (n = 3).

The data presented above suggest that the elevated intensity of fluorescence in cells incubated in low glucose concentrations may be due to an increase in the rate of channel synthesis. It is also apparent that the rate of channel synthesis is very rapidly increased following the switch from high to low glucose. The initial rate of channel synthesis following the initiation of low glucose incubation was therefore tested using a biochemical method. Briefly, INS1e cells were incubated in either high or low glucose conditions before switching to media containing either the same glucose concentration or to the opposite glucose concentration. The media used was deficient in cysteine and methionine and for the second incubation was supplemented with [^{35}S] methionine to label newly synthesized proteins. The labelled channel subunits were then isolated by immuno-precipitation with anti-SUR1 antibodies, separated by SDS-PAGE and examined by fluorography. Samples from cells incubated in 25 mM glucose overnight (O/N) followed by incubation with 3 mM glucose showed a very rapid increase in the amount of radiolabelled protein, with detectable bands apparent as early as 2 minutes following the switch to low glucose. Three major bands are evident with predicted sizes of (KDa) ~ 220, ~170, ~ 47. The bands of ~ 220 and ~ 170 KDa are thought to correspond to the mature glycosylated and immature non-glycosylated forms of SUR1 respectively, whereas the band at ~ 47 KDa is thought to represent Kir6.2 since SUR1 is predicted to be 177 KDa and Kir6.2 to be 44 KDa in size. However, from the literature, the sizes of bands corresponding to either the mature and immature forms of SUR1 and Kir6.2 vary quite considerably (Conti *et al.* 2002, Crane & Aguilar-Bryan 2004). In this case, since the sizes of the observed bands are so close to the predicted sizes and that they are only observed in samples where increased protein synthesis might be expected it has been assumed that these bands do indeed correspond to SUR1 and Kir6.2. Generally, the intensity of all bands increased with time but the comparative intensity of the two SUR1 bands changed from more immature-SUR1 at the earliest time points (< 5 minutes) to more mature-SUR1 at the later time points (> 5 minutes) as might be expected due to protein maturation. The intensities of the Kir6.2 and mature-SUR1 bands also appear to increase in parallel throughout, suggesting that the expression of both SUR1 and Kir6.2 may be very closely linked via a common mechanism. In addition to this, that both SUR1 and Kir6.2 are retrieved by immunoprecipitation with anti-SUR1 antibodies suggests that these newly formed subunits are rapidly assembled into

hetero-oligomeric channels, even as rapidly as two minutes following glucose depletion (figure 3.8 *top left panel*).

In contrast to the above results, no significant stimulation of the radiolabel incorporation into the channel subunits occurred during other conditions, that is when cells were shifted from 3 to 25 mM or from 25 to 25 mM, or even from 3 to 3 mM glucose. These data suggest that the channel synthesis is stimulated only in response to a sudden decline in glucose concentration; under other conditions channel synthesis is either switched off or occurs very slowly (figure 3.8 *other panels*). Synthesis of channel subunits over a longer time course has not been investigated using this approach.

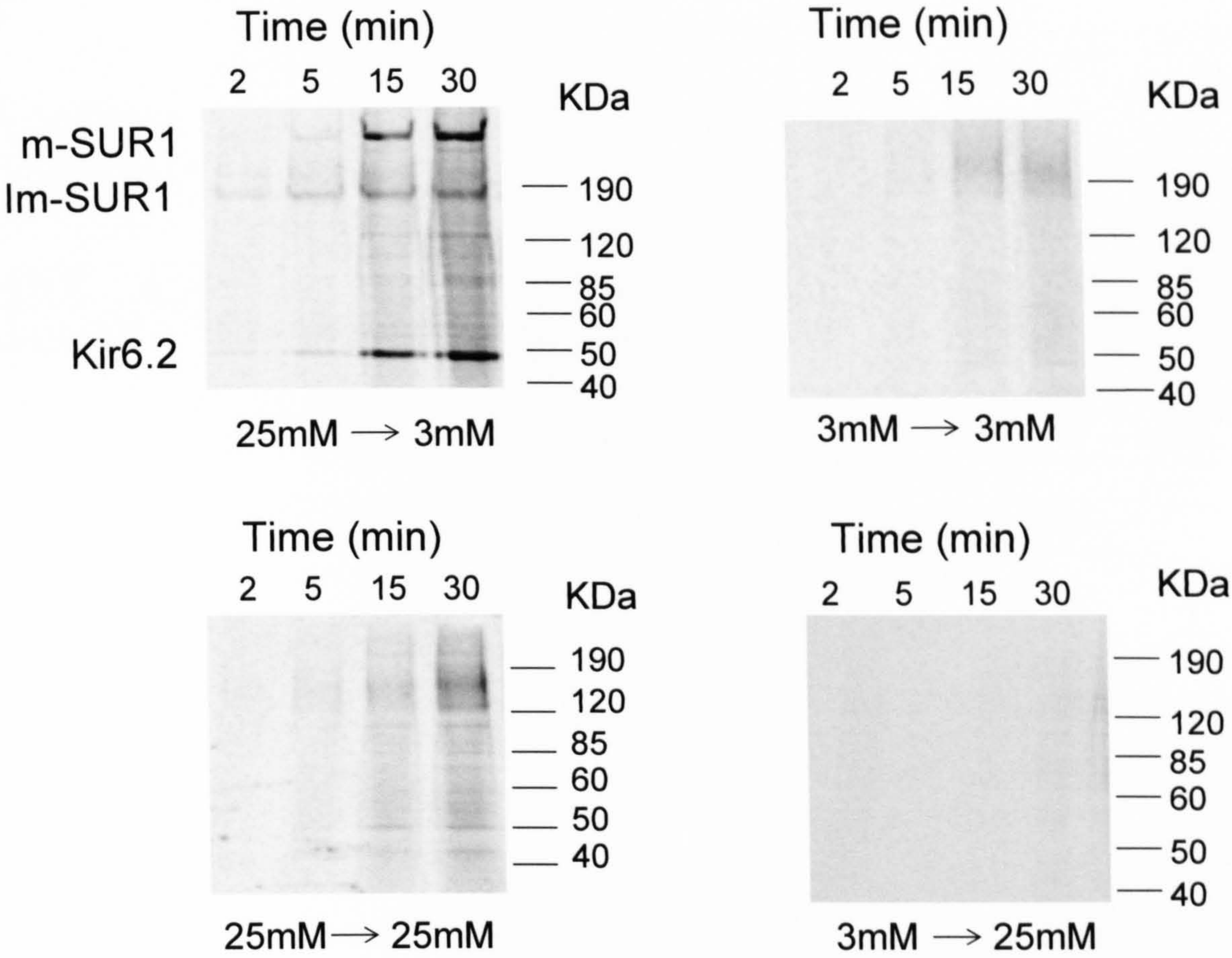

Figure 3.8 - *Pulse labelling of INS1e cells demonstrates a rapid increase in K_{ATP} channel synthesis stimulated by low glucose.* INS-1e cells were incubated overnight (16 hrs) in media containing the indicated pre-incubation glucose concentration (25 or 3 mM; corresponds to the first number at the bottom of each panel) before switching to cysteine/methionine deficient media containing the same glucose concentration for 30 min. The cells were then switched to media containing the test glucose concentration (3 or 25 mM, as indicated by the second number at the bottom of each panel) plus 200 μCi of [^{35}S]methionine. At the indicated time points, incorporation of [^{35}S]methionine into newly synthesised proteins was terminated, the radiolabelled K_{ATP} channels were immunoprecipiated from the cell lysates with anti-SUR1 antibodies, and subjected to SDS-PAGE (5-15% gradient gel) and fluorography. Representative phosphorimages are shown (n = 3).

3.2.5 – The rapid increase in K_{ATP} channel expression is due to an increase in the rate of translation and not transcription

An increase in protein synthesis can be brought about in two ways; either by producing more mRNA encoding the protein of interest by increasing the rate of transcription, or by increasing the rate of translation by utilising the existing mRNA more efficiently. Whether the increase in K_{ATP} channel expression in response to low glucose observed here is due to an increase in transcription or translation was therefore investigated using pharmacological agents to selectively inhibit either transcription or translation. Briefly, INS1e cells were incubated in media containing either 3 mM or 25 mM glucose overnight before being switched to media containing the opposite glucose concentration supplemented with various inhibitors of transcription or translation.

INS1e cells treated with either α-amanitin (5 μg ml^{-1}) or actinomycin D (1 μg ml^{-1}), both inhibitors of transcription, displayed a response to glucose comparable to that of untreated cells, with greater levels of fluorescence in the cells incubated in 3 mM glucose compared to those incubated in 25 mM glucose (figure 3.9). By contrast, cells treated with the translational inhibitor cycloheximide (25 μg ml^{-1}) showed much lower levels of fluorescence in the cells incubated with 3 mM glucose compared to the untreated cells. Indeed, the level of fluorescence in these cells was comparable to that observed in cells incubated with 25 mM glucose, suggesting that addition of cycloheximide had impaired the normal response to low glucose. In these cells, whilst the level of staining near the periphery of the cell remained relatively high, the intensity of the staining throughout the majority of the cytoplasm was clearly reduced in a similar fashion to the cells incubated in high glucose in figure 3.1. These data therefore suggest that the increase in K_{ATP} channel expression is due to an increase in the rate of translation and not transcription. If this is indeed true an examination of the levels of mRNA encoding either of the K_{ATP} channel subunits should show no difference in cells incubated in either 3 mM or 25 mM glucose. In order to investigate this, probes were designed against SUR1 to be used in northern blot analysis. As shown in figure 3.10, northern blot analysis of lysates of INS1e cells showed no difference in the levels of SUR1 mRNA isolated from cells treated with 3 mM or 25 mM glucose using two separate sets of probes. Densitometric analysis of the data showed no significant difference ($p > 0.05$) in the SUR1 mRNA content

(expressed as mean ± s.e.m. of SUR1/actin ratio) of cells treated with 3 mM glucose (3.00 ± 0.27) from that of 25 mM glucose (3.14 ± 0.4).

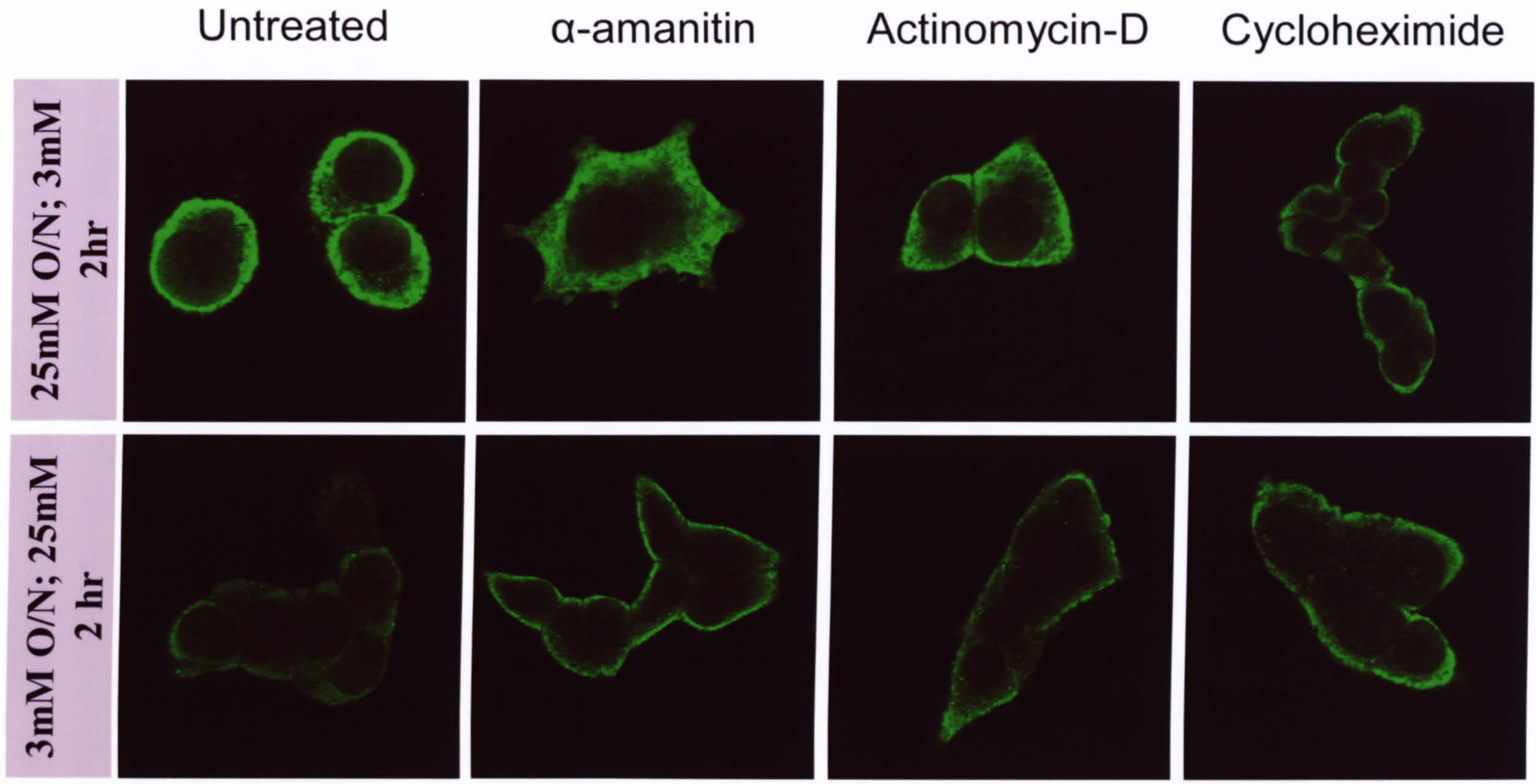

Figure 3.9 - *Inhibition of translation, but not transcription, inhibits the increase in K_{ATP} channel expression associated with low glucose.* INS-1 cells were pre-incubated overnight (16 hr) in media containing glucose as described. For the final 4 hours of this incubation media was supplemented with either α-amanitin (5 μg/ml), actinomycin-D (1 μg/ml) or cycloheximide (25 μg/ml) followed by a further 2 hr incubation in medium containing the second glucose concentration, supplemented with the relevant pharmacological agent. Cells were then fixed, permeabilised and stained using anti-SUR1 antibodies followed by FITC-conjugated secondary antibodies. Labelled cells were then examined by LSCM using identical settings for each image. (n = 2).

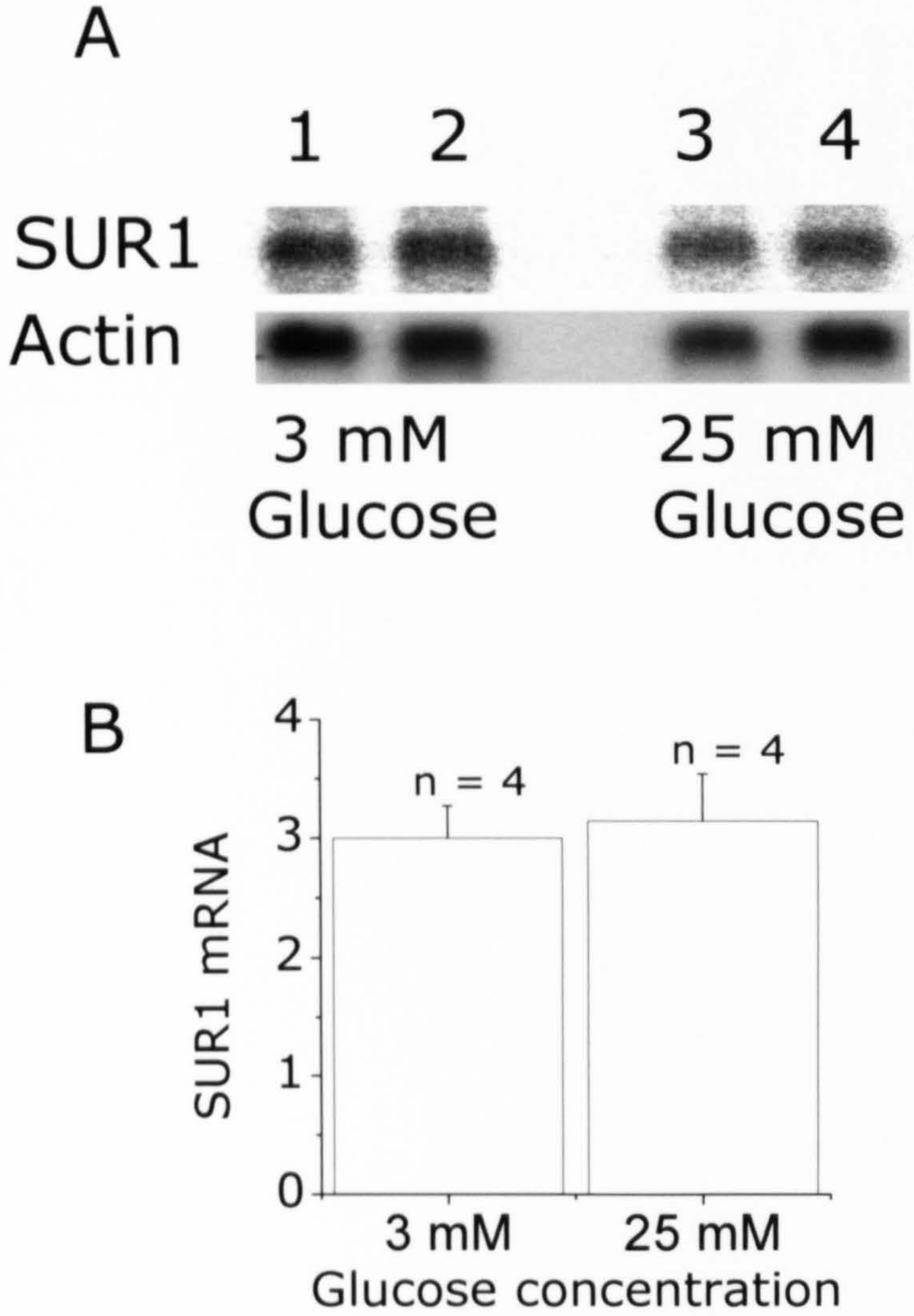

Figure 3.10 - *Northern blot analysis of SUR1 mRNA reveals no change in response to glucose.* **A** - Northern blots of total RNA isolated from INS-1e cells incubated in 3 mM (lanes 1,2) or 25 mM (lanes 3,4) glucose, showing the SUR1 and actin bands; data generated from RNA isolated two separate flasks of cells are shown for each glucose concentration. **B** - shows mean ± s.e.m (n =4) of SUR1 mRNA, normalised to actin mRNA band intensity; $P > 0.05$ (Student two-tailed t-test). *Northern blotting was performed by Dr A. Asipu (St James' University Hospital, Leeds)*

3.2.6 – Cell surface channel density is unaffected by glucose

An important question to address is whether the apparent increase in K_{ATP} channel expression in INS1e cells is translated into a concomitant increase in the density of channels at the cell surface. Since the vast majority of the fluorescent staining appeared to be cytoplasmic it was impossible to determine if such a difference existed. The cell surface density of K_{ATP} channels was therefore determined by electrophysiological means by functionally assaying whole cell currents using the patch-clamp technique. Recordings were taken from cells, which had previously been pre-incubated in media containing either 3 or 25 mM glucose, perfused with bath solution containing the same glucose concentration. Maximal K_{ATP} channel currents were elicited by the addition of diazoxide and were subsequently inhibited by addition of tolbutamide (figure 3.11 *A* + *B*). The maximal amplitude of the diazoxide-stimulated tolbutamide-sensitive currents, corresponding to K_{ATP} channel specific currents, were normalised to the capacitance of the cell (which provides a measure of cell surface area) to obtain an estimate of cell surface channel density. Whilst cells incubated in 3 mM glucose showed a higher mean density of channels at the cell surface (636 ± 125 pA/pF; n = 7) compared to those incubated with 25 mM glucose (428 ± 70 pA/pF; n = 8), the difference was not deemed to be statistically significant ($P > 0.1$) (figure 3.11 *C*).

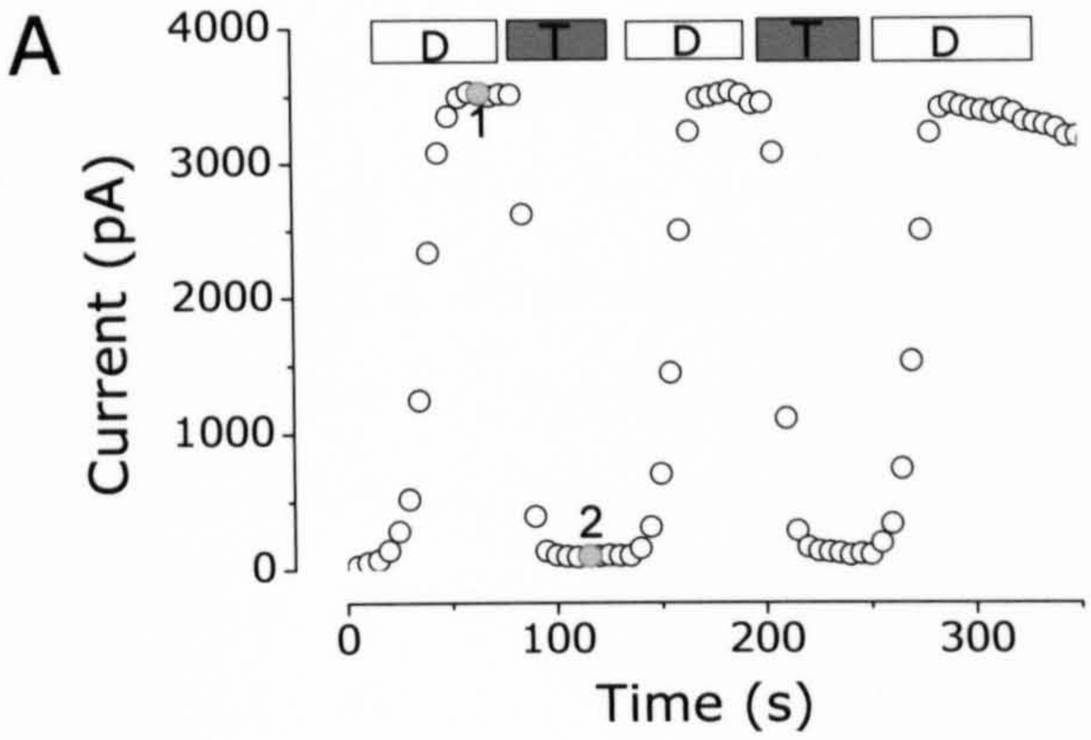

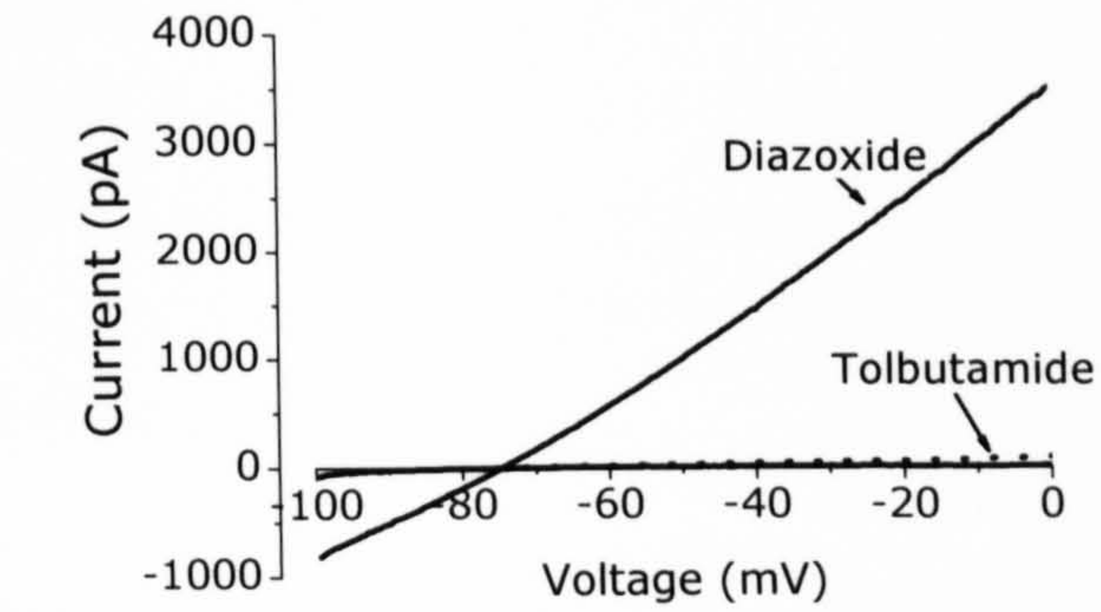

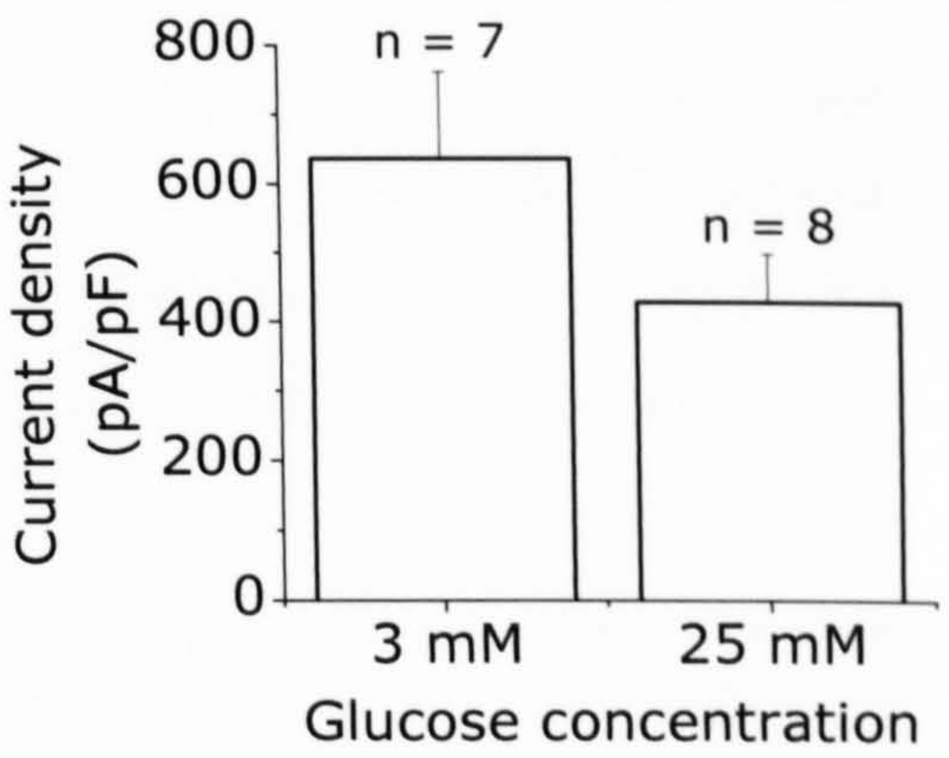

Figure 3.11 - *The cell surface density of K_{ATP} channels is unaffected by changes in glucose.* **A-B**, K_{ATP} channel currents measured from INS-1 cells cultured in 3 mM glucose. Currents were measured in the whole cell patch clamp configuration. Data points represent currents measured at 0 mV during perfusion of bath solution alone or bath solution supplemented with diazoxide (D) or tolbutamide (T), as indicated by horizontal bars. B shows current-voltage relationships measured during the application of diazoxide or tolbutamide, corresponding to time points (gray filled circles) labelled 1 and 2 in A. **C**. Histogram of mean ± s.e.m of currents from cells incubated in 3 and 25 mM glucose as indicated. *Whole cell patch-clamp was performed by Dr M. Hunter (School of Biomedical Sciences, University of Leeds)*

3.2.7 – The increase in K_{ATP} channel expression in low glucose may involve the activation of AMPK

For the expression of K_{ATP} channels to be affected by changing glucose concentrations, a metabolic sensor must be involved to sense the changes in glucose and then to translate this into a signal that the cell can recognize to initiate the increase in expression. Studies into the glucose regulated expression of a number of other proteins, for example pre-proinsulin and L-type pyruvate kinase (de Silva Xavier *et al.* 2000a) have lead to the identification of AMP-activated protein kinase (AMPK) as a possible candidate for this role (de Silva Xavier *et al.* 2000b). AMPK is a serine / threonine protein kinase which is activated by depletion of ATP and increase of AMP. It has recently been described as a "metabolic master-switch" responsible for down-regulating high energy demand processes within cells when metabolism is slowed. Whether this role extends to protecting the cell from low glucose by stimulating pathways which will actively act to protect from the effects of low glucose, like upregulating the expression of K_{ATP} channels in the pancreatic β–cell has yet to be shown.

The activity of AMPK in INS1e cells was stimulated by the addition of either 5-Aminoimidazole-4-carboxamide 1-b-D-ribofuranoside (AICAR) or the anti-diabetic drug metformin, both potent and selective activators of AMPK, but with varying mechanisms of action (Henin *et al.* 1996, Zhou *et al.* 2001). Addition of either agent to cells incubated in 3 mM glucose produced no effects on the level of observed fluorescence compared to untreated cells. However, when cells incubated in 25 mM glucose were exposed to either AICAR or metformin the levels of fluorescence were comparable to those observed in cells incubated in low glucose and noticeably higher than those cells incubated in 25 mM glucose alone (figure 3.12). These data suggest that activation of AMPK by low glucose may be central to the increase in K_{ATP} channel expression observed in INS1e cells.

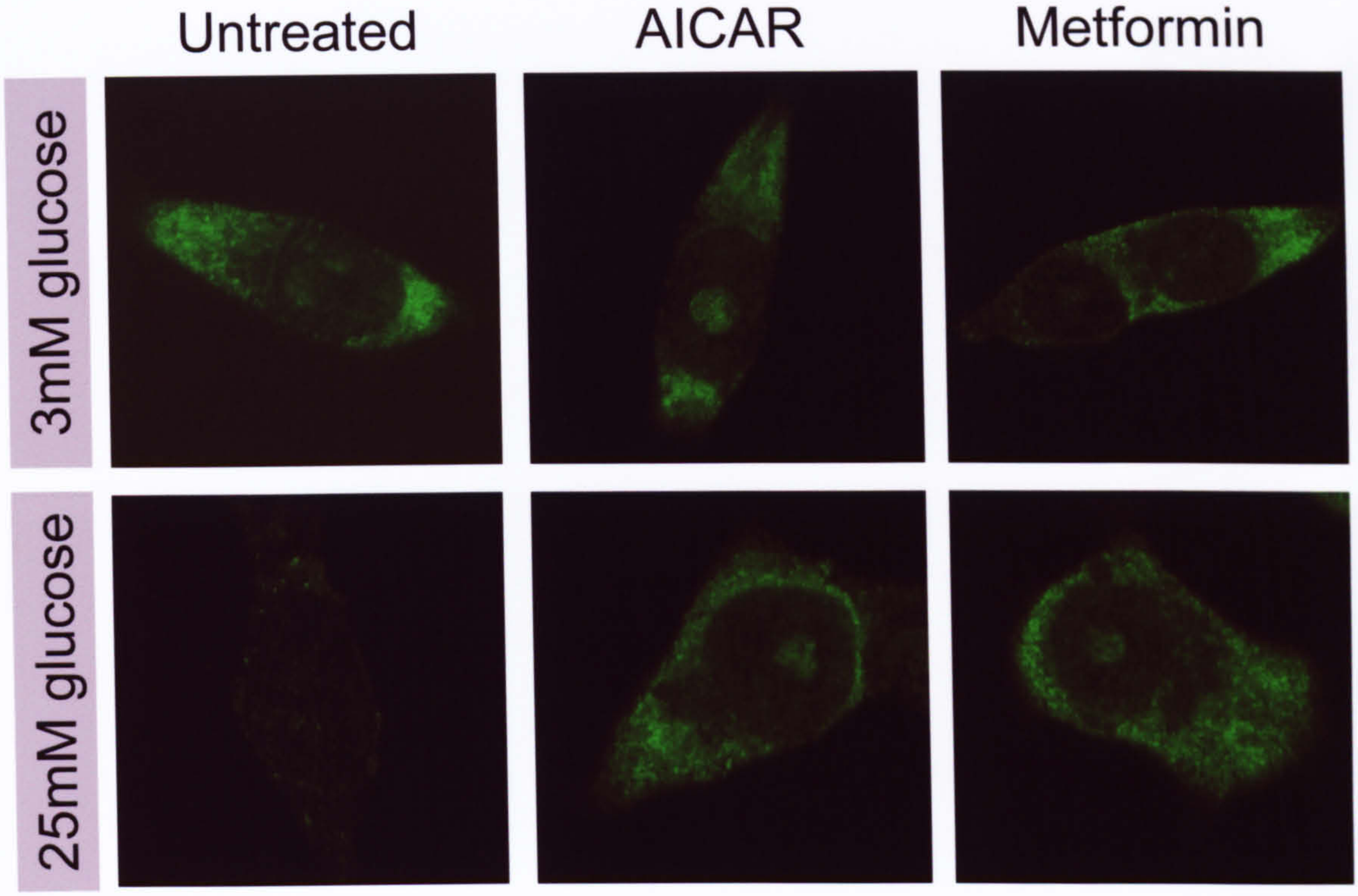

Figure 3.12 - *Pharmacological activation of AMPK mimics the effect of low glucose on the expression of K_{ATP} channels in INS1e cells.* INS1e cells were incubated for 2 hours in media containing either 3 mM glucose or 25 mM glucose supplemented with AICAR (0.5 mM) or metformin (0.5 mM) as required. Cells were then stained using anti-SUR1 antibodies followed by FITC-conjugated secondary antibodies. Labelled cells were then examined by LSCM using identical settings for each image. (n = 3)

3.2.8 – K_{ATP} channel expression is regulated by glucose in isolated mouse pancreatic β-cells

As a model system for pancreatic β–cells, INS1e cells are largely suitable for most purposes. However, during the establishment and subsequent long-term culture of these immortal model cell lines some aspects of normal β–cell function may be distorted or lost altogether, and some new traits not representative of native β–cells may arise (Minami *et al.* 2000, Rustenbeck 2002). In order to confirm that the data obtained in INS1e cells are indeed representative of native cells it was decided to repeat the key findings in β–cells freshly isolated from mouse pancreas. Following removal of the whole pancreas from freshly killed mice and subsequent collagenase digestion, whole islets were isolated from the surrounding exocrine tissue. These intact islets were further disrupted by gentle trypsin treatment to yield a suspension of islet cells including β–cells, but also α–cells and δ–cells. For the purposes of the experiments, the β–cells were counterstained with anti-insulin antibodies and in this way were easily distinguishable from the other cell types. It was also apparent that β–cells always appeared as more spherical in shape compared to other cell types which appeared flatter with more pronounced projections (figure 3.13).

Two strains of mice were used for the islet isolations. The first strain, BALB/c, is a popular, inbred mouse strain which has been used extensively for all areas of biomedical research. The second strain, C57bl/6J, is perhaps the most popular mouse model used in biomedical research. Recent research has shown that islets from the C57bl/6J mice show impaired insulin secretion in response to glucose which becomes more pronounced when fed on a high fat diet (Kaku *et al.* 1988, Surwit *et al.* 1988, Kooptiwut *et al.* 2002). Because of this, isolated β-cells from each strain were used to investigate the effect of low glucose on K_{ATP} channel expression.

Pancreatic β-cells isolated from BALB/c mice showed much higher levels of anti-SUR1 fluorescence in cells incubated in 3 mM glucose compared to those incubated in 25 mM glucose. This difference was comparable to that observed in INS1e cells. By contrast, β-cells isolated from C57bl/6J mice showed a difference in fluorescence which was far less pronounced than that observed with either INS1e cells or β-cells isolated from BALB/c mice (figure 3.14).

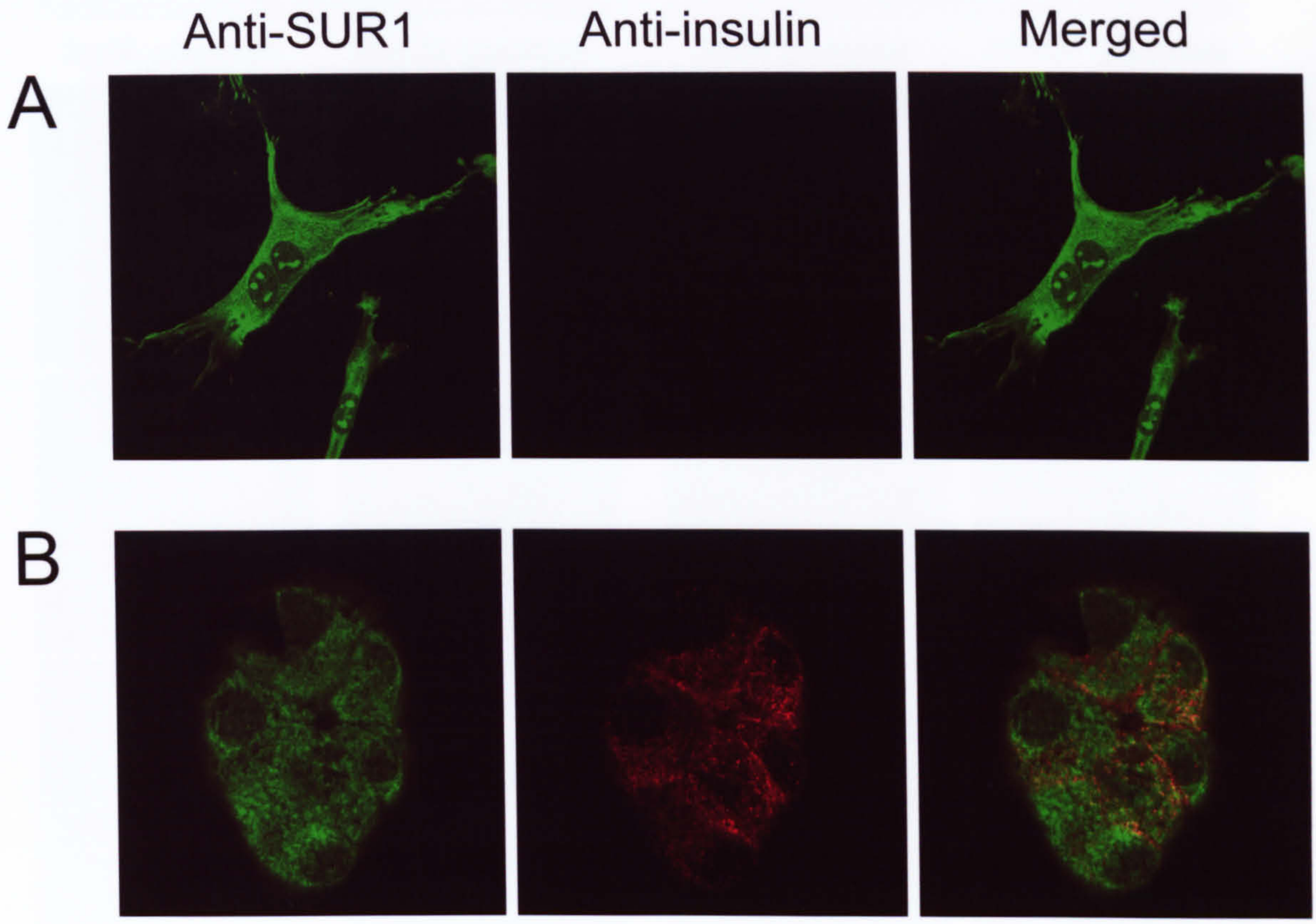

Figure 3.13 - *Pancreatic β-cells from isolated mouse islets can be easily distinguished from surrounding cells.* Isolated cells from pancreatic islets were stained using rabbit anti-SUR1 antibodies followed by FITC-conjugated anti-rabbit secondary antibodies and with mouse anti-insulin antibodies followed by Cy3-conjugated anti-mouse secondary antibodies. **(A)** - Non β-cell type cells not stained with anti-insulin antibodies. **(B)** - β-cells stained by anti-insulin antibodies. Cells were viewed by LSCM. (n = 2).

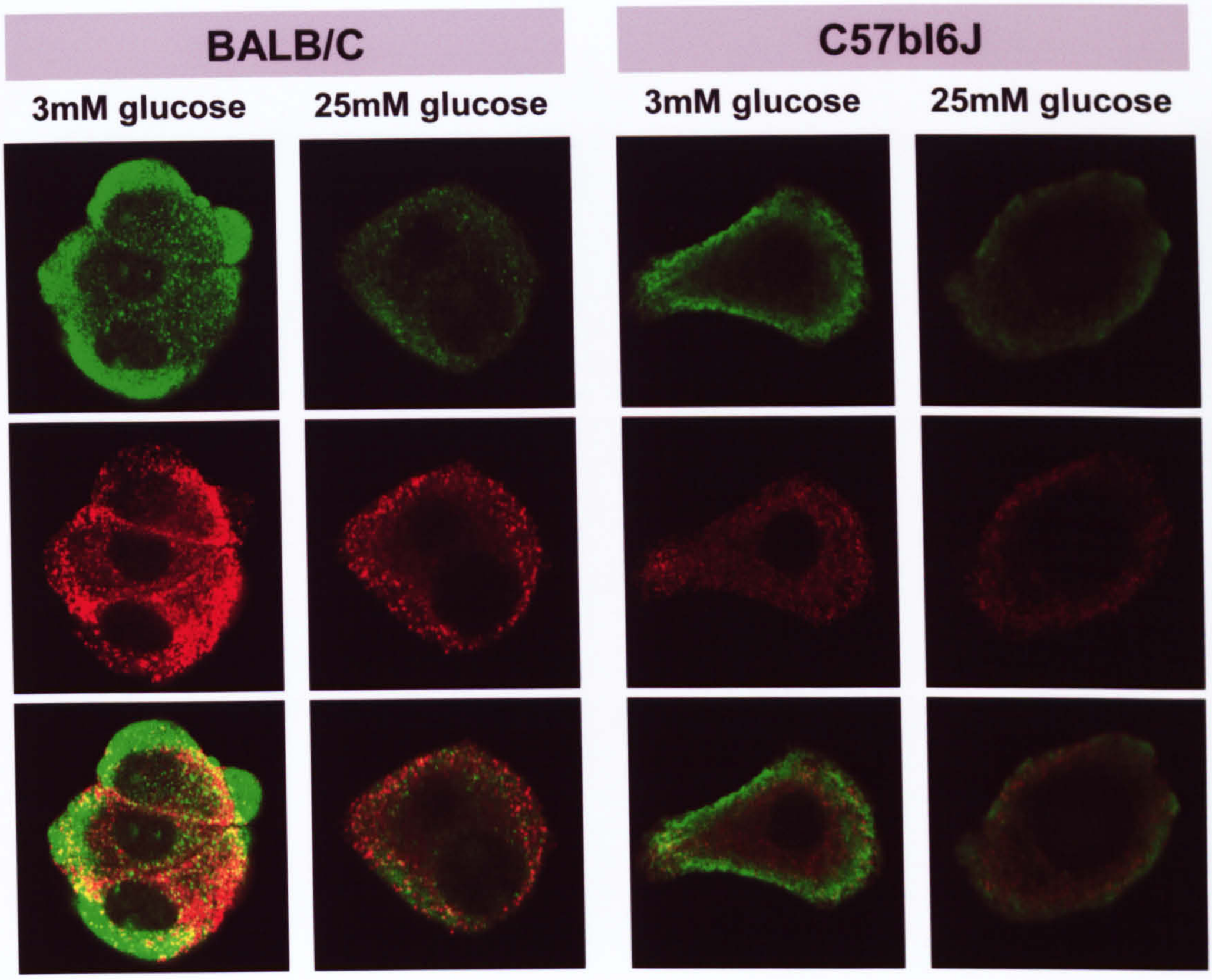

Figure 3.14 - *Glucose regulates the expression of K_{ATP} channels in β-cells of BALB/c mice, but not in C57bl/6J mice.* Cells from pancreatic islets isolated from either C57Bl6/J or Balb/C mice were incubated for 2 hours in media supplemented with either 3 mM or 25 mM glucose. They were then stained using rabbit anti-SUR1 antibodies followed by FITC-conjugated anti-rabbit secondary antibodies and with mouse anti-insulin antibodies followed by Cy3-conjugated anti-mouse secondary antibodies. Cells were viewed by LSCM using identical settings for each image. (n = 1).

3.3 - Discussion

3.3.1 - Overview

Described here is evidence to suggest that the expression of the pancreatic K_{ATP} channel is regulated by glucose. When incubated in low glucose, pancreatic β-cells are shown to increase the overall level of K_{ATP} channel subunits rapidly, not by increasing the rate of transcription, but by increasing the rate of translation of pre-existing mRNA (figures 3.1 - 3.10). It is also apparent that this regulation of K_{ATP} channel expression by glucose is specific for pancreatic β-cells which exhibit normal insulin secretory responses to elevated glucose levels, since the characteristic increase in expression was not observed in either HEK293 cells stably expressing K_{ATP} channels or more importantly pancreatic β-cells which have lost their ability to secrete insulin correctly (figure 3.5 and figure 3.14). Further to this it appears that this effect may be regulated by modulation of the activity of AMPK.

3.3.2 - Glucose regulation of expression

A number of groups, whose work is described below, have investigated the possibility that glucose may affect the expression of K_{ATP} channels in pancreatic β-cells. These studies however were limited to investigating the effect of glucose on the level of mRNA encoding Kir6.2 and SUR1 within cells which were chronically exposed to varying concentrations of glucose. Due to a wide range of cell types used, ranging from different model β-cell lines (e.g. INS, MIN6) to intact islets form different species (mouse, human), and the diverse range of culture conditions and durations of treatment, it is difficult to draw many conclusions as to the role which glucose may be playing in regulating K_{ATP} channel expression. For example, Shalev *et al.* (2002) suggested that incubation of intact isolated human islets in high glucose for 24 hours had no effect on SUR1 mRNA levels compared to those islets incubated in low glucose, as assayed by RT-PCR. In contrast, Moritz *et al.* (2001) reported that INS1 cells showed a ~70 % decrease in the levels of both Kir6.2 and SUR1 mRNA when incubated for 72 hours in high glucose compared to those cells incubated in low glucose, using northern blot analysis. Another study by Wang *et al.* (2002) demonstrated that mRNA levels in INS1e cells for either Kir6.2 of SUR1 were not affected by brief (8 hour) exposure to elevated glucose content of the culture medium. The findings of this third study support the findings of the present study, where brief

(2 hour) exposure to 25 mM glucose had no effect on the level of SUR1 mRNA as shown in figure 3.10. This may suggest that acute changes in glucose concentrations have no effect on the level of K_{ATP} channel mRNAs, whereas more prolonged exposure to elevated glucose may cause a reduction in these mRNA levels. This is supported by the observation that induced diabetes in mice, with associated long-term hyperglycaemia, leads to a marked reduction in K_{ATP} mRNAs (Jonas *et al.* 1999).

To my knowledge this is the first report describing glucose regulated expression of a protein by modulation of the rate of translation in preference to transcription. All other examples of glucose responsive genes from the literature describe changes in the rate of mRNA synthesis by the transcription of the gene of interest (Permutt *et al.* 1972, Vaulont *et al.* 1986, Asano *et al.* 1992, Marie *et al.* 1993, Roche *et al.* 1997). In this way, it would appear that the mode of regulation of pancreatic K_{ATP} channel expression in response to acute changes in glucose is at the present time unique. Similar mechanisms have, however, been previously described in other systems where nutrient supply must be tightly regulated (Eisenstein 2000). The expression of both ferritin and transferrin are regulated by changes in iron availability, and this has been shown to be via regulation at the translational level. When iron is particularly abundant the cell responds to an increase in cytosolic iron concentrations by increasing the synthesis of the iron binding protein ferritin and a parallel decrease in the synthesis of the plasma membrane iron transporter, transferrin receptor. When iron availability is low the opposite is true, with synthesis of ferritin slowed and transferrin receptor synthesis greatly increased in order to import more iron into the cell. It has been shown that these two responses are mediated by the action of a single iron-responsive regulatory protein, aconitase, which recognises and binds to common features in the mRNA structure of both ferritin and transferrin receptor. When iron availability is limited, aconitase is bound to the mRNA of both transferrin receptor and ferritin. Binding of aconitase to the 3'-UTR of transferrin receptor mRNA blocks an endonuclease cleavage site thus stabilising the mRNA allowing increased translation. Binding of aconitase to the 5'-UTR of ferritin mRNA blocks translational initiation thus preventing protein synthesis. When iron becomes abundant it binds to aconitase causing dissociation from the mRNA allowing translation of ferritin and destabilising transferrin receptor mRNA (Hentze *et al.* 1987, Casey *et al.* 1988). The existence of such a mechanism for the regulation of K_{ATP} channel expression is

currently not known but may warrant further examination on the strength of the presented data.

3.3.3 - The role of AMPK in regulating K_{ATP} channel expression

The data presented in figure 3.12 suggests that the increase in K_{ATP} channel synthesis following a switch to low glucose may be mediated by the activation of AMP-activated protein kinase. The lowering of glucose availability to the cells would lead to a lowering of glucose uptake and thus lead to a lowering in the rate of metabolism with a resulting decrease in the ATP / ADP ratio. As well as stimulating the activity of K_{ATP} channels within these cells, the lowering of the ATP / ADP ratio leads to an increase in the levels of AMP because of the action of the enzyme adenylate kinase which attempts to maintain the ATP / ADP ratio by the reaction [2ADP ↔ ATP + AMP] in equilibrium (Hardie & Hawley 2001). The increase in AMP within the cells due to the decrease in glucose availability would be sufficient to stimulate AMPK activity. Indeed several sources report a stimulation of AMPK activity by lowered glucose in pancreatic β-cells over the same concentration range in which insulin release is inhibited (Salt *et al.* 1998, da Silva Xavier *et al.* 2000b). Once active, AMPK has been shown to adapt the cell for short-term survival during periods of low ATP via a number of different mechanisms (see Kemp *et al.* 2003 for review). As a consequence of increased AMPK activity, both gene transcription (Kawaguchi *et al.* 2001, Leclerc *et al.* 2001, Yang *et al.* 2001) and protein synthesis are affected (Bolster *et al.* 2002, Horman *et al.* 2002). Interestingly, since the activation of AMPK tends to halt processes with high ATP demands, processes such as protein synthesis would be expected to be inhibited. It has been shown that an increase in AMPK activity leads to an increase in the activity of protein kinase elongation factor-2 kinase. This in turn leads to increased phosphorylation of elongation factor-2 leading to a decrease in translation (Horman *et al.* 2002, McLeod & Proud 2002). This is contrary to the findings reported in the current study where it appears that AMPK activation mediates an increase in the synthesis of K_{ATP} channel subunits. This could perhaps be attributed to the fact that an increase in K_{ATP} channel density might provide an additional protective mechanism by suppressing insulin secretion following a rapid decrease in glucose concentration and is therefore in some way exempt from the normal mechanisms which serve to prevent processes with high energy demands. A recent report suggests that the activation of AMPK may indeed lead to an increase in

the rate of vascular epithelial growth factor (VEGF) protein synthesis in vascular smooth muscle in response to metabolic stress (Ouchi *et al.* 2005) perhaps supporting the role of AMPK in protecting against metabolic injury. As described earlier (1.3.2) K_{ATP} channels have been proposed to play an important role in protecting against injury during ischemia and it is possible that AMPK may also play a part in this protective mechanism in these tissues. As well as being stimulated by the application of AICAR, the action of AMPK in regulation of glucose stimulated expression of K_{ATP} channels was stimulated by the action of metformin (figure 3.12). Metformin has been used to treat type-2 diabetes for many years and has recently been shown to activate AMPK by an as yet poorly understood mechanism (Zhou *et al.* 2001, Hawley *et al.* 2002, Fryer *et al.* 2002). Many of the actions of metformin in the treatment of type-2 diabetes were attributed to its actions on peripheral tissues (liver and skeletal muscle). However, it became evident that many of the actions of metformin may be mediated by directly acting on the insulin secreting pancreatic β-cell. It has been reported that treatment with metformin is able to restore correct insulin secretory capacity to β-cells which had previously lost this ability due to prolonged exposure to elevated levels of either glucose or fatty acids (Lupi *et al.* 1999, Patane *et al.* 2000). From these studies it is unclear whether these effects are mediated by the stimulation of AMPK or whether the drug may be acting in some other fashion. This does however propose a possible link between metformin stimulated AMPK activity and the onset of type-2 diabetes which becomes all the more prominent when considered alongside the data presented in figure 3.5. These data show that the ability for glucose regulation of K_{ATP} channel expression is very closely linked to the ability of the cell for GSIS. If the anti-diabetic action of metformin is mediated via AMPK activation, this suggests a possible link between the ability of a cell for GSIS, the activation of AMPK and the correct regulation of K_{ATP} channel expression. Taken together this may reinforce the importance of both the ability of the cell to regulate the expression of K_{ATP} channels and the role of AMPK in this mechanism for correct functioning of the pancreatic β-cell and maintenance of correct GSIS.

3.3.4 - Physiological significance of the findings

Immunofluorescence experiments showed that the expression of K_{ATP} channels decreased sharply when INS1e cells were bathed in medium containing > 5mM glucose (figure 3.1). Since the normal physiological range of glucose concentrations

is between 3 - 6 mM, this may imply that this response is a physiologically significant phenomenon and not merely due to adaptations of INS1e cells as a consequence of prolonged culture. Since this phenomenon is also apparent in mouse pancreatic β-cells freshly isolated from BALB/c mice (figure 3.14), it is likely that this is indeed an important regulatory mechanism possessed by β-cells to aid in the correct regulation of insulin secretion. This is further reinforced by the observation that β-cells lacking the ability to secrete insulin correctly in response to glucose, both glucose unresponsive RIN-m cells and isolated islets from the GSIS impaired C57bl6/J mouse strain, lack the same level of glucose regulated expression observed in INS1e cells. These observations may therefore have important implications for the understanding of the onset of type-2 diabetes, where often the normal glucose stimulated insulin secretion is disrupted. Whether the dysregulation of K_{ATP} channel expression by glucose is a cause or is caused by a loss of normal glucose stimulated insulin secretion remains to be shown.

Following the shift from high glucose to low glucose the onset of K_{ATP} channel synthesis has been shown to be very rapid as demonstrated using both immunostaining (figure 3.6) and pulse-labelling techniques (figure 3.8). Evidence from pulse-labelling suggests that detectable amounts of both SUR1 and Kir6.2 are produced within only 2 minutes of the change in glucose concentration from high to low. Also, since the presence of bands thought to correspond to Kir6.2 are present in samples immunoprecipitated using anti-SUR1 antibodies it would appear that these newly synthesised channel subunits are being very rapidly assembled to form complete channels under these particular conditions. In all other conditions tested (a switch from low glucose to high glucose as well as maintaining low or high glucose) synthesis of K_{ATP} channel subunits was absent. Thus it would appear that a rapid decline of glucose concentrations is sufficient to stimulate a rapid accumulation of newly synthesised and assembled channels rather than a steady rate of synthesis of channels in low glucose conditions. It is likely that the rapid nature of this response is due in part to the induction of increased expression by an increase in translation, rather than having to wait to produce more mRNA by transcription prior to protein expression. The physiological significance of such a mechanism becomes apparent if the need to prevent a severe hypoglycaemic episode is considered. If the blood glucose levels of an organism decrease sharply, the secretion of insulin will be

required to be halted to prevent any further residual lowering of systemic glucose levels. It is therefore preferable that the secretion of insulin would be halted rapidly rather than a gradual decrease. One way to do this would be through inducing a large current through K_{ATP} channels resident at the plasma membrane. It may be that the newly synthesised channels are intended to augment such a K_{ATP} current thus rapidly halting and maintaining the block of insulin secretion. When glucose levels are more stable, such tight control of insulin secretion may not be required.

If such a mechanism were true it might be expected that the cell surface density of K_{ATP} channels would increase sharply following challenge with low glucose. Patch-clamp recordings of whole-cell currents demonstrated that this was not the case, although a small increase in channel density was observed in cells incubated with low glucose compared to those incubated in high glucose, this was not significant (figure 3.11). In addition, this small observed difference in channel density was much smaller than the difference observed using immunocytochemistry, where a ~2.5 fold increase in fluorescence was observed between cells treated similarly (figures 3.1 and 3.2). The discrepancy between the two estimates (fluorescence intensity vs. electrophysiology) may be attributed to membrane trafficking of the channels. Under the experimental conditions, channels made in the cell might have either failed to traffic to the cell surface, or may be rapidly removed out of the cell surface. Consistent with this notion, we found that most of the channel density was seen in structures distributed throughout the cytoplasm, which might represent trafficking vesicles or storage compartments. Regulated insertion and removal has been described as being a major determinant of membrane density of a number of cell surface proteins including a number of ion channels, e.g. AMPA receptors (Ehlers 2000) and the possible existence of such mechanisms for K_{ATP} channels warrants further examination.

3.3.5 - Summary of findings

In conclusion, it would appear that the expression of the pancreatic K_{ATP} channel is regulated by glucose via a mechanism which modulates the rate of translation of pre-existing mRNA rather than increasing the rate of gene transcription to produce more mRNA. Because of this, the increase in K_{ATP} channel synthesis triggered by a sudden decrease in glucose levels is very rapid, eventually leading to an increase of ~2.5 fold

in channel numbers. The exact mechanisms controlling this has not been characterised, but some evident for involvement of AMPK was presented in this study. Despite the large increase in channel numbers, a similar increase in cell surface channel density is not observed and the majority of the channels appear to be confined to cytoplasmic compartments, suggesting a possible role for regulated trafficking of the channel which is addressed in chapter 5.

Chapter 4

Production and characterisation of Kir6.2HA+11aaHMKFLAG constructs

4.1 – Introduction

If the factors affecting the surface expression of K_{ATP} channels are to be fully investigated it is necessary to be able to label channels that have been inserted into the plasma membrane selectively. By labelling surface bound channels in this way, the internalisation and trafficking of channels through endocytic pathways can be investigated. Selective labelling of plasma membrane bound channels in intact cells can be achieved either through the use of antibodies targeted against extracellular epitopes or by the use of fluorescent membrane impermeable ligands to the channel. Since no suitable membrane impermeable ligands exist for K_{ATP} channels, it was decided to attempt the antibody labelling method. Unfortunately, the predicted topology of the channel subunit SUR1 (Raab-Graham *et al.* 1999, Conti *et al.* 2001) along with the crystal structure of bacterial Kir channel homologues (Doyle *et al.* 1998, Kuo *et al.* 2003) suggests that very little of the K_{ATP} channel complex would exist extracellularly, with only very short loops in both Kir6.2 and SUR1 accessible from outside of the cell. The size of these loops makes them unsuitable to be used as epitope targets for raising antibodies, thus making selective labelling of the membrane bound channel difficult. However, a number of groups (Sharma *et al.* 1999, Zerangue *et al.* 1999, Reimann et al. 2003) have shown that the insertion of antibody epitopes into various extracellular domains of either Kir6.2 or SUR1 can allow selective staining of cell surface channels without apparent alteration in regulation of normal channel function or trafficking. An approach similar to that described by Zerangue *et al.* (1999) has been used to insert a haemaglutinin A (HA) antibody epitope into the extracellular loop preceding the pore region of Kir6.2 (figure 4.1). The HA-epitope was inserted into the Kir6.2 sequence following residue 102 and in addition to this a second short sequence will also be inserted at position 98 of the Kir6.2 sequence. This 11 amino acid linker sequence (+11aa) is homologous to the corresponding region of Kir6.1 and has previously been shown to improve the accessibility of the HA-epitope following insertion into Kir6.2 (Zerangue *et al.* 1999). The insertions will be achieved using an approach based around insertion PCR methodology, as summarised in figure 4.2.

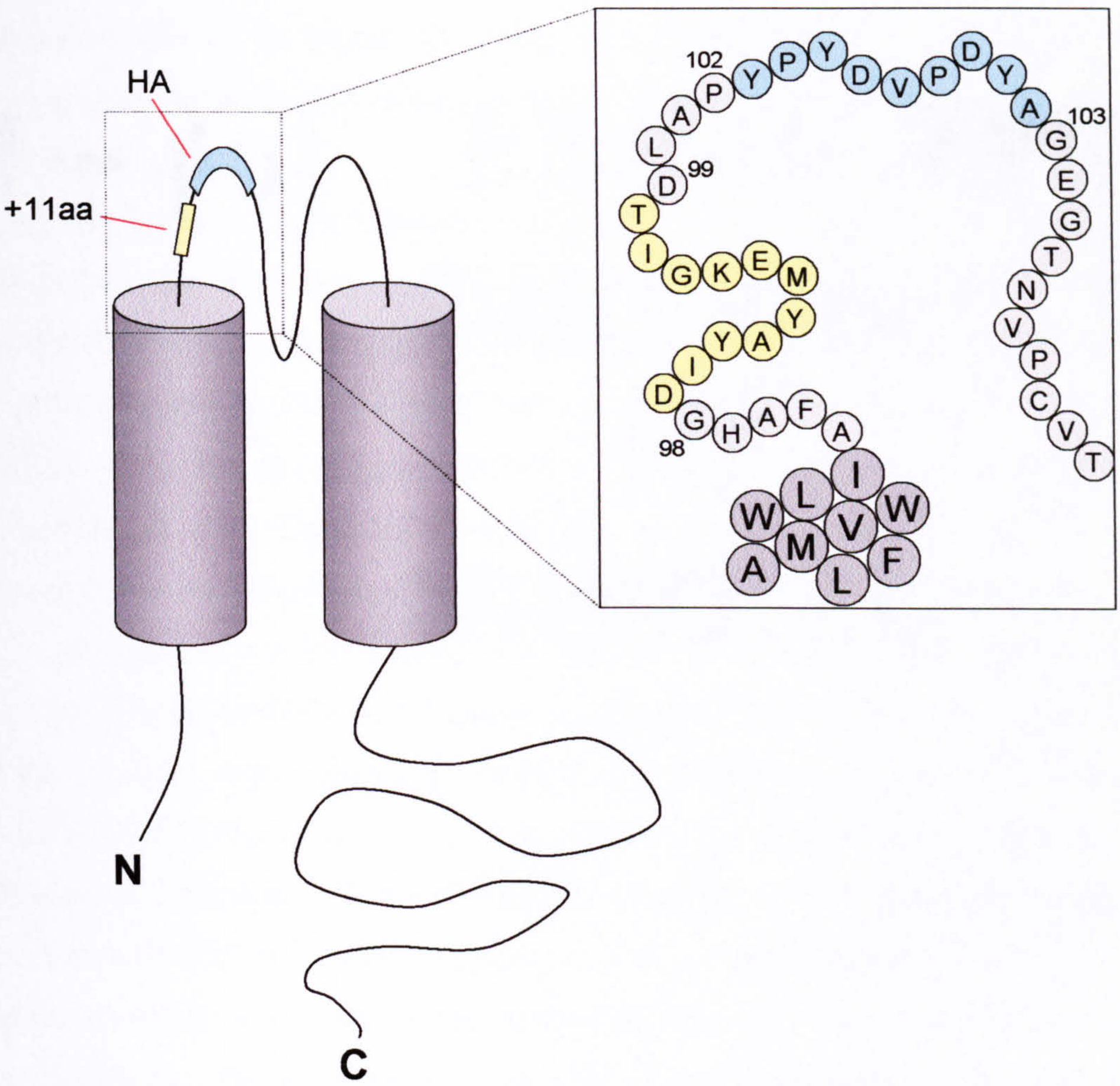

Figure 4.1 – *Schematic showing the location of both the HA and +11aa insertions in Kir6.2.* Inset shows an expansion of the predicted first extracellular loop with inserted sequences (+11aa – yellow, HA – blue). Numbering corresponds to the residue positions of wild-type Kir6.2.

4.2 – Results

4.2.1 – Production of the Kir6.2-HA+11aa-HMKFLAG construct

In order to selectively label plasma membrane bound channels a haemaglutanin-A (HA) antibody epitope was to be inserted into the first extracellular loop of Kir6.2. In addition to this an additional 11 amino acid (+11aa) linker sequence was to be inserted upstream of the HA epitope in order to improve antibody accessibility.

Shown in figure 2.2 is a schematic diagram of the strategy used to produce the Kir6.2-HA+11aa construct. Following the initial insertion of the HA epitope into pKS-Kir6.2-HMKFLAG a major PCR product of ~ 3.9 Kb was observed (figure 4.3 A) corresponding to the predicted size of pKS-Kir6.2-HA-HMKFLAG. Correct insertion of the HA epitope was confirmed by DNA sequencing (figure 4.3 B). For expression of the Kir6.2-HA-HMKFLAG construct in mammalian expression systems it was necessary to subclone the construct into the pcDNA3 plasmid vector. Since no suitable restriction sites were present in both the donor (pKS) and the recipient plasmid (pcDNA3), it became necessary to first subclone the construct into another plasmid vector, pSportII (figure 2.1). A BamHI / SalI restriction of pKS-Kir6.2-HA-HMKFLAG gave a ~ 1.6 Kb fragment which was ligated into BamHI / SalI restricted pSportII. This now enabled a BamHI / EcoRI fragment of pSportII-Kir6.2-HA-HMKFLAG to be subcloned into the BamHI / EcoRI sites of pcDNA3. Correct insertion was confirmed by restriction digestion and DNA sequencing. In order to improve the accessibility of the HA epitope to antibodies we also inserted an 11 amino acid linker sequence (+11aa) downstream of the HA insertion site. These 11 amino acids correspond to those found in the sequence of Kir6.1, but do not correspond to residues found in Kir6.2. As such they are not expected to impact on either the function or trafficking of the channels. The +11aa sequence was inserted into pcDNA3-Kir6.2-HA-HMKFLAG using a similar approach to that employed for insertion of the HA epitope. However, due to much higher levels of non-specific products being produced, a touch-down PCR protocol was utilised in an attempt to improve the final yield of the correct product. Following the PCR reaction, a major band of ~ 7.3 Kb was seen, corresponding to the predicted size of the construct. The PCR product was transformed into XL-blue competent cells and colonies were then subjected to plasmid mini-preparation protocol. Correct insertion of the +11aa

sequence was confirmed by DNA sequencing (figure 4.4). For expression of this construct in the *Xenopus* oocyte expression system, it was necessary to subclone the Kir6.2-HA+11aa-HMKFLAG construct into the pKSglobin plasmid vector. In order to achieve this, a BamHI / EcoRI fragment of pcDNA3-Kir6.2-HA+11aa-HMKFLAG was ligated into the BamHI / EcoRI sites of the pKSglobin vector.

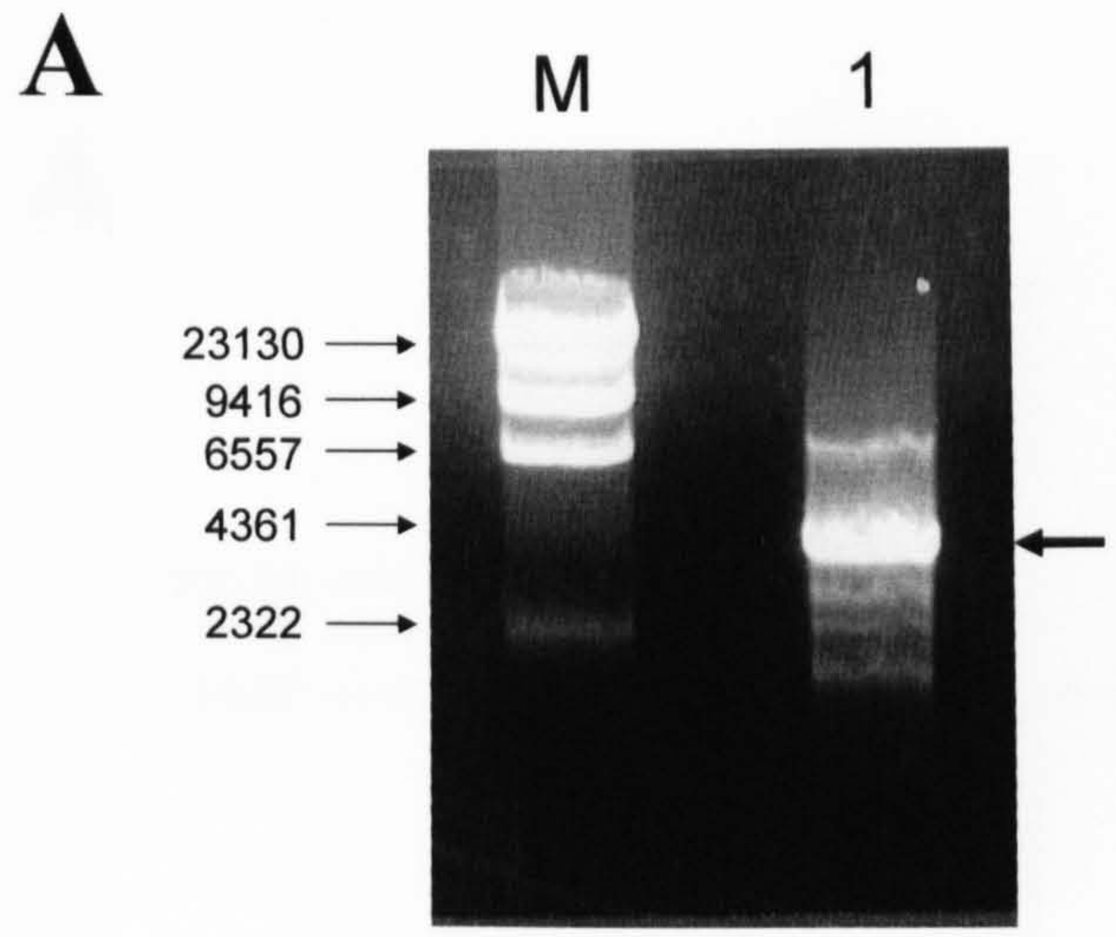

Figure 4.3 – *Production and sequencing of the pKS-Kir6.2-HA-HMKFLAG construct.*

A) PCR product analysed by electrophoresis on a 1 % agarose gel. Thick arrow denotes main PCR product. M = λ-HindIII markers (marker sizes (bp) are shown on the left); 1 = pKS-Kir6.2-HA-HMKFLAG PCR product.

B) Sequencing of PCR product. Both single letter amino acid code and nucleotide sequences are shown. Numbering refers to residue positions of wild-type Kir6.2.

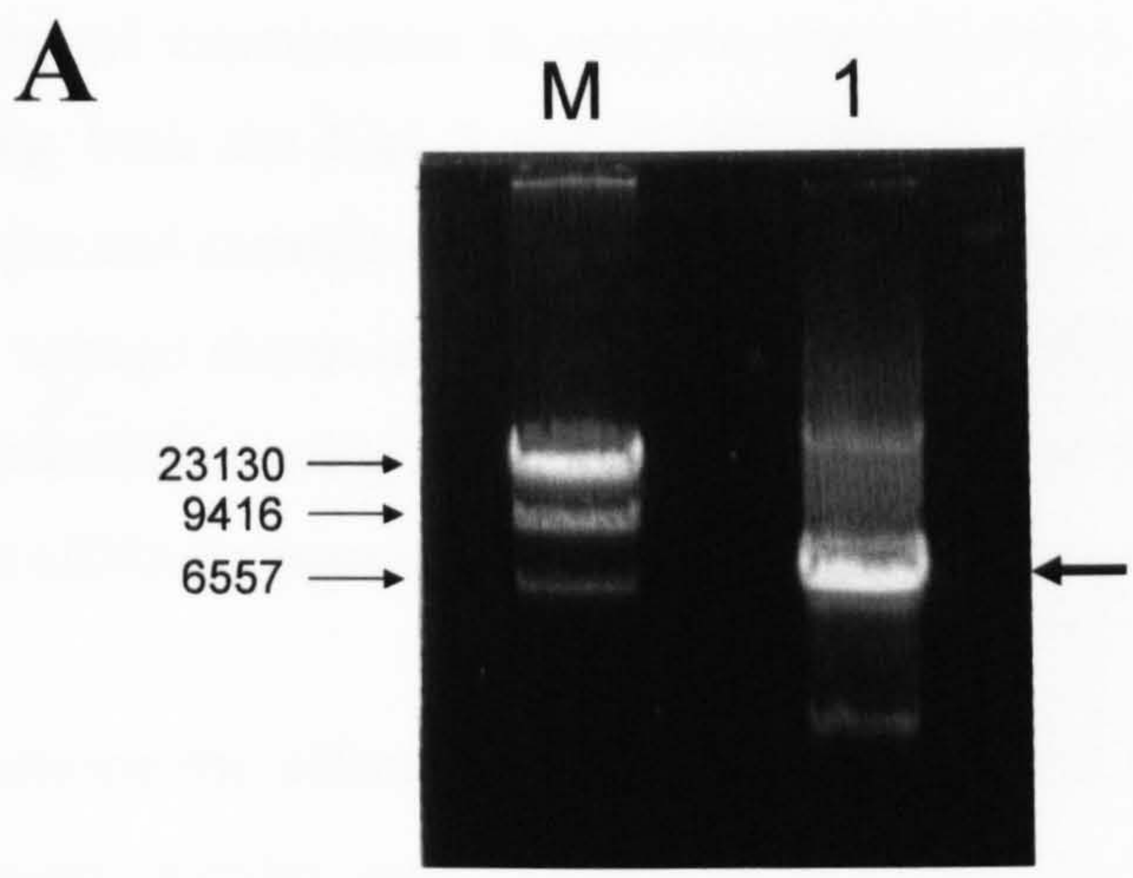

B

Kir6.2 ..... 98 +11aa linker sequence ——— 99

F A H G D I Y A Y M E K G I T D

.. TTC GCC CAC GGT GAC ATC TAT GCT TAC ATG GAG AAA GGC ATC ACG GAC

Kir6.2 ..... HA-epitope - - - - - - - - -

L A P Y P Y

CTG GCC CCC TAC CCA TAC ..

Figure 4.4 – *Production and sequencing of the pcDNA3-Kir6.2-HA+11aa-HMKFLAG construct.*

A) PCR product analysed by electrophoresis on a 1 % agarose gel. Thick arrow denotes main PCR product. M = λ-HindIII markers (marker sizes (bp) are shown on the left); 1 = pcDNA3-Kir6.2-HA+11aa-HMKFLAG PCR product.

B) Sequencing of PCR product. Both single letter amino acid code and nucleotide sequences are shown. Numbering refers to residue positions of wild-type Kir6.2.

4.2.2 – Functional expression of Kir6.2-HA+11aa-HMKFLAG in *Xenopus* oocytes

The function of ion channels can be easily tested by expression and electrophysiological examination in oocytes from *Xenopus laevis* frogs. For this, cRNA encoding both the Kir6.2 and SUR1 subunits are microinjected into each individual oocyte and currents from the resultant channels can be examined using the two electrode voltage clamp method. cRNA encoding SUR1 and Kir6.2 constructs were *in vitro* transcribed using T7-Megascript kit (Ambion) followed by examination of the resultant cRNA by agarose gel electrophoresis (figure 4.5).

In order to examine the effect of the HA+11aa insertions on the function of K_{ATP} channels, *Xenopus* oocytes were injected with cRNA for SUR1 along with either wild-type (wt) Kir6.2-HMKFLAG or Kir6.2-HA+11aa-HMKFLAG and currents were examined using the two electrode voltage clamp method. In both cases large currents were observed when injected oocytes were treated with 200 μM diazoxide (a selective K_{ATP} channel opener) and 3 mM sodium azide (a metabolic inhibitor). These currents were rapidly and completely inhibited by addition of 1 μM glibenclamide (selective K_{ATP} channel inhibitor), confirming that the observed currents were due to K_{ATP} channels (figure 4.6 A). No such currents were observed in water injected oocytes suggesting that the currents were due to introduced channels and not channels native to the cells. Consistent with this, fluorescent labelling of oocyte sections showed clear labelling in both the plasma membrane and cytoplasm in oocytes expressing either Kir6.2-wt or Kir6.2-HA-11aa containing channels.

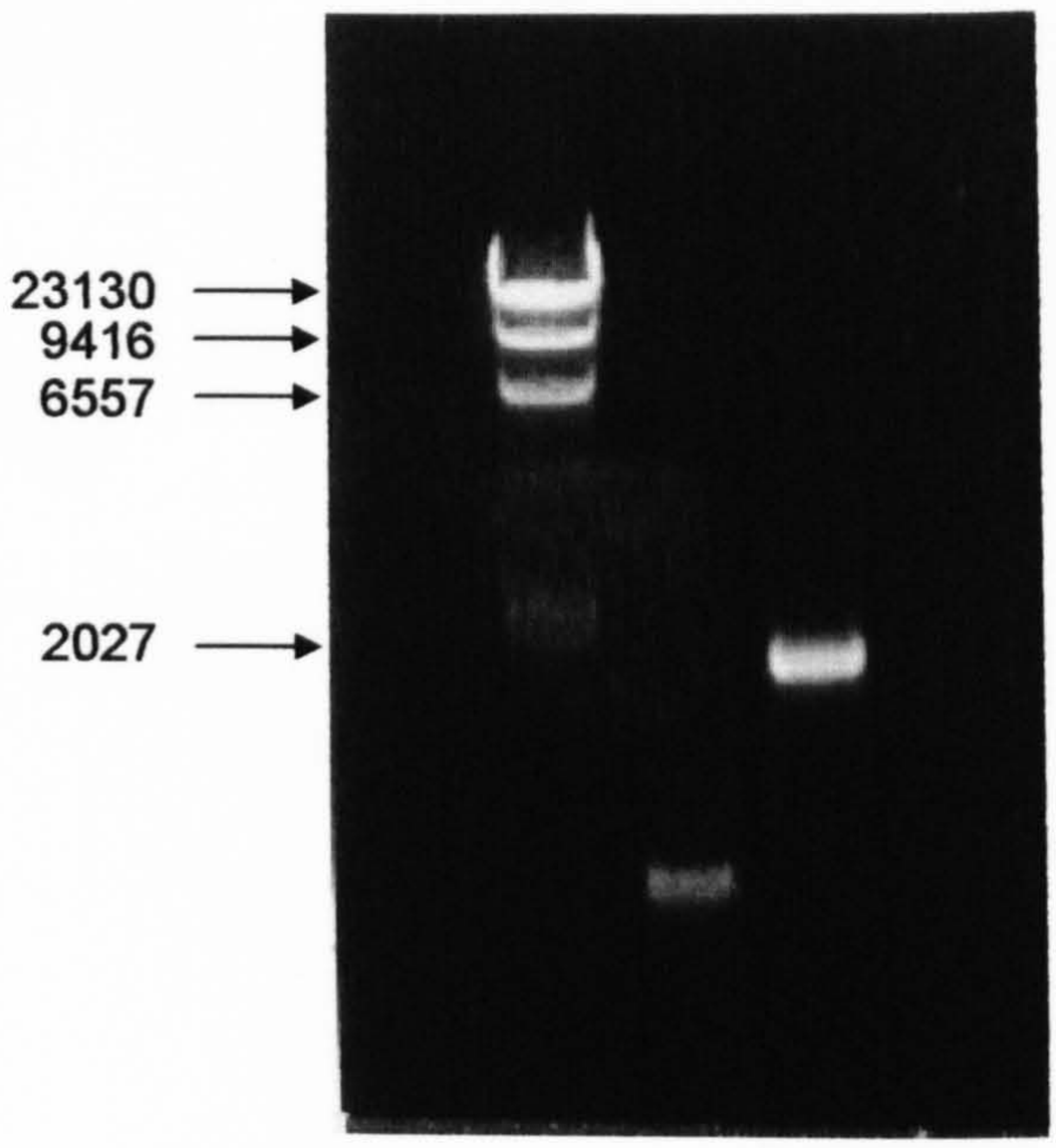

Figure 4.5 - *In vitro produced cRNA analysed by 1 % agarose gel electrophoresis.* M = λ-HindIII markers (marker sizes (bp) are shown on the left); 1 = Kir6.2-HA+11aa-HMKFLAG cRNA; 2 = His6-SUR1 cRNA.

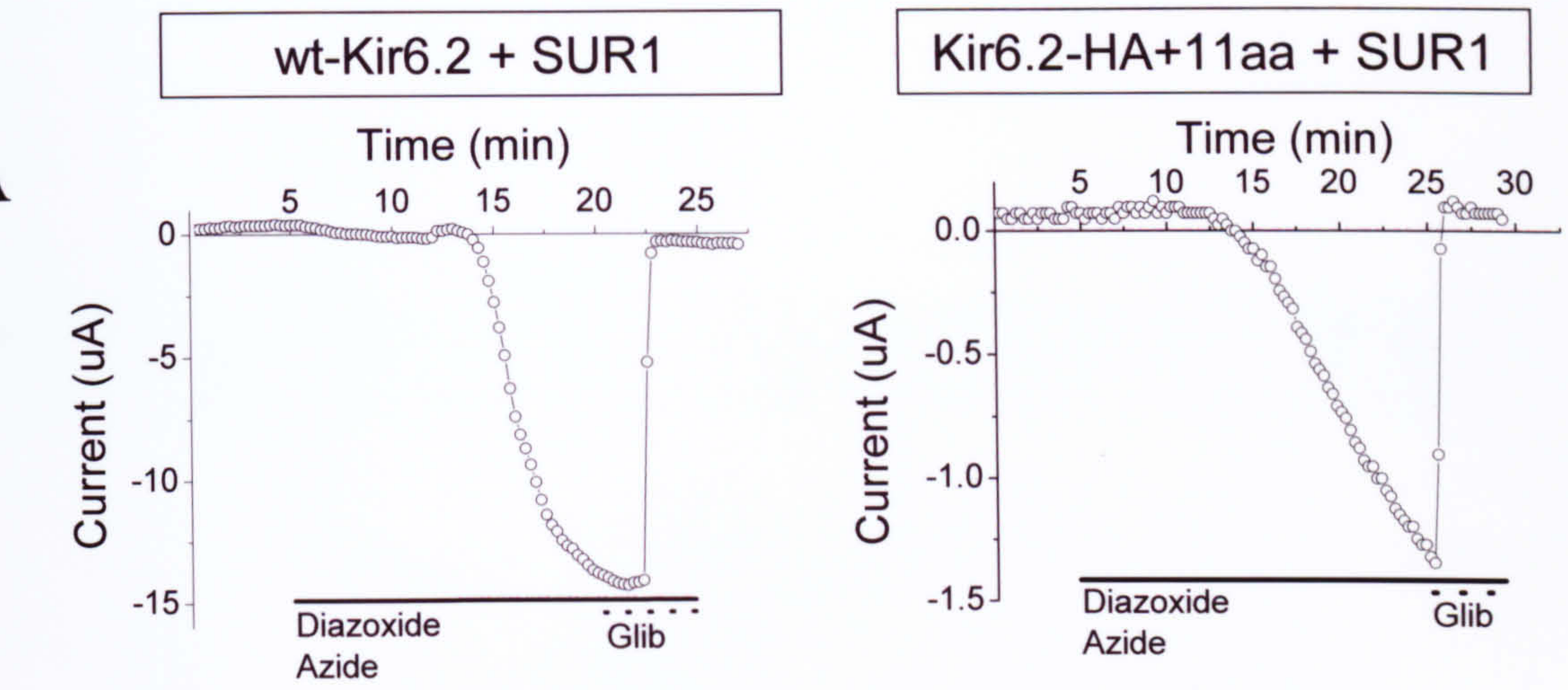

Figure 4.6 – *Comparison of wild-type Kir6.2 and Kir6.2HA+11aa in Xenopus oocytes.* **(A)** - Plot of current at -120 mV against time from an oocyte injected with cRNA encoding either wt-Kir6.2 or Kir6.2-HA+11aa both alongside His6-SUR1. Drugs were applied for the duration indicated by the horizontal bars at the following concentrations; diazoxide – 200 μM, sodium azide – 3 mM, glibenclamide – 1 μM. Currents were recorded using a ramp protocol from -150 mV to + 50 mV (0.22 $V.s^{-1}$) and a holding potential of -30 mV. **(B)** - Oocytes injected as above were sectioned at 20 μm and labelled with anti-Kir6.2 antibodies and appropriate FITC conjugated secondary antibodies before viewing by confocal microscopy.

4.2.3 – Expression of Kir6.2-HA+11aa containing channels in mammalian cells

It was next necessary to assess whether the HA+11aa insertions were affecting normal membrane trafficking of the channels in mammalian cells. This also provided an opportunity to assess the suitability of the HA epitope for surface labelling studies. Normal trafficking of wild-type K_{ATP} channels requires that both Kir6.2 and SUR1 subunits are present, and that complete channel assembly has occurred. Otherwise ER retention motifs (-RKR-) contained in each subunit prevents the export of channel subunits into the later biosynthetic pathway. To ensure that addition of the HA+11aa insertions have not interfered with this quality control mechanism, surface expression of Kir6.2-HA+11aa containing channels in HEK-293 and COS7 cells was investigated.

Expression of Kir6.2-HA+11aa-HMKFLAG along with SUR1 in either HEK-293 or COS7 cells showed strong surface staining in unpermeabilised cells when labelled with anti-HA antibodies coupled with complementary fluorescently labelled secondary antibodies (figure 4.8 *upper panels*). However, no surface labelling was observed in unpermeabilised cells when Kir6.2-HA+11aa-HMKFLAG was expressed in the absence of SUR1 (figure 4.8 *lower panels*). Immunofluorescence labelling of permeabilised cells revealed that in the absence of SUR1, anti-HA staining was largely limited to perinuclear regions, most probably the endoplasmic reticulum (figure 4.9). In untransfected cells, no labelling was observed in either permeabilised or unpermeabilised cells with the anti-HA and complementary secondary antibodies (figure 4.7).

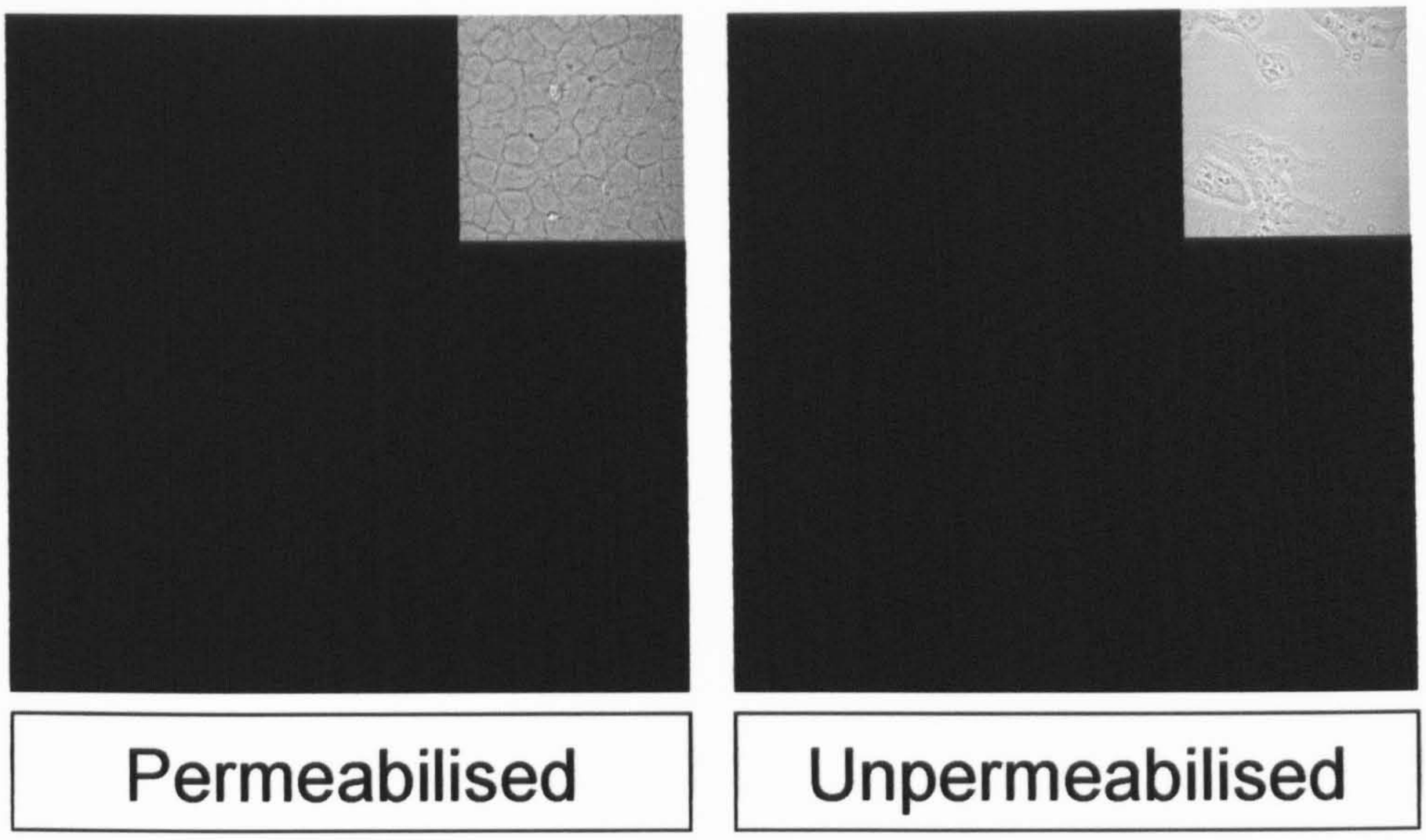

Figure 4.7 – *Anti-HA antibodies do not label untransfected cells.* HEK-293 cells were fixed, permeabilised where necessary and labelled with rat anti-HA primary antibodies followed by anti-rat Cy3 conjugated secondary antibodies prior to viewing by confocal microscopy. Insets show phase DIC phase contrast images of the cells within the fluorescent images.

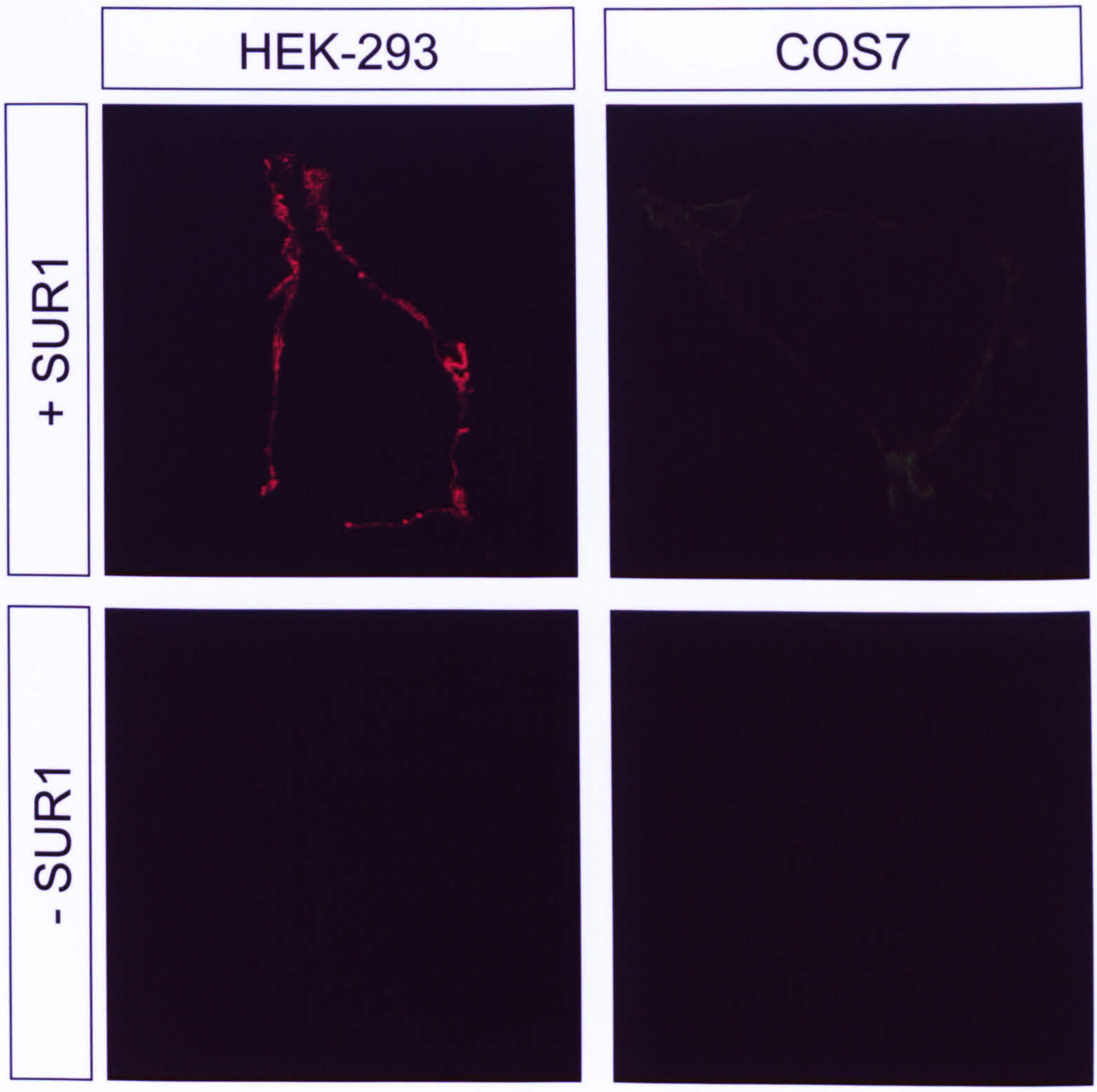

Figure 4.8 – *Kir6.2-HA+11aa-HMKFLAG requires SUR1 to traffic to the cell surface.* Both HEK-293 and COS7 cells were transiently transfected using Fugene6™ with pcDNA3-Kir6.2-HA+11aa-HMKFLAG with or without pcDNA6-His6-SUR1. Cells were fixed, left unpermeabilised and stained with rat anti-HA antibodies and complementary secondary antibodies. Where no fluorescently-labelled cells are evident the entire coverslip has been examined but no fluorescent cells were seen.

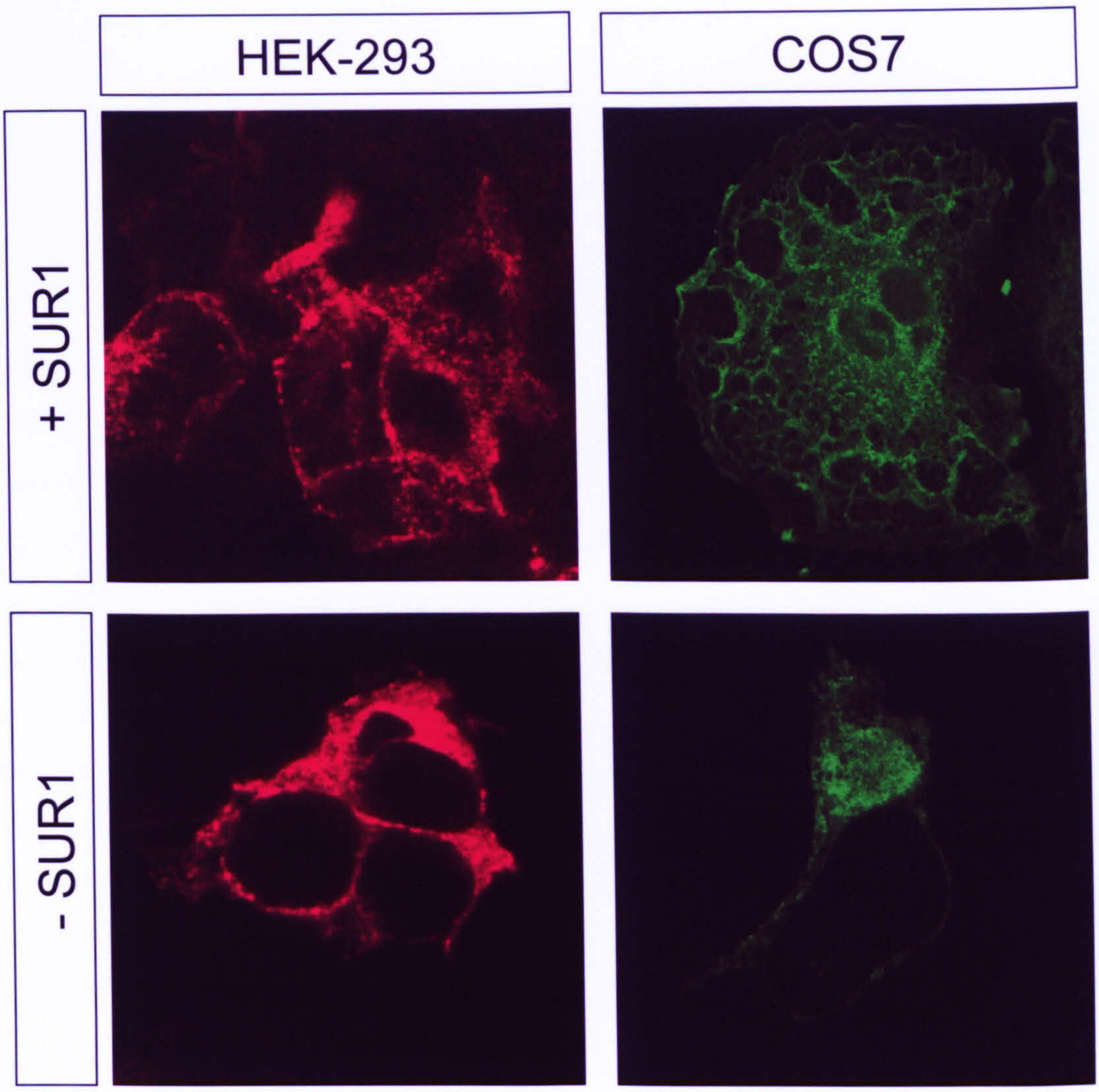

Figure 4.9 – *Kir6.2-HA+11aa-HMKFLAG is confined to perinuclear compartment in the absence of SUR1.* Both HEK-293 and COS7 cells were transiently transfected using Fugene6™ with pcDNA3-Kir6.2-HA+11aa-HMKFLAG with or without pcDNA6-His6-SUR1. Cells were fixed, permeabilised and stained with rat anti-HA antibodies and complementary secondary antibodies.

4.3 – Discussion

The successful insertion of both the HA-epitope and the 11 amino acid linker sequence into an extracellular domain of Kir6.2 will allow the examination of many aspects of K_{ATP} trafficking. Despite recent advances in the understanding of the mechanisms responsible for controlling K_{ATP} channel trafficking to the plasma membrane, little is known concerning the fate of the channels once they have reached the cell surface. Hu *et al.* (2003) recently reported a possible role for protein kinase C (PKC) in the regulation of K_{ATP} channel internalisation from the plasma membrane, but this study did not investigate the fate of the internalised channels very comprehensively. As such, it is still unclear what happens to the channels once they have been removed from the cell surface. Studies of the fates of numerous other proteins internalised from the cell surface have revealed a number of diverse trafficking pathways, all of which influence the normal physiological functioning of the protein. For example, the transferrin receptor is known to be very rapidly recycled back to the cell membrane via specialised early-endosomes following internalisation whereas the GLUT4 glucose transporter has been shown to be recruited into a highly specialised, TGN-associated storage compartment. EGF receptors however are targeted through late-endosomes ultimately ending with the degradation of the protein in the lysosome (see Maxfield & McGraw 2004 for review). To understand fully how the cell surface density of K_{ATP} channels is regulated the route by which the channels traverse the endosomal system must be elucidated.

An indication suggesting that regulated trafficking pathways may play a role in the normal function of K_{ATP} channels has already been shown in chapter 3. The investigation into the effects of glucose on K_{ATP} channel expression showed that although a large increase in K_{ATP} channels is observed in low glucose, the density of channels at the cell surface is not similarly increased. Indeed, much of the fluorescence associated with this increase in channel density is confined to structures in the cytoplasmic regions of the cell. Taken together these findings could indicate the existence of a K_{ATP} channel storage compartment within the cell or the existence of tightly controlled insertion / removal regulatory mechanisms governing the density of channels at the cell surface. The production of the Kir6.2-HA+11aa construct will

allow the investigation of these hypotheses as well as examining the pathways taken by K_{ATP} channels following internalisation from the cell surface. From these data it appears that the Kir6.2-HA+11aa construct behaves in the same fashion as the wild-type channel. The construct forms functional channels which are activated by azide and diazoxide treatment and inhibited by glibenclamide application when co-expressed alongside SUR1 in a similar manner as wild-type channels (figure 4.6). channels containing the HA-tagged Kir6.2 are also only able to traffic to the cell surface in mammalian cells when co-expressed with SUR1 (figure 4.8). Because the HA-tagged Kir6.2 does behave like the wild-type Kir6.2, this makes it a suitable tool for use in investigating the endocytic trafficking of K_{ATP} channels.

Chapter 5

Elucidation and regulation of the endocytic trafficking pathways of K_{ATP} channels

5.1 – Introduction

It has recently become apparent that regulated trafficking pathways play an important role in the regulation of the overall activity of a number of cell surface ion channels, transporters and receptors (Kleizen *et al.* 2000, Robinson 2002, Muth & Caplan 2003, Tan *et al.* 2004, Watson *et al.* 2004 - see for reviews). Since trafficking pathways of this kind have the potential to impact greatly on the physiological roles of these proteins it is important to understand the mechanisms which are responsible for regulating them as well as how proteins traverse through them. A diverse range of pathways which both upregulate and downregulate the density of a wide range of target proteins at the cell surface are already known, some of which are outlined below.

One of the best characterised of these mechanisms is that which regulates the desensitization of certain members of the G-protein coupled receptor (GPCR) family, as exemplified by the β-adrenoceptor. In this case, receptor activation by ligand binding results in phosphorylation of the receptor, allowing binding of the adaptor protein β-arrestin leading to the formation of clathrin coated pits (see Fergusson 2001 for review). Once endocytosed into the cytoplasm, the receptors are dephosphorylated, which results in receptor resensitization and allows reinsertion back into the plasma membrane. Another well characterised trafficking pathway is that which regulates the cell surface density of the GLUT4 glucose transporter in adipocytes and smooth muscle. The activity of GLUT4 was shown to be greatly increased in the presence of insulin, and it was later discovered that this was due to a massive, rapid, recruitment of GLUT4 to the cell surface (James *et al.* 1988). It became apparent that under normal conditions GLUT4 is retained in an insulin-responsive compartment which consists of TGN-derived endosomal compartments along with a number of specialised transport vesicles, collectively termed the peri-centriolar reticular-GLUT4 storage compartment (PR-GSC). Stimulation of GLUT4 expressing cells with insulin results in the release of GLUT4 from the PR-GSC and a rapid translocation to the cell surface (Kanai *et al.* 1993, Lund *et al.* 1995). It is becoming more apparent that the mechanisms governing cell surface density of many, if not all, channels are tightly regulated and physiologically significant processes. A wide range of channels have so far been identified as having their surface density

controlled in some manner. Examples include, members of the Kv channel family - Kv4.2 for example (Wang *et al.* 2004), the ENaC sodium channel (Carattino *et al.* 2003), the cystic fibrosis transmembrane regulator chloride channel (see Bertrand & Frizzell 2003 for review), the aquaporin-2 water channel (see Brown 2003 for review) and the AMPA receptor (Ehlers 2000) to name a few.

The mechanisms regulating K_{ATP} channel trafficking are poorly understood. As described earlier (section 1.1.4) the presence of an endoplasmic retention motif in both Kir6.2 and SUR1 is known to regulate the biosynthetic export of the channel. However, once the channel has reached the cell surface very little is known of its fate. A study by Hu *et al.* (2003) showed that activation of PKC resulted in a reduction in K_{ATP} channel surface density which they attributed to an increase in the rate of internalisation. They also showed that the kinase sites responsible for this effect were not present of the Kir6.2 subunit although a dileucine motif in Kir6.2 may have been involved in the initial internalisation. The fate of the channels following internalisation was not studied in any detail, and as such it is not clear whether the internalised channels are able to recycle back to the cell surface or indeed to which organelles they are targeted.

The data presented in chapter 3 showed that a decrease in glucose concentration led to an increase in the expression of K_{ATP} channel subunits. This rise in the number of K_{ATP} channels subunits appeared to translate into an increase in fully assembled mature channels but the density of channels at the cell surface did not appear to similarly change. This has led to the idea that perhaps the surface density of K_{ATP} channels is tightly regulated through trafficking of channels to and from the plasma membrane. If this were found to be true it could have significant implications for the understanding of the actions of K_{ATP} channels in relation to all of its physiological roles including the regulation of insulin secretion. Therefore the endocytic trafficking of K_{ATP} channels has been investigated, including elucidation of the trafficking pathway and the involvement of channel recycling. In addition, such studies are important for understanding the cellular basis of diseases associated with defective trafficking of K_{ATP} channels such as CHI and PNDM.

5.2 – Results

5.2.1 - Suitability of stably transfected cells for the examination of K_{ATP} channel internalisation

The HEK293 cells stably expressing HA-tagged K_{ATP} channels (K_{ATP}-HA) have been shown to be suitable for surface labelling studies (see chapter 4). It is however not clear from these experiments whether these cells are suitable for use for studies requiring the internalisation of labelled channels from the cell surface. It is possible that antibodies may internalise into cells via fluid phase uptake in a non-specific manner and not because of being bound to epitope-tagged channels. Figure 5.1 shows that this is not the case, and proves that uptake of the anti-HA antibodies requires the presence of K_{ATP}-HA channels (figure 5.1A) and that the fluorophore conjugated secondary antibodies require the prior application of anti-HA antibodies in order to bind (figure 5.1B).

5.2.2 - K_{ATP} channels are constitutively internalised from the plasma membrane in HEK293 cells into a perinuclear compartment

The internalisation of K_{ATP}-HA from the cell surface was investigated in the stably transfected HEK293 cells. Briefly, cells were incubated in the presence of anti-HA antibodies at 4°C for 1 hour to label channels present at the cell surface, before incubation for varying lengths of time at 37°C to allow internalisation. Labelled channels were then visualised using fluorophore-conjugated secondary antibodies in cells which were either unpermeabilised (to examine surface expression) or permeabilised (to examine distribution throughout the cell).

In cells which were unpermeabilised (figure 5.2) fluorescence at the cell membrane is clearly defined immediately following the 4°C incubation (t = 0 min). Following the subsequent incubations at 37°C the fluorescence can be seen to become less uniform before lessening in intensity. This lessening in the intensity of fluorescence presumably occurs due to the internalisation of anti-HA bound channels from the cell surface making then unavailable for subsequent binding with fluorescently-conjugated secondary antibodies. The intensity of the cell surface fluorescence decreases very rapidly, suggesting a very rapid rate internalisation. However, from 10 minutes onwards the level of fluorescence remains relatively unchanged, albeit at a

significantly lower level than at t = 0. It should be noted that at no point does the fluorescence disappear completely; indeed at the later time points the level of fluorescence appears to fluctuate slightly, perhaps indicating that some sort of recycling is occurring.

In cells which were permeabilised (figure 5.3), endocytosed material can be seen in vesicular structures close to the plasma membrane as early as 5 minutes of incubation at 37°C, supporting the observations of rapid internalisation from figure 5.2 above. At this time however the majority of the fluorescence still appears to be at, or very near to, the cell surface. From 10 minutes onwards, the fluorescence appears to move from the cell surface towards the centre of the cell, first in the form of smaller punctate structures, later accumulating in larger structures in the peri-nuclear region which begin to become apparent after 15 minutes.

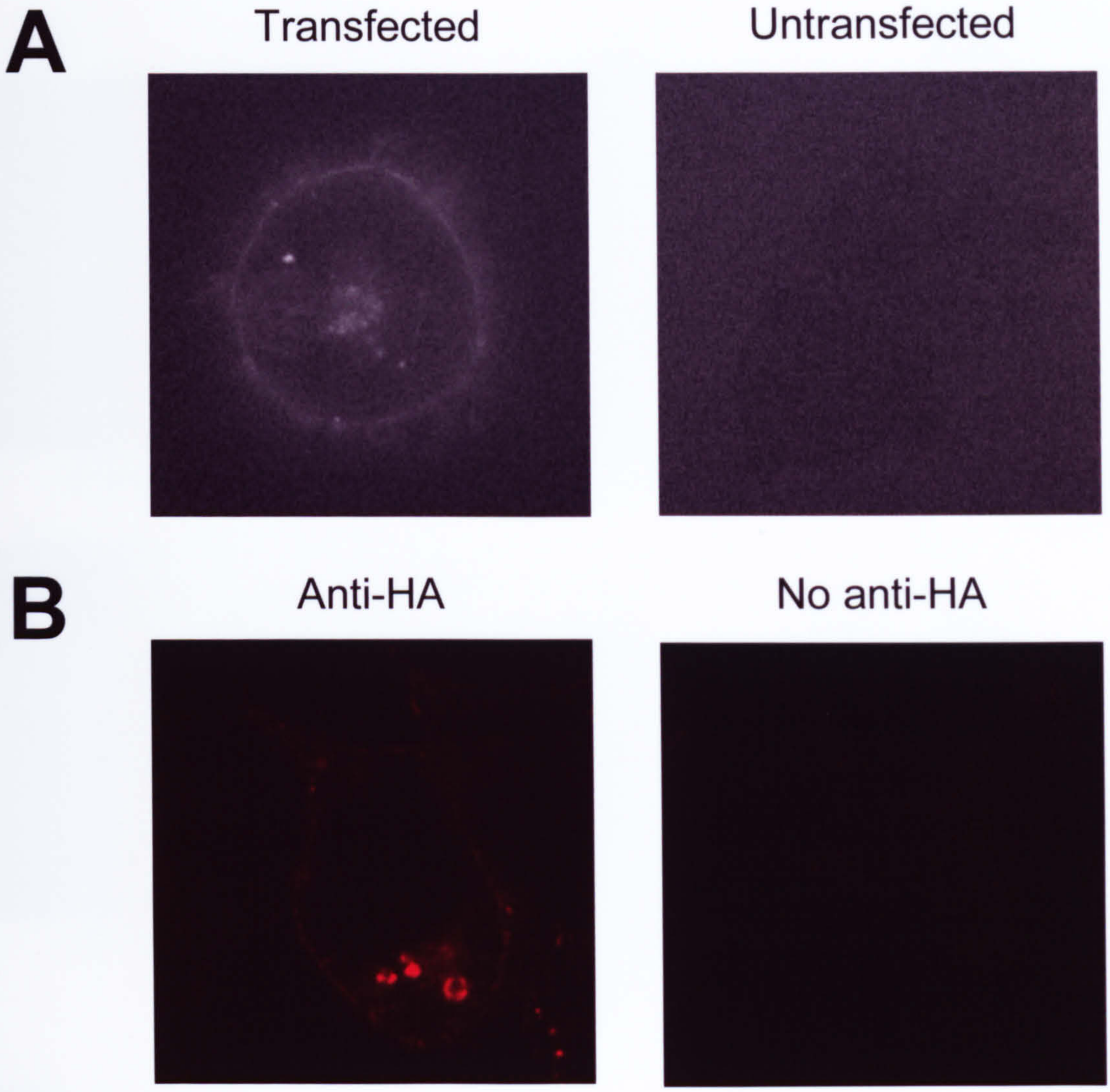

Figure 5.1 - *Stably transfected HEK293 cells are suitable for internalisation studies.* **(A)** Stably transfected and untransfected HEK293 cells were labelled with mouse anti-HA Alexafluor594-conjugated antibodies (2 μg ml^{-1}) and subsequently viewed by fluorescence microscopy using the live cell imaging protocol. Each image is a single frame taken from the movies included as supplementary material. (n = 3) **(B)** Stably transfected HEK293 cells were labelled using the internalisation protocol in the presence or absence of rat anti-HA antibodies (0.2 μg ml^{-1}) followed by fixation, permeabilisation and staining with anti-rat Cy3-conjugated secondary antibodies (n = 4). Labelled cells were subsequently viewed by LSCM.

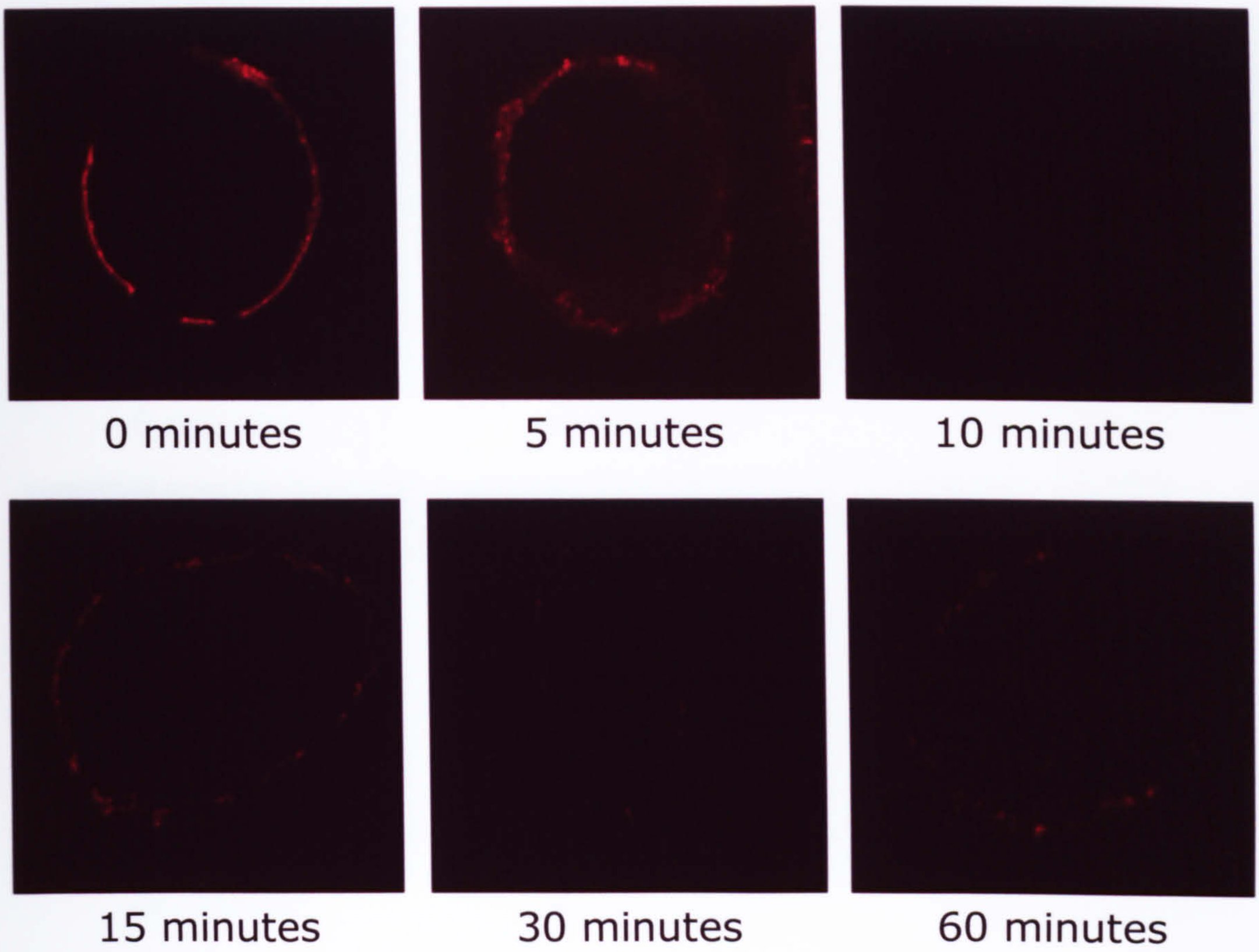

Figure 5.2 - *K_{ATP}-HA channels are rapidly removed from the surface of unpermeabilised cells.* Stably transfected HEK293 cells were incubated at 4˚C for 2 hours in the presence of rat anti-HA antibodies (0.2 μg ml^{-1}). The cells were then washed with chilled media before incubation at 37˚C for the indicated duration. Following this incubation the cells were fixed and labelled channels at the cell surface were stained with anti-rat Cy3 conjugated secondary antibodies. The cells were subsequently viewed by LSCM using identical settings for each image (n = 3). Representative images are shown.

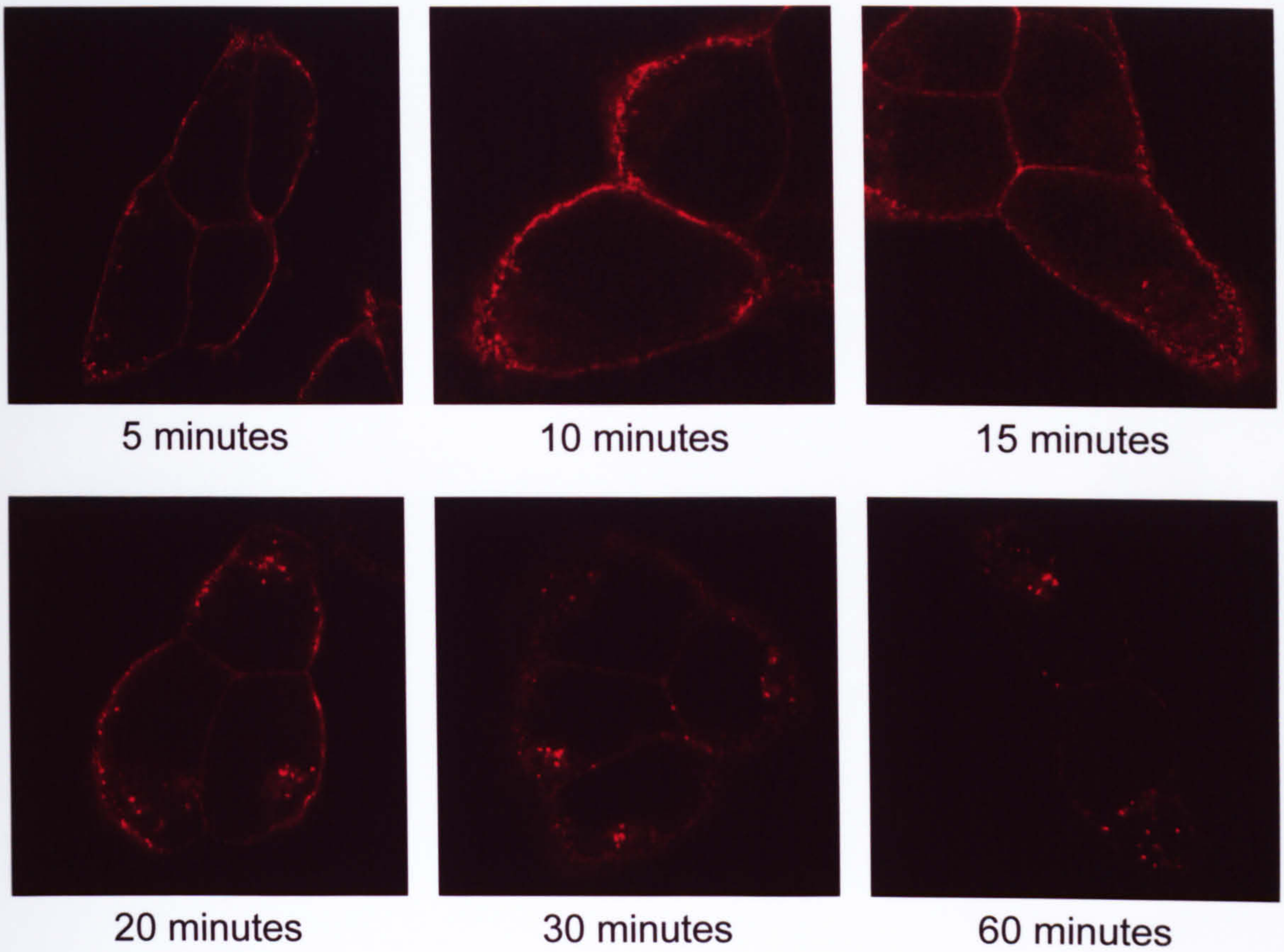

Figure 5.3 - *K_{ATP}-HA channels are rapidly internalised into perinuclear compartments.* Stably transfected HEK293 cells were incubated at 4˚C for 2 hours in the presence of rat anti-HA antibodies (0.2 μg ml^{-1}). The cells were then washed with chilled media before incubation at 37˚C for the indicated duration. Following this incubation the cells were fixed, permeabilised and labelled channels were stained with anti-rat Cy3 conjugated secondary antibodies. The cells were subsequently viewed by LSCM using identical settings for each image (n = 4). Representative images are shown.

5.2.3 - Effect of PKC activity on the internalisation of K_{ATP} channels

It was recently reported (Hu *et al.* 2003) that rapid K_{ATP} channel internalisation from the cell surface required the activation of protein kinase C (PKC). From the data presented above (figures 5.2 & 5.3) it would appear that in these stably transfected cells activation of PKC by pharmacological means was not required for rapid channel internalisation to occur. In an attempt to reconcile the differences between these two sets of data the effect of both activation and inhibition of PKC on the internalisation of K_{ATP} channels was investigated. Following 2 hours of antibody-labelled channel internalisation, cells which were untreated showed the majority of fluorescence in the fairly large punctate perinuclear structures as described earlier (figure 5.4 - *upper left panel*) and no fluorescence was seen at the cell surface. These structures were also present in cells which had been treated with PMA, an activator of PKC, and no significant fluorescence was observed at the cell surface (figure 5.4 - *upper right panel*). In cells treated with chelerythrine, an inhibitor of PKC, the majority of fluorescence was observed at the periphery of the cells, most likely at the cell surface (figure 5.4 - *lower left panel*). The perinuclear punctate structures were absent in these cells, and the only punctate structures in these cells were very small and located near the cell membrane. In cells treated with both PMA and chelerythrine staining was observed in both the perinuclear compartments and at the cell surface (figure 5.4 - *lower right panel*). One possible explanation for the difference in the PKC regulation of channel internalisation between the data presented here and the data reported in Hu *et al.* (2003) could be due to the constructs used in each study. The Kir6.2-HA construct that has been used here to establish the stably transfected cell line has an HMKFLAG tag attached to the C-terminus, whereas the construct used by Hu and colleagues does not and it possible that the presence this tag has in some way affected the characteristics of the internalisation event. In order to test this, a Kir6.2-HA construct lacking the HMKFLAG moiety was produced, as described in 2.3.9, (Kir6.2-HA-ΔHMKFLAG) (figure 5.5) and its internalisation characteristics were examined. When cells expressing Kir6.2-HA-ΔHMKFLAG and SUR1 were stained with anti-HA antibodies using the internalisation protocol the pattern of staining was very similar to that observed in the stably transfected cell line (figure 5.6). Untreated cells showed the majority of fluorescence in the large punctate perinuclear compartments and little near the cell surface (*upper left panel*). Cells treated with PMA showed a similar distribution of staining (*upper right panel*), whereas cells

treated with chelerythrine showed the majority of the staining at the periphery of the cell (*lower left panel*). As with the stably transfected cell line, the cells treated with both PMA and chelerythrine showed both the perinuclear staining as well as some staining at the cell surface (*lower right panel*). From these data it would appear that the presence of HMKFLAG tag at the C-terminus of Kir6.2 is not responsible for the differences observed between the present data and the previously published results.

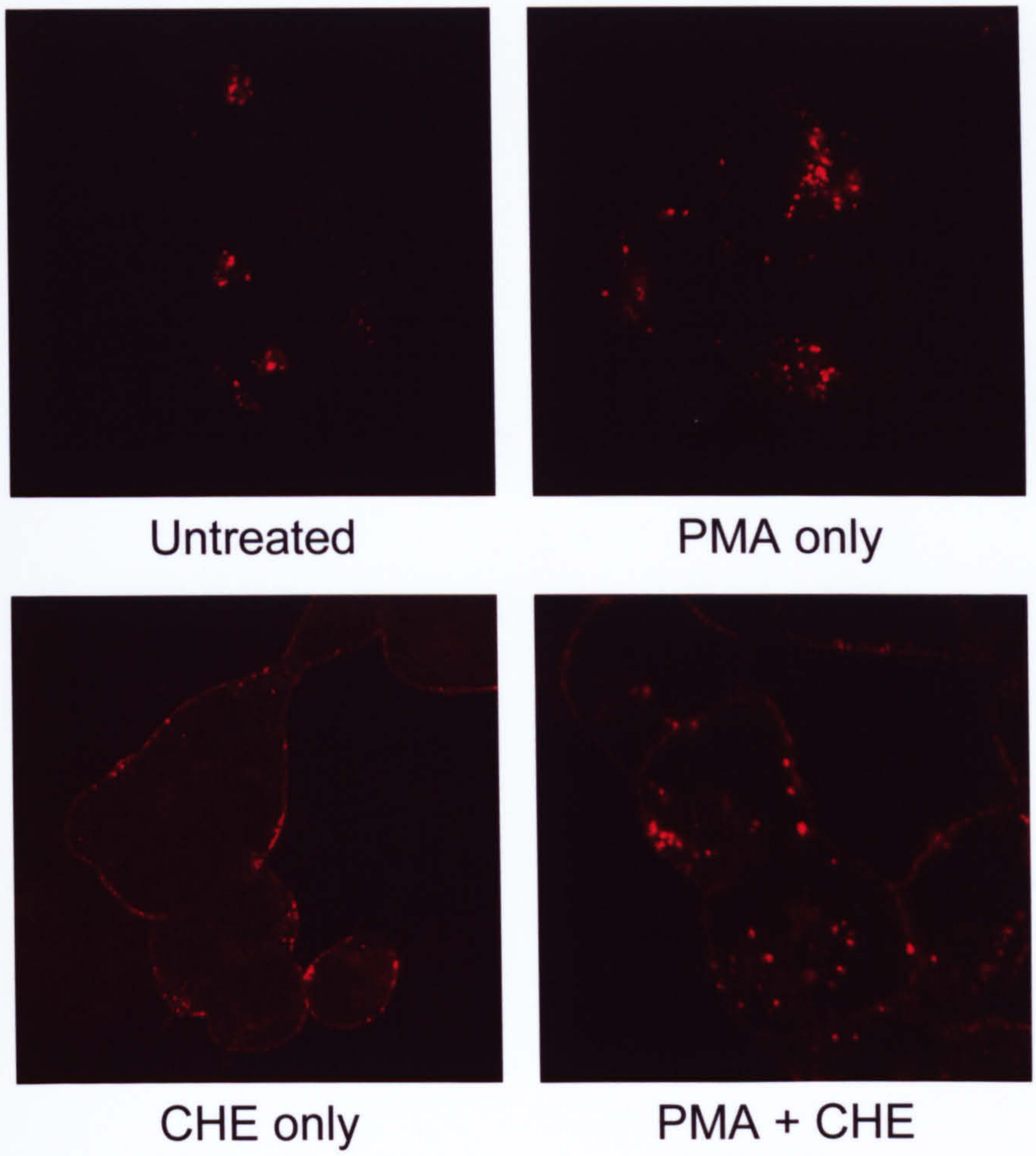

Figure 5.4 - *Effect of modulation of PKC activity on K_{ATP}-HA channel internalisation.* Stably transfected HEK293 cells were treated with drugs as described for 30 minutes prior to and throughout the labelling protocol. Cells were labelled with rat anti-HA antibodies (0.2 μg ml^{-1}) using the internalisation staining protocol. Cells were then fixed, permeabilised and labelled with anti-rat Cy3-conjugated antibodies (n = 3). The cells were subsequently viewed by LSCM. Representative images are shown. The drugs used were PMA (phorbol-12-myristate-13-acetate) - 100 nM, CHE (chelerythrine) - 10 μM .

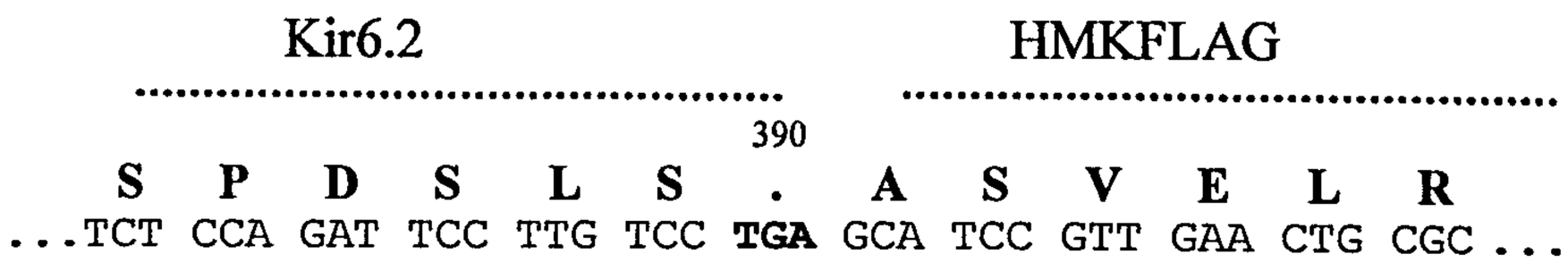

Figure 5.5 - *Confirmation of the correct insertion of a stop codon to produce Kir6.2-HA+11aa-ΔHMKFLAG.* A stop codon was introduced into pcDNA3-Kir6.2-HA+11aa-HMKFLAG to replace the first residue of the HMKFLAG epitope as described in 2.3.9. Correct insertion was confirmed by DNA sequencing. When expressed the produced protein will not have the C-terminal HMKFLAG attached (Kir6.2-HA+11aa-ΔHMKFLAG).

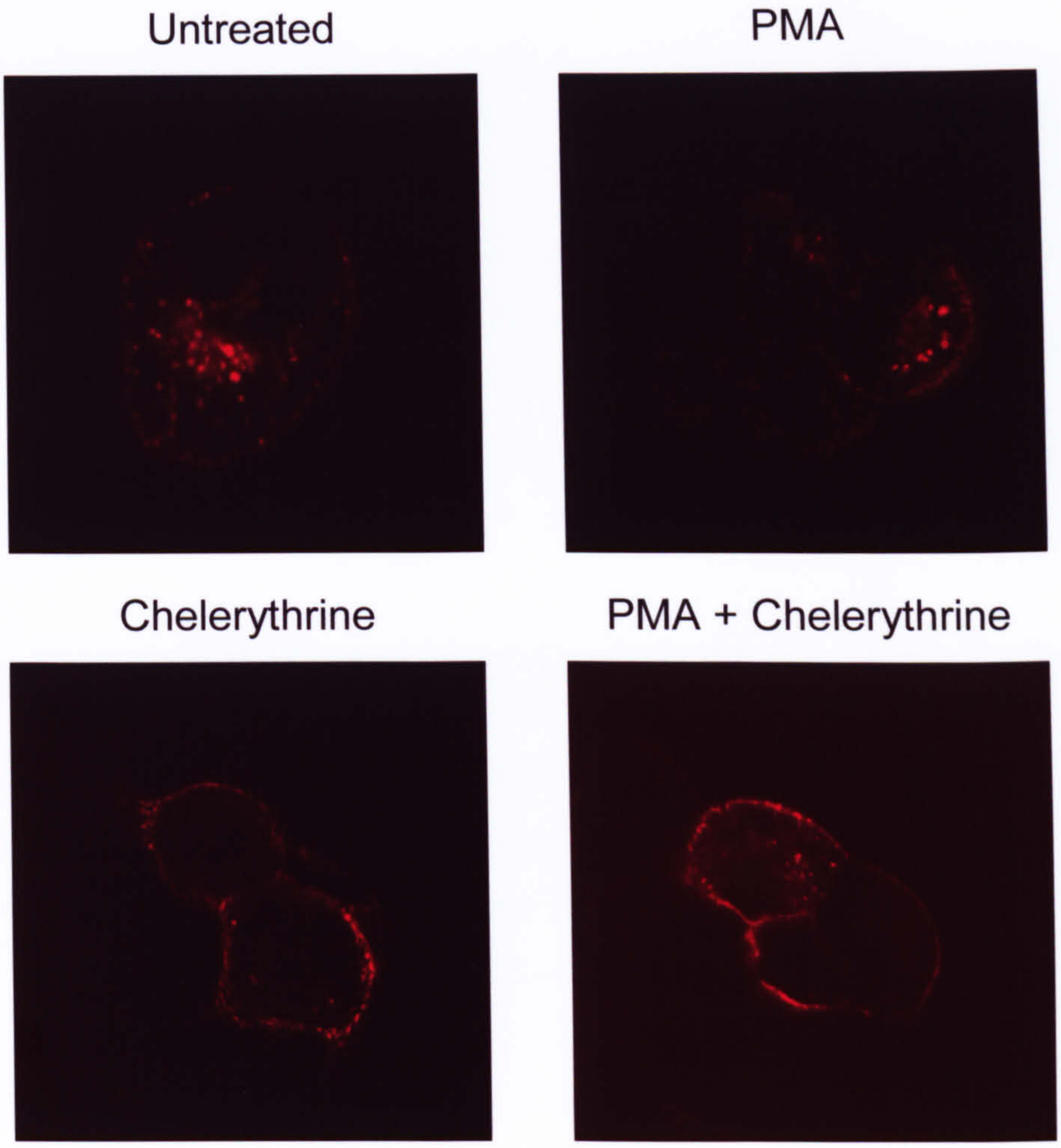

Figure 5.6 - *Removal of HMKFLAG from the C-terminus of Kir6.2-HA does not affect internalisation of K_{ATP}-HA channels.* HEK293MSRII cells were transiently transfected with SUR1 and Kir6.2-HA+11aa-ΔHMKFLAG. 48 hours post transfection the cells were stained with rat anti-HA antibodies (0.2 μg ml^{-1}) using the internalisation protocol before fixation and permeabilisation. The cells were then labelled with anti-rat Cy3-conjugated antibodies and were subsequently examined by LSCM. Representative images are shown (n = 3). The drugs used were PMA (phorbol-12-myristate-13-acetate) - 100 nM, CHE (chelerythrine) - 10 μM .

5.2.4 - Elucidation of the K_{ATP} channel endocytic trafficking pathway

Figures 5.2 and 5.3 suggest that in the stably transfected HEK293 cell line, K_{ATP} channels are constitutively internalised from the cell surface into numerous punctate structures in the perinuclear region of the cell. By identifying the identity of these structures it should be possible to elucidate the endocytic trafficking pathways through which K_{ATP} channels are translocated following internalisation from the cell surface. Cells were incubated at 37°C for two hours in the constant presence of anti-HA antibodies, so that all channels internalised channels from the cell surface during the duration of the incubation would be antibody bound. It was hoped that this would lead to labelled antibody being present in each compartment along the endocytic pathway of K_{ATP} channels and allow subsequent identification using fluorescent markers specific for each organelle.

The distribution of internalised channels was first compared to that of internalised fluorescent probes with well characterised trafficking pathways (figure 5.7). The first marker used was FITC-conjugated wheatgerm agglutinin (WGA) which is known to bind to glycoproteins at the cell surface before being internalised into the cell where it is eventually concentrated at the TGN. A fairly high degree of co-localisation was observed when the distribution of internalised K_{ATP} channels and WGA are compared; this is hardly surprising since most compartments will contain glycoproteins to some extent. The highest degree of co-localisation was apparent in the perinuclear regions of the cells where the WGA staining was at its most intense, perhaps suggesting the presence of K_{ATP} channels in the TGN or a TGN associated compartment. The second marker used was FITC-conjugated transferrin (Tf). Tf is known to bind to the transferrin receptor (TfR) at the cell surface leading to internalisation of the ligand-receptor complex. Following internalisation the ligand-receptor complex is rapidly recycled via a well characterised pathway involving the sorting endosome (SE) and the endocytic recycling compartment (ERC). Co-localisation between Tf staining and K_{ATP} channel staining was rather limited suggesting that K_{ATP} channels and Tf may not share a common trafficking itinerary to a significant extent.

Although these data give some indications as to the pathways which might be involved in K_{ATP} channel trafficking, further investigations are needed to confirm

what has been shown. In a similar series of experiments the distribution of internalised K_{ATP} channels was compared to the distribution of a number of organelle specific marker proteins. One way in which this was achieved was to transiently express GFP-tagged organelle marker proteins in the stably transfected HEK293 cells. A number of GFP-tagged markers were obtained including EEA1 (SE), Rab4 (SE & ERC), Rme-1 (ERC), Rab7 (LE & lysosome), Lamp1 (Lysosome) and TGN46 (TGN). As can be seen in figure 5.8 the most prominent co-localisation of fluorescence was observed between internalised K_{ATP} channels and EEA1 and TGN46. Slight co-localisation was observed with Rab7 and Rab4 and no co-localisation was observed with Rme-1 and Lamp1. Thus although a large amount of the internalised K_{ATP} channel fluorescence was co-localised with that of TGN46-GFP, the regions showing overlap accounted for only a small portion of the total TGN46-GFP fluorescence. This may imply that internalised K_{ATP}-HA channels are targeted only to specific regions of the TGN. Although the majority of internalised K_{ATP} channels did not co-localise with EEA1-GFP, the majority of EEA1-GFP positive structures did co-localise with internalised K_{ATP} channels. So whilst the majority of internalised K_{ATP} channels are not present in EEA1 containing compartments, it is likely that they do pass through these compartments at some point during the trafficking pathway. The slight co-localisation observed between internalised K_{ATP} channels and Rab4-GFP or Rab7-GFP suggests that these compartments may be involved at some point during the trafficking of the channels, albeit to a lesser extent. The lack of co-localisation between internalised K_{ATP} channels and Rme1-GFP or Lamp1-GFP would suggest that the compartments containing these markers are not involved in the trafficking pathways.

A second approach was used in order to confirm the previous co-localisation data using antibodies targeted against specific markers of the endocytic organelles (figure 5.9). The antibodies used were anti-CI-M6PR, anti-EEA1, anti-cathepsin-D, anti-TGN46 and anti-clathrin light chain. A very high degree of co-localisation was observed between internalised K_{ATP} channels and anti-CI-M6PR staining. At steady-state distribution, the majority of CI-M6PR is thought to reside in a recycling loop between the TGN and the late endosomes, although it is also supposed to be present at much lower levels at the cell surface and in the early endosomal system. The extent of co-localisation between internalised K_{ATP} channels and CI-M6PR suggests that

both the TGN and late endosomal compartments may be involved in the trafficking pathway. A high degree of co-localisation was also observed between internalised K_{ATP} channels and anti-clathrin light chain staining. Whilst a large proportion of this co-localisation was evident near the periphery of the cell, some co-localisation was also observed in larger structures in the perinuclear regions of the cell. The extent of co-localisation between anti-EEA1 and the internalised K_{ATP} channels was much lower by comparison but was still significant. Slight co-localisation was observed between internalised K_{ATP} channels and anti-cathepsin-D staining, but only in occasional isolated spots. No co-localisation was observed between internalised K_{ATP} channels and anti-TGN46.

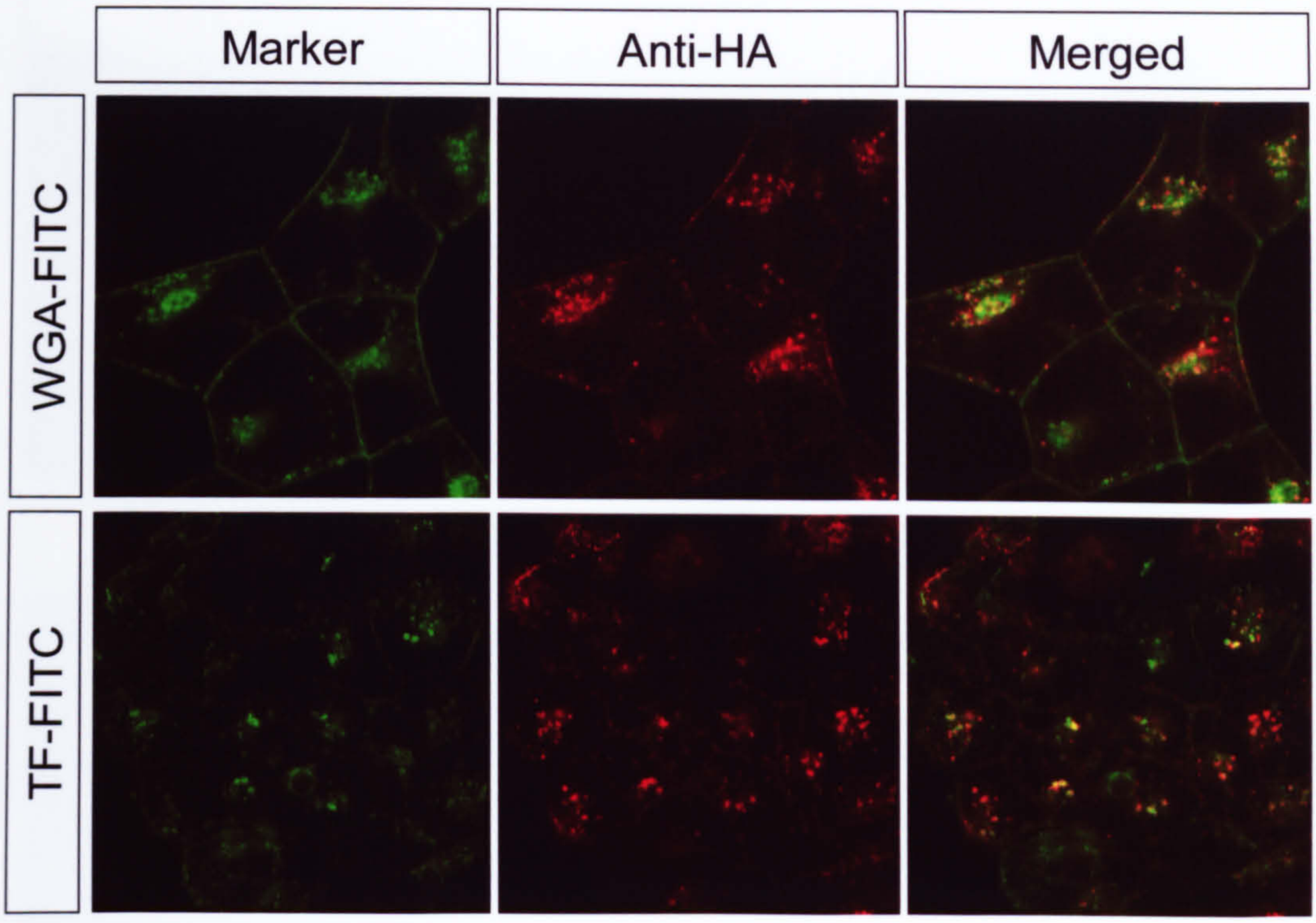

Figure 5.7 - *Co-localisation of internalised K_{ATP}-HA channels with internalised FITC-conjugated ligands.* Stably transfected HEK293 cells were stained with rat anti-HA antibodies (0.2 μg ml^{-1}) using the internalisation protocol. Media was supplemented with FITC-wheat germ agglutinin (WGA) (5 μg ml^{-1}) or FITC-transferrin (TF) (25 μg ml^{-1}) for the final 15 minutes of the incubation. Following this the cells were fixed, permeabilised and stained with anti-rat Cy3-conjugated antibodies. The cells were then viewed by LSCM. Representative images are shown (n = 3).

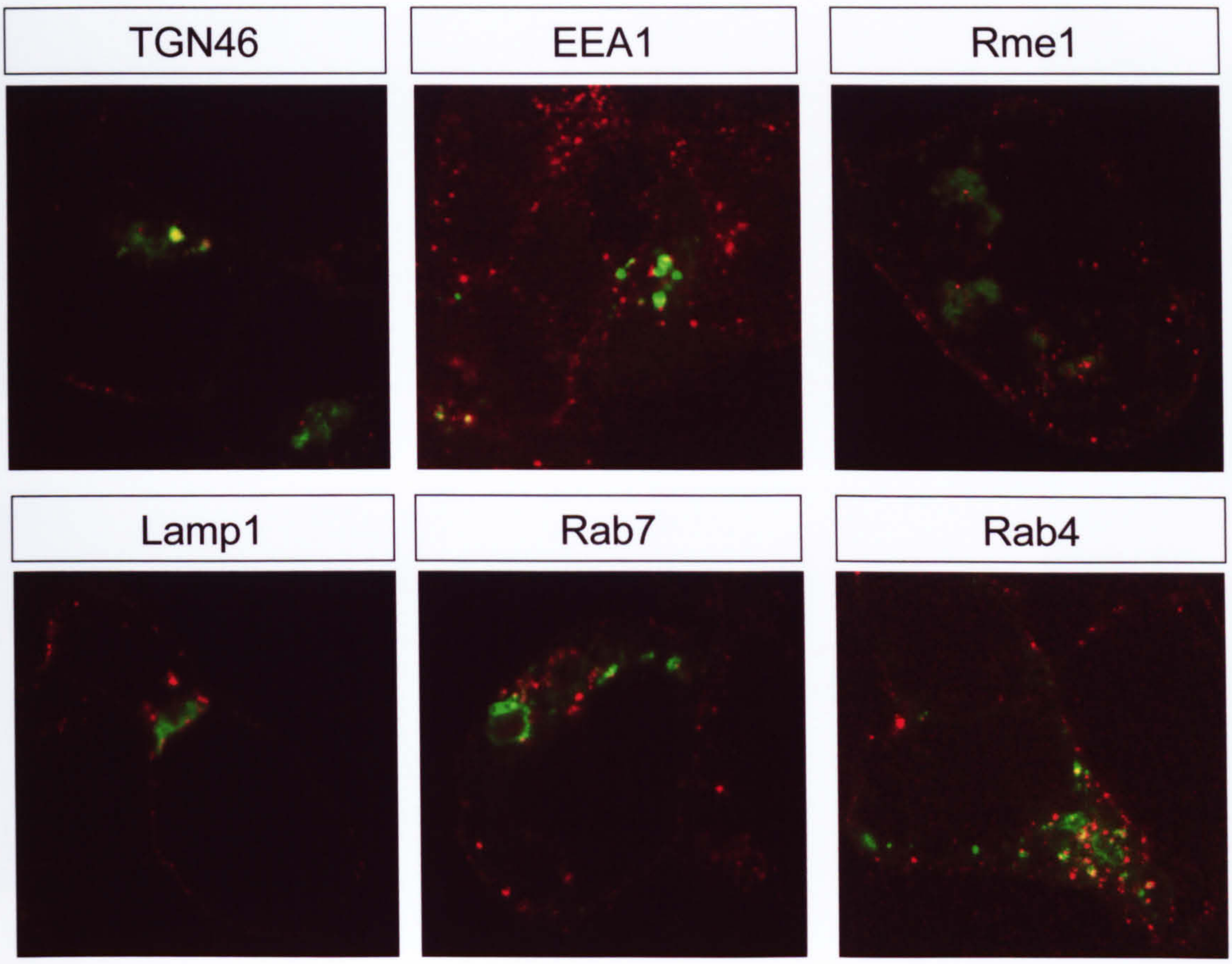

Figure 5.8 - *Co-localisation of internalised K_{ATP}-HA channels with EGFP-tagged organelle markers.* Stably transfected HEK293 cells were transfected with various EGFP-tagged organelle markers. 48 hours post-transfection cells were stained with rat anti-HA antibodies (0.2 μg ml^{-1}) using the internalisation protocol. Following this the cells were fixed, permeabilised and stained with anti-rat Cy3-conjugated antibodies (n = 4). The cells were then viewed by LSCM. Representative images are shown.

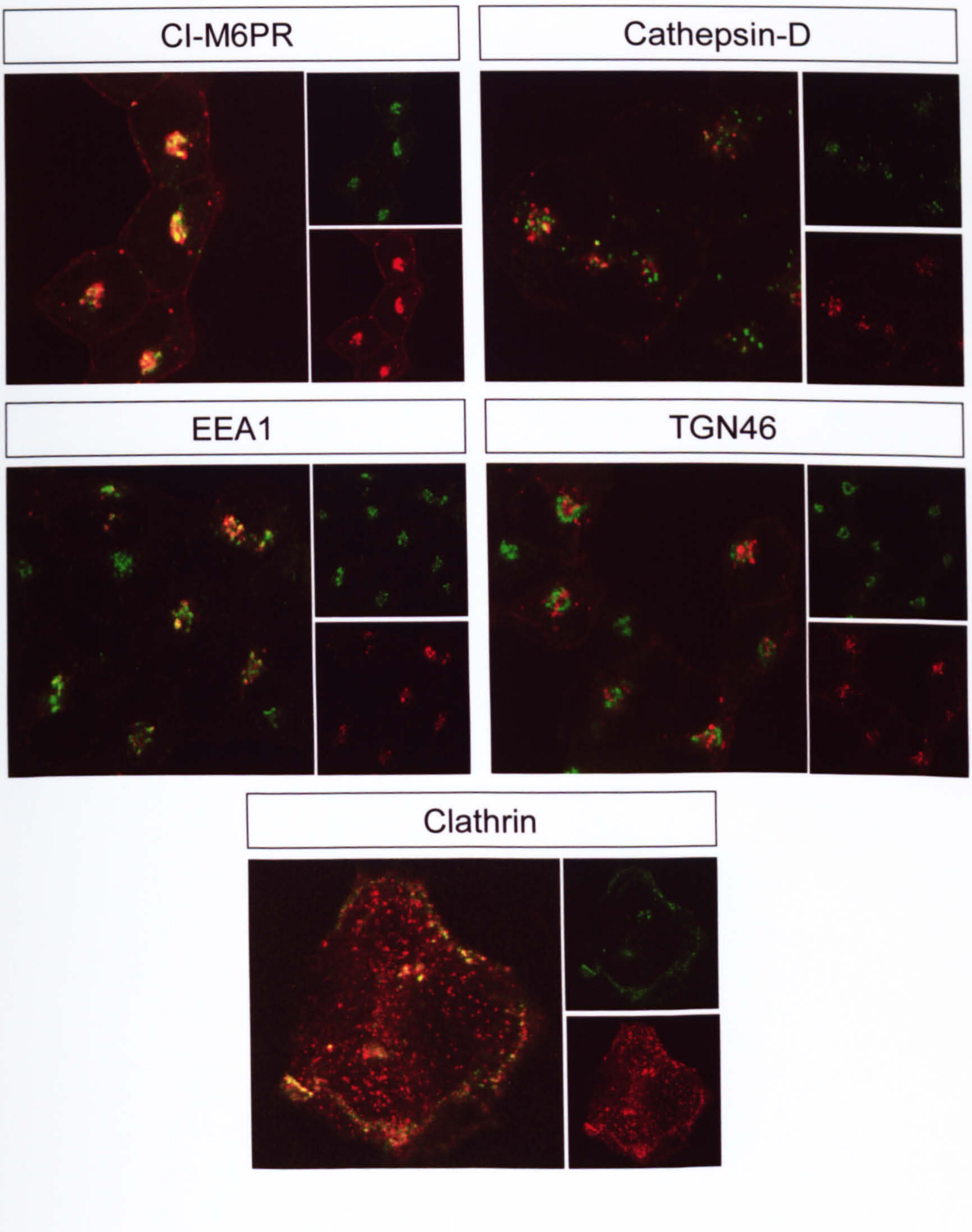
CI-M6PR
Cathepsin-D
EEA1
TGN46
Clathrin

Figure 5.9 - *Co-localisation of internalised K_{ATP}-HA with antibody labelled organelles.* Stably transfected cells were labelled with rat anti-HA antibodies (0.2 μg ml^{-1}) using the internalisation staining protocol. Cells were then fixed, permeabilised and labelled with antibodies targeted against various endocytic organelles. The antibodies used were mouse anti-cation independent mannose-6-receptor (CI-M6PR) antibody (10 μg ml^{-1}), mouse anti-cathepsin-D antibody (1 μg ml^{-1}), mouse anti-early endosome 1 (EEA1) antibody (2.5 μg ml^{-1}), sheep anti-TGN46 antibody (2.5 μg ml^{-1}) and mouse anti-clathrin light chain antibodies (0.5 μg ml^{-1}). Following this all cells were labelled with anti-rat Cy3-conjugated antibodies along with either anti-mouse FITC conjugated antibodies or anti-sheep FITC-conjugated antibodies as required (n = 3). Cells were subsequently examined by LSCM. Images of the cells stained with anti-clathrin light chain antibodies were taken in an optical plane near the coverslip attached membrane. Shown are the merged images along with the staining associated with each individual fluorophore (HA - red, organelle - green).

5.2.5 - Internalised K_{ATP} channels are recycled back to the cell surface

Many channels and transporters which are internalised from the cell surface enter into rapidly recycling pathways, leading to their reinsertion into the plasma membrane. The possibility that K_{ATP} channels are also similarly recycled was investigated. K_{ATP}-HA channels were labelled with anti-HA antibodies for 2 hours at 37°C so that HA-labelled internalised channels saturate the endocytic trafficking pathways. The cells were then incubated in acidic buffer at 4°C to strip any bound anti-HA antibodies from the cell surface whilst halting any other channel movement. Following the acid wash, cells were returned to media at 37°C containing FITC-conjugated secondary antibodies. Any channels bound with anti-HA antibodies which had previously been internalised which then recycled back to the cell surface would therefore be labelled with FITC. The remainder of the anti-HA-labelled channels which had remained within the cell throughout the FITC-labelling step were subsequently labelled with Cy3-conjugated antibodies. For the recycling assay to be effective it is vital that the acid strip step removes all bound anti-HA antibodies from the cell surface. The data presented in figure 5.10 shows that this is indeed the case. Cells were labelled with anti-HA antibodies using the internalisation protocol. Following internalisation, the cells were rapidly chilled to 4°C to halt trafficking, before incubation with either chilled acidic strip buffer or chilled phosphate buffered saline (PBS). The cells were subsequently fixed and surface fluorescence examined by LSCM. Those cells which had been treated with acidic strip buffer showed no surface fluorescence. This is in contrast with the cells treated with chilled PBS which displayed prominent fluorescence at the cell surface.

Shown in figure 5.11 is representative data depicting apparent K_{ATP} channel recycling. When the cells were allowed to recycle for 0 minutes no FITC staining is observed, suggesting that the acidic stripping buffer is removing all of the anti-HA antibodies from channels at the cell surface. FITC-staining begins to become apparent after only 5 minutes, with faint fluorescence at the cell surface. After a further 10 minutes (t = 15 min) the faint staining at the cell surface is still apparent at as well as some fluorescence in punctate structures within the cytoplasm of the cell. For the remainder of the first hour the staining is seen at both the cell surface and in the cell interior but the intensity of the FITC-fluorescence (recycled channels) increases whilst the intensity of the Cy3-fluorescence (non-recycled channels)

decreases. At later time points (t = 2 hr and t = 3 hr) the intensity of fluorescence at the cell surface becomes less intense and the vast majority of fluorescence is apparent in the perinuclear compartments. These data suggest that K_{ATP} channels are recycled back to the cell surface following internalisation.

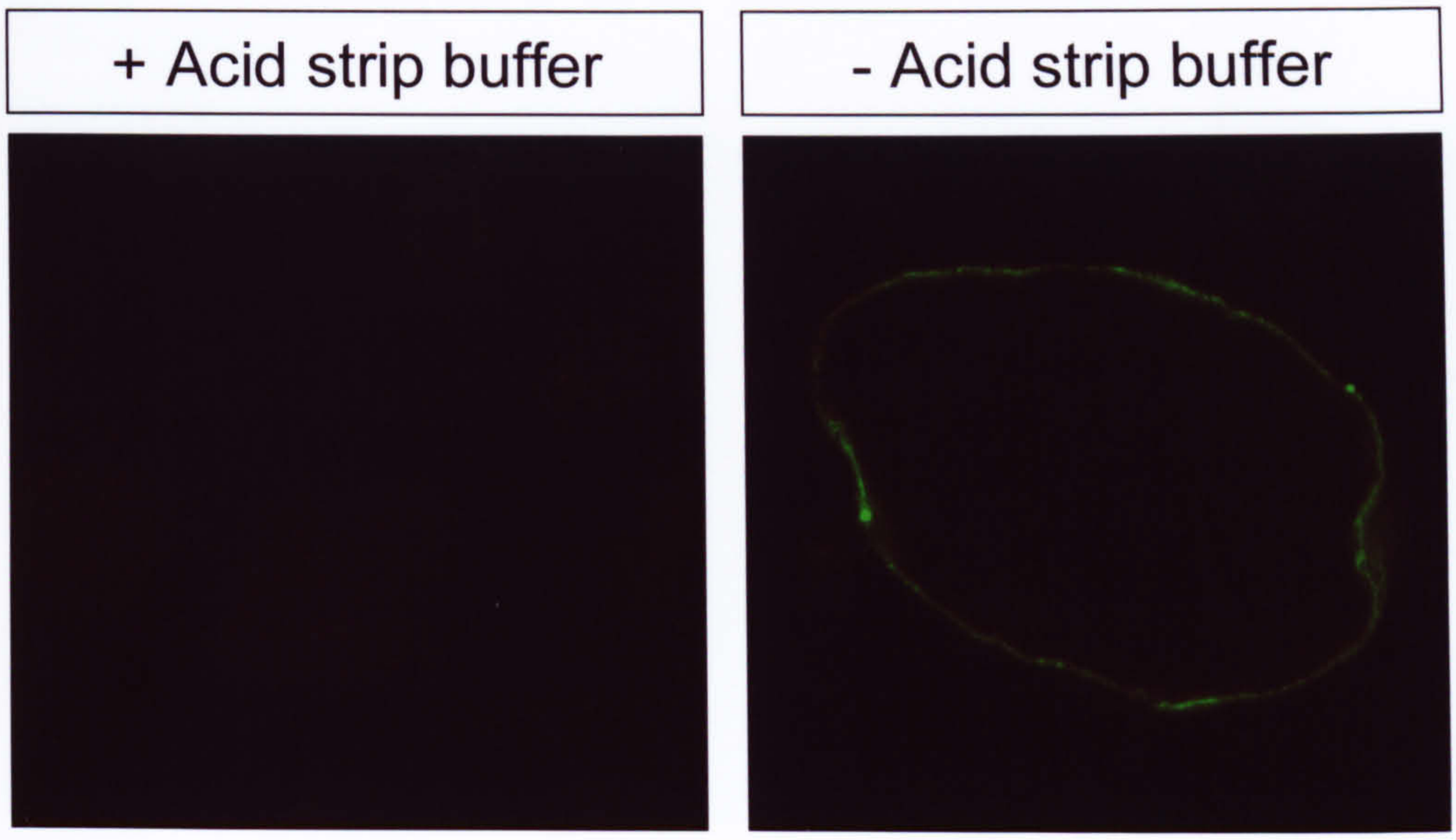

Figure 5.10 - *Treatment with acidic stripping buffer removes surface bound anti-HA antibodies.* Cells were labelled with rat anti-HA antibodies (0.2 μg ml^{-1}) for 2 hours at 37°C. The cells were then rapidly chilled to 4°C and incubated in either chilled acidic stripping buffer (+ acid strip buffer) or in chilled PBS (- acid strip buffer) for 30 minutes at 4°C. The cells were then fixed and labelled with anti-rat FITC conjugated secondary antibodies (n = 3). The labelled cells were subsequently viewed by LSCM.

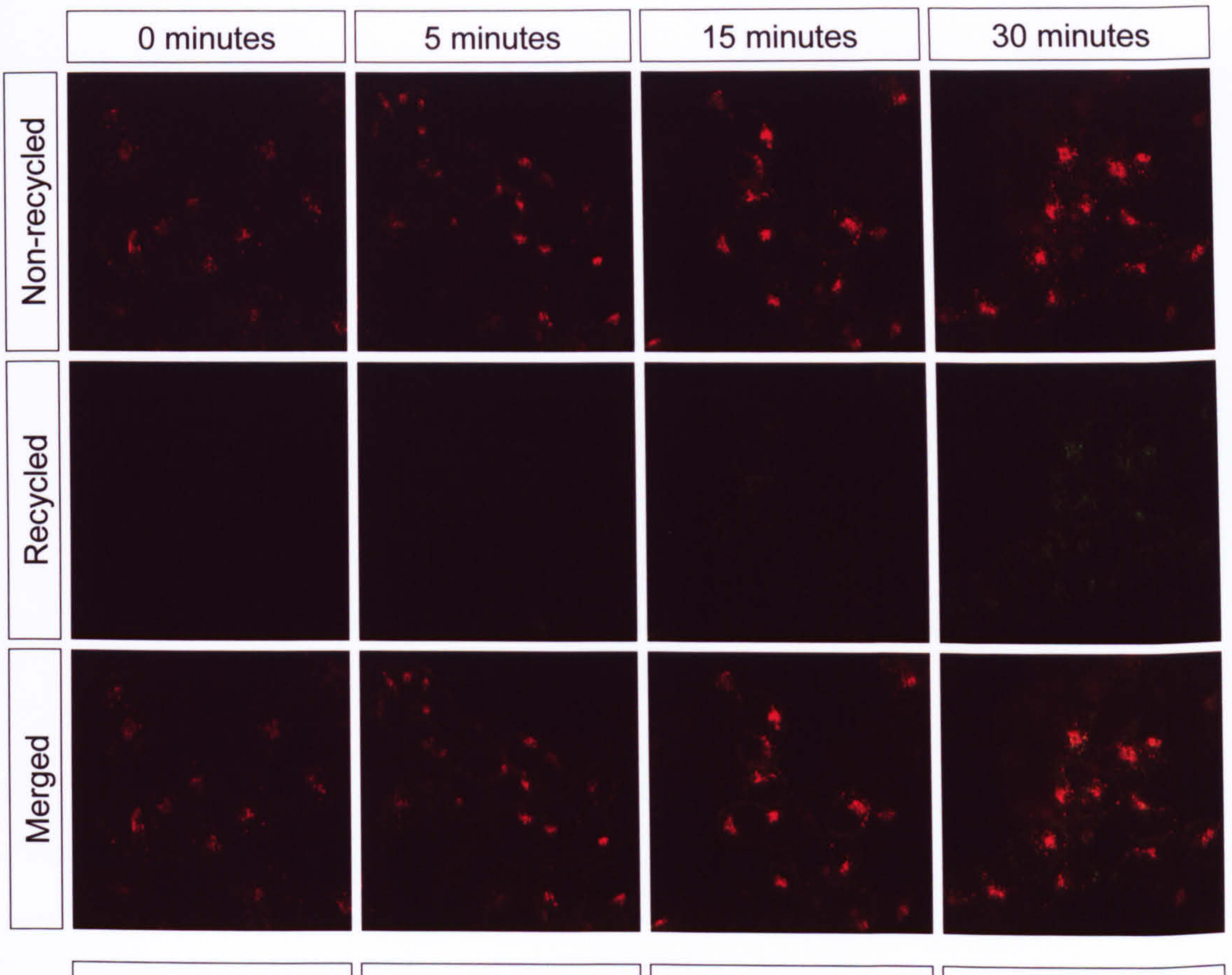
0 minutes
5 minutes
15 minutes
30 minutes
Non-recycled
Recycled
Merged
45 minutes
1 hour
2 hours
3 hours
Non-recycled
Recycled
Merged

Figure 5.11 - K_{ATP}-*HA channels recycle following internalisation from the cell surface.* HEK293 cells stably expressing K_{ATP}-HA channels were labelled with rat anti-HA antibodies (0.2 μg ml^{-1}) using the recycling protocol. Recycled channels were labelled with anti-rat FITC-conjugated antibodies and non-recycled channels were recycled with anti-rat Cy3-conjugated antibodies. Cells were then viewed by LSCM using identical settings for each image. Representative images are shown (n = 2).

5.2.6 - Channel recycling is PKC dependent

The data reported in chapter 5.3.3 supports the observations of Hu *et al.* (2003) that the internalisation of K_{ATP} channels appears to be dependent on PKC activation. It is shown in figure 5.3 that PKC activation leads to a redistribution of channels from the cell surface into a perinuclear compartment. When PKC activity is inhibited the channels remain at the cell surface. This effect may be achieved in two ways; either by preventing internalisation of channels when PKC is inhibited or by increasing the recycling of internalised channels. The effect of PKC activity on the recycling of K_{ATP} channels was investigated using the recycling assay as described in chapter 2.4.5 with cells treated with either PMA or chelerythrine.

Cells treated with PMA behaved very similarly to those cells which were untreated (figure 5.12). In cells where recycling had not been allowed (t = 0) the majority of Cy3-fluorescence, corresponding to non-recycled channels, was located in the perinuclear compartments with some also present at the periphery of the cell, possibly in vesicles near the cell surface. No FITC-fluorescence was observed in these cells, confirming that no recycling had occurred. At later time points the amount of FITC-fluorescence increases and is apparent at both the cell surface and in the perinuclear compartment following 30 minutes of recycling whilst the Cy3 fluorescence is confined to the perinuclear compartment. From 60 minutes of recycling and onwards all of the fluorescence is seen only in the perinuclear compartment and not at the cell surface. At this stage the FITC-labelled channels co-localise fairly well with those channels labelled with Cy3, suggesting that those channels which have initially recycled (green) were later sequestered to the same compartment as those channels which where never recycled (red) to the cell surface during the recycling step.

By contrast, cells treated with chelerythrine showed a marked difference between the distribution of recycled channels to that observed in cells which were either untreated or treated with PMA (figure 5.13). In cells where recycling had not been allowed (t = 0) no FITC-fluorescence was observed, consistent with no channel recycling, and the majority of the Cy3-fluorescence was observed towards the periphery of the cell with very little visible in the perinuclear compartments. After 30, 60 and 120 minutes of recycling, both the FITC and Cy3-fluorescence remains near at the periphery of the cell and little is observed in the perinuclear compartments.

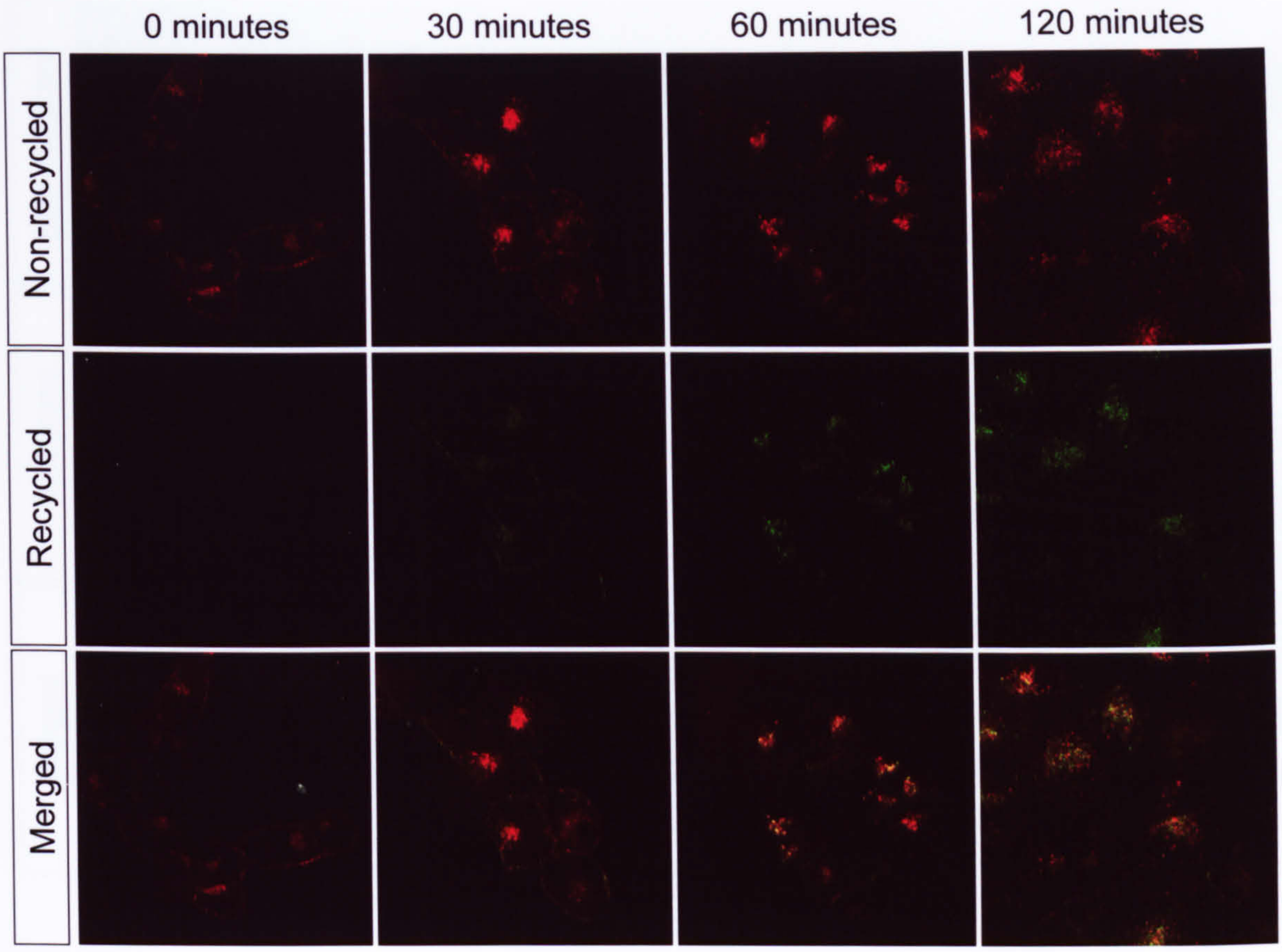

Figure 5.12 - *Effect of PKC activation on recycling of K_{ATP}-HA channels*. Stably transfected cells were treated with PMA (100 nM) for 30 minutes prior to and for the duration of labelling with rat anti-HA antibodies (0.2 μg ml^{-1}) using the recycling protocol. Recycled channels were labelled with anti-rat FITC-conjugated antibodies and non-recycled channels were labelled with anti-rat Cy3-conjugated antibodies. Cells were then viewed by LSCM using identical settings for each image. Representative images are shown (n = 1).

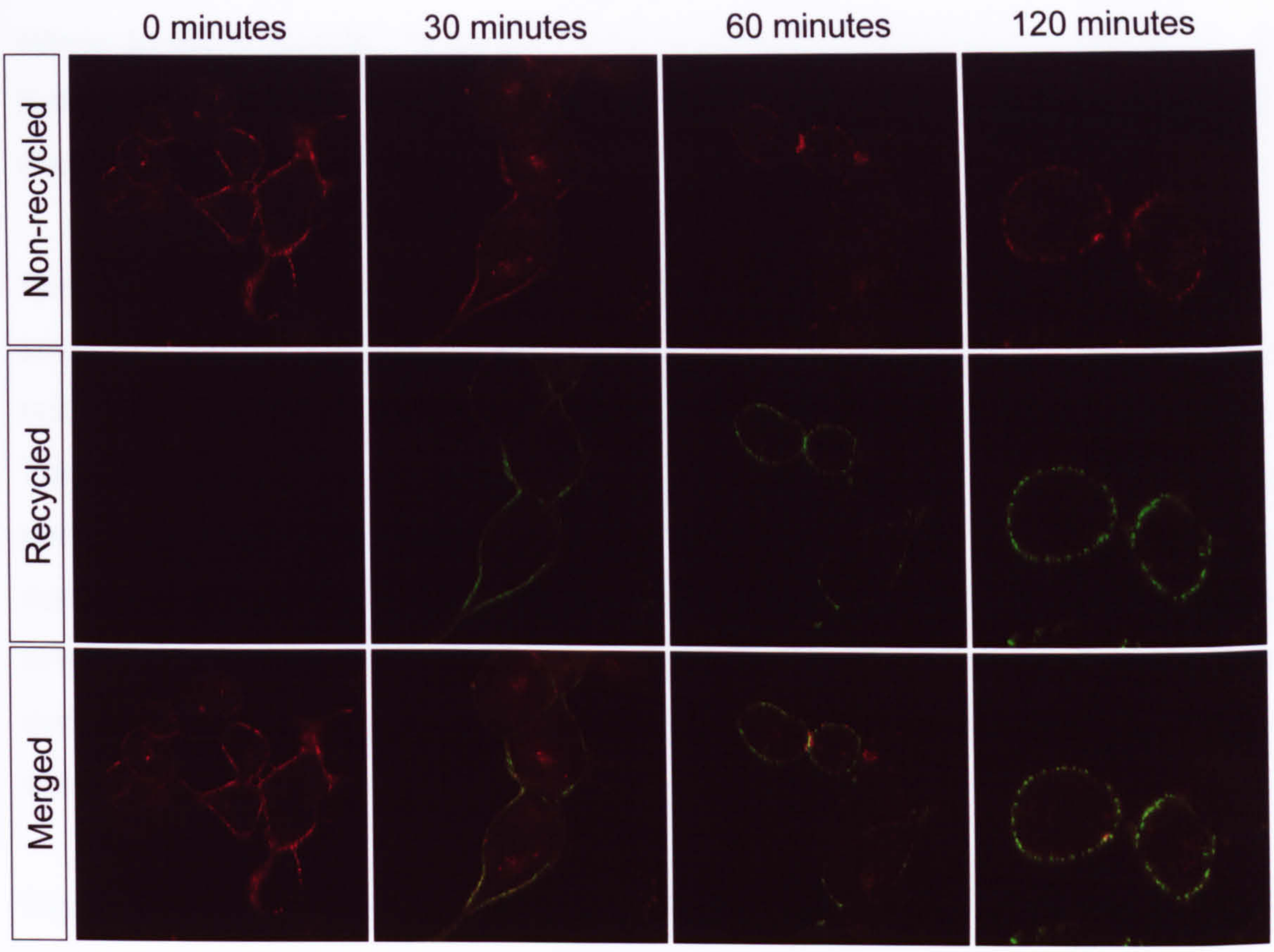

Figure 5.13 - *Effect of PKC inhibition on recycling of K_{ATP}-HA channels*. Stably transfected cells were treated with chelerythrine (10 μM) for 30 minutes prior to and for the duration of labelling with rat anti-HA antibodies (0.2 μg ml^{-1}) using the recycling protocol. Recycled channels were labelled with anti-rat FITC-conjugated antibodies and non-recycled channels were labelled with anti-rat Cy3-conjugated antibodies. Cells were then viewed by LSCM using identical settings for each image. Representative images are shown (n = 1).

5.2.7 - Live cell imaging reveals two potential pools of trafficking vesicles

The previous data suggest that both the internalisation and recycling of K_{ATP} channels is very rapid and that the channels may be present in two pools of vesicles; those that rapidly recycle and those which are trafficked to the perinuclear compartment and appear to not to recycle. In an attempt to confirm these observations and to gain a further understanding of the properties of these vesicles, the movement of labelled channels was investigated in live cells.

For the purposes of viewing the movements of K_{ATP}-HA laden vesicles within live cells, Alexafluor594-conjugated anti-HA antibodies were used to label channels at the cell surface and then to follow any subsequent internalisation and trafficking events. The uptake of the anti-HA antibodies relies on the presence of the HA epitope and is not due to uptake of fluorophore by fluid phase uptake as shown in figure 5.2A. The resulting movies are included as supplementary material. Figures 5.14 and 5.15 show several still images taken from sequential frames of one of these movies and demonstrate two of the most common types of trafficking vesicles observed in these cells.

Figure 5.14 shows an example of a vesicle which is trafficked from near the periphery of the cell into the perinuclear compartment. This vesicle is fairly large compared to a number of other vesicles in the cell and may possibly represent part of an endosomal compartment. The vesicle is first located in the cytoplasm approximately one-third of the way between the cell surface and the mass of fluorescence in the perinuclear compartment and appears to be spherical in shape *(upper left and right panels)*. The vesicle then begins to move rapidly towards the perinuclear compartment. As it does so the vesicle can be seen to elongate, possibly as it translocates along microtubules *(lower left and right panels)*. This vesicle and others like it may represent a population of vesicles which are translocated away from the plasma membrane into the perinuclear compartments.

Figure 5.15 shows an example of a vesicle which appears to recycle directly back to the cell surface following internalisation. This vesicle is much smaller than those described above and may represent an endocytic vesicle of some description. Throughout the duration of the time course shown the vesicle never moves very far

from the plasma membrane. The highlighted vesicle appears to be very short lived, rejoining the plasma membrane only ~ 10 seconds after appearing in the cytoplasm. The size and shape of this vesicle appears to remain unchanged throughout this trafficking in contrast to the vesicle shown in figure 5.14. This vesicle and others which behaves in a similar fashion may represent vesicles which rapidly recycle to the plasma membrane following internalisation.

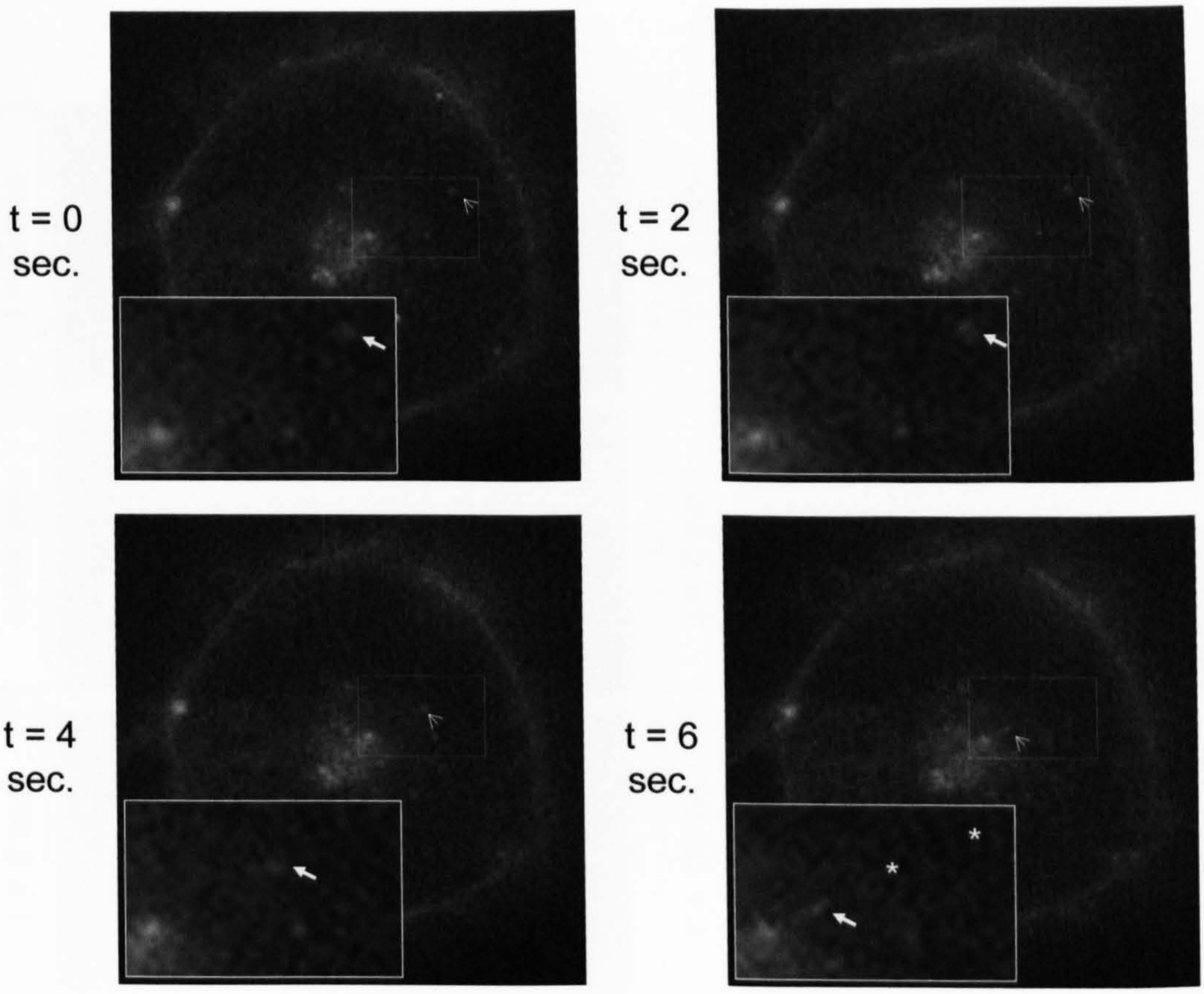

Figure 5.14 - *Live cell imaging of K_{ATP}-HA channel internalisation reveals a population of rapidly moving vesicles.* Stably transfected HEK293 cells were labelled with mouse anti-HA Alexafluor594-conjugated antibodies (2 μg ml^{-1}) using the live cell imaging protocol. Each frame was captured at 2 second intervals. Shown are four sequential frames corresponding to frames 170 - 173 of the movie included in the supplementary material (see animation 1 on the attached CD). Inset images correspond to expanded versions of the outlined area shown in the main image. The arrows highlight a vesicle of interest as it traverses the cell. The positions of the vesicle in the previous frames are denoted by * in the final image. The experiment was repeated three times and similar results were obtained each time.

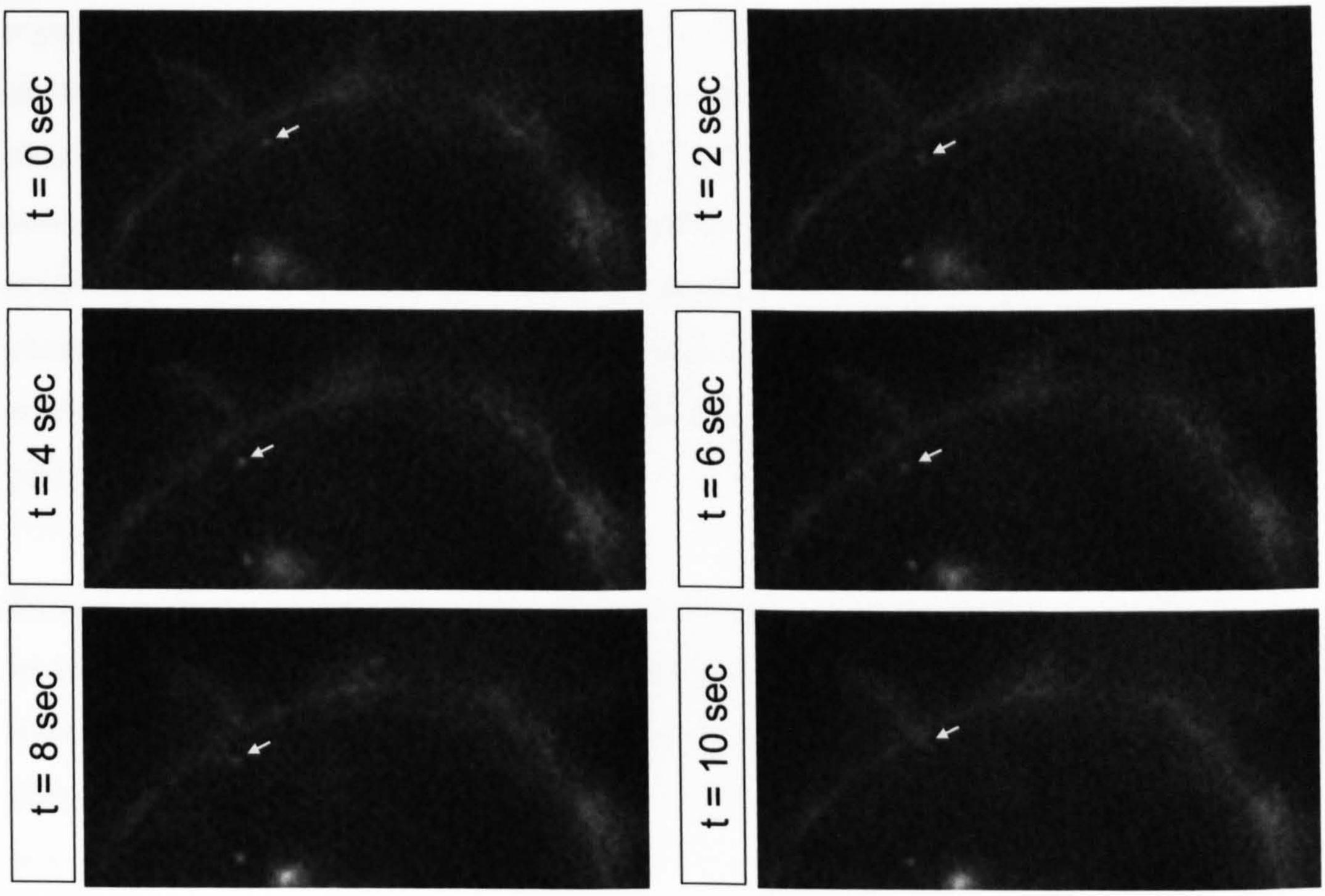

Figure 5.15 - *Live cell imaging of K_{ATP}-HA channel internalisation reveals a population of rapidly recycling vesicles.* Stably transfected HEK293 cells were labelled with mouse anti-HA Alexafluor594-conjugated antibodies (2 μg ml^{-1}) using the live cell imaging protocol. Each frame was captured at 2 second intervals. Shown are eight sequential frames corresponding to frames 40 - 45 of the movie included in the supplementary material (see animation 1 on the attached CD). The arrows highlight a vesicle of interest as it enters the cell and recycles back to the cell membrane. The experiment was repeated three times and similar results were obtained each time.

5.3 - Discussion

5.3.1 - Overview

Shown in the results section is evidence in support of the endocytic trafficking pathways of K_{ATP} channels. Also presented are data suggesting that this trafficking is regulated by the activity of protein kinase C (PKC). HA-tagged K_{ATP} channels are shown to internalise constitutively and rapidly into HEK293 cells. Internalised channels have been demonstrated to be present in a number of perinuclear compartments including the sorting endosome, late endosomes and the *trans*-Golgi network (TGN) or a TGN associated compartment. A proportion of internalised channels are rapidly recycled back to the cell surface, a process which is enhanced when PKC activity is suppressed. The final fate of the channels internalised into the perinuclear compartments is still not clear.

Shown in figure 5.16 are the likely endocytic trafficking pathways for K_{ATP} channels as suggested by the current data. It is suggested that the channels are first rapidly internalised from the cell surface and enter the sorting endosome. At this stage the channels are either recycled directly back to the cell surface in a pathway which does not appear to involve the endocytic recycling compartment or they are directed towards the late endosomal compartment. It would appear that this sorting step is regulated by PKC. From the late endosome the vast majority of the internalised channels are directed towards the TGN or a TGN-associated compartment although it appears possible that a small fraction of internalised channels may be targeted to lysosomes for degradation. The fate of the channels once at this destination is not known, although many possibilities exist, including recycling and storage, as will be discussed in more detail below.

5.3.2 - Residency at the membrane and mechanisms of endocytosis

These data suggest that the residence time of K_{ATP} channels at the cell membrane is fairly short. Two lines of evidence point toward this. Firstly, internalisation of channels from the cell surface is very rapid, with almost complete removal of labelled channels from the surface within 10 minutes (figure 5.4). Secondly, labelling of recycled channels reveals that newly recycled channels can be seen to move rapidly from the cell membrane into cytoplasmic vesicular structures (compare figure 5.11, at

5 minutes and 15 minutes). This suggests that channels which are recycled back to the cell surface from the cell interior may remain in the cell membrane for as short a time as 5-10 minutes before re-internalisation.

The exact mechanisms of channel internalisation are not clear. The rapid nature of internalisation, almost all surface labelled channels internalised within 10 minutes (figure 5.4), suggests that clathrin mediated endocytosis is the most likely mechanism, since internalisation via other means is thought to be much slower (Conner & Schmidt 2003). Indeed, internalised channels show a very high degree of co-localisation with anti-clathrin light chain antibodies near the periphery of the cell (figure 5.9). If clathrin mediated endocytosis were responsible for the removal of channels from the cell surface it would be expected that this process would be inhibited by overexpression of dominant negative forms of dynamin (Damke *et al.* 1994). An examination of the role of dynamin in the internalisation of K_{ATP} channels by Hu *et al.* (2003) suggested that dominant-negative forms of dynamin did indeed slow the rate of endocytosis further reinforcing its potential role in this initial internalisation step. However, a large proportion of the anti-clathrin light chain co-localisation is located near the centre of the cell. These structures could represent endosomal or TGN-associated compartments through which K_{ATP}-HA channels are trafficked, since clathrin has been shown to be present on these compartments where it is thought to regulate movement to and from one compartment and the next (Nicoziani *et al.* 2000).

If the exact mechanisms which mediate K_{ATP} channel endocytosis are to be elucidated, further investigation must be undertaken. Should channel endocytosis not be clathrin mediated it is possible that the process might be mediated by caveolin, with internalisation of channels via caveolae. For internalisation by this mechanism to occur the channels must first be present in lipid-rafts in the plasma membrane of the cell. It has been reported that K_{ATP} channels consisting of SUR1 and Kir6.2 (the same composition as the channels examined in the present study) are excluded from lipid rafts in pancreatic β-cell membranes (Xia *et al.* 2004). However, a more recent study has isolated K_{ATP} channels containing Kir6.1 from lipid rafts in aortic smooth muscle (Sampson *et al.* 2004) raising the possibility that pancreatic-like K_{ATP} channels (Kir6.2 + SUR1) might also be present in lipid rafts, even if only in a transient manner. The rapid nature of internalisation suggests that uptake via

caveolae is not very likely as this form of uptake is thought to be fairly slow (t½ > 20 minutes) (Conner & Schmidt 2003) although the involvement of caveolin and lipid rafts in the internalisation process may warrant further investigation. Other areas on which to focus further research could involve the role of the adaptor-proteins, such as AP-2, on channel internalisation. Dominant negative forms of AP-2 should selectively inhibit clathrin coated vesicle formation at the cell membrane whilst not affecting clathrin dependent intracellular trafficking mechanisms which are thought to rely on AP-1, AP-3 and AP-4 (Dell'Angelica *et al.* 1997, Simpson *et al.* 1997, Meyer *et al.* 2000, Ihrke *et al.* 2004, Peden *et al.* 2004). One approach which could prove particularly useful in further elucidating these processes is electron microscopy, which might provide a much higher resolution view of the processes occurring.

5.3.3 - Trafficking through early endosomes

For all material internalised from the cell surface which is destined for the endosomal system the point of entry is the sorting endosome. The entry of endocytosed material relies on the fusion of endocytic vesicles with the sorting endosome, a process which is regulated by Rab5 and EEA1 (Rubino *et al.* 2000). Once in the sorting endosome some material, such as the transferrin receptor, is targeted to the endocytic recycling compartment (ERC) from where they are returned to the cell surface in a process dependent on the action of Rab4, Rab11 and Rme1 (Ward *et al.* 2005). The trafficking of internalised K_{ATP} channels through the early endosomal compartments was investigated by several approaches. Internalised K_{ATP} channels co-localised fairly well with both GFP-tagged EEA1 (figure 5.8) and anti-EEA1 antibody associated fluorescent staining (figure 5.9). This suggests that K_{ATP} channels are indeed present in the sorting endosome following internalisation from the cell surface. Limited co-localisation was evident when the distribution of internalised K_{ATP} channels was examined alongside that of GFP-tagged Rab4 (figure 5.8), which is known to be present in both the sorting endosome and ERC (Sonnichsen *et al.* 2000). Limited staining was also observed when the distribution of internalised channels was compared to that of internalised FITC-conjugated transferrin (figure 5.7) which would also be expected to be present in both the sorting endosomes and ERC. No co-localisation of staining was observed when comparing internalised channels along with GFP-tagged dominant negative form of Rme1 (figure 5.8), which is known to accumulate ERC cargo proteins (Lin *et al.* 2001). Taken together it appears likely

that K_{ATP} channels are present in sorting endosomes following internalisation from the cell surface as indicated by co-localisation between the channels and EEA1 and to a smaller extent Rab4. Since residency time in the sorting endosome is thought to be very short ($t_{1/2} \sim 2$ - 4 minutes) (Conner & Schmid 2003) the extent of co-localisation observed may not be as robust as that observed in other organelles where cargo accumulation may have more opportunity to occur. It does not appear likely that the internalised channels are present in the ERC, since no co-localisation was observed with Rme1-DN-GFP (figure 5.8). It could be argued that the limited co-localisation observed with FITC-conjugated transferrin (figure 5.7) could imply that the internalised channels are indeed present in the ERC since transferrin will only be present in either the sorting endosome or the ERC. However, if the internalised channels were present in the ERC, a higher degree of co-localisation might be expected, with all FITC-transferrin staining overlapping to some degree with staining associated with internalised channels. Since this is not the case it is likely that the overlap of staining observed with FITC-transferrin is due to the proportion of transferrin which is still contained within the sorting endosome. In conclusion, it appears that internalised K_{ATP} channels enter the endocytic system via the sorting endosome but are excluded from the ERC. Any rapid recycling which occurs must be occurring directly from the sorting endosome, and will be discussed in more detail below. These findings are supported by the observations of Hu *et al.* (2003) who described only very slight co-localisation with Rme1-GFP following PKC stimulated K_{ATP} internalisation in COS1 cells.

5.3.4 - Trafficking through late endosomes and lysosomes

Since it does not appear that the internalised channels are targeted into the ERC from the sorting endosome, it is likely that they are translocated towards the late endosomal compartments. Evidence for this comes from extensive co-localisation of internalised channels with fluorescence associated with anti-cation-independent mannose-6-phosphate receptor (CI-M6PR) antibodies (figure 5.9). CI-M6PR has been shown to be enriched in the late endosomal compartment as well as the TGN of most cell types and has been used extensively as a marker for these compartments (Dintzis *et al.* 1994). Another marker for late endosomes, albeit less selective, is Rab7 which is involved in late endosomal maturation as part of lysosome biogenesis (Bucci *et al.* 2000). Internalised K_{ATP} channels do show some co-localisation with Rab7-GFP,

although only to a lesser extent (figure 5.8). This may be because the compartments enriched in Rab7 are already undergoing the maturation necessary for its conversion into lysosomes, and that internalised channels have been excluded for traffic to different compartment. Consistent with this, lysosomal markers such as Lamp1-GFP or anti-cathepsin-D antibody associated fluorescence (both proteolytic enzymes enriched in the lysosome) (Dean & Barrett 1976, Diment *et al.* 1988) display very little, if any, co-localisation with internalised K_{ATP} channels. This could suggest that the majority of internalised channels are diverted away from the lysosome mediated protein degradation pathways and to another destination. Another possibility for the lack of co-localisation of internalised channels with markers for lysosomes could be that the low luminal pH of these compartments, coupled with the enrichment of proteolytic enzymes, could interfere with anti-HA antibody binding to the channel. The targeting of internalised K_{ATP} channels to a degradative pathway, is however, unlikely, since the half life of mature channels has been reported to be as long as 7.3 hours (Crane & Aguilar-Bryan 2004). If internalised channels were targeted towards lysosomes the rapid nature of channel endocytosis would surely mean that channel turnover would be much more rapid than that reported, but labelling remains intense for a number of hours following the internalisation into the perinuclear compartments (figure 5.11). In conclusion, it would appear that internalised K_{ATP} channels are targeted from the sorting endosome to the late endosome where further sorting occurs to divert the bulk of the channels away from entering the lysosome. These findings are supported by the observations of Hu *et al.* (2003) who described a fairly high degree of co-localisation between internalised K_{ATP} channels and Rab7-GFP in COS1 cells.

5.3.5 - Trafficking to the *trans*-Golgi network (TGN)

The direct trafficking pathways between the late endosome and TGN have been fairly well characterised and it is possible that the internalised K_{ATP} channels could utilise one of these routes following sorting in the late endosome. As with the investigation of earlier compartments, a number of markers were used in an attempt to evaluate the role of the TGN in K_{ATP} channel endocytic trafficking. Firstly, FITC-conjugated wheat-germ agglutinin (WGA) accumulation in the TGN was used as a crude marker. WGA binds to glycoproteins and so will label any region of the cell where glycoproteins are found. Apart from the cell membrane the main concentration of

glycoproteins in cells is found at the TGN, so any regions of strong intracellular perinuclear fluorescence would most likely be associated with the TGN. A fair degree of co-localisation was observed between internalised K_{ATP} channels and FITC-conjugated WGA suggesting the possibility that the TGN may play a role in the endocytic trafficking pathways (figure 5.7). These findings are supported by the observations of Hu *et al.* (2003) who described a very high degree of co-localisation between internalised K_{ATP} channels and fluorescent-WGA in COS1 cells. However, WGA is not selective enough for the TGN to be sure that the co-localisation observed is due to internalised channels in this compartment. To confirm the above data the distribution of internalised channels was compared to that of the TGN resident protein TGN46, visualised by both TGN46-GFP and anti-TGN46 antibodies. Significant co-localisation was observed between internalised K_{ATP} channels and TGN46-GFP (figure 5.8) suggesting that the channels are indeed targeted to the TGN. In contrast, no co-localisation was observed when the distribution of internalised channels was compared to that of anti-TGN46 antibodies (figure 5.9). It is possible that this discrepancy has arisen because the TGN46-GFP has become overexpressed and so has 'over-flowed' into other compartments which are peripheral to the TGN. It is also possible that internalised K_{ATP} channels are directed to areas of the TGN in which TGN46 is not normally found at steady state, since it has been reported that many TGN resident proteins are segregated from cargo proteins (Hirschberg *et al.* 1998) especially in the more peripheral regions of the TGN. In conclusion, it appears possible that internalised K_{ATP}-HA channels are directed to the TGN or to a TGN-derived endosomal compartment following passage through the late endosome. This is suggested by the high degree of co-localisation observed between internalised K_{ATP} channels with both WGA in the perinuclear region and TGN46-GFP. These findings are also supported by the very good co-localisation observed between internalised K_{ATP} channels and CI-M6PR which at steady state is found to some extent in the TGN as well as the late endosome.

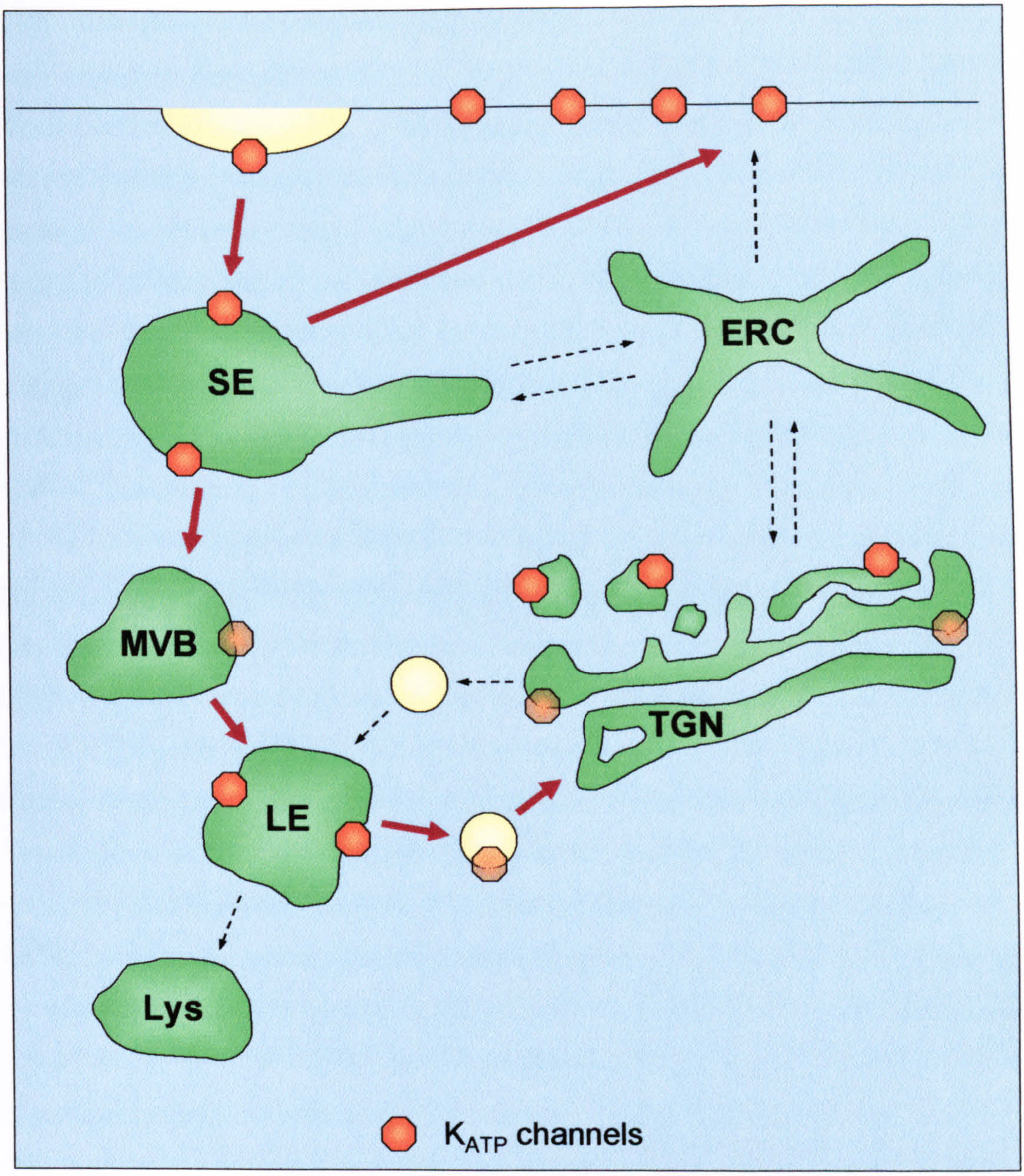

Figure 5.16 - *Schematic of the suggested endocytic trafficking pathways of K_{ATP} channels.* Where strong evidence for K_{ATP} channel residency of a compartment is shown solid symbols are shown. Where evidence for K_{ATP} channel residency is less convincingly shown symbols are semi-transparent. The suggested trafficking pathways are shown by the thick red arrows. Other trafficking pathways which are not thought to be involved are shown by dashed arrows. SE - sorting endosome, ERC - endocytic recycling compartment, MVB - multi-vesicular body, LE - Late endosome, TGN - *trans*-Golgi network, Lys - lysosome.

5.3.6 - Recycling of internalised K_{ATP} channels

K_{ATP} channels have the ability to recycle back to the cell surface following internalisation (figure 5.13). An antibody-capture assay was devised allowing examination of recycling dynamics of K_{ATP} channels as described earlier (2.4.5). As a result of the antibody-capture assay, anti-HA bound channels which had previously been internalised, and so were protected from the acid stripping step, and had then subsequently been recycled back to the cell surface were labelled with FITC-conjugated secondary antibodies. The remaining HA-bound antibodies which had not recycled would be labelled with Cy3-conjugated secondary antibodies. The absence of FITC fluorescence at the beginning of the experiment (t = 0) where no recycling has been allowed suggests that the acid-stripping has successfully removed all bound-HA from the cell surface. This means that any FITC fluorescence observed at later time points will be as a result of recycled channels and not due to contamination from labelled channels already at the cell surface. Recycled channels, i.e. those which have bound FITC-conjugated antibodies, begin appearing at 5 minutes of recycling at the surface of the cell. This is hardly surprising since the entire endocytic pathways of these cells will have HA-labelled antibodies within them following the 2 hours of antibody internalisation. As such, the rapid appearance of recycled channels gives no indication as to the actual rates of channels recycling. This will have to be examined by other means. Following 15 minutes of recycling, FITC-labelled channels are more prominent at the cell surface and are beginning to become apparent in vesicular structures in the perinuclear region of the cell. The appearance of these vesicles at this location suggests that recycled K_{ATP} channels do not reside for very long at the cell surface, < 10 minutes, possibly even less since they have already been returned to the cell surface and re-internalised and translocated to these compartments in a very short space of time. As the duration of the recycling step increases, FITC labelling in the intracellular structures becomes more pronounced whilst the staining at the surface becomes more indistinct. This suggests that whilst channels may pass through multiple recycling cycles, a proportion of these channels may be removed from the recycling pool at each pass diminishing the numbers of HA-labelled channels competent to recycle (compare t = 15 minutes with t = 1 hour in figure 5.11). It also appears that those FITC-labelled channels which enter the perinuclear compartments are entering the same compartment as the population of channels which have not recycled back to the cell surface (the Cy3-labelled channels). Indeed, the existence of

this population of channels suggests that residency in this compartment may be fairly long lived since a large proportion of channels always appears to be resident here.

The dynamics of channels recycling were also investigated by live cell imaging which revealed two populations of trafficking vesicles. The first type of vesicle were fairly large in nature and appeared to move rapidly from near the periphery of the cell towards the perinuclear compartments, possibly along microtubules (figure 5.14). Vesicles similar to these are likely to represent the trafficking pathways of the perinuclear targeted channels. The second type of trafficking vesicles were small and were located near to the plasma membrane (figure 5.15). They were seen budding away from the plasma membrane before rapidly recombining again and may represent a mechanism for rapid recycling of K_{ATP} channels, although further research into this area is required to substantiate these hypotheses.

5.3.7 - Regulation of K_{ATP} channel recycling by PKC

It was recently reported by Hu *et al.* (2003) that the endocytosis of K_{ATP} channels was regulated by the activity of PKC. They described that PKC activation was required for rapid channel internalisation and that in the absence of PKC activity channels were internalised only very slowly from the cell surface. Analysis of the current data would suggest that this is not strictly the case in the system used here. The internalisation which is observed with the HEK293 cells which are stably expressing K_{ATP} shown in figure 5.1 and 5.2 is constitutive, although this effect could possibly be due to an elevated basal level of PKC in the HEK293 cells compared to the COS1 cells used by Hu *et al.* (2003). Indeed, initial studies using an inhibitor (chelerythrine) and an activator (PMA) of PKC validated the observations of Hu *et al.* (2003), with internalised channels present in a perinuclear region following PKC activation but apparently confined to the cell membrane following PKC inactivation (figure 5.4). It is worth noting that although the vast majority of channels were present in the cell membrane there were also some small vesicular structures present in the cytoplasm near the cell surface of these cells, indicating that internalisation was continuing under these conditions. Indeed, the presence of these vesicles in the cytoplasm suggests that the apparent retention of labelled channels at the cell surface could be due to an increased rate of recycling as opposed to a decrease in the rate of internalisation *per se*. The effect of PKC activation and inhibition on channel

recycling was therefore investigated. It was discovered that whilst in the presence of PKC activation channels are internalised and a small proportion of these will indeed rapidly recycle back to the cell surface for a short time, although recycled channels at the cell surface are only apparent at early time points (< 1 hour) (figure 5.12). It is likely that during each cycle of internalisation and recycling a proportion of the recycling channels are sequestered into the perinuclear compartments thus reducing the overall population of recycling HA-labelled channels. In the presence of reduced PKC activity very few channels appear able to enter the perinuclear compartment and the vast majority of channels appear to be present at or near the cell surface (figure 5.13). A large proportion of channels are labelled with FITC-conjugated antibodies, suggesting that they have been recycled, and are present in punctate regions of the cell membrane. The fact that these channels are labelled with FITC-conjugated antibodies suggests that they were internalised into the cell and so were protected from the acid-stripping of anti-HA antibodies prior to the commencement of the recycling assay. This suggests that internalisation of K_{ATP} channels is indeed constitutive even in the absence of PKC activity. That the recycled channels remain at or near the cell surface rather than being sequestered into the perinuclear compartment suggests that it is the recycling of K_{ATP} channels which is regulated by PKC and not the initial endocytic event as has been proposed by Hu *et al.* (2003)

In summary, the data suggest that it is not the endocytosis as such which is regulated by PKC, but rather the ability of the channels to traffic to the perinuclear compartments in preference to recycling back to the cell surface. With reference to the current data it is proposed that PKC is responsible for regulating an intracellular trafficking step which in the presence of elevated PKC activity causes a redistribution of internalised channels to the perinuclear compartments and out of a rapid recycling pathway. Inhibition of PKC activity allows all of the internalised channels to rapidly recycle back to the cell surface avoiding the perinuclear compartments. These two pathways are summarised in figure 5.17.

The sorting of a number of other membrane proteins including many channels and transporters have been shown to be regulated in some manner by PKC as described below. A number of different effects on protein trafficking and sorting are associated with PKC activation with a number of channels and transporters being upregulated

and a number downregulated in response to increased PKC activity. The cell surface density of the glutamate transporter EEAC1 is greatly increased when PKC activity is elevated (Dowd & Robinson 1996, Davis *et al.* 1998). Under basal conditions EEAC1 cycles between the cell surface and an intracellular pool but when PKC is activated the rate of endocytosis is slowed and a massive recruitment of transporters to the cell surface is stimulated (Fournier *et al.* 2004). Two other proteins whose cell surface density is increased by PKC activation are NMDA receptors (Lan *et al.* 2001) and the glucose transporter GLUT2 in intestinal brush borders (Helliwell *et al.* 2000). An example of a protein whose recycling to the cell surface is PKC dependent is the EGF receptor, which is diverted away from a degradative pathway into a recycling compartment following PKC stimulation (Bao *et al.* 2000). The activation of PKC has also been implicated in the downregulation of a number of proteins at the cell surface, a phenomenon which is perhaps more applicable to the current study. Activation of PKC is associated with the down regulation of the neurotransmitter transporters GAT1 - GABA transporter (Beckman *et al.* 1999), SERT - serotonin transporter (Qian *et al.* 1997) and GLT1 - glutamate transporter (Kalandadze *et al.* 2002) by mechanisms which are still poorly understood. In the case of GAT1 a parallel inhibition of activity by the direct association of syntaxin1A is seen, a phenomenon which is also observed with K_{ATP} channels (Pasyk *et al.* 2003, Kang *et al.* 2004, Cui *et al.* 2004). Increases in the rate of endocytosis associated with an increase in PKC activity have been observed with the dopamine receptor DAT (Pristupa *et al.* 1998) and E-cadherin (Le *et al.* 2002), a component of adherens junctions in epithelial cells. In both cases the increase of internalisation is associated with an accumulation of protein in the endocytic recycling compartment (Melikian & Buckley 1999, Le *et al.* 2002, Lodler & Melikian 2003). In the case of DAT internalisation it appears that direct phosphorylation by PKC of DAT itself is not required for internalisation (Torres *et al.* 2001). The retention in the endocytic recycling compartment observed with both DAT and E-cadherin results in a reduced rate of recycling back to the cell surface. A similar reduction in the rate of recycling as a result of increased PKC activity has been observed with the hepatocyte growth factor receptor, c-Met (Kermorgant *et al.* 2003) and the chloride channel, $GABA_A$ (Connolly *et al.* 1999). In both cases endocytosed proteins were seen to traffic to perinuclear endosomal compartments which in the case of c-Met includes the TGN (Kermorgant *et al.* 2003). In the case of $GABA_A$ channels, PKC was shown not to

affect the rate of endocytosis, affecting only the rate of recycling (Connolly *et al.* 1999), characteristics which are apparently shared by K_{ATP} channels.

5.3.8 - Summary of findings

It has been shown that following internalisation into cells, K_{ATP} channels move along a trafficking pathway which most likely includes the early sorting endosome, the late endosome and a compartment which is associated with the *trans*-Golgi network (TGN). Both the mechanism of endocytosis and the fate of the channels once they reach the TGN-associated compartment remain unclear. It is also apparent that following endocytosis K_{ATP} channels are able to recycle back to the cell surface rapidly and that this process is dependent on the activity of protein kinase C (PKC). An elevation in PKC activity results in the sequestration of channels in the trafficking pathway outlined above, whereas inhibition of PKC activity results in the majority of internalised K_{ATP} channels returning rapidly back to the cell surface. The exact mechanisms responsible for this phenomenon are yet to be understood.

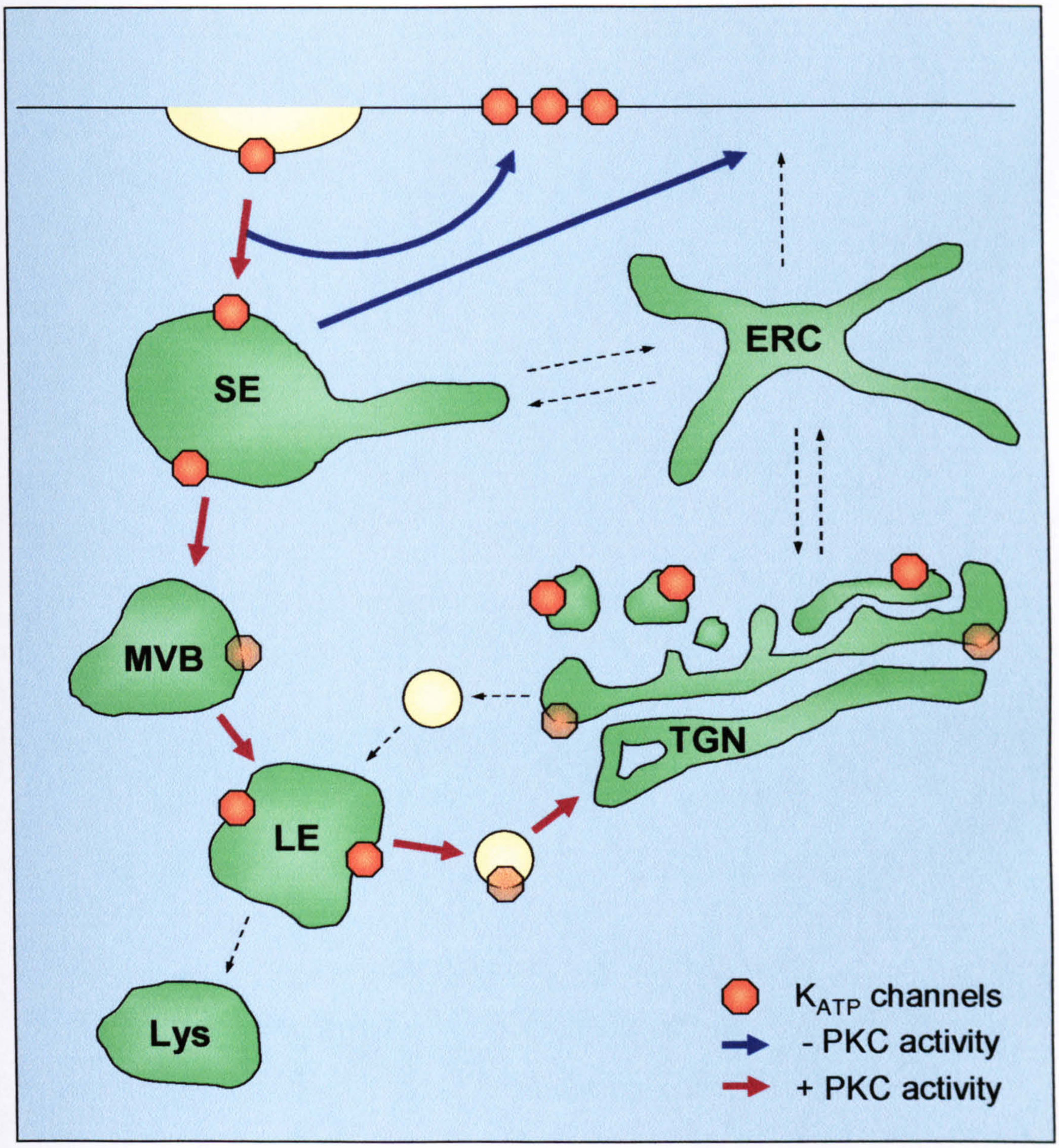

Figure 5.17 - *Effect of PKC on the endocytic trafficking of K_{ATP}-HA channels.* The suggested trafficking pathways when PKC activity is elevated are shown by the thick red arrows. The suggested trafficking pathways when PKC activity is attenuated are shown by the thick blue arrows. Other trafficking pathways which are not thought to be involved are shown by dashed arrows. SE - sorting endosome, ERC - endocytic recycling compartment, MVB - multi-vesicular body, LE - late endosome, TGN - *trans*-Golgi network, Lys - lysosome.

Chapter 6

Characterisation of two mutations of Kir6.2 known to cause congenital hyperinsulinism

6.1 – Introduction

Congenital hyperinsulinism (CHI), also known as persistent hyperinsulinaemic hyperglycaemia of infancy (PHHI) and familial hyperinsulinism is an insulin secretory disorder characterised by an inappropriately high level of insulin secretion for the level of blood glucose (see Dunne *et al.* 2004 for a comprehensive review).

Cases of CHI are not common, with an incidence of ~ 1 : 50000 live births in Finland and 1 : 27000 in Ireland, although in some isolated communities the incidence is significantly higher, for example in a central region of Finland (1 : 3200) or in the Arabian peninsular (1 : 2500) (Glaser *et al.* 2000). CHI can not currently be diagnosed *in utero* and only becomes apparent following birth. The majority of sufferers are born with inappropriately high birth weight due to the anabolic effects of prolonged hyperinsulinaemia *in utero* leading to increased muscle, adipose tissue and liver mass (Aynsley-Green *et al.* 2000) although this is not always the case. The first symptoms of CHI usually become apparent soon after birth and may include cyanosis, respiratory distress, sweating, hypothermia, irritability, poor feeding, hunger, jitteriness, lethargy, and apnea, which can progress to vomiting, seizures, tachycardia, and neonatal death. In older children and adults symptoms tend to be typical of those of hypoglycemia including confusion, headaches, dizziness, syncope, and, when severe, loss of consciousness. Clinical diagnosis of CHI relies on several features; 1) blood glucose levels of < 2.6 mM, 2) a glucose requirement of > 6 - 8 mg glucose kg^{-1} min^{-1} to maintain euglycaemia, 3) detectable levels of insulin and elevated C-peptide levels in the blood during hypoglycaemia, 4) inappropriately low free-fatty acids and ketone bodies during hypoglycaemia, 5) the absence of ketonuria, 6) and a glycaemic response to glucagon during hypoglycaemia (Aynsley-Green *et al.* 2000).

Following diagnosis several strategies may be employed in an attempt to treat the disorder, and these are ultimately targeted at either lowering insulin secretion or increasing glucose availability. Glucose availability is most commonly increased by a simple infusion of glucose into the blood, although this may not be practical for long-term management of the disorder. In some cases glucagon has been used to treat CHI by mobilizing glucose from hepatic glycogen stores, although this mode of treatment is far from ideal as glucagon also has actions as an insulin secretagogue and prolonged

administration may contribute to the tendency for insulin hypersecretion. Many other therapies are targeted at preventing insulin secretion, such as administration of somatostatin or its analogues octreotide and sandostatin which act to hyperpolarize the β-cell membrane preventing the opening of voltage dependent calcium channels (VDCC). Other drugs such as nifedipine block the VDCC directly, preventing the Ca^{2+} influx required for insulin release. Another possible therapy is the use of diazoxide to open the pancreatic K_{ATP} channel directly, meaning that the resultant membrane hyperpolarization blocks insulin release. Unfortunately, a large proportion of CHI cases do not respond to pharmacological intervention, leaving a partial pancreatectomy as the last resort in treatment, often with up to 95 % of the pancreatic mass being removed to limit the insulin secretory capabilities (Aynsley-Green *et al.* 2000).

CHI has been shown to occur in two main types, namely diffuse and focal CHI. Diffuse CHI is so called because all pancreatic islets are affected and arises predominantly because of autosomal recessive inheritance of K_{ATP} channel subunit mutations (Glaser *et al.* 2000). The focal form of the disorder is characterised by a number of so-called focal lesions, areas of the pancreas where hyperplasia of the β-cells has occurred. Focal lesions appear histologically as small regions of islet adenomatosis measuring 2 – 5 mm in size and appear to develop through imbalanced expression of maternally imprinted tumor suppressor genes H19 and p57kip2, and the paternally derived insulin-like growth factor II gene (see Dunne *et al.* 2004 for review).

The cause of CHI has been discovered in only about half of those cases diagnosed. To date mutations in five genes have been implicated. These genes are *ABCC8* (SUR1), *KCNJ11* (Kir6.2) (see Dunne *et al.* 2004 for review), *GLUD1* (glutamate dehydrogenase) (see Kelly *et al.* 2001 for review), *HADHSC* (short-chain L-3-hydroxyacyl-CoA dehydrogenase) (Clayton *et al.* 2001) and the glucokinase gene (Glaser *et al.* 1998, Christesen *et al.* 2002). Over 100 mutations of either *ABCC8* or *KCNJ11* have been described as causing CHI (Fournet & Junien 2003), although the vast majority of these mutations are associated with *ABCC8*. Mutations of these genes have been shown to cause CHI by disrupting the normal function of the pancreatic β-cell K_{ATP} channel. This may occur by several processes such as by reducing the rate of channel synthesis, by reducing the stability, thus increasing the rate of channel degradation, by interfering with channel trafficking, or by interfering with the function

of the channel. Many of these scenarios have been shown to occur, for example several *ABCC8* mutations have been shown to prevent trafficking of the channel to the cell surface (Cartier *et al.* 2001, Partridge *et al.* 2001, Taschenberger *et al.* 2002). Other mutations associated with *ABCC8*, for example the mutation resulting in the V1479R mutation of SUR1, have been shown to interfere with function of the channels by interfering with normal nucleotide binding (Nichols *et al.* 1996). Several mutations have also been described in *KCNJ11*. These mutations have not been very well characterized, and the aim of the current study is to investigate the effect of two of these Kir6.2 mutations on K_{ATP} channel trafficking and function.

The first Kir6.2 mutation to be investigated in the current study involves the substitution of the tryptophan residue at position 91 for an arginine (W91R). This mutation was first described by Aguilar-Bryan & Bryan (1999) and was identified in a neonate suffering from severe hyperinsulinaemia which was unresponsive to treatment with either diazoxide or somatostatin. Treatment of this individual required a partial pancreatectomy at an age of two weeks, followed by a second resection four weeks later. This tryptophan residue is one of a pair of tryptophan residues which are thought to be located at the top (extracellular) side of TM1 of Kir6.2 (figure 6.1). The model shown in figure 6.3, constructed by threading the amino-acid sequence of Kir6.2 onto the crystal structure coordinates of Kirbac1.1 (Kuo *et al.* 2003), supports this idea, clearly showing that W91 is likely to be found near the top of TM1, facing outwardly at the periphery of the channel complex. Some aspects of channels containing this mutation have previously been investigated. Aguilar-Bryan & Bryan (1999) have suggested that channels containing this mutation are non-functional. Further to this it has been reported that channels containing the W91R mutation are much less stable than those containing wild-type Kir6.2 subunits as demonstrated by an apparent increase in the turnover of mutant Kir6.2 subunits compared to that of wild-type (Crane & Aguilar-Bryan 2004). However, the same study showed that W91R mutant Kir6.2 subunits were able to associate with SUR1 subunits raising the possibility that ER exit and further trafficking of fully assembled channels may occur.

The second Kir6.2 mutation to be investigated in the current study involves the substitution of a leucine residue at position 147 for a proline (L147P). This mutation

was first described by Thomas *et al.* (1996) and was the first mutation to be discovered in Kir6.2 which was shown to be associated with CHI. The affected individual presented with profound hyperinsulinaemia soon after birth, which was unresponsive to treatment with diazoxide, somatostatin or glucagon. Final treatment required a 95 % pancreatectomy, and histopathological analysis of the excised tissue revealed a diffuse nesidioblastosis. The leucine residue in question is thought to reside near the top of TM2 of Kir6.2 (figure 6.2). The model shown in figure 6.3 again supports this idea, clearly showing that L147 is likely to be found near the top of TM1, facing outwardly at the periphery of the channel complex. Very little is known about the effect that the L147P mutation has on K_{ATP} channels other than that the channels appear to be non-functional (Aguilar-Bryan & Bryan 1999).

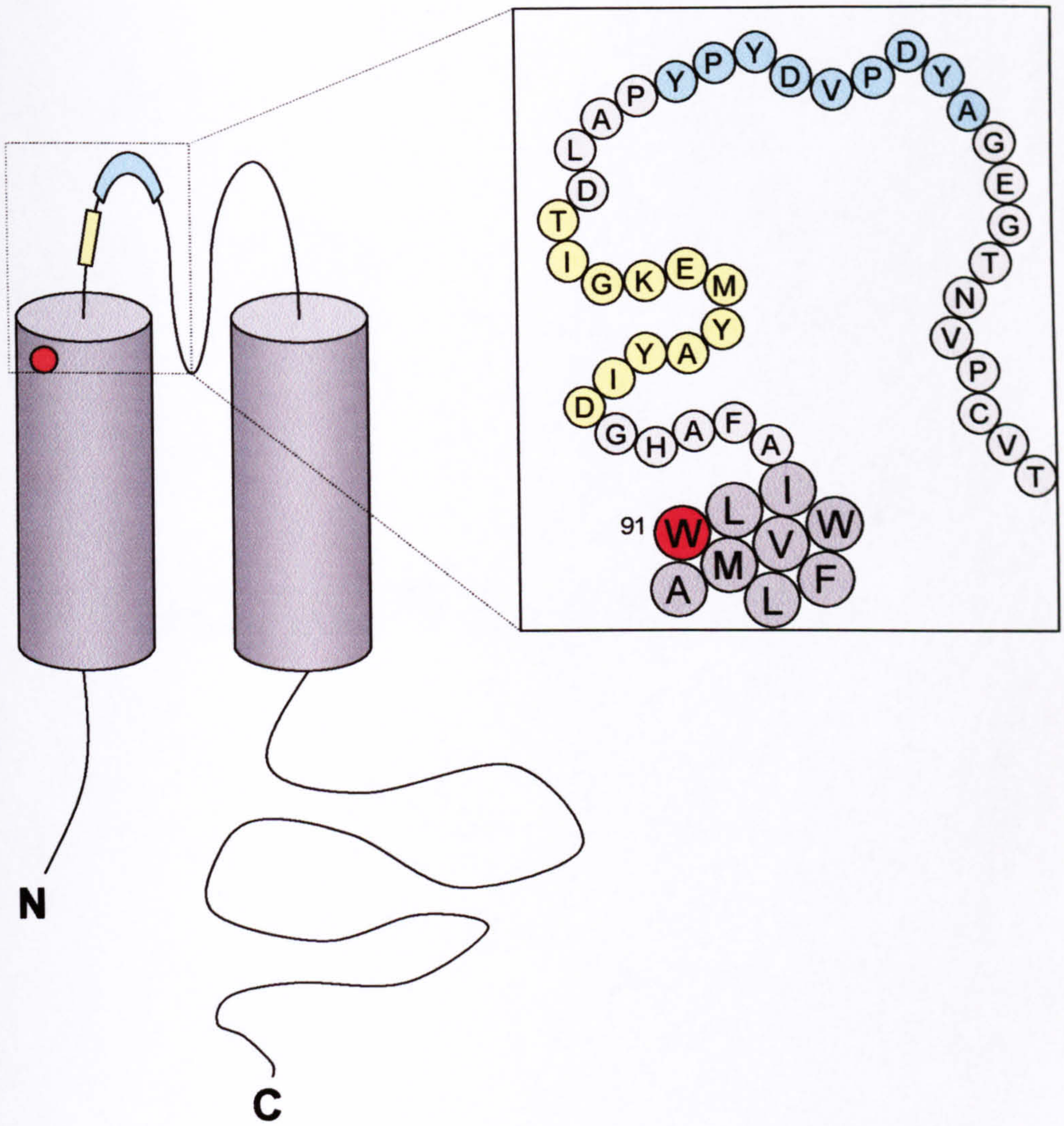

Figure 6.1 - *The proposed location of the W91R mutation in Kir6.2.* W91 is thought to reside near the top of the first transmembrane domain of Kir6.2. The inset shows an expansion of the predicted first extracellular loop showing the proposed location of W91 (red circle) and both the 11aa (yellow) and HA (blue) insertions. Numbering corresponds to the residue positions of wild-type Kir6.2.

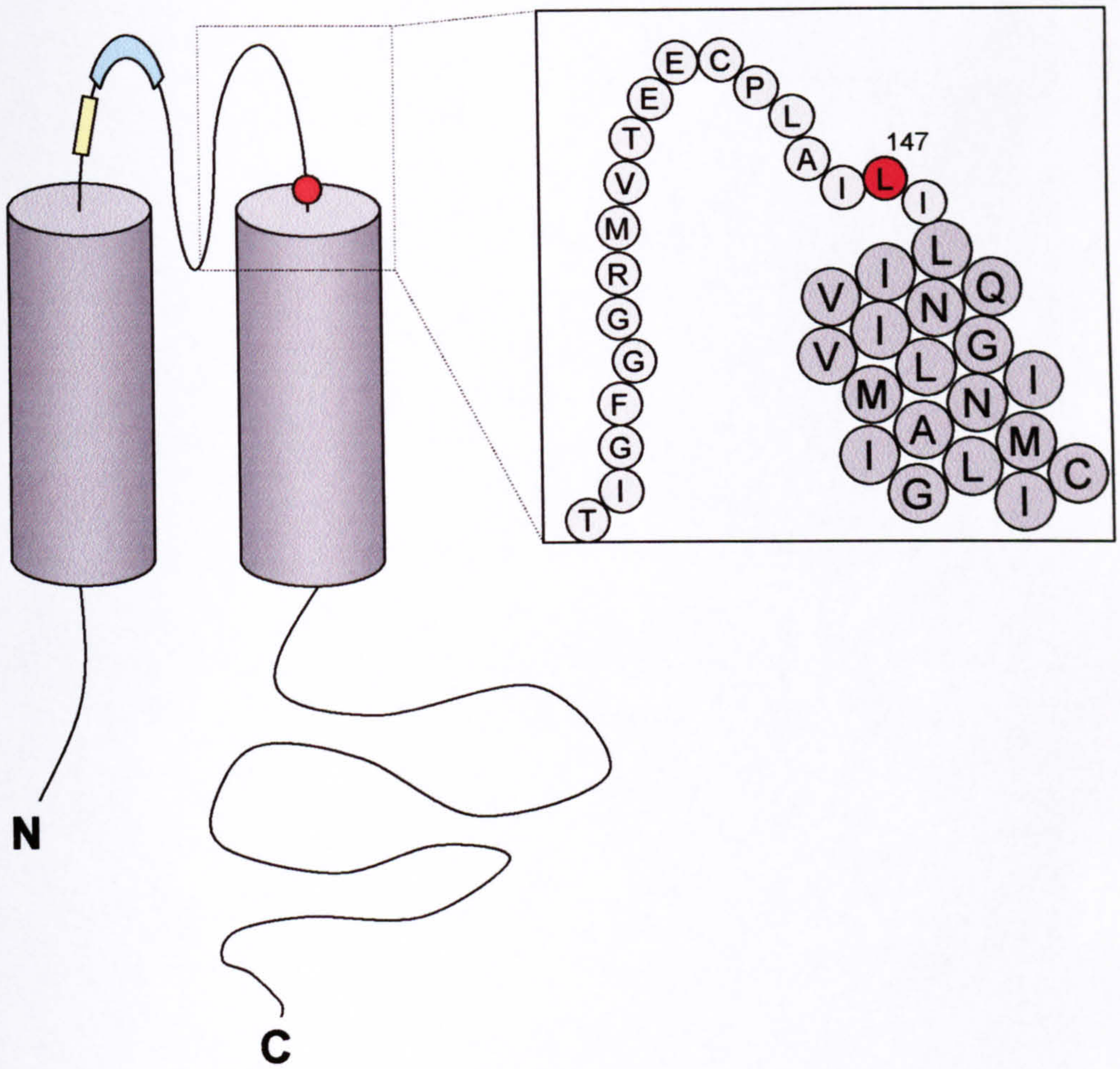

Figure 6.2 - *The proposed location of the L147P mutation in Kir6.2.* L147 is thought to reside near the top of the second transmembrane domain of Kir6.2. The predicted location of L147 is depicted by the red circle. Also shown are the locations of the +11aa (yellow) and HA (blue) insertions. The inset shows an expansion of the predicted second extracellular loop and also shows the proposed location of L147. Numbering corresponds to the residue positions of wild-type Kir6.2.

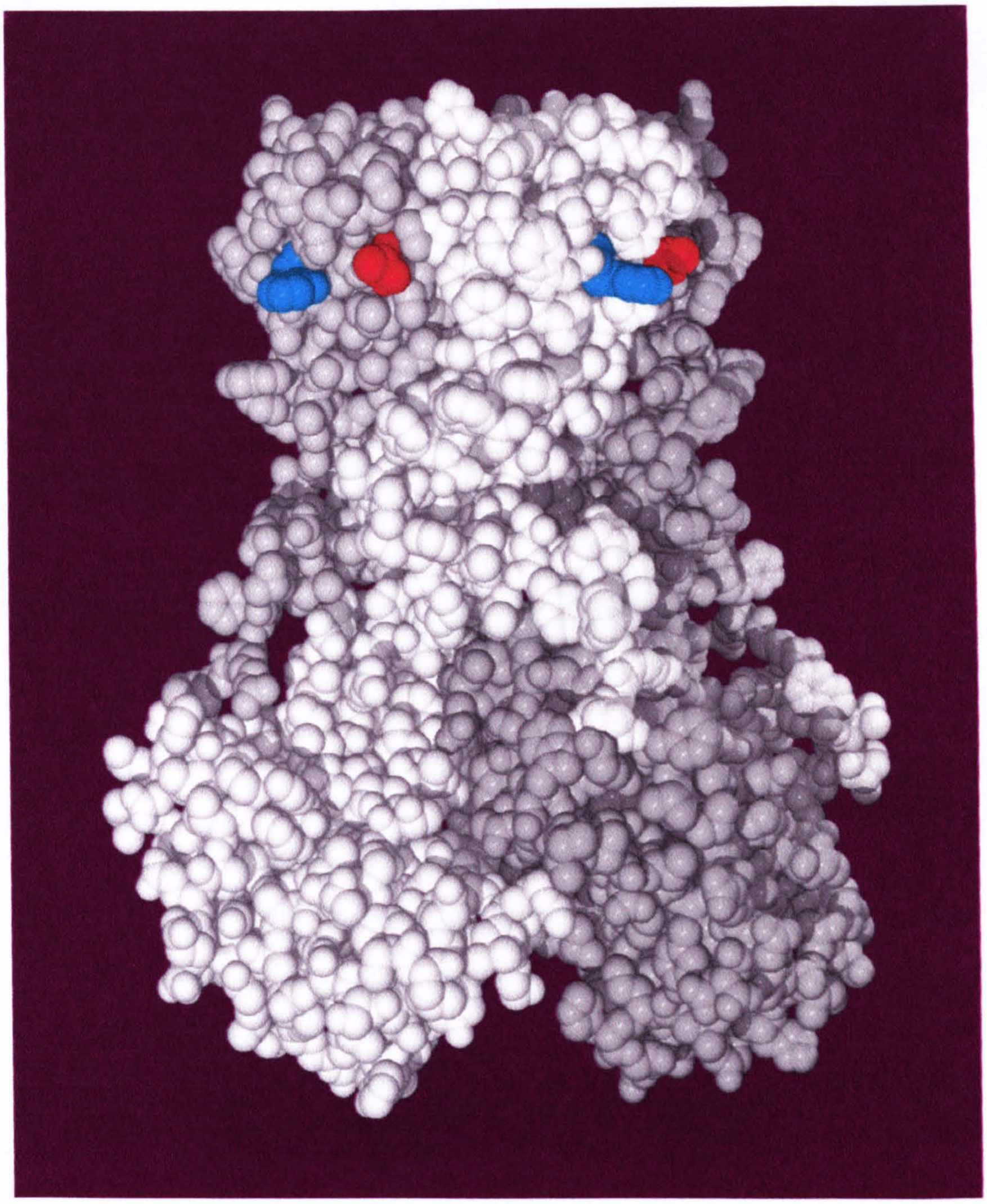

Figure 6.3 - *Both W91R and L147P are predicted to be found at the periphery of the Kir6.2 tetramer.* The amino acid sequence of Kir6.2 was aligned to that of the bacterial Kir channel homologue Kirbac1.1. A model of Kir6.2 was then constructed using the coordinates 1P7B (obtained from the protein data bank) using Deepview / Swiss-PdbViewer software. The individual subunits are coloured alternately light and dark for clarity. The predicted positions of W91 (blue) and L147 (red) are shown.

	86					91					96
	F	**A**	**M**	**V**	**W**	**W**	**L**	**I**	**A**	**F**	**A**
WT	5' - TTT	GCC	ATG	GTC	TGG	TGG	CTC	ATC	GCC	TTC	GCC - 3'
W91R	5' - TTT	GCC	ATG	GTC	TGG	CGT	CTC	ATC	GCC	TTC	GCC - 3'
	F	**A**	**M**	**V**	**W**	**R**	**L**	**I**	**A**	**F**	**A**

Figure 6.4 - *Sequence of Kir6.2 surrounding W91 in both wild-type and W91R mutant subunits.* The sequence of W91R-Kir6.2-HA+11aa-HMKFLAG was confirmed by DNA sequencing. Shown is a comparison of the DNA and protein sequences of the area surrounding W91 of both wild-type (WT) and W91R mutant Kir6.2 constructs. The mutated codon and the resultant amino-acid change are highlighted in grey. The numbering corresponds to that of wild-type Kir6.2.

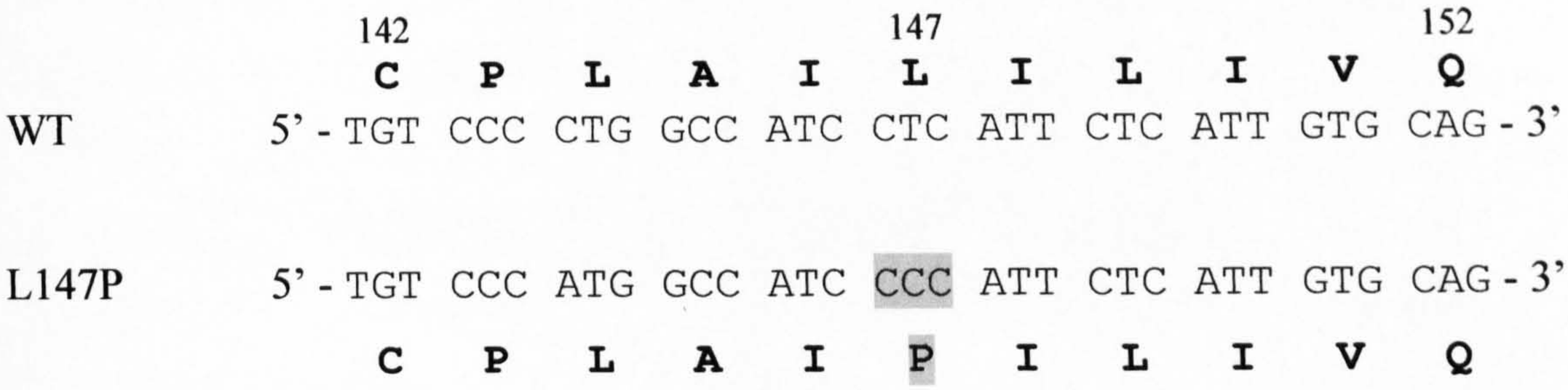

Figure 6.5 - *Sequence of Kir6.2 surrounding L147 in both wild-type and L147P mutant subunits.* The sequence of L147P-Kir6.2-HA+11aa-HMKFLAG was confirmed by DNA sequencing. Shown is a comparison of the DNA and protein sequences of the area surrounding L147 of both wild-type (WT) and L147P mutant Kir6.2 constructs. The mutated codon and the resultant amino-acid change are highlighted in grey. The numbering corresponds to that of wild-type Kir6.2.

6.2 - Results

6.2.1 - Both W91R and L147P mutant containing channels are non-functional in *Xenopus* oocytes

Point mutations were inserted into pcDNA3-Kir6.2-HA+11aa-HMKFLAG using the QuikChange™ mutagenesis protocol (2.3.9) and correct insertion of the point mutation was confirmed by DNA sequenceing (figure 6.4 & 6.5). The function of K_{ATP} channels containing either the W91R or L147P mutations were examined in *Xenopus* oocytes using the two-electrode voltage clamp (TEVC) method. Oocytes from *Xenopus* laevis frogs were injected with cRNA encoding His6-SUR1 and Kir6.2-HA+11aa-HMKFLAG containing one of the two mutations. Neither mutant Kir6.2 subunit formed channels which elicited currents upon channel stimulation by metabolic poisoning with azide and the channel opener diazoxide (figure 6.6A). This is in contrast to *Xenopus* oocytes expressing wild-type channels in which robust currents were elicited in response to the same stimuli (see figure 4.7A for comparison).

6.2.2 - K_{ATP} channels containing the L147P mutation traffic to the cell surface whereas those containing W91R do not

The lack of functional channels observed in *Xenopus* oocytes expressing the mutant channels could be due to two reasons; either the channels have been rendered non-functional by the mutations or that the mutations have in someway prevented the normal trafficking of the channels to the cell surface. These possibilities were investigated by sectioning the *Xenopus* oocytes and antibody labelling the channels present in the sections to examine their cellular distribution. It was discovered that whilst channels containing the L147P mutation were present largely in the cell membrane, channels containing the W91R mutation were not present at the cell surface and were confined to the cytoplasm of the oocytes (figure 6.6B). It was confirmed that these findings also applied in mammalian cells by expressing mutant channels in both COS7 and HEK293-MSRII cells, where channels containing the L147P mutation were observed at the cell surface whereas those containing W91R were not (figure 6.7).

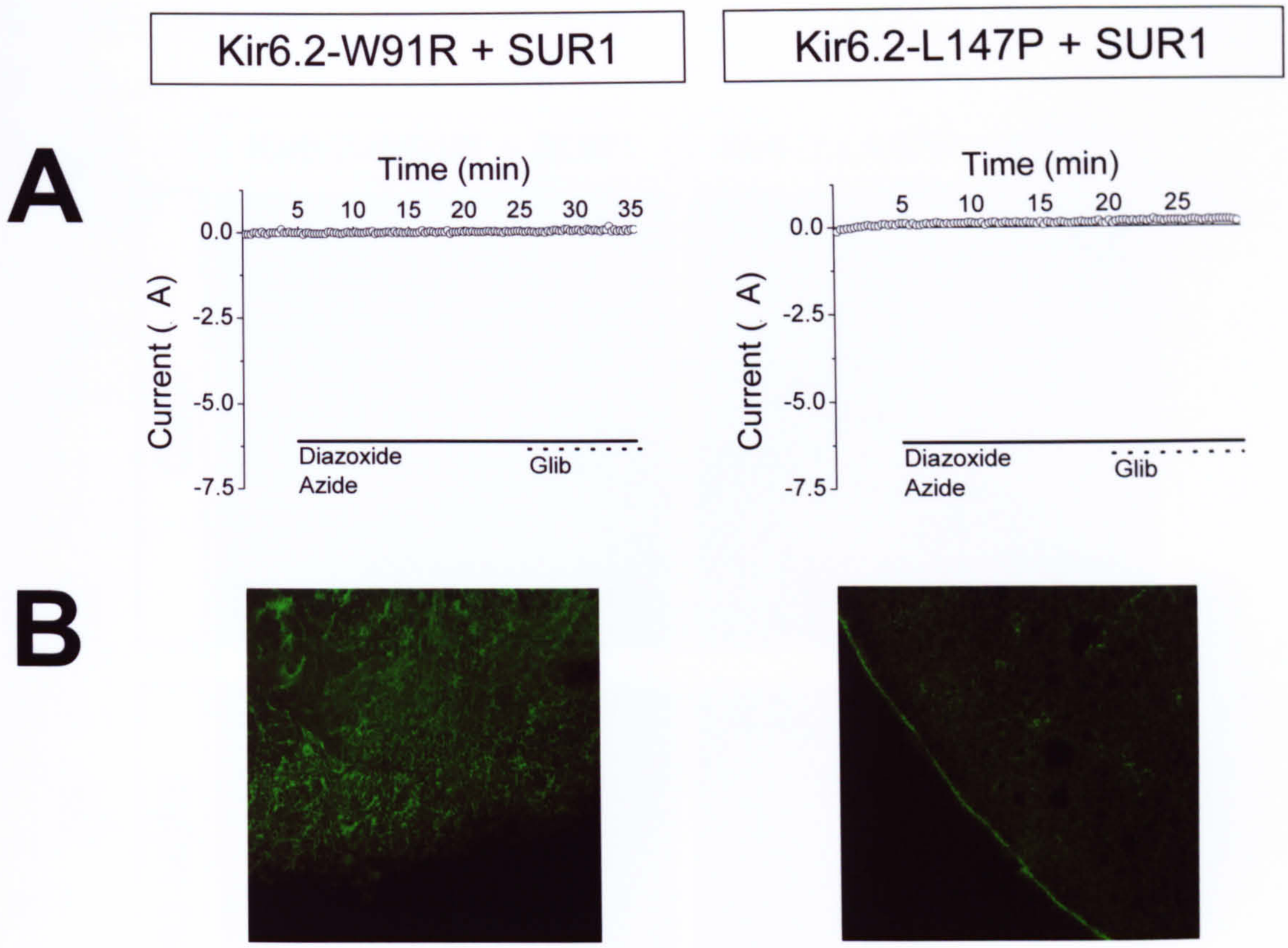

Figure 6.6 - *Channels containing either the W91R or L147P mutant Kir6.2 subunit are non-functional.* **(A)** - Xenopus oocytes co-injected with SUR1 and either W91R or L147P-Kir6.2HA cRNA were examined by two electrode voltage clamp (TEVC). K_{ATP} channels currents were elicited by perfusion in 90 mM K^+ Ringers supplemented with azide (3 mM) and diazoxide (200 μM) and were inhibited by glibenclamide (1 μM) for the duration of the time indicated by the horizontal bars. Currents were recorded using a ramp protocol from -150 mV to + 50 mV (0.22 $V.s^{-1}$) and a holding potential of -30 mV. Data points correspond to currents recorded at -120 mV. **(B)** - Oocytes injected in parallel with those used for TEVC were sectioned and stained with rabbit anti-SUR1 and anti-rabbit FITC-conjugated antibodies. The sections were then examined by LSCM. Representative images are shown. Oocytes injected with wild-type Kir6.2HA + SUR1 are shown in figure 4.7 for comparison. (n = 3).

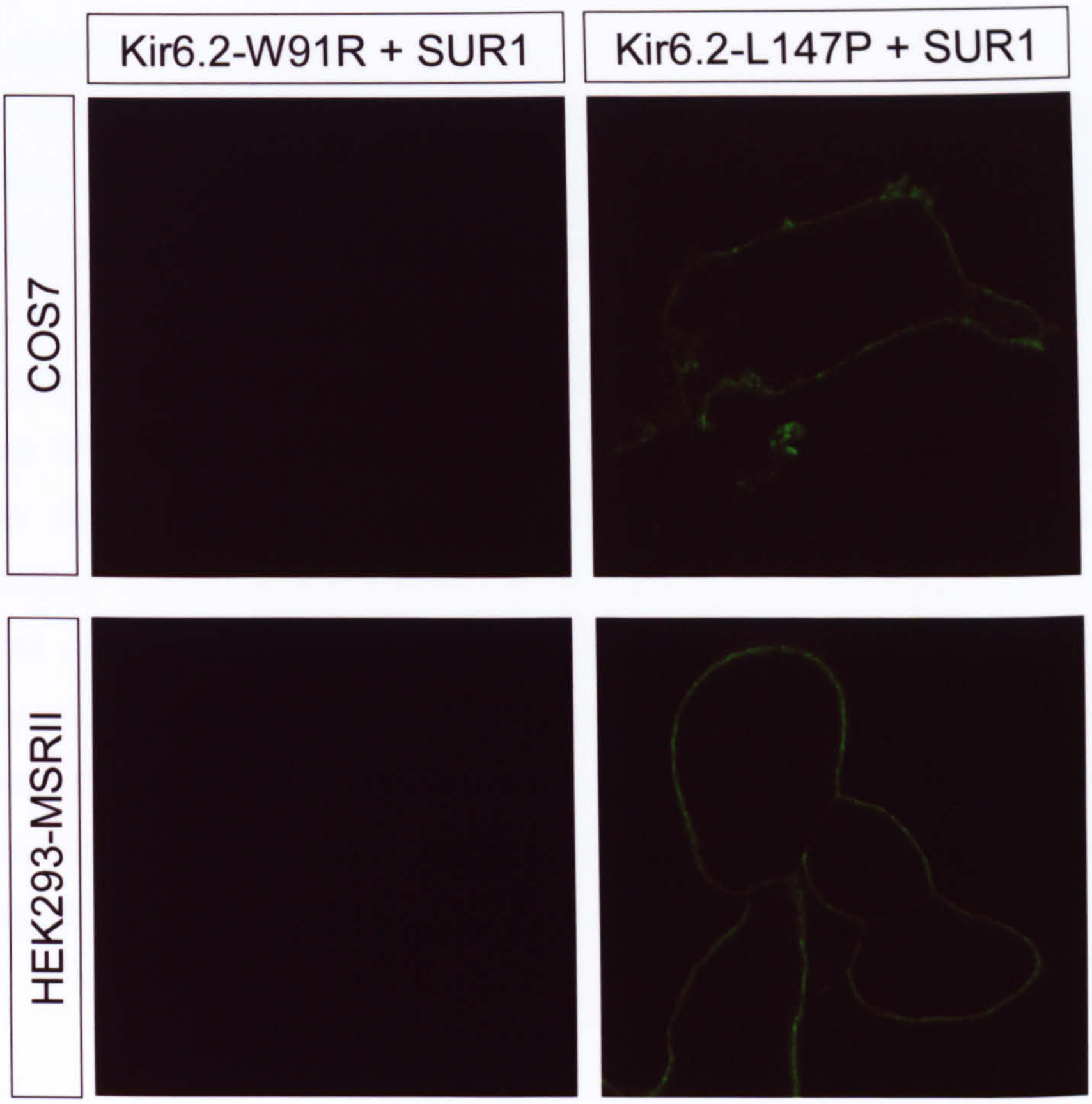

Figure 6.7 - *Channels containing the L147P mutation traffic to the cell surface whereas those containing the W91R mutation do not.* Cells were transiently transfected with His6-SUR1 and either W91R or L147P mutant Kir6.2-HA+11aa-HMKFLAG. They were then fixed and stained without permeabilisation of the cell membranes using rat anti-HA antibodies followed by anti-rat FITC-conjugated secondary antibodies. The cells were subsequently viewed by LSCM. Representative images are shown. (n = 4). Where no fluorescently-labeled cells are evident the entire coverslip has been examined but no fluorescent cells were seen.

6.2.3 - Intracellular distribution of channels containing the W91R mutation

Since channels containing the W91R mutation do not traffic to the cell surface it was necessary to investigate the fate of the channels within the cell. In order to accomplish this, channels were stained in permeabilised cells which had previously been treated with the translational inhibitor cycloheximide. The purpose of the cycloheximide treatment was to prevent synthesis of new channel subunits for a brief period prior to the commencement of staining so that any channels in the cells which had been synthesised before the cycloheximide treatment would achieve a steady-state distribution. It was hoped that staining in this manner would give a better indication of the exact site of channels' retention. The stained channels were seen to be concentrated in an often spherical perinuclear structure, with staining absent in the remainder of the cytoplasm (figure 6.8 *upper left panel*). The nature of this compartment was investigated by comparing the distribution of channel associated staining with that of a number of organelle markers. No co-localisation was observed with anti-EEA1 antibodies (sorting endosome marker). However, a moderate degree of co-localisation was observed between the labelled channels and anti-mannose-6-phosphate receptor antibodies (late endosome / TGN marker) and a very high degree of co-localisation with anti-syntaxin6 antibodies (TGN marker) (figure 6.8).

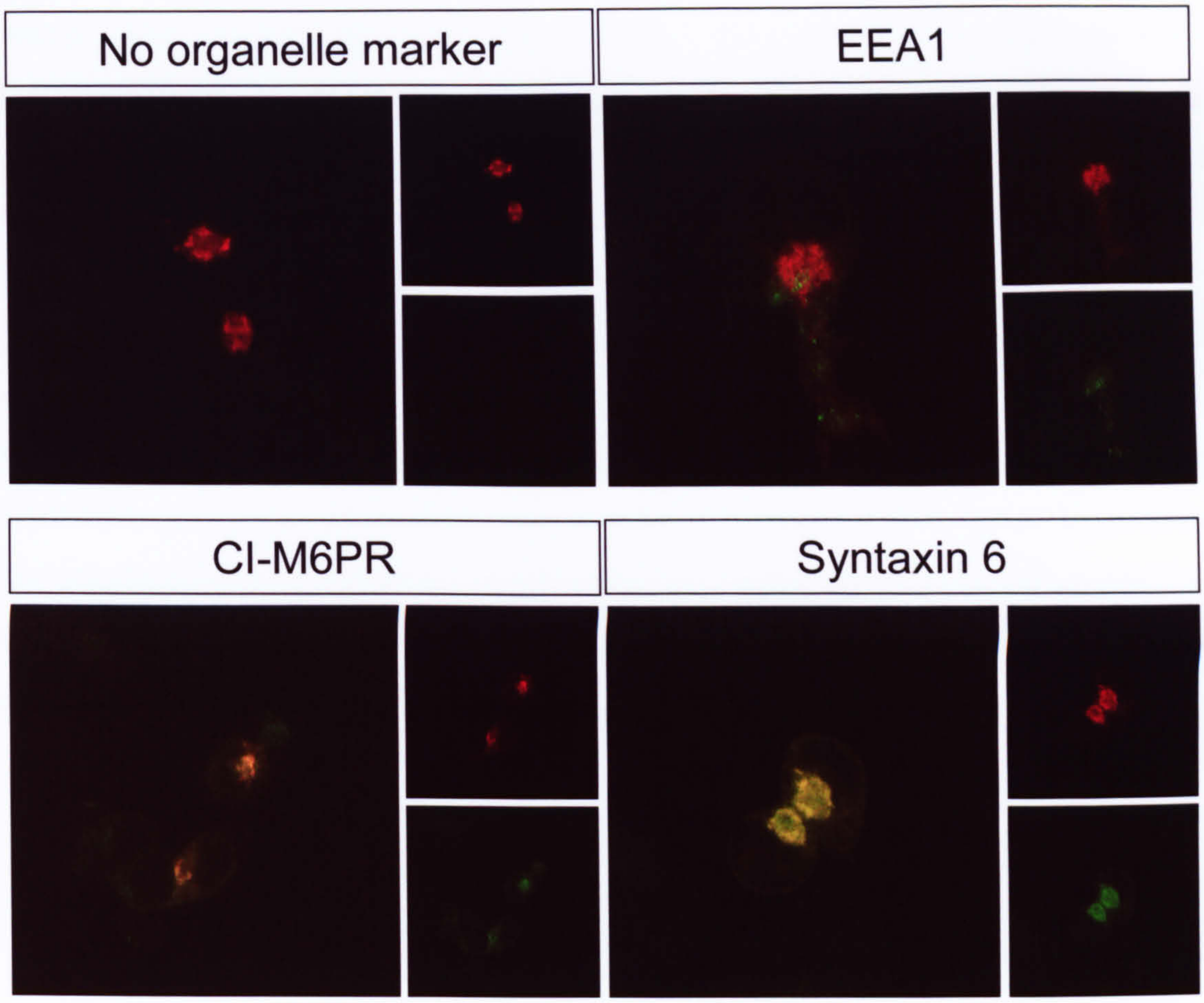

Figure 6.8 - *Co-localisation of W91R mutant containing channels with antibody labelled organelles.* HEK293-MSRII cells were transiently transfected with His6-SUR1 and W91R-Kir6.2-HA+11aa-HMKFLAG. Prior to staining the cells were treated cycloheximide (25 μg ml^{-1}) for 4 hours at 37°C in order to remove channels from the biosynthetic pathway and allow channels already produced to achieve a steady-state distribution. The cells were then fixed, permeabilised and the channels stained using rat anti-HA antibodies followed by anti-rat Cy3 conjugated secondary antibodies. Intracellular organelles were then stained using appropriate primary and secondary antibodies. Antibodies used were mouse anti-EEA1, mouse anti-M6PR and mouse anti-syntaxin6 primary antibodies and anti-mouse FITC-conjugated secondary antibodies. Cells were subsequently viewed by LSCM. Shown are the merged images along with the staining associated with each individual fluorophore (HA - red, organelle - green). Representative images are shown. (n = 3).

6.2.4 - The trafficking defect associated with the W91R mutation is not reversed by pharmacological intervention

Recent reports suggest that trafficking defects of K_{ATP} channels associated with PHHI may be reversed by pharmacological intervention by treatment with either the K_{ATP} channel opening drug diazoxide or inhibitor glibenclamide (Partridge *et al.* 2001, Yan *et al.* 2004). Several reports have also suggested that cell surface trafficking of certain mutant forms of CFTR may be rescued by lowering the incubation temperature to 27°C (Denning *et al.* 1992). The possibility that some or all of these treatments might rescue the surface expression of channels containing the W91R mutation was investigated. Cells expressing W91R containing channels were incubated in media supplemented with either glibenclamide or diazoxide or in normal media at 27°C for 24 hours prior to the commencement of staining. None of the treatments appeared to induce trafficking of the mutant channels to the cell surface as illustrated by a lack of staining at the cell surface in unpermeabilised cells (Figure 6.9).

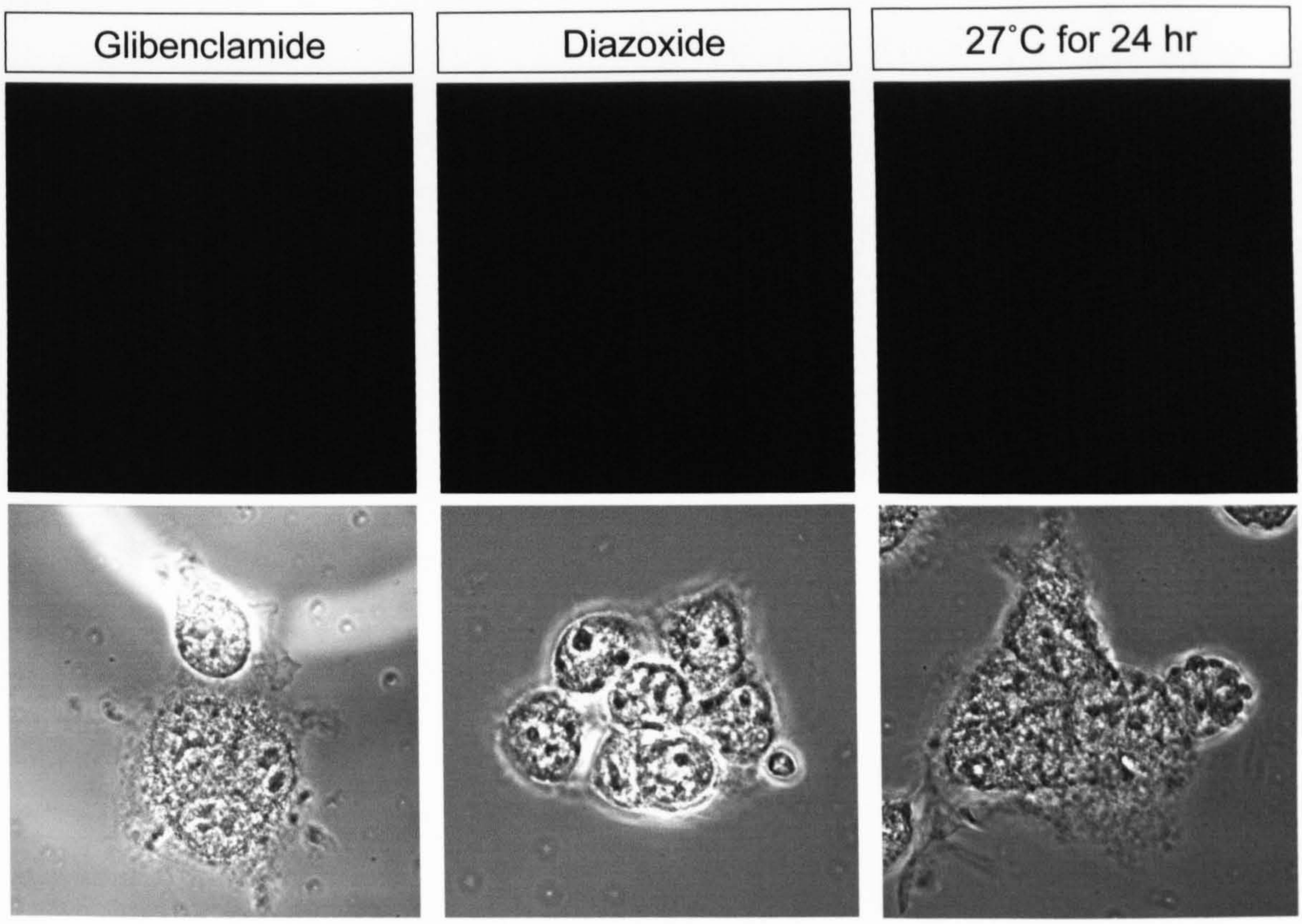

Figure 6.9 - *Neither drug treatments nor lowered temperature incubations are able to reverse the trafficking defect associated with W91R-Kir6.2.* HEK293-MSRII cells were transiently transfected with HA-tagged W91R-Kir6.2 + SUR1. For the final 24 hours of culture prior to staining cells were incubated at 27˚C or in media supplemented with either glibenclamide (10 μM) or diazoxide (200 μM). Cells were stained using rat anti-HA antibodies followed by anti-rat Cy3 conjugated antibodies *(upper panels)*. The lower panels show phase contrast images corresponding to those shown above each one. Wild-type channels (containing wt-Kir6.2 + SUR1) were stained in parallel and displayed strong fluorescence in all cases (data not shown).

6.3 - Discussion

Described in this chapter is an examination of the functional and cell biological consequences of two mutations of the Kir6.2 subunit of K_{ATP} channels known to cause the disorder CHI. The first mutation, W91R, has been shown to cause retention of K_{ATP} channels in an intracellular compartment which has been identified as likely being the *trans*-Golgi network (TGN). Retention of the channels in this compartment could not be reversed by any intervention attempted. The second mutation, L147P, was shown to traffic to the cell surface in both *Xenopus* oocytes and in mammalian cells, but was not able to pass currents when stimulated with diazoxide and azide. Figure 6.10 summarizes these findings.

6.3.1 - The W91R mutation

Of the characterised mutations known to cause CHI, two broad mechanisms have been demonstrated whereby the channel defects arise. The first type of channel defect is those which result from impairments to the function of the channel. The second mechanism results from a disruption of the correct trafficking of channels leading to a reduction or complete abolition of currents. The W91R mutation of Kir6.2 has been shown to cause a trafficking defect of K_{ATP} channels in both *Xenopus* oocytes and in mammalian cells (figures 6.6 and 6.7). In addition to this, it has also been demonstrated that these W91R mutantion containing channels are retained in a post-ER cytoplasmic compartment which stains positive for syntaxin 6, which implies that this compartment is most likely part of a TGN / endosomal population of structures. That the channels are capable of exiting the ER and to move into TGN-associated structures implies that Kir6.2 subunits harbouring the W91R mutation are capable of assembling with SUR1. These observations are supported by the findings of Crane and Aguilar-Bryan (2004) who showed association between SUR1 and W91R mutant containing Kir6.2.

A number of K_{ATP} channel mutations known to cause CHI have been described as causing a trafficking defect. Indeed, the vast majority of characterised channel mutations display some degree of change in cell surface numbers, even those mutations which are known to primarily cause functional defects (for example the L1551V mutation of SUR1 which displays both impaired function and a small decrease in channel density (Reimann *et al.* 2003)). Other than the mutations which have been

shown to reduce cell surface density, several mutations, in both Kir6.2 and SUR1, have been shown to totally abolish channel trafficking to the cell surface in a similar manner to that reported here for the W91R mutation. The Kir6.2 mutation P254L is thought to cause K_{ATP} channels to be retained within the endoplasmic reticulum (Tornovsky *et al.* 2004) perhaps due to incorrect shielding of the -RKR- retention motifs in either of the two subunits. The same is also true of a number of SUR1 mutations including ΔF1388 (Cartier *et al.* 2001), A1457T, V1550D (both Reimann *et al.* 2003), A116P and V187D (both Yan *et al.* 2004) which all lead to retention in the ER. In contrast, the R1394H mutation of SUR1 has been shown to lead to retention of the channel in the TGN (Partridge *et al.* 2001) in a similar manner to that described here for the W91R Kir6.2 mutation. Partridge *et al.* (2001) also reported that the TGN retention of the R1394H mutation containing channel could be overcome by treatment of the cells with the K_{ATP} channel activator diazoxide, however, this type of treatment was not effective in restoring the trafficking of W91R mutation containing channels (figure 6.9). It has also been reported that treatment with sulphonylureas can reverse the ER retention of certain SUR1 mutant channels (A116P and V187D (Yan *et al.* 2004)) but such treatments were again not effective in restoring the membrane trafficking of W91R containing channels (figure 6.9).

The exact mechanisms which have led to TGN retention of channels containing the W91R mutation remain unclear. The tryptophan residue at this position is the second of a pair of tryptophan residues which are fairly well conserved throughout the Kir channel family suggesting the potential for an important role (figure 6.11). Aromatic residues are commonly found at the membrane / water interfaces of membrane spanning regions of integral membrane proteins (Killian & Von Heijne 2000, Ulmscheider & Sansom 2001). It is thought that they stabilize transmembrane α-helices by anchoring proteins into the membrane via interactions with lipid head-groups. These interactions were first proposed to exist in the photoreaction center (Deisenhofer & Michel 1989) and were subsequently proposed to play a role in maintaining the structure of bacterial porins (Cowan *et al.* 1992). More recently, bioinformatical studies using crystal structures of a number of integral proteins have confirmed the tendency for aromatic residues to be present at the membrane boundary (Landolt-Marticorena *et al.* 1993, Ulmscheider & Sansom 2001). It may be that the tryptophan residues located at the top of TM1 of Kir6.2 are acting in a similar fashion, and that substitution of one of the tryptophan

residues with arginine is destabilizing the structure of the channel. Further evidence for this is demonstrated by the crystal structure of the KcsA archetypal bacterial K^+ ion channel, where two rings of tryptophan residues appear to form a 'collar' at the periphery of the membrane embedded portions of the channel (Doyle *et al.* 1998). Another contributing factor behind the defect cause by the mutation may be due to the nature of the amino acid change. The tryptophan to arginine change has substituted a very hydrophobic amino acid with a hydrophilic charged amino acid and it is conceivable that this drastic change may affect the stability of the protein in this region.

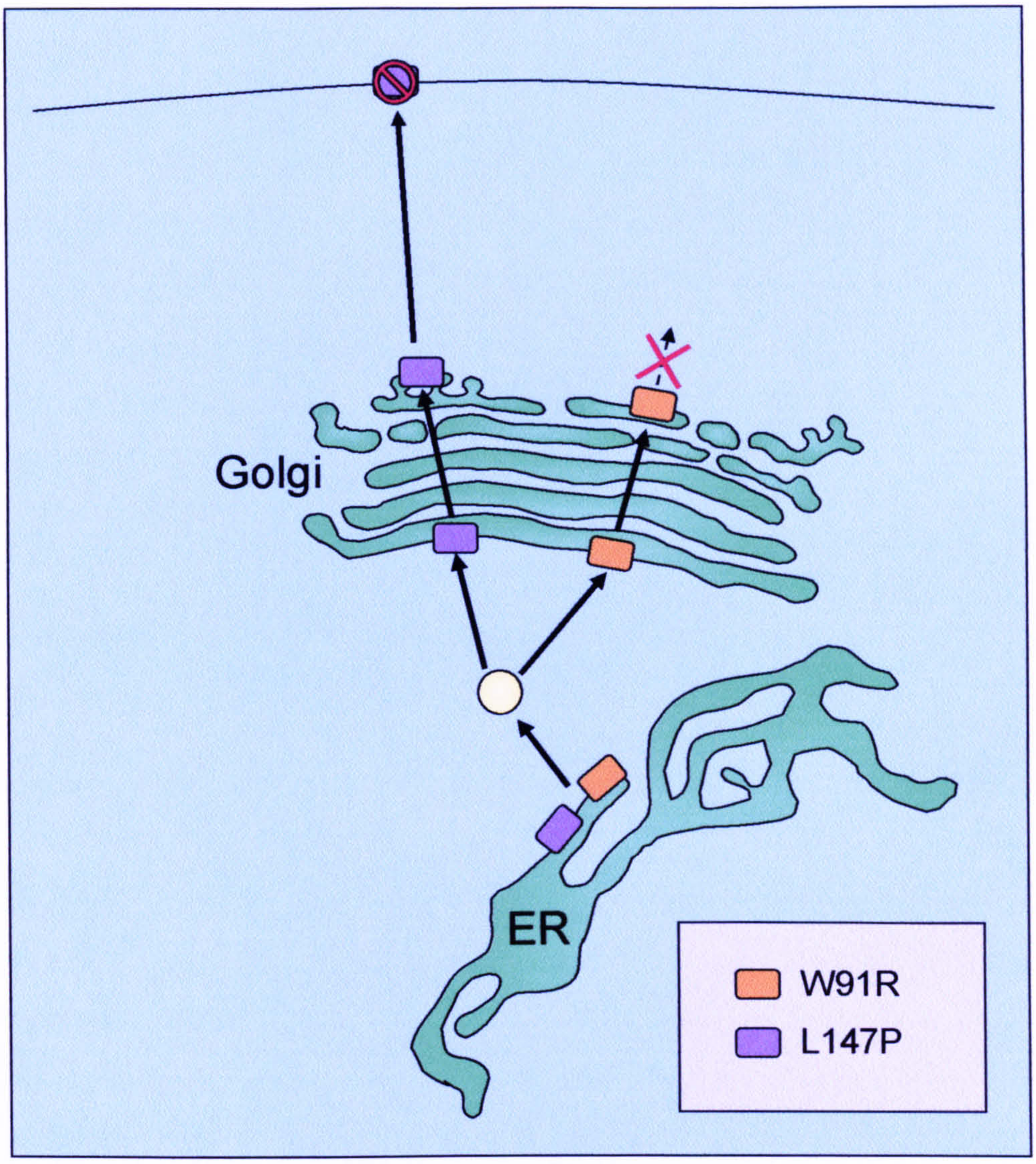

Figure 6.10 - *A schematic summarizing the different effects of the W91R and L147P mutations of Kir6.2.* Channels containing either the W91R or L147P mutation are able to exit the endoplasmic reticulum (ER) and traffic to the Golgi apparatus. The channels containing the W91R mutation are retained (✕) in elements of the *trans*-Golgi network whereas channels containing the L147P mutation are able to traffic to the cell surface. Once at the cell surface the L147P containing channels are unable to pass current, suggesting a functional defect (⊘).

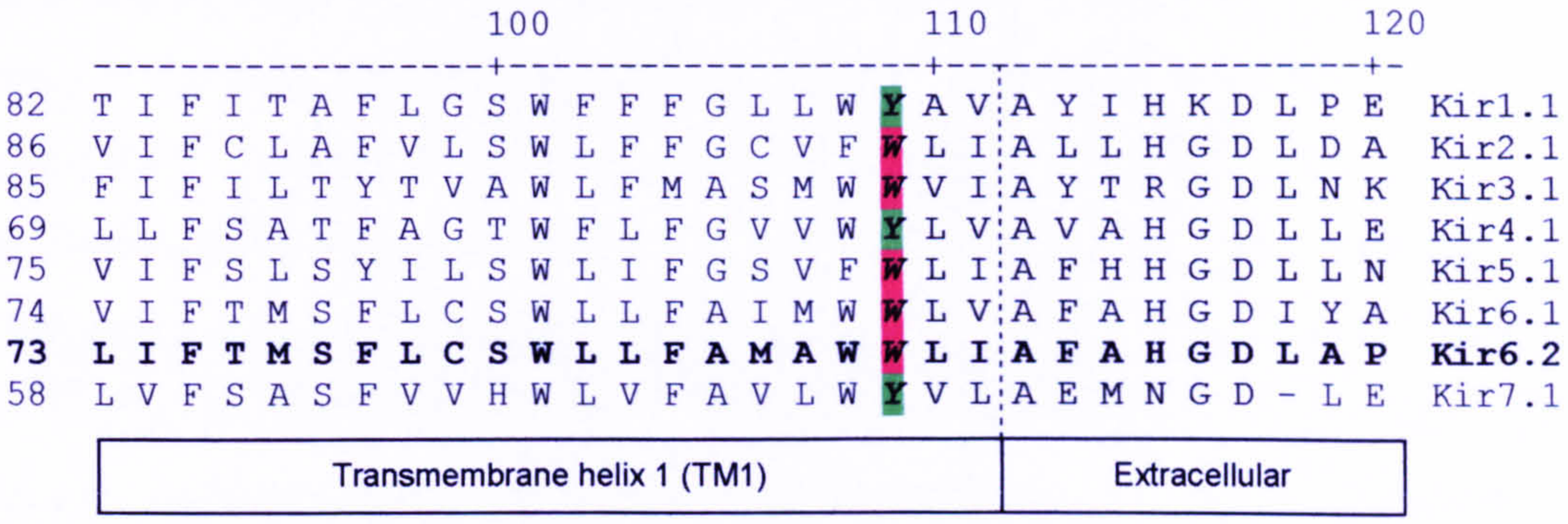

Figure 6.11 - *Sequence alignment of the Kir channel members surrounding the location of the W91R mutation.* The sequences of human KirX.1 family members are shown. The full length protein sequences of each subunit were aligned using the ClustalW function of DNA star - Megalign programme. The sequence of Kir6.2 is shown in **bold** and the location of W91 is denoted in ***italics.*** The corresponding residues in alignments are highlighted red if identical or green if similar. The predicted boundaries of the first transmembrane helix (TM1) are shown. Numbering down the left hand side corresponds to the position of the first amino acid of the sequence shown.

6.3.2 - The L147P mutation

The basis of the functional defect which affects L147P containing channels is unclear. Several possibilities exist, however, which could explain this functional defect. Firstly, the introduction of a proline residue at this position may cause a deformation in TM2 which may interfere with the movements of this transmembrane helix thought to be important for gating of the channel. The introduction of the proline residue could cause a 'kink' in the helix which might cause an occlusion of the channel gate located at the bundle crossing at the cytoplasmic end of TM2 thus preventing the passage of ions into the K^+ conduction pathway. It seems unlikely that this is responsible for the functional defect purely because of the distance between the site of the mutation and the cytoplasmic gate. It is possible however that a mutation in this region could interfere with the channel pore, where a second gate has been postulated to reside (Claydon *et al.* 2003) Secondly, the introduction of the proline residue into TM2 of Kir6.2 might interfere with its assembly with SUR1. It seems unlikely that such interference would totally disrupt the interactions between the two subunits since the channels are able to traffic to the cell surface suggesting that assembly has occurred sufficiently to allow ER-export. However, the overall structure of the channel might be sufficiently disrupted so that normal functional coupling between the Kir6.2 tetramer and SUR1 might not be able to occur. A third possibility is that the introduction of the proline residue into the top of TM2 could in some way affect the packing of the pore region of the channel. The location of the mutation lies very close to both the pore and pore helices and it is conceivable that misfolding of the transmembrane domain may interfere with the architecture of either the pore or may interfere with the orientation of the pore helices. All of the above possibilities are purely speculative however, and the exact reason for the functional defect remains unknown.

Examples of functional defects have previously been reported in both Kir6.2 and SUR1. The K67N mutation of Kir6.2 has been shown to lead to no loss of cell surface density of the channel but *Xenopus* oocytes expressing the mutant channels yielded currents reduced by about a half compared to wild-type channels, although the exact impact of this mutation remains unknown (Reimann *et al.* 2003). Several SUR1 mutations have been described where channel function has been shown to be defective. These include the R1420C mutation (Matsuo *et al.* 2000) in which it has been shown that nucleotide binding to NBF2 is disrupted and the L1551V mutation (Reimann *et al.* 2003) which

showed a loss of sensitivity to both MgADP and diazoxide stimulation as well as a mild reduction in cell surface expression.

6.3.3 - Summary of findings

Described in the current chapter is characterization of two mutations of the Kir6.2 subunit of K_{ATP} channels which are known to cause CHI. Functional analysis of the mutant channels reveals that neither the W91R- nor L147P-containing channels are functional in *Xenopus* oocytes. It has been demonstrated that in the case of the W91R mutation containing channels the lack of currents results from a trafficking defect which prevents channels from reaching the cell surface. The channels have been found to be retained within a compartment which is enriched in syntaxin 6 and is therefore thought to be associated with the TGN or a TGN derived endosomal population. The lack of currents observed with L147P mutation containing channels is thought to result from a loss of channel function since membrane trafficking of these channels appears normal. Taken together these findings demonstrate two ways in which mutations associated with Kir6.2 can adversely affect the function of the pancreatic-type K_{ATP} channel.

Chapter 7

General discussion

7.1 - Overview

The aim of the current study was to investigate the possible mechanisms by which the cell surface density of K_{ATP} channels could be regulated. It has been shown that:

(i) The expression of K_{ATP} channel subunits is increased ~ 2.5 fold in response to a sudden lowering of glucose in the bathing medium in both INS-1e cells and freshly isolated mouse pancreatic β-cells. These findings are discussed in more detail in chapter 3. (ii) It has been demonstrated that regulated trafficking pathways play some part in regulating the cell surface density of K_{ATP} channels. Under basal conditions, channels are rapidly internalised into the cell and accumulate in a perinuclear compartment which includes elements of the early endosome, late endosome and *trans*-Golgi network (TGN) / TGN derived endosomal compartments. In the presence of PKC inhibitors these internalised channels are redirected into a pathway which allows rapid recycling back to the cell surface. These data are discussed in more detail in chapter 5. (iii) It has also been demonstrated that mutations of the Kir6.2 subunit known to cause the disorder congenital hyperinsulinism can affect both channel function and channel trafficking. These findings are discussed in more detail in chapter 6.

7.2 - Physiological relevance of the findings & future perspectives

Glucose regulation of K_{ATP} channel expression

A sudden decrease in glucose availability results in a rapid upregulation of K_{ATP} channel numbers. It seems most likely that the purpose of this increase in channel numbers would be to enable the cell to respond to the lowering of glucose by increasing the numbers of channels available to be inserted into the cell membrane. Together with decreased [ATP], this may prevent insulin secretion from the β-cell, and it is likely that this mechanism has evolved to protect the body from the effects of a sudden hypoglycaemic shock. A corresponding difference was not however observed in the cell surface density of K_{ATP} channels when examined by the patch clamp analysis. This prompted the investigation of the possibility that channel turnover at the cell surface might also be tightly regulated, that is, in low glucose conditions the rate of both channel insertion and removal at the membrane might be greatly increased, a process which might only be possible with a larger population of channels within the cells (see *endocytic trafficking of K_{ATP} channels* below). The precise role that AMP-activated protein kinase plays in mediating the glucose

stimulated upregulation of the pancreatic K_{ATP} channel following glucose withdrawal remains unclear. However, there is mounting evidence to suggest that AMPK is one of the most important sensors of cellular energy status and it is becoming increasingly evident that a multitude of processes which depend on the energetic state of the cell are regulated by the action of this kinase. The role that AMPK activation plays in mediating the upregulation of K_{ATP} channels in pancreatic β-cells requires further examination. The potential roles that AMPK may play in this process are further discussed in chapter 3 (3.4.3). These data also do not rule out another role for K_{ATP} channels within these cells, for example a role for K_{ATP} channels has been proposed at the level of the insulin secreting granule (Geng *et al.* 2003). The physiological significance of these findings is discussed in more detail in chapter 3.

Endocytic trafficking of K_{ATP} channels

The pathway through which K_{ATP} channels are internalised appears to involve the early sorting endosomes, late endosomes, eventually leading to accumulation in a TGN / TGN-derived endosomal compartment in the perinuclear region of the cell. In the presence of PKC inhibitors, internalised channels appear to bypass this trafficking pathway in favour of an alternative pathway which allows rapid recycling of the channels back to the cell surface. This pathway outlined for the endocytic trafficking of K_{ATP} channels will hopefully lead to a better understanding of how the density, and hence the overall activity, of these channels is regulated by the cell, although a great deal of further research is required to answer a number of questions raised.

Firstly, the fate of the channels once they have been internalised into the perinuclear (TGN / TGN-derived endosomal) compartment remains unclear. It is possible that the channels could traffic back to the cell surface, be targeted for degradation by the either the proteasome or lysosome or that they will remain in the peri-nuclear region in some sort of storage compartment. The most likely outcome from the data presented (the presence of internalised channels in long-lived perinuclear structures) is that the channels are internalised into the TGN-associated perinuclear compartment where they accumulate. No significant loss of internalised channels is observed in cells where channels have been allowed to internalise for > 3 hours, suggesting that significant degradation of channels is not occurring. The live cell imaging of K_{ATP} movement showed many vesicles moving towards the centre of the cell but very few

moving back towards the periphery, supporting the idea that K_{ATP} channels internalised into the perinuclear compartment were largely retained for some purpose. If there is a TGN-associated K_{ATP} storage compartment within the cell this may provide an explanation as to why certain CHI causing mutations are retained in TGN-like / derived structures. It is conceivable that channels harbouring either of the two mutations currently known to lead to TGN retention (W91R - current study and R1394H - Partridge *et al.* 2001) may be unable to interact correctly with whatever machinery which might be required for entry to or export from this compartment. This is however highly speculative. The purpose of such a mechanism is unclear; however, parallels do exist with other proteins, for example the GLUT4 glucose transporter, which is retained in a TGN-derived endosomal storage compartment until stimulated by the presence of insulin (Kanai *et al.* 1993, Lund *et al.* 1995). It is not clear if such a mechanism is at play with K_{ATP} channels, but a further characterisation of this compartment may provide clues as to its exact function with respect to K_{ATP} channel trafficking.

A very clear difference in the endocytic trafficking of the channels can be seen when PKC activity is impaired. With the activity of PKC absent the channels appear to enter a cycle of repeated internalisation and rapid recycling back to the plasma membrane. As mentioned above, when PKC activity is promoted the internalised channels appear to be sequestered in the perinuclear compartments. This may explain why PKC activation stimulates insulin secretion. PKC has been shown to augment the second phase of insulin secretion by potentiating the primary signals derived from fuel metabolism (see Nesher *et al.* 2002 for review). It has been suggested that PKC acts in this manner by recruiting secretory vesicles from a reserve pool in the cell into the readily releasable pool of vesicles close to the plasma membrane (Yaney *et al.* 2002, Lee *et al.* 2003) and by sensitising the secretory machinery to Ca^{2+} (Wan *et al.* 2004). If the action of elevated PKC activity is to augment insulin secretion it follows that K_{ATP} channel activity should preferably be suppressed. One way to achieve this is to reduce the overall K_{ATP} channel activity by removing the channels from the cell surface into an intracellular compartment or by inhibiting their return to the cell surface. This hypothesis offers a plausible explanation for both the apparent sequestration of the channels in the perinuclear compartment and for the regulation of this process by PKC. These findings were however made in a recombinant system

and it would be necessary to attempt to replicate these findings in a native cell line, such as the INS-1e cells or in isolated pancreatic β-cells.

Trafficking motifs of SUR1 and Kir6.2 which may mediate channel trafficking

The targeting of proteins into the various compartments of the endocytic trafficking system relies on a number of specific signalling motifs located in the cytoplasmic domains of membrane bound proteins. These motifs consist of short stretches of protein sequence which are recognised by various components of the trafficking machinery, for example the adaptor protein complexes AP1 - 4. They allow cargo proteins to be concentrated into specific membrane domains of each compartment where the recruitment of the accessory proteins necessary for movement to the next destination occurs (see Bonifacino & Traub 2003 for a comprehensive review).

Several different trafficking motifs have been identified which allow the internalisation of integral membrane proteins from the cell surface. One of these trafficking motifs is the YXXΦ tyrosine based motif (where Y - tyrosine, X - any amino acid, Φ - any amino acid with a bulky, hydrophobic sidechain; F,W,L,I) (Jadot *et al.* 1992). These trafficking motifs have been implicated in clathrin coated vesicle formation where they interact with the μ subunit of the adaptor protein complexes (Ohno *et al.* 1995, Boll *et al.* 1996, Honing *et al.* 1996), and they also may have a role in lysosomal targeting (Williams & Fukuda 1990, Harter & Mellman 1992, Marks *et al.* 1995, Gough *et al.* 1999). Those tyrosine based motifs which mediate lysosomal targeting commonly have a glycine residue immediately upstream of the tyrosine residue (Harter & Mellman 1992). The tyrosine residue of theses motifs is critical for function whereas the X positions can accommodate almost any amino acid, although the exact nature of these residues is believed to specify the properties of the motif (Gough *et al.* 1999, Rous *et al.* 2002). Most, but not all, of the YXXΦ motifs responsible for mediating endocytosis are found within 10 - 40 residues of transmembrane domains whereas the majority of lysosomal targeting motifs are thought to be found either within 6-9 residues of transmembrane domains or in the distal C-terminus of proteins.

Two candidate sequences can be found in the sequence of both Kir6.2 and SUR1. The motifs in SUR1 are -Y^{367}VAI- and -Y^{386}NKI- (numbering refers to hamster

SUR1) and are both located in a large cytoplasmic loop between TM 7 and 8 in TMD1. The motifs in Kir6.2 are -Y^{258}HVI- and -Y^{330}SKF- (numbering refers to mouse Kir6.2) and are both located in the C-terminus. If these motifs do indeed play a role in regulating the trafficking of K_{ATP} channels, it is likely that they are involved in the process of rapid internalisation from the cell surface. Further investigation is required in order to ascertain whether these motifs do indeed function in the endocytic trafficking of K_{ATP} channels at either the site of internalisation from the cell surface or during a particular sorting step in the endosomal system.

A second class of trafficking motifs have been implicated in the initial endocytic event as well as several intracellular trafficking steps. These motifs are characterised by the presence of two leucine residues (-LL-) and are thus called dileucine motifs (Johnson & Kornfeld 1992). Since their initial discovery two distinct types of dileucine motifs have been found, one which allows interactions with the AP1-4 adaptor complexes throughout the endocytic trafficking system (Heilker *et al.* 1996, Dietrich *et al.* 1997, Honing *et al.* 1998, Fujita *et al.* 1999, Peden *et al.* 2001) and a second motif which binds to the Golgi-localised γ-ear containing ADP-ribosylation-factor binding proteins (GGAs), adaptor proteins which are thought to mediate trafficking from the *trans*-Golgi network to endosomes (Puertollano *et al.* 2001, Zhu *et al.* 2001, Jacobsen *et al.* 2002). The motif responsible for interacting with AP1-4 is the [D/E]XXXL[L/I] motif. In this motif, the first leucine residue is necessary for function but the second leucine can tolerate the change to isoleucine (Letourneur & Klausner 1992). The acidic residue at the beginning of the motif is not thought to be required for internalisation to occur, but is thought to target internalised proteins towards lysosomes (Pond *et al.* 1995, Sandoval *et al.* 2000). Some [D/E]XXXL[L/I] motifs have two arginine residues substituted for the acid residue at the beginning of the motif, although to date they have only been found in proteins which are targeted into insulin responsive storage compartments, for example GLUT4 and IRAP (Sandoval *et al.* 2000). The motif responsible for interactions with GGA proteins is DXXLL. As mentioned above these motifs appear to mediate trafficking from the TGN to the endosomes (Puertollano *et al.* 2001, Doray *et al.* 2002, Puertollano *et al.* 2003). It has been shown that these motifs are recognised by the amino-terminal VHS domain of the GGA adaptor proteins (Zhu *et al.* 2001, Takatsu *et al.* 2001). This interaction is specific for the VHS domain of the GGAs since other VHS containing

proteins do not bind to the DXXLL motif (Puertollano *et al.* 2001). The requirement for both the aspartate and the dileucine pair for this motif to function is absolute, with alanine substitutions of any of the three residues sufficient to abolish function, leading to an increased expression of the protein at the cell surface (Johnson & Kornfeld 1992, Chen *et al.* 1997).

Dileucine motifs are fairly common features in the cytoplasmic domains of most integral membrane proteins, and SUR1 and Kir6.2 are no different, with 11 such pairs in hamster SUR1 and 1 in the sequence of mouse Kir6.2. The role of each of these motifs in K_{ATP} internalisation and trafficking would have to be individually investigated. Of the motifs present in SUR1 only one motif shows significant similarities to the [D/E]XXXL[L/I] type motif whereas no motifs resemble the DXXLL type motif. The -E^{654}EVRDLLG- motif of SUR1 is located in the large cytoplasmic loop between TMD1 and TMD2 and appears to resemble the dileucine motifs responsible for lysosomal targeting due to the presence of the glutamate residue at -4 positions from the dileucine pair. The dileucine pair contained within Kir6.2 conforms to the DXXLL type motif. The dileucine pair of the -D^{350}RSLL- has previously been studied by Hu *et al.* (2003) who reported that substitution of the dileucine pair with alanine resulted in increased surface expression of K_{ATP} channels. Their interpretation of this was that internalisation was being interrupted, but it remains possible that the increase in apparent surface expression was due to decreased GGA binding in the TGN resulting in increased surface expression in a similar manner to that reported by Johnson & Kornfeld (1992) and Chen *et al.* (1997). If indeed the internalised channels are being trafficked to the TGN or into TGN-derived endosomal compartments (as shown in chapter 5), it is plausible that GGA binding may be required at some stage. In support of this motif being involved in traffic in and around the TGN as opposed to its involvement in channel internalisation from the cell membrane, unpublished work (by Mr J. Mankouri) from this laboratory has shown that channels composed of SUR1 and Kir6.2 containing a dileucine to dialanine substitution (-LL- to -AA-) are still able to internalise into the cell. The potential role of the motifs described here in regulating K_{ATP} channel traffic requires further investigation.

Proteins which traffic from the late endosome to the *trans*-Golgi network have been shown to contain acidic motifs (many D and E residues) in their cytoplasmic domains (Schafer *et al.* 1995, Voorhees *et al.* 1995, Alconada *et al.* 1996, Mauxion *et al.* 1996, Dittie *et al.* 1997). Also associated with the acidic motif is a casein kinase II (CKII) phosphorylation site (Meresse *et al.* 1990). When this CKII site is phosphorylated the acidic motif is able to interact with a similar acidic motif contained in a chaperone protein called PACS-1 (Wan et al. 1998). It is this interaction which allows trafficking to the TGN to occur via AP-1 or AP-3 binding to PACS-1 to allow clathrin coat formation (Crump *et al.* 2001). An almost identical acidic motif (-D^{971}EEEEEAAESEEDDNL-) containing a CKII phosphorylation site (underlined) is contained within the cytoplasmic loop found between TMD1 and TMD2 of SUR1 and its potential role in the late endosome to TGN trafficking of K_{ATP} channels could warrant further investigation.

7.3 - Final summary

In this thesis it was shown that a sudden decrease in glucose stimulated a rapid induction of K_{ATP} channel synthesis, but a similar increase in the cell surface channel density was not observed. This may imply that separate regulated insertion / removal mechanisms are involved in regulating the cell surface channel density. The data presented in chapter 5 did indeed show that this is the case. Recombinant K_{ATP} channels are rapidly internalised from the cell surface into a perinuclear compartment under basal conditions and into a rapid recycling pathway upon PKC inhibition.

It is not clear how these two modes of regulation might interact directly. Certainly, further research must be undertaken to elucidate the individual roles of each mechanism in regulating the overall cell surface density of the K_{ATP} channel. What the current study does underline, however, is that the regulation of both expression and trafficking are likely to be very important factors in determining the overall numbers of K_{ATP} channels at the cell surface, and thus regulate overall channel function.

References

AGUILAR-BRYAN L., NICHOLS C.G., WECHSLER S.W., CLEMENT J.P., BOYD A.E., III, GONZALEZ G., HERRERA-SOSA H., NGUY K., BRYAN J. & NELSON D.A. (1995). Cloning of the beta cell high-affinity sulfonylurea receptor: a regulator of insulin secretion. *Science.* **268.** 423-426.

AGUILAR-BRYAN L. & BRYAN J. (1999). Molecular biology of adenosine triphosphate-sensitive potassium channels. *Endocr. Rev.* **20.** 101-135.

AHMET I., SAWA Y., NISHIMURA M. & MATSUDA H. (2000). Cardioprotective effect of diadenosine tetraphosphate (AP4A) cardioplegia in isolated rat hearts. *Heart Vessels.* **15.** 30-34.

ALCONADA A., BAUER U. & HOFLACK B. (1996). A tyrosine-based motif and a casein kinase II phosphorylation site regulate the intracellular trafficking of the varicella-zoster virus glycoprotein I, a protein localized in the *trans*-Golgi network. *EMBO J.* **15.** 6096-6110.

ANDERSON H.A., CHEN Y. & NORKIN L.C. (1998). MHC class I molecules are enriched in caveolae but do not enter with simian virus 40. *J. Gen. Virol.* **79 (Pt 6).** 1469-1477.

ANIENTO F., EMANS N., GRIFFITHS G. & GRUENBERG J. (1993). Cytoplasmic dynein-dependent vesicular transport from early to late endosomes. *J. Cell Biol.* **123.** 1373-1387.

ANTCLIFF J.F., HAIDER S., PROKS P., SANSOM M.S. & ASHCROFT F.M. (2005). Functional analysis of a structural model of the ATP-binding site of the K_{ATP} channel Kir6.2 subunit. *EMBO J.* **24.** 229-239.

ASANO T., KATAGIRI H., TSUKUDA K., LIN J.L., ISHIHARA H., YAZAKI Y. & OKA Y. (1992). Upregulation of GLUT2 mRNA by glucose, mannose, and fructose in isolated rat hepatocytes. *Diabetes.* **41.** 22-25.

ASHCROFT F. & RORSMAN P. (2004a). Type 2 diabetes mellitus: not quite exciting enough? *Hum. Mol. Genet.* **13 Spec No 1.** R21-R31.

ASHCROFT F.M., HARRISON D.E. & ASHCROFT S.J. (1984). Glucose induces closure of single potassium channels in isolated rat pancreatic beta-cells. *Nature.* **312.** 446-448.

ASHCROFT F.M. & RORSMAN P. (1989). Electrophysiology of the pancreatic beta-cell. *Prog. Biophys. Mol. Biol.* **54.** 87-143.

ASHCROFT F.M. & GRIBBLE F.M. (2000). New windows on the mechanism of action of K(ATP) channel openers. *Trends Pharmacol. Sci.* **21.** 439-445.

ASHCROFT F.M. & RORSMAN P. (2004b). Molecular defects in insulin secretion in type-2 diabetes. *Rev. Endocr. Metab Disord.* **5.** 135-142.

ASHCROFT S.J. & ASHCROFT F.M. (1990). Properties and functions of ATP-sensitive K-channels. *Cell Signal.* **2.** 197-214.

ASHFIELD R., GRIBBLE F.M., ASHCROFT S.J. & ASHCROFT F.M. (1999). Identification of the high-affinity tolbutamide site on the SUR1 subunit of the K_{ATP} channel. *Diabetes.* **48.** 1341-1347.

ASHFORD M.L., BODEN P.R. & TREHERNE J.M. (1990a). Tolbutamide excites rat glucoreceptive ventromedial hypothalamic neurones by indirect inhibition of ATP-K+ channels. *Br. J. Pharmacol.* **101.** 531-540.

ASHFORD M.L., BODEN P.R. & TREHERNE J.M. (1990b). Glucose-induced excitation of hypothalamic neurones is mediated by ATP-sensitive K+ channels. *Pflugers Arch.* **415.** 479-483.

AUER R.N., HALL P., INGVAR M. & SIESJO B.K. (1986). Hypotension as a complication of hypoglycemia leads to enhanced energy failure but no increase in neuronal necrosis. *Stroke.* **17.** 442-449.

AYNSLEY-GREEN A., HUSSAIN K., HALL J., SAUDUBRAY J.M., NIHOUL-FEKETE C., LONLAY-DEBENEY P., BRUNELLE F., OTONKOSKI T., THORNTON P. & LINDLEY K.J. (2000). Practical management of hyperinsulinism in infancy. *Arch. Dis. Child Fetal Neonatal Ed.* **82.** F98-F107.

BABENKO A.P., GONZALEZ G. & BRYAN J. (1999). The tolbutamide site of SUR1 and a mechanism for its functional coupling to K_{ATP} channel closure. *FEBS Lett.* **459.** 367-376.

BABENKO A.P. & BRYAN J. (2003). SUR domains that associate with and gate K_{ATP} pores define a novel gatekeeper. *J. Biol. Chem.* **278.** 41577-41580.

BAO J., ALROY I., WATERMAN H., SCHEJTER E.D., BRODIE C., GRUENBERG J. & YARDEN Y. (2000). Threonine phosphorylation diverts internalized epidermal growth factor receptors from a degradative pathway to the recycling endosome. *J. Biol. Chem.* **275.** 26178-26186.

BAUKROWITZ T., SCHULTE U., OLIVER D., HERLITZE S., KRAUTER T., TUCKER S.J., RUPPERSBERG J.P. & FAKLER B. (1998). PIP_2 and PIP as determinants for ATP inhibition of K_{ATP} channels. *Science.* **282.** 1141-1144.

BECKMAN M.L., BERNSTEIN E.M. & QUICK M.W. (1999). Multiple G protein-coupled receptors initiate protein kinase C redistribution of GABA transporters in hippocampal neurons. *J. Neurosci.* **19.** RC9.

BEGUIN P., NAGASHIMA K., NISHIMURA M., GONOI T. & SEINO S. (1999). PKA-mediated phosphorylation of the human K_{ATP} channel: separate roles of Kir6.2 and SUR1 subunit phosphorylation. *EMBO J.* **18.** 4722-4732.

BELLES B., HESCHELER J. & TRUBE G. (1987). Changes of membrane currents in cardiac cells induced by long whole-cell recordings and tolbutamide. *Pflugers Arch.* **409.** 582-588.

BELLONI F.L. & HINTZE T.H. (1991). Glibenclamide attenuates adenosine-induced bradycardia and coronary vasodilatation. *Am. J. Physiol.* **261.** H720-H727.

BERNARDI H., FOSSET M. & LAZDUNSKI M. (1988). Characterization, purification, and affinity labeling of the brain [^{3}H]glibenclamide-binding protein, a putative neuronal ATP-regulated K^+ channel. *Proc. Natl. Acad. Sci. U. S. A.* **85.** 9816-9820.

BERTRAND C.A. & FRIZZELL R.A. (2003). The role of regulated CFTR trafficking in epithelial secretion. *Am. J. Physiol Cell Physiol.* **285.** C1-18.

BIENENGRAEBER M., ALEKSEEV A.E., ABRAHAM M.R., CARRASCO A.J., MOREAU C., VIVAUDOU M., DZEJA P.P. & TERZIC A. (2000). ATPase activity of the sulfonylurea receptor: a catalytic function for the K_{ATP} channel complex. *FASEB J.* **14.** 1943-1952.

BOKVIST K., OLSEN H.L., HOY M., GOTFREDSEN C.F., HOLMES W.F., BUSCHARD K., RORSMAN P. & GROMADA J. (1999). Characterisation of sulphonylurea and ATP-regulated K^+ channels in rat pancreatic A-cells. *Pflugers Arch.* **438.** 428-436.

BOLL W., OHNO H., SONGYANG Z., RAPOPORT I., CANTLEY L.C., BONIFACINO J.S. & KIRCHHAUSEN T. (1996). Sequence requirements for the recognition of tyrosine-based endocytic signals by clathrin AP-2 complexes. *EMBO J.* **15.** 5789-5795.

BOLSTER D.R., CROZIER S.J., KIMBALL S.R. & JEFFERSON L.S. (2002). AMP-activated protein kinase suppresses protein synthesis in rat skeletal muscle through down-regulated mammalian target of rapamycin (mTOR) signaling. *J. Biol. Chem.* **277.** 23977-23980.

BOMSEL M., PARTON R., KUZNETSOV S.A., SCHROER T.A. & GRUENBERG J. (1990). Microtubule- and motor-dependent fusion in vitro between apical and basolateral endocytic vesicles from MDCK cells. *Cell.* **62.** 719-731.

BONEV A.D. & NELSON M.T. (1996). Vasoconstrictors inhibit ATP-sensitive K^+ channels in arterial smooth muscle through protein kinase C. *J. Gen. Physiol.* **108.** 315-323.

BONIFACINO J.S. & TRAUB L.M. (2003). Signals for sorting of transmembrane proteins to endosomes and lysosomes. *Annu. Rev. Biochem.* **72.** 395-447.

BORG M.A., BORG W.P., TAMBORLANE W.V., BRINES M.L., SHULMAN G.I. & SHERWIN R.S. (1999). Chronic hypoglycemia and diabetes impair counterregulation induced by localized 2-deoxy-glucose perfusion of the ventromedial hypothalamus in rats. *Diabetes.* **48.** 584-587.

BORG W.P., SHERWIN R.S., DURING M.J., BORG M.A. & SHULMAN G.I. (1995). Local ventromedial hypothalamus glucopenia triggers counterregulatory hormone release. *Diabetes.* **44.** 180-184.

BROWN D. (2003). The ins and outs of aquaporin-2 trafficking. *Am. J. Physiol Renal Physiol.* **284.** F893-F901.

BUCCI C., THOMSEN P., NICOZIANI P., MCCARTHY J. & VAN DEURS B. (2000). Rab7: a key to lysosome biogenesis. *Mol. Biol. Cell.* **11.** 467-480.

BUDAS G.R., JOVANOVIC S., CRAWFORD R.M. & JOVANOVIC A. (2004). Hypoxia-induced preconditioning in adult stimulated cardiomyocytes is mediated by the opening and trafficking of sarcolemmal K_{ATP} channels. *FASEB J.* **18.** 1046-1048.

BURTON F.L. & SMITH G.L. (1997). The effect of cromakalim on intracellular [Ca^{2+}] in isolated rat skeletal muscle during fatigue and metabolic blockade. *Exp. Physiol.* **82.** 469-483.

CAMPBELL J.D., SANSOM M.S. & ASHCROFT F.M. (2003). Potassium channel regulation. *EMBO Rep.* **4.** 1038-1042.

CARATTINO M.D., HILL W.G. & KLEYMAN T.R. (2003). Arachidonic acid regulates surface expression of epithelial sodium channels. *J. Biol. Chem.* **278.** 36202-36213.

CARTIER E.A., CONTI L.R., VANDENBERG C.A. & SHYNG S.L. (2001). Defective trafficking and function of K_{ATP} channels caused by a sulfonylurea receptor 1 mutation associated with persistent hyperinsulinemic hypoglycemia of infancy. *Proc. Natl. Acad. Sci. U. S. A.* **98.** 2882-2887.

CASEY J.L., HENTZE M.W., KOELLER D.M., CAUGHMAN S.W., ROUAULT T.A., KLAUSNER R.D. & HARFORD J.B. (1988). Iron-responsive elements: regulatory RNA sequences that control mRNA levels and translation. *Science.* **240.** 924-928.

CERAMI A., STEVENS V.J. & MONNIER V.M. (1979). Role of nonenzymatic glycosylation in the development of the sequelae of diabetes mellitus. *Metabolism.* **28.** 431-437.

CHANG G. (2003). Structure of MsbA from Vibrio cholera: a multidrug resistance ABC transporter homolog in a closed conformation. *J. Mol. Biol.* **330.** 419-430.

CHEN H.J., YUAN J. & LOBEL P. (1997). Systematic mutational analysis of the cation-independent mannose 6-phosphate/insulin-like growth factor II receptor cytoplasmic domain. An acidic cluster containing a key aspartate is important for function in lysosomal enzyme sorting. *J. Biol. Chem.* **272.** 7003-7012.

CHEN W., FENG Y., CHEN D. & WANDINGER-NESS A. (1998). Rab11 is required for *trans*-Golgi network-to-plasma membrane transport and a preferential target for GDP dissociation inhibitor. *Mol. Biol. Cell.* **9.** 3241-3257.

CHRISSOBOLIS S. & SOBEY C.G. (2003). Inwardly rectifying potassium channels in the regulation of vascular tone. *Curr. Drug Targets.* **4.** 281-289.

CHRISTESEN H.B., JACOBSEN B.B., ODILI S., BUETTGER C., CUESTA-MUNOZ A., HANSEN T., BRUSGAARD K., MASSA O., MAGNUSON M.A., SHIOTA C., MATSCHINSKY F.M. & BARBETTI F. (2002). The second activating glucokinase mutation (A456V): implications for glucose homeostasis and diabetes therapy. *Diabetes.* **51.** 1240-1246.

CHUTKOW W.A., SAMUEL V., HANSEN P.A., PU J., VALDIVIA C.R., MAKIELSKI J.C. & BURANT C.F. (2001). Disruption of SUR2-containing K_{ATP} channels enhances insulin-stimulated glucose uptake in skeletal muscle. *Proc. Natl. Acad. Sci. U. S. A.* **98.** 11760-11764.

CLAYDON T.W., MAKARY S.Y., DIBB K.M. & BOYETT M.R. (2003). The selectivity filter may act as the agonist-activated gate in the G protein-activated Kir3.1/Kir3.4 K^+ channel. *J. Biol. Chem.* **278.** 50654-50663.

CLAYTON P.T., EATON S., AYNSLEY-GREEN A., EDGINTON M., HUSSAIN K., KRYWAWYCH S., DATTA V., MALINGRE H.E., BERGER R. & VAN DEN BERG., I (2001). Hyperinsulinism in short-chain L-3-hydroxyacyl-CoA dehydrogenase deficiency reveals the importance of beta-oxidation in insulin secretion. *J. Clin. Invest.* **108.** 457-465.

CLEMENT J.P., KUNJILWAR K., GONZALEZ G., SCHWANSTECHER M., PANTEN U., AGUILAR-BRYAN L. & BRYAN J. (1997). Association and stoichiometry of K_{ATP} channel subunits. *Neuron.* **18.** 827-838.

CONDLIFFE S.B., ZHANG H. & FRIZZELL R.A. (2004). Syntaxin 1A regulates ENaC channel activity. *J. Biol. Chem.* **279.** 10085-10092.

CONNER S.D. & SCHMID S.L. (2003). Regulated portals of entry into the cell. *Nature.* **422.** 37-44.

CONNOLLY C.N., KITTLER J.T., THOMAS P., UREN J.M., BRANDON N.J., SMART T.G. & MOSS S.J. (1999). Cell surface stability of gamma-aminobutyric acid type A receptors. Dependence on protein kinase C activity and subunit composition. *J. Biol. Chem.* **274.** 36565-36572.

CONTI L.R., RADEKE C.M., SHYNG S.L. & VANDENBERG C.A. (2001). Transmembrane topology of the sulfonylurea receptor SUR1. *J. Biol. Chem.* **276.** 41270-41278.

CONTI L.R., RADEKE C.M. & VANDENBERG C.A. (2002). Membrane targeting of ATP-sensitive potassium channel. Effects of glycosylation on surface expression. *J. Biol. Chem.* **277.** 25416-25422.

COOK D.L. & HALES C.N. (1984). Intracellular ATP directly blocks K^+ channels in pancreatic B-cells. *Nature.* **311.** 271-273.

COURTOIS P., LOUCHAMI K., LAGHMICH A., PICTON S., JIJAKLI H., SENER A. & MALAISSE W.J. (2000). Possible role of diadenosine polyphosphates in glucose-stimulated insulin release: effects of NaF upon metabolic and functional variables in rat isolated islets. *Int. J. Mol. Med.* **5.** 493-503.

COWAN S.W., SCHIRMER T., RUMMEL G., STEIERT M., GHOSH R., PAUPTIT R.A., JANSONIUS J.N., ROSENBUSCH J.P. (1992). Crystal structures explain functional properties of two E. coli porins. *Nature.* **358.** 727-733

CRANE A. & AGUILAR-BRYAN L. (2004). Assembly, maturation, and turnover of K(ATP) channel subunits. *J. Biol. Chem.* **279.** 9080-9090.

CRAWFORD R.M., RANKI H.J., BOTTING C.H., BUDAS G.R. & JOVANOVIC A. (2002). Creatine kinase is physically associated with the cardiac ATP-sensitive K^+ channel in vivo. *FASEB J.* **16.** 102-104.

CRAWFORD R.M., JOVANOVIC S., BUDAS G.R., DAVIES A.M., LAD H., WENGER R.H., ROBERTSON K.A., ROY D.J., RANKI H.J. & JOVANOVIC A. (2003). Chronic mild hypoxia protects heart-derived H9c2 cells against acute hypoxia/reoxygenation by regulating expression of the SUR2A subunit of the ATP-sensitive K+ channel. *J. Biol. Chem.* **278.** 31444-31455.

CRUMP C.M., XIANG Y., THOMAS L., GU F., AUSTIN C., TOOZE S.A. & THOMAS G. (2001). PACS-1 binding to adaptors is required for acidic cluster motif-mediated protein traffic. *EMBO J.* **20.** 2191-2201.

CRYER P.E. & GERICH J.E. (1985). Glucose counterregulation, hypoglycemia, and intensive insulin therapy in diabetes mellitus. *N. Engl. J. Med.* **313.** 232-241.

CUI N., KANG Y., HE Y., LEUNG Y.M., XIE H., PASYK E.A., GAO X., SHEU L., HANSEN J.B., WAHL P., TSUSHIMA R.G. & GAISANO H.Y. (2004). H3 domain of syntaxin 1A inhibits K_{ATP} channels by its actions on the sulfonylurea receptor 1 nucleotide-binding folds-1 and -2. *J. Biol. Chem.* **279.** 53259-53265.

D'HAHAN N., JACQUET H., MOREAU C., CATTY P. & VIVAUDOU M. (1999). A transmembrane domain of the sulfonylurea receptor mediates activation of ATP-sensitive K^+ channels by K^+ channel openers. *Mol. Pharmacol.* **56.** 308-315.

DA SILVA XAVIER, VARADI A., AINSCOW E.K. & RUTTER G.A. (2000a). Regulation of gene expression by glucose in pancreatic beta -cells (MIN6) via insulin secretion and activation of phosphatidylinositol 3'-kinase. *J. Biol. Chem.* **275.** 36269-36277.

DA SILVA XAVIER, LECLERC I., SALT I.P., DOIRON B., HARDIE D.G., KAHN A. & RUTTER G.A. (2000b). Role of AMP-activated protein kinase in the regulation by glucose of islet beta cell gene expression. *Proc. Natl. Acad. Sci. U. S. A.* **97.** 4023-4028.

DA SILVA XAVIER, LECLERC I., VARADI A., TSUBOI T., MOULE S.K. & RUTTER G.A. (2003). Role for AMP-activated protein kinase in glucose-stimulated insulin secretion and preproinsulin gene expression. *Biochem. J.* **371.** 761-774.

DAMKE H., BABA T., WARNOCK D.E. & SCHMID S.L. (1994). Induction of mutant dynamin specifically blocks endocytic coated vesicle formation. *J. Cell Biol.* **127.** 915-934.

DAUT J., MAIER-RUDOLPH W., VON BECKERATH N., MEHRKE G., GUNTHER K. & GOEDEL-MEINEN L. (1990). Hypoxic dilation of coronary arteries is mediated by ATP-sensitive potassium channels. *Science.* **247.** 1341-1344.

DAVIS K.E., STRAFF D.J., WEINSTEIN E.A., BANNERMAN P.G., CORREALE D.M., ROTHSTEIN J.D. & ROBINSON M.B. (1998). Multiple signaling pathways regulate cell surface expression and activity of the excitatory amino acid carrier 1 subtype of Glu transporter in C6 glioma. *J. Neurosci.* **18.** 2475-2485.

DE SARRO G., MELDRUM B.S. & REAVILL C. (1984). Anticonvulsant action of 2-amino-7-phosphonoheptanoic acid in the substantia nigra. *Eur. J. Pharmacol.* **106.** 175-179.

DEAN R.T. & BARRETT A.J. (1976). Lysosomes. *Essays Biochem.* **12.** 1-40.

DEISENHOFER J., MICHEL H. (1989). The photosynthetic reaction centre from the purple bacterium Rhodopseudomonas viridis. *EMBO J.* **8.** 2149-2170.

DIETRICH J., KASTRUP J., NIELSEN B.L., ODUM N. & GEISLER C. (1997). Regulation and function of the CD3gamma DxxxLL motif: a binding site for adaptor protein-1 and adaptor protein-2 in vitro. *J. Cell Biol.* **138.** 271-281.

DELL'ANGELICA E.C., OHNO H., OOI C.E., RABINOVICH E., ROCHE K.W. & BONIFACINO J.S. (1997). AP-3: an adaptor-like protein complex with ubiquitous expression. *EMBO J.* **16.** 917-928.

DENNING G.M., ANDERSON M.P., AMARA J.F., MARSHALL J., SMITH A.E., WELSH M.J. (1992). Processing of mutant cystic fibrosis transmembrane conductance regulator is temperature-sensitive. *Nature.* **358.** 761-764

DEPAULIS A., KEAY K.A. & BANDLER R. (1994). Quiescence and hyporeactivity evoked by activation of cell bodies in the ventrolateral midbrain periaqueductal gray of the rat. *Exp. Brain Res.* **99.** 75-83.

DIAZ E. & PFEFFER S.R. (1998). TIP47: a cargo selection device for mannose 6-phosphate receptor trafficking. *Cell.* **93.** 433-443.

DIMENT S., LEECH M.S. & STAHL P.D. (1988). Cathepsin D is membrane-associated in macrophage endosomes. *J. Biol. Chem.* **263.** 6901-6907.

DINTZIS S.M., VELCULESCU V.E. & PFEFFER S.R. (1994). Receptor extracellular domains may contain trafficking information. Studies of the 300-kDa mannose 6-phosphate receptor. *J. Biol. Chem.* **269.** 12159-12166.

DITTIE A.S., THOMAS L., THOMAS G. & TOOZE S.A. (1997). Interaction of furin in immature secretory granules from neuroendocrine cells with the AP-1 adaptor complex is modulated by casein kinase II phosphorylation. *EMBO J.* **16.** 4859-4870.

DORAY B., GHOSH P., GRIFFITH J., GEUZE H.J. & KORNFELD S. (2002). Cooperation of GGAs and AP-1 in packaging MPRs at the *trans*-Golgi network. *Science.* **297.** 1700-1703.

DOWD L.A. & ROBINSON M.B. (1996). Rapid stimulation of EAAC1-mediated Na^+-dependent L-glutamate transport activity in C6 glioma cells by phorbol ester. *J. Neurochem.* **67.** 508-516.

DOYLE D.A., MORAIS C.J., PFUETZNER R.A., KUO A., GULBIS J.M., COHEN S.L., CHAIT B.T. & MACKINNON R. (1998). The structure of the potassium channel: molecular basis of K+ conduction and selectivity. *Science.* **280.** 69-77.

DRAB M., VERKADE P., ELGER M., KASPER M., LOHN M., LAUTERBACH B., MENNE J., LINDSCHAU C., MENDE F., LUFT F.C., SCHEDL A., HALLER H. & KURZCHALIA T.V. (2001). Loss of caveolae, vascular dysfunction, and pulmonary defects in caveolin-1 gene-disrupted mice. *Science.* **293.** 2449-2452.

DUNN K.W., MCGRAW T.E. & MAXFIELD F.R. (1989). Iterative fractionation of recycling receptors from lysosomally destined ligands in an early sorting endosome. *J. Cell Biol.* **109.** 3303-3314.

DUNNE M.J. (1994). Phorbol myristate acetate and ATP-sensitive potassium channels in insulin-secreting cells. *Am. J. Physiol.* **267.** C501-C506.

DUNNE M.J., COSGROVE K.E., SHEPHERD R.M., AYNSLEY-GREEN A. & LINDLEY K.J. (2004). Hyperinsulinism in infancy: from basic science to clinical disease. *Physiol Rev.* **84.** 239-275.

ECHARD A., JOLLIVET F., MARTINEZ O., LACAPERE J.J., ROUSSELET A., JANOUEIX-LEROSEY I. & GOUD B. (1998). Interaction of a Golgi-associated kinesin-like protein with Rab6. *Science.* **279.** 580-585.

EDIDIN M. (2001). Shrinking patches and slippery rafts: scales of domains in the plasma membrane. *Trends Cell Biol.* **11.** 492-496.

EHLERS M.D. (2000). Reinsertion or degradation of AMPA receptors determined by activity-dependent endocytic sorting. *Neuron.* **28.** 511-525.

EISENSTEIN R.S. (2000). Iron regulatory proteins and the molecular control of mammalian iron metabolism. *Annu. Rev. Nutr.* **20.** 627-662.

FAN Z. & MAKIELSKI J.C. (1997). Anionic phospholipids activate ATP-sensitive potassium channels. *J. Biol. Chem.* **272.** 5388-5395.

FARQUHAR M.G. & PALADE G.E. (1998). The Golgi apparatus: 100 years of progress and controversy. *Trends Cell Biol.* **8.** 2-10.

FELDER S., MILLER K., MOEHREN G., ULLRICH A., SCHLESSINGER J. & HOPKINS C.R. (1990). Kinase activity controls the sorting of the epidermal growth factor receptor within the multivesicular body. *Cell.* **61.** 623-634.

FERGUSON S.S. (2001). Evolving concepts in G protein-coupled receptor endocytosis: the role in receptor desensitization and signaling. *Pharmacol. Rev.* **53.** 1-24.

FERRER J.C., FAVRE C., GOMIS R.R., FERNANDEZ-NOVELL J.M., GARCIA-ROCHA M., DE l., I, CID E. & GUINOVART J.J. (2003). Control of glycogen deposition. *FEBS Lett.* **546.** 127-132.

FINDLAY I. (1988). Effects of ADP upon the ATP-sensitive K^+ channel in rat ventricular myocytes. *J. Membr. Biol.* **101.** 83-92.

FLORES N.A., STAVROU B.M. & SHERIDAN D.J. (1999). The effects of diadenosine polyphosphates on the cardiovascular system. *Cardiovasc. Res.* **42.** 15-26.

FOJO A.T., WHANG-PENG J., GOTTESMAN M.M. & PASTAN I. (1985). Amplification of DNA sequences in human multidrug-resistant KB carcinoma cells. *Proc. Natl. Acad. Sci. U. S. A.* **82.** 7661-7665.

FOSSET M., DE WEILLE J.R., GREEN R.D., SCHMID-ANTOMARCHI H. & LAZDUNSKI M. (1988). Antidiabetic sulfonylureas control action potential properties in heart cells via high affinity receptors that are linked to ATP-dependent K+ channels. *J. Biol. Chem.* **263.** 7933-7936.

FOURNET J.C. & JUNIEN C. (2003). The genetics of neonatal hyperinsulinism. *Horm. Res.* **59 Suppl 1.** 30-34.

FOURNIER K.M., GONZALEZ M.I. & ROBINSON M.B. (2004). Rapid trafficking of the neuronal glutamate transporter, EAAC1: evidence for distinct trafficking pathways differentially regulated by protein kinase C and platelet-derived growth factor. *J. Biol. Chem.* **279.** 34505-34513.

FRYER L.G., PARBU-PATEL A. & CARLING D. (2002). The Anti-diabetic drugs rosiglitazone and metformin stimulate AMP-activated protein kinase through distinct signaling pathways. *J. Biol. Chem.* **277.** 25226-25232.

FUJITA H., SAEKI M., YASUNAGA K., UEDA T., IMOTO T. & HIMENO M. (1999). In vitro binding study of adaptor protein complex (AP-1) to lysosomal targeting motif (LI-motif). *Biochem. Biophys. Res. Commun.* **255.** 54-58.

FURUKAWA T., YAMANE T., TERAI T., KATAYAMA Y. & HIRAOKA M. (1996). Functional linkage of the cardiac ATP-sensitive K+ channel to the actin cytoskeleton. *Pflugers Arch.* **431.** 504-512.

GAINES K.L., HAMILTON S. & BOYD A.E., III (1988). Characterization of the sulfonylurea receptor on beta cell membranes. *J. Biol. Chem.* **263.** 2589-2592.

GIBLIN J.P., QUINN K. & TINKER A. (2002). The cytoplasmic C-terminus of the sulfonylurea receptor is important for K_{ATP} channel function but is not key for complex assembly or trafficking. *Eur. J. Biochem.* **269.** 5303-5313.

GENG X., LI L., WATKINS S., ROBBINS P.D., DRAIN P. (2003). The insulin secretory granule is the major site of K(ATP) channels of the endocrine pancreas. *Diabetes.* **52.** 767-776.

GLASER B., KESAVAN P., HEYMAN M., DAVIS E., CUESTA A., BUCHS A., STANLEY C.A., THORNTON P.S., PERMUTT M.A., MATSCHINSKY F.M. & HEROLD K.C. (1998). Familial hyperinsulinism caused by an activating glucokinase mutation. *N. Engl. J. Med.* **338.** 226-230.

GLEESON P.A., LOCK J.G., LUKE M.R. & STOW J.L. (2004). Domains of the TGN: coats, tethers and G proteins. *Traffic.* **5.** 315-326.

GLOYN A.L., HASHIM Y., ASHCROFT S.J., ASHFIELD R., WILTSHIRE S. & TURNER R.C. (2001). Association studies of variants in promoter and coding regions of beta-cell ATP-sensitive K-channel genes SUR1 and Kir6.2 with Type 2 diabetes mellitus (UKPDS 53). *Diabet. Med.* **18.** 206-212.

GLOYN A.L., WEEDON M.N., OWEN K.R., TURNER M.J., KNIGHT B.A., HITMAN G., WALKER M., LEVY J.C., SAMPSON M., HALFORD S., MCCARTHY M.I., HATTERSLEY A.T. & FRAYLING T.M. (2003). Large-scale association studies of variants in genes encoding the pancreatic beta-cell K_{ATP} channel subunits Kir6.2 (KCNJ11) and SUR1 (ABCC8) confirm that the KCNJ11 E23K variant is associated with type 2 diabetes. *Diabetes.* **52.** 568-572.

GLOYN A.L., CUMMINGS E.A., EDGHILL E.L., HARRIES L.W., SCOTT R., COSTA T., TEMPLE I.K., HATTERSLEY A.T. & ELLARD S. (2004a). Permanent neonatal diabetes due to paternal germline mosaicism for an activating mutation of the KCNJ11 Gene encoding the Kir6.2 subunit of the beta-cell potassium adenosine triphosphate channel. *J. Clin. Endocrinol. Metab.* **89.** 3932-3935.

GLOYN A.L., PEARSON E.R., ANTCLIFF J.F., PROKS P., BRUINING G.J., SLINGERLAND A.S., HOWARD N., SRINIVASAN S., SILVA J.M., MOLNES J., EDGHILL E.L., FRAYLING T.M., TEMPLE I.K., MACKAY D., SHIELD J.P., SUMNIK Z., VAN RHIJN A., WALES J.K., CLARK P., GORMAN S., AISENBERG J., ELLARD S., NJOLSTAD P.R., ASHCROFT F.M. & HATTERSLEY A.T. (2004b). Activating mutations in the gene encoding the ATP-sensitive potassium-channel subunit Kir6.2 and permanent neonatal diabetes. *N. Engl. J. Med.* **350.** 1838-1849.

GLOYN A.L., REIMANN F., GIRARD C., EDGHILL E.L., PROKS P., PEARSON E.R., TEMPLE I.K., MACKAY D.J., SHIELD J.P., FREEDENBERG D., NOYES K., ELLARD S., ASHCROFT F.M., GRIBBLE F.M. & HATTERSLEY A.T. (2005). Relapsing diabetes can result from moderately activating mutations in KCNJ11. *Hum. Mol. Genet.*

GODA Y. & PFEFFER S.R. (1988). Selective recycling of the mannose 6-phosphate/IGF-II receptor to the *trans*-Golgi network in vitro. *Cell.* **55.** 309-320.

GONZALEZ L., Jr. & SCHELLER R.H. (1999). Regulation of membrane trafficking: structural insights from a Rab/effector complex. *Cell.* **96.** 755-758.

GOPEL S.O., KANNO T., BARG S. & RORSMAN P. (2000). Patch-clamp characterisation of somatostatin-secreting -cells in intact mouse pancreatic islets. *J. Physiol.* **528.** 497-507.

GOPEL S.O., KANNO T., BARG S., WENG X.G., GROMADA J. & RORSMAN P. (2000). Regulation of glucagon release in mouse α-cells by K_{ATP} channels and inactivation of TTX-sensitive Na^+ channels. *J. Physiol.* **528.** 509-520.

GOSSET P., GHEZALA G.A., KORN B., YASPO M.L., POUTSKA A., LEHRACH H., SINET P.M. & CREAU N. (1997). A new inward rectifier potassium channel gene (KCNJ15) localized on chromosome 21 in the Down syndrome chromosome region 1 (DCR1). *Genomics.* **44.** 237-241.

GOUGH N.R., ZWEIFEL M.E., MARTINEZ-AUGUSTIN O., AGUILAR R.C., BONIFACINO J.S. & FAMBROUGH D.M. (1999). Utilization of the indirect lysosome targeting pathway by lysosome-associated membrane proteins (LAMPs) is influenced largely by the C-terminal residue of their GYXXphi targeting signals. *J. Cell Sci.* **112 (Pt 23).** 4257-4269.

GRAMOLINI A. & RENAUD J.M. (1997). Blocking ATP-sensitive K^+ channel during metabolic inhibition impairs muscle contractility. *Am. J. Physiol.* **272.** C1936-C1946.

GRIBBLE F.M., TUCKER S.J. & ASHCROFT F.M. (1997). The essential role of the Walker A motifs of SUR1 in K-ATP channel activation by Mg-ADP and diazoxide. *EMBO J.* **16.** 1145-1152.

GRIBBLE F.M., TUCKER S.J., SEINO S. & ASHCROFT F.M. (1998). Tissue specificity of sulfonylureas: studies on cloned cardiac and beta-cell K_{ATP} channels. *Diabetes.* **47.** 1412-1418.

GRIBBLE F.M. & ASHCROFT F.M. (1999). Differential sensitivity of beta-cell and extrapancreatic K_{ATP} channels to gliclazide. *Diabetologia.* **42.** 845-848.

GRIFFITHS G., HOFLACK B., SIMONS K., MELLMAN I. & KORNFELD S. (1988). The mannose 6-phosphate receptor and the biogenesis of lysosomes. *Cell.* **52.** 329-341.

GROSS G.J. & PEART J.N. (2003). K_{ATP} channels and myocardial preconditioning: an update. *Am. J. Physiol Heart Circ. Physiol.* **285.** H921-H930.

GRUENBERG J. & STENMARK H. (2004). The biogenesis of multivesicular endosomes. *Nat. Rev. Mol. Cell Biol.* **5.** 317-323.

GUILLAM M.T., DUPRAZ P. & THORENS B. (2000). Glucose uptake, utilization, and signaling in GLUT2-null islets. *Diabetes.* **49.** 1485-1491.

HANI E.H., CLEMENT K., VELHO G., VIONNET N., HAGER J., PHILIPPI A., DINA C., INOUE H., PERMUTT M.A., BASDEVANT A., NORTH M., DEMENAIS F., GUY-GRAND B. & FROGUEL P. (1997). Genetic studies of the sulfonylurea receptor gene locus in NIDDM and in morbid obesity among French Caucasians. *Diabetes.* **46.** 688-694.

HANI E.H., BOUTIN P., DURAND E., INOUE H., PERMUTT M.A., VELHO G. & FROGUEL P. (1998). Missense mutations in the pancreatic islet beta cell inwardly rectifying K^+ channel gene (KIR6.2/BIR): a meta-analysis suggests a role in the polygenic basis of Type II diabetes mellitus in Caucasians. *Diabetologia.* **41.** 1511-1515.

HANSEN A.M., CHRISTENSEN I.T., HANSEN J.B., CARR R.D., ASHCROFT F.M. & WAHL P. (2002). Differential interactions of nateglinide and repaglinide on the human beta-cell sulphonylurea receptor 1. *Diabetes.* **51.** 2789-2795.

HARDIE D.G. & HAWLEY S.A. (2001). AMP-activated protein kinase: the energy charge hypothesis revisited. *Bioessays.* **23.** 1112-1119.

HARTER C. & MELLMAN I. (1992). Transport of the lysosomal membrane glycoprotein lgp120 (lgp-A) to lysosomes does not require appearance on the plasma membrane. *J. Cell Biol.* **117.** 311-325.

HAWLEY S.A., GADALLA A.E., OLSEN G.S. & HARDIE D.G. (2002). The antidiabetic drug metformin activates the AMP-activated protein kinase cascade via an adenine nucleotide-independent mechanism. *Diabetes.* **51.** 2420-2425.

HAYABUCHI Y., DAVIES N.W. & STANDEN N.B. (2001). Angiotensin II inhibits rat arterial K_{ATP} channels by inhibiting steady-state protein kinase A activity and activating protein kinase Ce. *J. Physiol.* **530.** 193-205.

HEILKER R., MANNING-KRIEG U., ZUBER J.F. & SPIESS M. (1996). In vitro binding of clathrin adaptors to sorting signals correlates with endocytosis and basolateral sorting. *EMBO J.* **15.** 2893-2899.

HEIMBERG H., DE VOS A., PIPELEERS D., THORENS B. & SCHUIT F. (1995). Differences in glucose transporter gene expression between rat pancreatic alpha- and beta-cells are correlated to differences in glucose transport but not in glucose utilization. *J. Biol. Chem.* **270.** 8971-8975.

HELLIWELL P.A., RICHARDSON M., AFFLECK J. & KELLETT G.L. (2000). Stimulation of fructose transport across the intestinal brush-border membrane by PMA is mediated by GLUT2 and dynamically regulated by protein kinase C. *Biochem. J.* **350 Pt 1.** 149-154.

HENIN N., VINCENT M.F. & VAN DEN B.G. (1996). Stimulation of rat liver AMP-activated protein kinase by AMP analogues. *Biochim. Biophys. Acta.* **1290.** 197-203.

HENTZE M.W., CAUGHMAN S.W., ROUAULT T.A., BARRIOCANAL J.G., DANCIS A., HARFORD J.B. & KLAUSNER R.D. (1987). Identification of the iron-responsive element for the translational regulation of human ferritin mRNA. *Science.* **238.** 1570-1573.

HERNANDEZ-SANCHEZ C., BASILE A.S., FEDOROVA I., ARIMA H., STANNARD B., FERNANDEZ A.M., ITO Y. & LEROITH D. (2001). Mice transgenically overexpressing sulfonylurea receptor 1 in forebrain resist seizure induction and excitotoxic neuron death. *Proc. Natl. Acad. Sci. U. S. A.* **98.** 3549-3554.

HEURTEAUX C., BERTAINA V., WIDMANN C. & LAZDUNSKI M. (1993). K^+ channel openers prevent global ischemia-induced expression of c-fos, c-jun, heat shock protein, and amyloid beta-protein precursor genes and neuronal death in rat hippocampus. *Proc. Natl. Acad. Sci. U. S. A.* **90.** 9431-9435.

HILGEMANN D.W. & BALL R. (1996). Regulation of cardiac Na^+,$Ca2^+$ exchange and K_{ATP} potassium channels by PIP_2. *Science.* **273.** 956-959.

HILLE B. (2001). Ionic channels of excitable membranes, 3rd edition. *Sinauer publishing company.*

HIRSCHBERG K., MILLER C.M., ELLENBERG J., PRESLEY J.F., SIGGIA E.D., PHAIR R.D. & LIPPINCOTT-SCHWARTZ J. (1998). Kinetic analysis of secretory protein traffic and characterization of golgi to plasma membrane transport intermediates in living cells. *J. Cell Biol.* **143.** 1485-1503.

HO K., NICHOLS C.G., LEDERER W.J., LYTTON J., VASSILEV P.M., KANAZIRSKA M.V. & HEBERT S.C. (1993). Cloning and expression of an inwardly rectifying ATP-regulated potassium channel. *Nature.* **362.** 31-38.

HONING S., GRIFFITH J., GEUZE H.J. & HUNZIKER W. (1996). The tyrosine-based lysosomal targeting signal in lamp-1 mediates sorting into Golgi-derived clathrin-coated vesicles. *EMBO J.* **15.** 5230-5239.

HONING S., SANDOVAL I.V. & VON FIGURA K. (1998). A di-leucine-based motif in the cytoplasmic tail of LIMP-II and tyrosinase mediates selective binding of AP-3. *EMBO J.* **17.** 1304-1314.

HOPKINS C.R. (1983). The importance of the endosome in intracellular traffic. *Nature.* **304.** 684-685.

HORIE M. & IRISAWA H. (1987). Rectification of muscarinic K^+ current by magnesium ion in guinea pig atrial cells. *Am. J. Physiol.* **253.** H210-H214.

HORMAN S., BROWNE G., KRAUSE U., PATEL J., VERTOMMEN D., BERTRAND L., LAVOINNE A., HUE L., PROUD C. & RIDER M. (2002). Activation of AMP-activated protein kinase leads to the phosphorylation of elongation factor 2 and an inhibition of protein synthesis. *Curr. Biol.* **12.** 1419-1423.

HOUGH E. (2000). Cellular and molecular studies on the K_{ATP} potassium channel. *Thesis - University of Leeds.*

HU K., HUANG C.S., JAN Y.N. & JAN L.Y. (2003). ATP-sensitive potassium channel traffic regulation by adenosine and protein kinase C. *Neuron.* **38.** 417-432.

HUOPIO H., REIMANN F., ASHFIELD R., KOMULAINEN J., LENKO H.L., RAHIER J., VAUHKONEN I., KERE J., LAAKSO M., ASHCROFT F. & OTONKOSKI T. (2000). Dominantly inherited hyperinsulinism caused by a mutation in the sulfonylurea receptor type 1. *J. Clin. Invest.* **106.** 897-906.

HUOPIO H., OTONKOSKI T., VAUHKONEN I., REIMANN F., ASHCROFT F.M. & LAAKSO M. (2003). A new subtype of autosomal dominant diabetes attributable to a mutation in the gene for sulfonylurea receptor 1. *Lancet.* **361.** 301-307.

IADAROLA M.J. & GALE K. (1982). Substantia nigra: site of anticonvulsant activity mediated by gamma-aminobutyric acid. *Science.* **218.** 1237-1240.

IHRKE G., KYTTALA A., RUSSELL M.R., ROUS B.A. & LUZIO J.P. (2004). Differential use of two AP-3-mediated pathways by lysosomal membrane proteins. *Traffic.* **5.** 946-962.

INAGAKI N., TSUURA Y., NAMBA N., MASUDA K., GONOI T., HORIE M., SEINO Y., MIZUTA M. & SEINO S. (1995). Cloning and functional characterization of a novel ATP-sensitive potassium channel ubiquitously expressed in rat tissues, including pancreatic islets, pituitary, skeletal muscle, and heart. *J. Biol. Chem.* **270.** 5691-5694.

INAGAKI N., GONOI T., CLEMENT J.P., WANG C.Z., AGUILAR-BRYAN L., BRYAN J. & SEINO S. (1996). A family of sulfonylurea receptors determines the pharmacological properties of ATP-sensitive K^+ channels. *Neuron.* **16.** 1011-1017.

INAGAKI N., GONOI T. & SEINO S. (1997). Subunit stoichiometry of the pancreatic beta-cell ATP-sensitive K^+ channel. *FEBS Lett.* **409.** 232-236.

ISOMOTO S. & KURACHI Y. (1997). Function, regulation, pharmacology, and molecular structure of ATP-sensitive K^+ channels in the cardiovascular system. *J. Cardiovasc. Electrophysiol.* **8.** 1431-1446.

JACOB R. & NAIM H.Y. (2001). Apical membrane proteins are transported in distinct vesicular carriers. *Curr. Biol.* **11.** 1444-1450.

JACOBSEN L., MADSEN P., NIELSEN M.S., GERAERTS W.P., GLIEMANN J., SMIT A.B. & PETERSEN C.M. (2002). The sorLA cytoplasmic domain interacts with GGA1 and -2 and defines minimum requirements for GGA binding. *FEBS Lett.* **511.** 155-158.

JADOT M., CANFIELD W.M., GREGORY W. & KORNFELD S. (1992). Characterization of the signal for rapid internalization of the bovine mannose 6-phosphate/insulin-like growth factor-II receptor. *J. Biol. Chem.* **267.** 11069-11077.

JAMES D.E., BROWN R., NAVARRO J. & PILCH P.F. (1988). Insulin-regulatable tissues express a unique insulin-sensitive glucose transport protein. *Nature.* **333.** 183-185.

JEDD G., MULHOLLAND J. & SEGEV N. (1997). Two new Ypt GTPases are required for exit from the yeast trans-Golgi compartment. *J. Cell Biol.* **137.** 563-580.

JIANG G. & ZHANG B.B. (2003). Glucagon and regulation of glucose metabolism. *Am. J. Physiol Endocrinol. Metab.* **284.** E671-E678.

JIANG Y., LEE A., CHEN J., CADENE M., CHAIT B.T. & MACKINNON R. (2002). Crystal structure and mechanism of a calcium-gated potassium channel. *Nature.* **417.** 515-522.

JOHN S.A., MONCK J.R., WEISS J.N. & RIBALET B. (1998). The sulphonylurea receptor SUR1 regulates ATP-sensitive mouse Kir6.2 K^+ channels linked to the green fluorescent protein in human embryonic kidney cells (HEK 293). *J. Physiol.* **510 (Pt 2).** 333-345.

JOHN S.A., WEISS J.N. & RIBALET B. (2001). Regulation of cloned ATP-sensitive K channels by adenine nucleotides and sulfonylureas: interactions between SUR1 and positively charged domains on Kir6.2. *J. Gen. Physiol.* **118.** 391-405.

JOHN S.A., WEISS J.N., XIE L.H. & RIBALET B. (2003). Molecular mechanism for ATP-dependent closure of the K^+ channel Kir6.2. *J. Physiol.* **552.** 23-34.

JOHNSON K.F. & KORNFELD S. (1992). The cytoplasmic tail of the mannose 6-phosphate/insulin-like growth factor-II receptor has two signals for lysosomal enzyme sorting in the Golgi. *J. Cell Biol.* **119.** 249-257.

JOHNSON L.S., DUNN K.W., PYTOWSKI B. & MCGRAW T.E. (1993). Endosome acidification and receptor trafficking: bafilomycin A1 slows receptor externalization by a mechanism involving the receptor's internalization motif. *Mol. Biol. Cell.* **4.** 1251-1266.

JOHNSTON M. (1999). Feasting, fasting and fermenting. Glucose sensing in yeast and other cells. *Trends Genet.* **15.** 29-33.

JONAS J.C., SHARMA A., HASENKAMP W., ILKOVA H., PATANE G., LAYBUTT R., BONNER-WEIR S. & WEIR G.C. (1999). Chronic hyperglycemia triggers loss of pancreatic beta cell differentiation in an animal model of diabetes. *J. Biol. Chem.* **274.** 14112-14121.

JONES S., JEDD G., KAHN R.A., FRANZUSOFF A., BARTOLINI F. & SEGEV N. (1999). Genetic interactions in yeast between Ypt GTPases and Arf guanine nucleotide exchangers. *Genetics.* **152.** 1543-1556.

JOVANOVIC A., ALEKSEEV A.E. & TERZIC A. (1997). Intracellular diadenosine polyphosphates: a novel family of inhibitory ligands of the ATP-sensitive K^+ channel. *Biochem. Pharmacol.* **54.** 219-225.

JOVANOVIC S. & JOVANOVIC A. (2001). Diadenosine tetraphosphate-gating of recombinant pancreatic ATP-sensitive K^+ channels. *Biosci. Rep.* **21.** 93-99.

JUN J.Y., KONG I.D., KOH S.D., WANG X.Y., PERRINO B.A., WARD S.M. & SANDERS K.M. (2001). Regulation of ATP-sensitive K^+ channels by protein kinase C in murine colonic myocytes. *Am. J. Physiol Cell Physiol.* **281.** C857-C864.

KAJIOKA S., KITAMURA K. & KURIYAMA H. (1991). Guanosine diphosphate activates an adenosine 5'-triphosphate-sensitive K^+ channel in the rabbit portal vein. *J. Physiol.* **444.** 397-418.

KAKU K., FIEDOREK F.T., Jr., PROVINCE M. & PERMUTT M.A. (1988). Genetic analysis of glucose tolerance in inbred mouse strains. Evidence for polygenic control. *Diabetes.* **37.** 707-713.

KALANDADZE A., WU Y. & ROBINSON M.B. (2002). Protein kinase C activation decreases cell surface expression of the GLT-1 subtype of glutamate transporter. Requirement of a carboxyl-terminal domain and partial dependence on serine 486. *J. Biol. Chem.* **277.** 45741-45750.

KANAI F., NISHIOKA Y., HAYASHI H., KAMOHARA S., TODAKA M. & EBINA Y. (1993). Direct demonstration of insulin-induced GLUT4 translocation to the surface of intact cells by insertion of a c-myc epitope into an exofacial GLUT4 domain. *J. Biol. Chem.* **268.** 14523-14526.

KANG Y., LEUNG Y.M., MANNING-FOX J.E., XIA F., XIE H., SHEU L., TSUSHIMA R.G., LIGHT P.E. & GAISANO H.Y. (2004). Syntaxin-1A inhibits cardiac K_{ATP} channels by its actions on nucleotide binding folds 1 and 2 of sulfonylurea receptor 2A. *J. Biol. Chem.* **279.** 47125-47131.

KATSURADA A., IRITANI N., FUKUDA H., MATSUMURA Y., NISHIMOTO N., NOGUCHI T. & TANAKA T. (1990). Effects of nutrients and hormones on transcriptional and post-transcriptional regulation of fatty acid synthase in rat liver. *Eur. J. Biochem.* **190.** 427-433.

KAUBISCH N., HAMMER R., WOLLHEIM C., RENOLD A.E. & OFFORD R.E. (1982). Specific receptors for sulfonylureas in brain and in a beta-cell tumor of the rat. *Biochem. Pharmacol.* **31.** 1171-1174.

KAWAGUCHI T., OSATOMI K., YAMASHITA H., KABASHIMA T. & UYEDA K. (2002). Mechanism for fatty acid "sparing" effect on glucose-induced transcription: regulation of carbohydrate-responsive element-binding protein by AMP-activated protein kinase. *J. Biol. Chem.* **277.** 3829-3835.

KELLER P., TOOMRE D., DIAZ E., WHITE J. & SIMONS K. (2001). Multicolour imaging of post-Golgi sorting and trafficking in live cells. *Nat. Cell Biol.* **3.** 140-149.

KELLY A. & STANLEY C.A. (2001). Disorders of glutamate metabolism. *Ment. Retard. Dev. Disabil. Res. Rev.* **7.** 287-295.

KEMP B.E., STAPLETON D., CAMPBELL D.J., CHEN Z.P., MURTHY S., WALTER M., GUPTA A., ADAMS J.J., KATSIS F., VAN DENDEREN B., JENNINGS I.G., ISELI T., MICHELL B.J. & WITTERS L.A. (2003). AMP-activated protein kinase, super metabolic regulator. *Biochem. Soc. Trans.* **31.** 162-168.

KERMORGANT S., ZICHA D. & PARKER P.J. (2003). Protein kinase C controls microtubule-based traffic but not proteasomal degradation of c-Met. *J. Biol. Chem.* **278.** 28921-28929.

KILLIAN J.A., von HEIJNE G. (2000). How proteins adapt to a membrane-water interface. *Trends Biochem Sci.* **25.** 429-434.

KLEIZEN B., BRAAKMAN I. & DE JONGE H.R. (2000). Regulated trafficking of the CFTR chloride channel. *Eur. J. Cell Biol.* **79.** 544-556.

KLEPPISCH T. & NELSON M.T. (1995). Adenosine activates ATP-sensitive potassium channels in arterial myocytes via A2 receptors and cAMP-dependent protein kinase. *Proc. Natl. Acad. Sci. U. S. A.* **92.** 12441-12445.

KOBAYASHI T., STANG E., FANG K.S., DE MOERLOOSE P., PARTON R.G. & GRUENBERG J. (1998). A lipid associated with the antiphospholipid syndrome regulates endosome structure and function. *Nature.* **392.** 193-197.

KOOPTIWUT S., ZRAIKA S., THORBURN A.W., DUNLOP M.E., DARWICHE R., KAY T.W., PROIETTO J. & ANDRIKOPOULOS S. (2002). Comparison of insulin secretory function in two mouse models with different susceptibility to beta-cell failure. *Endocrinology.* **143.** 2085-2092.

KORNFELD S. & MELLMAN I. (1989). The biogenesis of lysosomes. *Annu. Rev. Cell Biol.* **5.** 483-525.

KOSTER J.C., MARSHALL B.A., ENSOR N., CORBETT J.A. & NICHOLS C.G. (2000). Targeted overactivity of beta cell K_{ATP} channels induces profound neonatal diabetes. *Cell.* **100.** 645-654.

KOSTER J.C., KNOPP A., FLAGG T.P., MARKOVA K.P., SHA Q., ENKVETCHAKUL D., BETSUYAKU T., YAMADA K.A. & NICHOLS C.G. (2001). Tolerance for ATP-insensitive K_{ATP} channels in transgenic mice. *Circ. Res.* **89.** 1022-1029.

KRAPIVINSKY G., MEDINA I., ENG L., KRAPIVINSKY L., YANG Y. & CLAPHAM D.E. (1998). A novel inward rectifier K^+ channel with unique pore properties. *Neuron.* **20.** 995-1005.

KRAUTER T., RUPPERSBERG J.P. & BAUKROWITZ T. (2001). Phospholipids as modulators of K_{ATP} channels: distinct mechanisms for control of sensitivity to sulphonylureas, K^+ channel openers, and ATP. *Mol. Pharmacol.* **59.** 1086-1093.

KUBO M., QUAYLE J.M. & STANDEN N.B. (1997). Angiotensin II inhibition of ATP-sensitive K^+ currents in rat arterial smooth muscle cells through protein kinase C. *J. Physiol.* **503 (Pt 3).** 489-496.

KUBO Y., BALDWIN T.J., JAN Y.N. & JAN L.Y. (1993). Primary structure and functional expression of a mouse inward rectifier potassium channel. *Nature.* **362.** 127-133.

KUO A., GULBIS J.M., ANTCLIFF J.F., RAHMAN T., LOWE E.D., ZIMMER J., CUTHBERTSON J., ASHCROFT F.M., EZAKI T. & DOYLE D.A. (2003). Crystal structure of the potassium channel KirBac1.1 in the closed state. *Science.* **300.** 1922-1926.

KURATA H.T., PHILLIPS L.R., ROSE T., LOUSSOUARN G., HERLITZE S., FRITZENSCHAFT H., ENKVETCHAKUL D., NICHOLS C.G. & BAUKROWITZ T. (2004). Molecular basis of inward rectification: polyamine interaction sites located by combined channel and ligand mutagenesis. *J. Gen. Physiol.* **124.** 541-554.

LADINSKY M.S., KREMER J.R., FURCINITTI P.S., MCINTOSH J.R. & HOWELL K.E. (1994). HVEM tomography of the trans-Golgi network: structural insights and identification of a lace-like vesicle coat. *J. Cell Biol.* **127.** 29-38.

LADINSKY M.S., WU C.C., MCINTOSH S., MCINTOSH J.R. & HOWELL K.E. (2002). Structure of the Golgi and distribution of reporter molecules at 20 degrees C reveals the complexity of the exit compartments. *Mol. Biol. Cell.* **13.** 2810-2825.

LAN J.Y., SKEBERDIS V.A., JOVER T., GROOMS S.Y., LIN Y., ARANEDA R.C., ZHENG X., BENNETT M.V. & ZUKIN R.S. (2001). Protein kinase C modulates NMDA receptor trafficking and gating. *Nat. Neurosci.* **4.** 382-390.

LANDOLT-MARTICORENA C., WILIAMS K.A., DEBER C.M., REITHMEIR R.A. (1993). Non-random distribution of amino acids in the transmembrane segments of human type I single span membrane proteins. *J Mol. Biol.* **229.** 602-608

LE T.L., JOSEPH S.R., YAP A.S. & STOW J.L. (2002). Protein kinase C regulates endocytosis and recycling of E-cadherin. *Am. J. Physiol Cell Physiol.* **283.** C489-C499.

LECLERC I., LENZNER C., GOURDON L., VAULONT S., KAHN A. & VIOLLET B. (2001). Hepatocyte nuclear factor-4alpha involved in type 1 maturity-onset diabetes of the young is a novel target of AMP-activated protein kinase. *Diabetes.* **50.** 1515-1521.

LECLERC I., VIOLLET B., DA S., X, KAHN A. & RUTTER G.A. (2002). Role of AMP-activated protein kinase in the regulation of gene transcription. *Biochem. Soc. Trans.* **30.** 307-311.

LECLERC I., WOLTERSDORF W.W., DA S., X, ROWE R.L., CROSS S.E., KORBUTT G.S., RAJOTTE R.V., SMITH R. & RUTTER G.A. (2004). Metformin, but not leptin, regulates AMP-activated protein kinase in pancreatic islets: impact on glucose-stimulated insulin secretion. *Am. J. Physiol Endocrinol. Metab.* **286.** E1023-E1031.

LEE I.S., HUR E.M., SUH B.C., KIM M.H., KOH D.S., RHEE I.J., HA H. & KIM K.T. (2003). Protein kinase A- and C-induced insulin release from Ca^{2+} -insensitive pools. *Cell Signal.* **15.** 529-537.

LERMAN J.C., ROBBLEE J., FAIRMAN R. & HUGHSON F.M. (2000). Structural analysis of the neuronal SNARE protein syntaxin-1A. *Biochemistry.* **39.** 8470-8479.

LESAGE F., DUPRAT F., FINK M., GUILLEMARE E., COPPOLA T., LAZDUNSKI M. & HUGNOT J.P. (1994). Cloning provides evidence for a family of inward rectifier and G-protein coupled K^+ channels in the brain. *FEBS Lett.* **353.** 37-42.

LETOURNEUR F. & KLAUSNER R.D. (1992). A novel di-leucine motif and a tyrosine-based motif independently mediate lysosomal targeting and endocytosis of CD3 chains. *Cell.* **69.** 1143-1157.

LIGHT P.E., BLADEN C., WINKFEIN R.J., WALSH M.P. & FRENCH R.J. (2000). Molecular basis of protein kinase C-induced activation of ATP-sensitive potassium channels. *Proc. Natl. Acad. Sci. U. S. A.* **97.** 9058-9063.

LIN S.X., GRANT B., HIRSH D. & MAXFIELD F.R. (2001). Rme-1 regulates the distribution and function of the endocytic recycling compartment in mammalian cells. *Nat. Cell Biol.* **3.** 567-572.

LIN Y.F., JAN Y.N. & JAN L.Y. (2000). Regulation of ATP-sensitive potassium channel function by protein kinase A-mediated phosphorylation in transfected HEK293 cells. *EMBO J.* **19.** 942-955.

LIPPINCOTT-SCHWARTZ J., COLE N. & PRESLEY J. (1998). Unravelling Golgi membrane traffic with green fluorescent protein chimeras. *Trends Cell Biol.* **8.** 16-20.

LIPPINCOTT-SCHWARTZ J. & ZAAL K.J. (2000). Cell cycle maintenance and biogenesis of the Golgi complex. *Histochem. Cell Biol.* **114.** 93-103.

LISS B., BRUNS R. & ROEPER J. (1999). Alternative sulfonylurea receptor expression defines metabolic sensitivity of K-ATP channels in dopaminergic midbrain neurons. *EMBO J.* **18.** 833-846.

LIU Y., MCKENNA E., FIGUEROA D.J., BLEVINS R., AUSTIN C.P., BENNETT P.B. & SWANSON R. (2000). The human inward rectifier K^+ channel subunit kir5.1 (KCNJ16) maps to chromosome 17q25 and is expressed in kidney and pancreas. *Cytogenet. Cell Genet.* **90.** 60-63.

LODER M.K. & MELIKIAN H.E. (2003). The dopamine transporter constitutively internalizes and recycles in a protein kinase C-regulated manner in stably transfected PC12 cell lines. *J. Biol. Chem.* **278.** 22168-22174.

LORENZ E., ALEKSEEV A.E., KRAPIVINSKY G.B., CARRASCO A.J., CLAPHAM D.E. & TERZIC A. (1998). Evidence for direct physical association between a K^+ channel (Kir6.2) and an ATP-binding cassette protein (SUR1) which affects cellular distribution and kinetic behavior of an ATP-sensitive K^+ channel. *Mol. Cell Biol.* **18.** 1652-1659.

LORENZ E. & TERZIC A. (1999). Physical association between recombinant cardiac ATP-sensitive K^+ channel subunits Kir6.2 and SUR2A. *J. Mol. Cell Cardiol.* **31.** 425-434.

LOVE-GREGORY L., WASSON J., LIN J., SKOLNICK G., SUAREZ B. & PERMUTT M.A. (2003). E23K single nucleotide polymorphism in the islet ATP-sensitive potassium channel gene (Kir6.2) contributes as much to the risk of Type II diabetes in Caucasians as the PPARgamma Pro12Ala variant. *Diabetologia.* **46.** 136-137.

LUND S., HOLMAN G.D., SCHMITZ O. & PEDERSEN O. (1995). Contraction stimulates translocation of glucose transporter GLUT4 in skeletal muscle through a mechanism distinct from that of insulin. *Proc. Natl. Acad. Sci. U. S. A.* **92.** 5817-5821.

LUPI R., DEL GUERRA S., TELLINI C., GIANNARELLI R., COPPELLI A., LORENZETTI M., CARMELLINI M., MOSCA F., NAVALESI R. & MARCHETTI P. (1999). The biguanide compound metformin prevents desensitization of human pancreatic islets induced by high glucose. *Eur. J. Pharmacol.* **364.** 205-209.

LUPO B. & BATAILLE D. (1987). A binding site for [^{3}H]glipizide in the rat cerebral cortex. *Eur. J. Pharmacol.* **140.** 157-169.

LUZIO J.P., ROUS B.A., BRIGHT N.A., PRYOR P.R., MULLOCK B.M. & PIPER R.C. (2000). Lysosome-endosome fusion and lysosome biogenesis. *J. Cell Sci.* **113 (Pt 9).** 1515-1524.

LUZIO J.P., POUPON V., LINDSAY M.R., MULLOCK B.M., PIPER R.C. & PRYOR P.R. (2003). Membrane dynamics and the biogenesis of lysosomes. *Mol. Membr. Biol.* **20.** 141-154.

MALLARD F., TANG B.L., GALLI T., TENZA D., SAINT-POL A., YUE X., ANTONY C., HONG W., GOUD B. & JOHANNES L. (2002). Early/recycling endosomes-to-TGN transport involves two SNARE complexes and a Rab6 isoform. *J. Cell Biol.* **156.** 653-664.

MANNHOLD R. (2004). K_{ATP} channel openers: structure-activity relationships and therapeutic potential. *Med. Res. Rev.* **24.** 213-266.

MARIE S., DIAZ-GUERRA M.J., MIQUEROL L., KAHN A. & IYNEDJIAN P.B. (1993). The pyruvate kinase gene as a model for studies of glucose-dependent regulation of gene expression in the endocrine pancreatic beta-cell type. *J. Biol. Chem.* **268.** 23881-23890.

MARKS M.S., ROCHE P.A., VAN DONSELAAR E., WOODRUFF L., PETERS P.J. & BONIFACINO J.S. (1995). A lysosomal targeting signal in the cytoplasmic tail of the beta chain directs HLA-DM to MHC class II compartments. *J. Cell Biol.* **131.** 351-369.

MARSH B.J., MASTRONARDE D.N., MCINTOSH J.R. & HOWELL K.E. (2001). Structural evidence for multiple transport mechanisms through the Golgi in the pancreatic beta-cell line, HIT-T15. *Biochem. Soc. Trans.* **29.** 461-467.

MASSA O., IAFUSCO D., D'AMATO E., GLOYN A.L., HATTERSLEY A.T., PASQUINO B., TONINI G., DAMMACCO F., ZANETTE G., MESCHI F., PORZIO O., BOTTAZZO G., CRINO A., LORINI R., CERUTTI F., VANELLI M. & BARBETTI F. (2005). KCNJ11 activating mutations in Italian patients with permanent neonatal diabetes. *Hum. Mutat.* **25.** 22-27.

MASUZAWA K., ASANO M., MATSUDA T., IMAIZUMI Y. & WATANABE M. (1990). Possible involvement of ATP-sensitive K^+ channels in the relaxant response of dog middle cerebral artery to cromakalim. *J. Pharmacol. Exp. Ther.* **255.** 818-825.

MATSCHINSKY F.M. (1990). Glucokinase as glucose sensor and metabolic signal generator in pancreatic beta-cells and hepatocytes. *Diabetes.* **39.** 647-652.

MATSUO H., CHEVALLIER J., MAYRAN N., LE B., I, FERGUSON C., FAURE J., BLANC N.S., MATILE S., DUBOCHET J., SADOUL R., PARTON R.G., VILBOIS F. & GRUENBERG J. (2004). Role of LBPA and Alix in multivesicular liposome formation and endosome organization. *Science.* **303.** 531-534.

MATSUO M., TRAPP S., TANIZAWA Y., KIOKA N., AMACHI T., OKA Y., ASHCROFT F.M. & UEDA K. (2000). Functional analysis of a mutant sulfonylurea receptor, SUR1-R1420C, that is responsible for persistent hyperinsulinemic hypoglycemia of infancy. *J. Biol. Chem.* **275.** 41184-41191.

MATTEONI R. & KREIS T.E. (1987). Translocation and clustering of endosomes and lysosomes depends on microtubules. *J. Cell Biol.* **105.** 1253-1265.

MAUXION F., LE BORGNE R., MUNIER-LEHMANN H. & HOFLACK B. (1996). A casein kinase II phosphorylation site in the cytoplasmic domain of the cation-dependent mannose 6-phosphate receptor determines the high affinity interaction of the AP-1 Golgi assembly proteins with membranes. *J. Biol. Chem.* **271.** 2171-2178.

MAXFIELD F.R. & MCGRAW T.E. (2004). Endocytic recycling. *Nat. Rev. Mol. Cell Biol.* **5.** 121-132.

MAYOR S., PRESLEY J.F. & MAXFIELD F.R. (1993). Sorting of membrane components from endosomes and subsequent recycling to the cell surface occurs by a bulk flow process. *J. Cell Biol.* **121.** 1257-1269.

MCGRAW T.E., DUNN K.W. & MAXFIELD F.R. (1993). Isolation of a temperature-sensitive variant Chinese hamster ovary cell line with a morphologically altered endocytic recycling compartment. *J. Cell Physiol.* **155.** 579-594.

MCLAUCHLAN H., NEWELL J., MORRICE N., OSBORNE A., WEST M. & SMYTHE E. (1998). A novel role for Rab5-GDI in ligand sequestration into clathrin-coated pits. *Curr. Biol.* **8.** 34-45.

MCLEOD L.E. & PROUD C.G. (2002). ATP depletion increases phosphorylation of elongation factor eEF2 in adult cardiomyocytes independently of inhibition of mTOR signalling. *FEBS Lett.* **531.** 448-452.

MELIKIAN H.E. & BUCKLEY K.M. (1999). Membrane trafficking regulates the activity of the human dopamine transporter. *J. Neurosci.* **19.** 7699-7710.

MERESSE S., LUDWIG T., FRANK R. & HOFLACK B. (1990). Phosphorylation of the cytoplasmic domain of the bovine cation-independent mannose 6-phosphate receptor. Serines 2421 and 2492 are the targets of a casein kinase II associated to the Golgi-derived HAI adaptor complex. *J. Biol. Chem.* **265.** 18833-18842.

MEYER C., ZIZIOLI D., LAUSMANN S., ESKELINEN E.L., HAMANN J., SAFTIG P., VON FIGURA K. & SCHU P. (2000). mu1A-adaptin-deficient mice: lethality, loss of AP-1 binding and rerouting of mannose 6-phosphate receptors. *EMBO J.* **19.** 2193-2203.

MIKI T., TASHIRO F., IWANAGA T., NAGASHIMA K., YOSHITOMI H., AIHARA H., NITTA Y., GONOI T., INAGAKI N., MIYAZAKI J. & SEINO S. (1997). Abnormalities of pancreatic islets by targeted expression of a dominant-negative K_{ATP} channel. *Proc. Natl. Acad. Sci. U. S. A.* **94.** 11969-11973.

MIKI T., NAGASHIMA K., TASHIRO F., KOTAKE K., YOSHITOMI H., TAMAMOTO A., GONOI T., IWANAGA T., MIYAZAKI J. & SEINO S. (1998). Defective insulin secretion and enhanced insulin action in K_{ATP} channel-deficient mice. *Proc. Natl. Acad. Sci. U. S. A.* **95.** 10402-10406.

MIKI T., SUZUKI M., SHIBASAKI T., UEMURA H., SATO T., YAMAGUCHI K., KOSEKI H., IWANAGA T., NAKAYA H. & SEINO S. (2002). Mouse model of Prinzmetal angina by disruption of the inward rectifier Kir6.1. *Nat. Med.* **8.** 466-472.

MINAMI K., YANO H., MIKI T., NAGASHIMA K., WANG C.Z., TANAKA H., MIYAZAKI J.I. & SEINO S. (2000). Insulin secretion and differential gene expression in glucose-responsive and -unresponsive MIN6 sublines. *Am. J. Physiol Endocrinol. Metab.* **279.** E773-E781.

MINAMI T., OOMURA Y. & SUGIMORI M. (1986). Electrophysiological properties and glucose responsiveness of guinea-pig ventromedial hypothalamic neurones in vitro. *J. Physiol.* **380.** 127-143.

MINTY A.J., ALONSO S., GUENET J.L. & BUCKINGHAM M.E. (1983). Number and organization of actin-related sequences in the mouse genome. *J. Mol. Biol.* **167.** 77-101.

MIYOSHI H. & NAKAYA Y. (1995). Calcitonin gene-related peptide activates the K^+ channels of vascular smooth muscle cells via adenylate cyclase. *Basic Res. Cardiol.* **90.** 332-336.

MIYOSHI Y. & NAKAYA Y. (1991). Angiotensin II blocks ATP-sensitive K^+ channels in porcine coronary artery smooth muscle cells. *Biochem. Biophys. Res. Commun.* **181.** 700-706.

MOHRMANN K. & VAN DER SLUIJS R. (1999). Regulation of membrane transport through the endocytic pathway by rabGTPases. *Mol. Membr. Biol.* **16.** 81-87.

MORITZ W., LEECH C.A., FERRER J. & HABENER J.F. (2001). Regulated expression of adenosine triphosphate-sensitive potassium channel subunits in pancreatic beta-cells. *Endocrinology.* **142.** 129-138.

MOURRE C., BEN ARI Y., BERNARDI H., FOSSET M. & LAZDUNSKI M. (1989). Antidiabetic sulfonylureas: localization of binding sites in the brain and effects on the hyperpolarization induced by anoxia in hippocampal slices. *Brain Res.* **486.** 159-164.

MULLINS C. & BONIFACINO J.S. (2001). The molecular machinery for lysosome biogenesis. *Bioessays.* **23.** 333-343.

MURPHY M.E. & BRAYDEN J.E. (1995). Nitric oxide hyperpolarizes rabbit mesenteric arteries via ATP-sensitive potassium channels. *J. Physiol.* **486 (Pt 1).** 47-58.

MUTH T.R. & CAPLAN M.J. (2003). Transport protein trafficking in polarized cells. *Annu. Rev. Cell Dev. Biol.* **19.** 333-366.

NAREN A.P., QUICK M.W., COLLAWN J.F., NELSON D.J. & KIRK K.L. (1998). Syntaxin 1A inhibits CFTR chloride channels by means of domain-specific protein-protein interactions. *Proc. Natl. Acad. Sci. U. S. A.* **95.** 10972-10977.

NELSON M.T., HUANG Y., BRAYDEN J.E., HESCHELER J. & STANDEN N.B. (1990). Arterial dilations in response to calcitonin gene-related peptide involve activation of K^+ channels. *Nature.* **344.** 770-773.

NESHER R, ANTEBY E, YEDOVIZSKY M, WARWAR N, KAISERN & CERASI E. (2002). Beta-cell protein kinases and the dynamics of the insulin response to glucose. *Diabetes.* **51 Suppl. 1.** 68-73.

NICHOLS B.J., KENWORTHY A.K., POLISHCHUK R.S., LODGE R., ROBERTS T.H., HIRSCHBERG K., PHAIR R.D. & LIPPINCOTT-SCHWARTZ J. (2001). Rapid cycling of lipid raft markers between the cell surface and Golgi complex. *J. Cell Biol.* **153.** 529-541.

NICHOLS C.G., SHYNG S.L., NESTOROWICZ A., GLASER B., CLEMENT J.P., GONZALEZ G., AGUILAR-BRYAN L., PERMUTT M.A. & BRYAN J. (1996). Adenosine diphosphate as an intracellular regulator of insulin secretion. *Science.* **272.** 1785-1787.

NICHOLS C.G. & KOSTER J.C. (2002). Diabetes and insulin secretion: whither K_{ATP}? *Am. J. Physiol Endocrinol. Metab.* **283.** E403-E412.

NICOZIANI P., VILHARDT F., LLORENTE A., HILOUT L., COURTOY P.J., SANDVIG K. & VAN DEURS B. (2000). Role for dynamin in late endosome dynamics and trafficking of the cation-independent mannose 6-phosphate receptor. *Mol. Biol. Cell.* **11.** 481-495.

NIELSEN E., SEVERIN F., BACKER J.M., HYMAN A.A. & ZERIAL M. (1999). Rab5 regulates motility of early endosomes on microtubules. *Nat. Cell Biol.* **1.** 376-382.

NIELSEN E.M., HANSEN L., CARSTENSEN B., ECHWALD S.M., DRIVSHOLM T., GLUMER C., THORSTEINSSON B., BORCH-JOHNSEN K., HANSEN T. & PEDERSEN O. (2003). The E23K variant of Kir6.2 associates with impaired post-OGTT serum insulin response and increased risk of type 2 diabetes. *Diabetes.* **52.** 573-577.

NOMA A. (1983). ATP-regulated K+ channels in cardiac muscle. *Nature.* **305.** 147-148.

OHNO H., STEWART J., FOURNIER M.C., BOSSHART H., RHEE I., MIYATAKE S., SAITO T., GALLUSSER A., KIRCHHAUSEN T. & BONIFACINO J.S. (1995). Interaction of tyrosine-based sorting signals with clathrin-associated proteins. *Science.* **269.** 1872-1875.

OHNO-SHOSAKU T. & YAMAMOTO C. (1992). Identification of an ATP-sensitive K+ channel in rat cultured cortical neurons. *Pflugers Arch.* **422.** 260-266.

OOMURA Y., ONO T., OOYAMA H. & WAYNER M.J. (1969). Glucose and osmosensitive neurones of the rat hypothalamus. *Nature.* **222.** 282-284.

OUCHI N., SHIBATA R. & WALSH K. (2005). AMP-Activated Protein Kinase Signaling Stimulates VEGF Expression and Angiogenesis in Skeletal Muscle. *Circ. Res.* **In press.**

PAGANO A., CROTTET P., PRESCIANOTTO-BASCHONG C. & SPEISS M. (2004). In vitro formation of recycling vesicles from endosomes requires adaptor protein-1/clathrin and is regulated by rab4 and the connector rabaptin-5. *Mol. Biol. Cell.* **15.** 4990-5000.

PAPE M.E., LOPEZ-CASILLAS F. & KIM K.H. (1988). Physiological regulation of acetyl-CoA carboxylase gene expression: effects of diet, diabetes, and lactation on acetyl-CoA carboxylase mRNA. *Arch. Biochem. Biophys.* **267.** 104-109.

PARTRIDGE C.J., BEECH D.J. & SIVAPRASADARAO A. (2001). Identification and pharmacological correction of a membrane trafficking defect associated with a mutation in the sulfonylurea receptor causing familial hyperinsulinism. *J. Biol. Chem.* **276.** 35947-35952.

PASYK E.A., KANG Y., HUANG X., CUI N., SHEU L. & GAISANO H.Y. (2004). Syntaxin-1A binds the nucleotide-binding folds of sulphonylurea receptor 1 to regulate the K_{ATP} channel. *J. Biol. Chem.* **279.** 4234-4240.

PATANE G., PIRO S., RABUAZZO A.M., ANELLO M., VIGNERI R. & PURRELLO F. (2000). Metformin restores insulin secretion altered by chronic exposure to free fatty acids or high glucose: a direct metformin effect on pancreatic beta-cells. *Diabetes.* **49.** 735-740.

PAULAUSKIS J.D. & SUL H.S. (1989). Hormonal regulation of mouse fatty acid synthase gene transcription in liver. *J. Biol. Chem.* **264.** 574-577.

PEDEN A.A., PARK G.Y. & SCHELLER R.H. (2001). The Di-leucine motif of vesicle-associated membrane protein 4 is required for its localization and AP-1 binding. *J. Biol. Chem.* **276.** 49183-49187.

PEDEN A.A., OORSCHOT V., HESSER B.A., AUSTIN C.D., SCHELLER R.H. & KLUMPERMAN J. (2004). Localization of the AP-3 adaptor complex defines a novel endosomal exit site for lysosomal membrane proteins. *J. Cell Biol.* **164.** 1065-1076.

PELKMANS L., PUNTENER D. & HELENIUS A. (2002). Local actin polymerization and dynamin recruitment in SV40-induced internalization of caveolae. *Science.* **296.** 535-539.

PERMUTT M.A. & KIPNIS D.M. (1972). Insulin biosynthesis. I. On the mechanism of glucose stimulation. *J. Biol. Chem.* **247.** 1194-1199.

PETTITT D.J., KNOWLER W.C., LISSE J.R. & BENNETT P.H. (1980). Development of retinopathy and proteinuria in relation to plasma-glucose concentrations in Pima Indians. *Lancet.* **2.** 1050-1052.

PFEFFER S. (2003). Membrane domains in the secretory and endocytic pathways. *Cell.* **112.** 507-517.

POITOUT V., OLSON L.K. & ROBERTSON R.P. (1996). Insulin-secreting cell lines: classification, characteristics and potential applications. *Diabetes Metab.* **22.** 7-14.

POLAK M. & SHIELD J. (2004). Neonatal and very-early-onset diabetes mellitus. *Semin. Neonatol.* **9.** 59-65.

POND L., KUHN L.A., TEYTON L., SCHUTZE M.P., TAINER J.A., JACKSON M.R. & PETERSON P.A. (1995). A role for acidic residues in di-leucine motif-based targeting to the endocytic pathway. *J. Biol. Chem.* **270.** 19989-19997.

POSTIC C., SHIOTA M. & MAGNUSON M.A. (2001). Cell-specific roles of glucokinase in glucose homeostasis. *Recent Prog. Horm. Res.* **56.** 195-217.

PRESLEY J.F., MAYOR S., MCGRAW T.E., DUNN K.W. & MAXFIELD F.R. (1997). Bafilomycin A1 treatment retards transferrin receptor recycling more than bulk membrane recycling. *J. Biol. Chem.* **272.** 13929-13936.

PRISTUPA Z.B., MCCONKEY F., LIU F., MAN H.Y., LEE F.J., WANG Y.T. & NIZNIK H.B. (1998). Protein kinase-mediated bidirectional trafficking and functional regulation of the human dopamine transporter. *Synapse.* **30.** 79-87.

PROKS P., REIMANN F., GREEN N., GRIBBLE F. & ASHCROFT F. (2002). Sulfonylurea stimulation of insulin secretion. *Diabetes.* **51 Suppl 3.** S368-S376.

PUERTOLLANO R., AGUILAR R.C., GORSHKOVA I., CROUCH R.J. & BONIFACINO J.S. (2001). Sorting of mannose 6-phosphate receptors mediated by the GGAs. *Science.* **292.** 1712-1716.

PUERTOLLANO R., VAN DER WEL N.N., GREENE L.E., EISENBERG E., PETERS P.J. & BONIFACINO J.S. (2003). Morphology and dynamics of clathrin/GGA1-coated carriers budding from the *trans*-Golgi network. *Mol. Biol. Cell.* **14.** 1545-1557.

QIAN Y., GALLI A., RAMAMOORTHY S., RISSO S., DEFELICE L.J. & BLAKELY R.D. (1997). Protein kinase C activation regulates human serotonin transporters in HEK-293 cells via altered cell surface expression. *J. Neurosci.* **17.** 45-57.

QUAYLE J.M., NELSON M.T. & STANDEN N.B. (1997). ATP-sensitive and inwardly rectifying potassium channels in smooth muscle. *Physiol Rev.* **77.** 1165-1232.

QUINN K.V., GIBLIN J.P. & TINKER A. (2004). Multisite phosphorylation mechanism for protein kinase A activation of the smooth muscle ATP-sensitive K^+ channel. *Circ. Res.* **94.** 1359-1366.

RAAB-GRAHAM K.F., CIRILO L.J., BOETTCHER A.A., RADEKE C.M. & VANDENBERG C.A. (1999). Membrane topology of the amino-terminal region of the sulfonylurea receptor. *J. Biol. Chem.* **274.** 29122-29129.

RAINBOW R.D., JAMES M., HUDMAN D., AL JOHI M., SINGH H., WATSON P.J., ASHMOLE I., DAVIES N.W., LODWICK D. & NORMAN R.I. (2004). Proximal C-terminal domain of sulphonylurea receptor 2A interacts with pore-forming Kir6 subunits in K_{ATP} channels. *Biochem. J.* **379.** 173-181.

RAJAN A.S., AGUILAR-BRYAN L., NELSON D.A., NICHOLS C.G., WECHSLER S.W., LECHAGO J. & BRYAN J. (1993). Sulfonylurea receptors and ATP-sensitive K+ channels in clonal pancreatic alpha cells. Evidence for two high affinity sulfonylurea receptors. *J. Biol. Chem.* **268.** 15221-15228.

RALSTON E. & PLOUG T. (1996). GLUT4 in cultured skeletal myotubes is segregated from the transferrin receptor and stored in vesicles associated with TGN. *J. Cell Sci.* **109 (Pt 13).** 2967-2978.

RAMM G., SLOT J.W., JAMES D.E. & STOORVOGEL W. (2000). Insulin recruits GLUT4 from specialized VAMP2-carrying vesicles as well as from the dynamic endosomal/trans-Golgi network in rat adipocytes. *Mol. Biol. Cell.* **11.** 4079-4091.

RANKI H.J., CRAWFORD R.M., BUDAS G.R. & JOVANOVIC A. (2002). Ageing is associated with a decrease in the number of sarcolemmal ATP-sensitive K^+ channels in a gender-dependent manner. *Mech. Ageing Dev.* **123.** 695-705.

RAZANI B., WOODMAN S.E. & LISANTI M.P. (2002). Caveolae: from cell biology to animal physiology. *Pharmacol. Rev.* **54.** 431-467.

REIMANN F., GRIBBLE F.M. & ASHCROFT F.M. (2000). Differential response of K_{ATP} channels containing SUR2A or SUR2B subunits to nucleotides and pinacidil. *Mol. Pharmacol.* **58.** 1318-1325.

REIMANN F., PROKS P. & ASHCROFT F.M. (2001). Effects of mitiglinide (S 21403) on Kir6.2/SUR1, Kir6.2/SUR2A and Kir6.2/SUR2B types of ATP-sensitive potassium channel. *Br. J. Pharmacol.* **132.** 1542-1548.

REIMANN F., HUOPIO H., DABROWSKI M., PROKS P., GRIBBLE F.M., LAAKSO M., OTONKOSKI T., ASHCROFT F.M. (2003). Characterisation of new K_{ATP}-channel mutations associated with congenital hyperinsulinism in the Finnish population. *Diabetologia.* **46.** 241-249

REN M., ZENG J., LEMOS-CHIARANDINI C., ROSENFELD M., ADESNIK M. & SABATINI D.D. (1996). In its active form, the GTP-binding protein rab8 interacts with a stress-activated protein kinase. *Proc. Natl. Acad. Sci. U. S. A.* **93.** 5151-5155.

REN M., XU G., ZENG J., LEMOS-CHIARANDINI C., ADESNIK M. & SABATINI D.D. (1998). Hydrolysis of GTP on rab11 is required for the direct delivery of transferrin from the pericentriolar recycling compartment to the cell surface but not from sorting endosomes. *Proc. Natl. Acad. Sci. U. S. A.* **95.** 6187-6192.

RENCUREL F., WAEBER G., ANTOINE B., ROCCHICCIOLI F., MAULARD P., GIRARD J. & LETURQUE A. (1996). Requirement of glucose metabolism for regulation of glucose transporter type 2 (GLUT2) gene expression in liver. *Biochem. J.* **314 (Pt 3).** 903-909.

RHODES C.J. & WHITE M.F. (2002). Molecular insights into insulin action and secretion. *Eur. J. Clin. Invest.* **32 Suppl 3.** 3-13.

RIEDERER M.A., SOLDATI T., SHAPIRO A.D., LIN J. & PFEFFER S.R. (1994). Lysosome biogenesis requires Rab9 function and receptor recycling from endosomes to the trans-Golgi network. *J. Cell Biol.* **125.** 573-582.

RIORDAN J.R., ROMMENS J.M., KEREM B., ALON N., ROZMAHEL R., GRZELCZAK Z., ZIELENSKI J., LOK S., PLAVSIC N., CHOU J.L. & . (1989). Identification of the cystic fibrosis gene: cloning and characterization of complementary DNA. *Science.* **245.** 1066-1073.

RIPOLL C., MARTIN F., MANUEL R.J., PINTOR J., MIRAS-PORTUGAL M.T. & SORIA B. (1996). Diadenosine polyphosphates. A novel class of glucose-induced intracellular messengers in the pancreatic beta-cell. *Diabetes.* **45.** 1431-1434.

ROBINSON M.B. (2002). Regulated trafficking of neurotransmitter transporters: common notes but different melodies. *J. Neurochem.* **80.** 1-11.

ROCHE E., ASSIMACOPOULOS-JEANNET F., WITTERS L.A., PERRUCHOUD B., YANEY G., CORKEY B., ASFARI M. & PRENTKI M. (1997). Induction by glucose of genes coding for glycolytic enzymes in a pancreatic beta-cell line (INS-1). *J. Biol. Chem.* **272.** 3091-3098.

RODUIT R., MORIN J., MASSE F., SEGALL L., ROCHE E., NEWGARD C.B., ASSIMACOPOULOS-JEANNET F. & PRENTKI M. (2000). Glucose down-regulates the expression of the peroxisome proliferator-activated receptor-alpha gene in the pancreatic beta -cell. *J. Biol. Chem.* **275.** 35799-35806.

RONNER P., MATSCHINSKY F.M., HANG T.L., EPSTEIN A.J. & BUETTGER C. (1993). Sulfonylurea-binding sites and ATP-sensitive K^+ channels in alpha-TC glucagonoma and beta-TC insulinoma cells. *Diabetes.* **42.** 1760-1772.

ROPER J. & ASHCROFT F.M. (1995). Metabolic inhibition and low internal ATP activate $K\text{-}_{ATP}$ channels in rat dopaminergic substantia nigra neurones. *Pflugers Arch.* **430.** 44-54.

ROUS B.A., REAVES B.J., IHRKE G., BRIGGS J.A., GRAY S.R., STEPHENS D.J., BANTING G. & LUZIO J.P. (2002). Role of adaptor complex AP-3 in targeting wild-type and mutated CD63 to lysosomes. *Mol. Biol. Cell.* **13.** 1071-1082.

RUBINO M., MIACZYNSKA M., LIPPE R. & ZERIAL M. (2000). Selective membrane recruitment of EEA1 suggests a role in directional transport of clathrin-coated vesicles to early endosomes. *J. Biol. Chem.* **275.** 3745-3748.

RUSTENBECK I. (2002). Desensitization of insulin secretion. *Biochem. Pharmacol.* **63.** 1921-1935.

RUSTOM A., BAJOHRS M., KAETHER C., KELLER P., TOOMRE D., CORBEIL D. & GERDES H.H. (2002). Selective delivery of secretory cargo in Golgi-derived carriers of nonepithelial cells. *Traffic.* **3.** 279-288.

RUTTER G.A., DA S., X & LECLERC I. (2003). Roles of 5'-AMP-activated protein kinase (AMPK) in mammalian glucose homoeostasis. *Biochem. J.* **375.** 1-16.

SALT I.P., JOHNSON G., ASHCROFT S.J. & HARDIE D.G. (1998). AMP-activated protein kinase is activated by low glucose in cell lines derived from pancreatic beta cells, and may regulate insulin release. *Biochem. J.* **335 (Pt 3).** 533-539.

SAMBROOK J. & RUSSELL D.W. (2001). Molecular cloning: A laboratory manual. *Cold Spring Harbour Laboratory Press, New York.*

SAMPSON L.J., HAYABUCHI Y., STANDEN N.B. & DART C. (2004). Caveolae localize protein kinase A signaling to arterial ATP-sensitive potassium channels. *Circ. Res.* **95.** 1012-1018.

SANDOVAL I.V., MARTINEZ-ARCA S., VALDUEZA J., PALACIOS S. & HOLMAN G.D. (2000). Distinct reading of different structural determinants modulates the dileucine-mediated transport steps of the lysosomal membrane protein LIMPII and the insulin-sensitive glucose transporter GLUT4. *J. Biol. Chem.* **275.** 39874-39885.

SANDVIG K. & VAN DEURS B. (2002). Transport of protein toxins into cells: pathways used by ricin, cholera toxin and Shiga toxin. *FEBS Lett.* **529.** 49-53.

SANTERRE R.F., COOK R.A., CRISEL R.M., SHARP J.D., SCHMIDT R.J., WILLIAMS D.C. & WILSON C.P. (1981). Insulin synthesis in a clonal cell line of simian virus 40-transformed hamster pancreatic beta cells. *Proc. Natl. Acad. Sci. U. S. A.* **78.** 4339-4343.

SCHAFER W., STROH A., BERGHOFER S., SEILER J., VEY M., KRUSE M.L., KERN H.F., KLENK H.D. & GARTEN W. (1995). Two independent targeting signals in the cytoplasmic domain determine trans-Golgi network localization and endosomal trafficking of the proprotein convertase furin. *EMBO J.* **14.** 2424-2435.

SCHIMMOLLER F., SIMON I. & PFEFFER S.R. (1998). Rab GTPases, directors of vesicle docking. *J. Biol. Chem.* **273.** 22161-22164.

SCHULZE D., KRAUTER T., FRITZENSCHAFT H., SOOM M. & BAUKROWITZ T. (2003). Phosphatidylinositol 4,5-bisphosphate (PIP_2) modulation of ATP and pH sensitivity in Kir channels. A tale of an active and a silent PIP_2 site in the N terminus. *J. Biol. Chem.* **278.** 10500-10505.

SCHWANSTECHER C., DICKEL C. & PANTEN U. (1992). Cytosolic nucleotides enhance the tolbutamide sensitivity of the ATP-dependent K^+ channel in mouse pancreatic B cells by their combined actions at inhibitory and stimulatory receptors. *Mol. Pharmacol.* **41.** 480-486.

SCHWANSTECHER C., NEUGEBAUER B., SCHULZ M. & SCHWANSTECHER M. (2002a). The common single nucleotide polymorphism E23K in K(IR)6.2 sensitizes pancreatic beta-cell ATP-sensitive potassium channels toward activation through nucleoside diphosphates. *Diabetes.* **51 Suppl 3.** S363-S367.

SCHWANSTECHER C., MEYER U. & SCHWANSTECHER M. (2002b). K(IR)6.2 polymorphism predisposes to type 2 diabetes by inducing overactivity of pancreatic beta-cell ATP-sensitive K^+ channels. *Diabetes.* **51.** 875-879.

SCHWANSTECHER C. & SCHWANSTECHER M. (2002). Nucleotide sensitivity of pancreatic ATP-sensitive potassium channels and type 2 diabetes. *Diabetes.* **51 Suppl 3.** S358-S362.

SEABRA M.C., MULES E.H. & HUME A.N. (2002). Rab GTPases, intracellular traffic and disease. *Trends Mol. Med.* **8.** 23-30.

SEGHERS V., NAKAZAKI M., DEMAYO F., AGUILAR-BRYAN L. & BRYAN J. (2000). SUR1 knockout mice. A model for K_{ATP} channel-independent regulation of insulin secretion. *J. Biol. Chem.* **275.** 9270-9277.

SHALEV A., PISE-MASISON C.A., RADONOVICH M., HOFFMANN S.C., HIRSHBERG B., BRADY J.N. & HARLAN D.M. (2002). Oligonucleotide microarray analysis of intact human pancreatic islets: identification of glucose-responsive genes and a highly regulated TGFbeta signaling pathway. *Endocrinology.* **143.** 3695-3698.

SHEWAN A.M., VAN DAM E.M., MARTIN S., LUEN T.B., HONG W., BRYANT N.J. & JAMES D.E. (2003). GLUT4 recycles via a *trans*-Golgi network (TGN) subdomain enriched in Syntaxins 6 and 16 but not TGN38: involvement of an acidic targeting motif. *Mol. Biol. Cell.* **14.** 973-986.

SHIELD J.P. (2000). Neonatal diabetes: new insights into aetiology and implications. *Horm. Res.* **53 Suppl 1.** 7-11.

SHIGEMATSU S., WATSON R.T., KHAN A.H. & PESSIN J.E. (2003). The adipocyte plasma membrane caveolin functional/structural organization is necessary for the efficient endocytosis of GLUT4. *J. Biol. Chem.* **278.** 10683-10690.

SHUCK M.E., PISER T.M., BOCK J.H., SLIGHTOM J.L., LEE K.S. & BIENKOWSKI M.J. (1997). Cloning and characterization of two K^+ inward rectifier (Kir) 1.1 potassium channel homologs from human kidney (Kir1.2 and Kir1.3). *J. Biol. Chem.* **272.** 586-593.

SHYNG S., FERRIGNI T. & NICHOLS C.G. (1997). Control of rectification and gating of cloned K_{ATP} channels by the Kir6.2 subunit. *J. Gen. Physiol.* **110.** 141-153.

SHYNG S. & NICHOLS C.G. (1997). Octameric stoichiometry of the K_{ATP} channel complex. *J. Gen. Physiol.* **110.** 655-664.

SHYNG S., FERRIGNI T. & NICHOLS C.G. (1997). Regulation of K_{ATP} channel activity by diazoxide and MgADP. Distinct functions of the two nucleotide binding folds of the sulfonylurea receptor. *J. Gen. Physiol.* **110.** 643-654.

SHYNG S.L. & NICHOLS C.G. (1998). Membrane phospholipid control of nucleotide sensitivity of K_{ATP} channels. *Science.* **282.** 1138-1141.

SHYNG S.L., CUKRAS C.A., HARWOOD J. & NICHOLS C.G. (2000). Structural determinants of PIP_2 regulation of inward rectifier K_{ATP} channels. *J. Gen. Physiol.* **116.** 599-608.

SIMPSON F., PEDEN A.A., CHRISTOPOULOU L. & ROBINSON M.S. (1997). Characterization of the adaptor-related protein complex, AP-3. *J. Cell Biol.* **137.** 835-845.

SOMSEL R.J. & WANDINGER-NESS A. (2000). Rab GTPases coordinate endocytosis. *J. Cell Sci.* **113 Pt 2.** 183-192.

SONG D.K. & ASHCROFT F.M. (2001). Glimepiride block of cloned beta-cell, cardiac and smooth muscle K_{ATP} channels. *Br. J. Pharmacol.* **133.** 193-199.

SONNICHSEN B., DE RENZIS S., NIELSEN E., RIETDORF J. & ZERIAL M. (2000). Distinct membrane domains on endosomes in the recycling pathway visualized by multicolor imaging of Rab4, Rab5, and Rab11. *J. Cell Biol.* **149.** 901-914.

SPRUCE A.E., STANDEN N.B. & STANFIELD P.R. (1985). Voltage-dependent ATP-sensitive potassium channels of skeletal muscle membrane. *Nature.* **316.** 736-738.

STANFORD I.M. & LACEY M.G. (1996). Electrophysiological investigation of adenosine trisphosphate-sensitive potassium channels in the rat substantia nigra pars reticulata. *Neuroscience.* **74.** 499-509.

STENMARK H., VITALE G., ULLRICH O. & ZERIAL M. (1995). Rabaptin-5 is a direct effector of the small GTPase Rab5 in endocytic membrane fusion. *Cell.* **83.** 423-432.

STUHMER W. & PAREKH A.B. (1995). Electrophysiological recordings from *Xenopus* oocytes. In *Single-channel recording, 2nd edition.* Ed. SAKMANN B. & NEHER E., Ch. 15, pp 341-356, Plenum Press, New York

STURGESS N.C., ASHFORD M.L., COOK D.L. & HALES C.N. (1985). The sulphonylurea receptor may be an ATP-sensitive potassium channel. *Lancet.* **2.** 474-475.

SUMIYOSHI R., NISHIMURA J., KAWASAKI J., KOBAYASHI S., TAKAHASHI S. & KANAIDE H. (1997). Diadenosine polyphosphates directly relax porcine coronary arterial smooth muscle. *J. Pharmacol. Exp. Ther.* **283.** 548-556.

SUNAGA Y., GONOI T., SHIBASAKI T., ICHIKAWA K., KUSAMA H., YANO H. & SEINO S. (2001). The effects of mitiglinide (KAD-1229), a new anti-diabetic drug, on ATP-sensitive K^+ channels and insulin secretion: comparison with the sulfonylureas and nateglinide. *Eur. J. Pharmacol.* **431.** 119-125.

SURWIT R.S., KUHN C.M., COCHRANE C., MCCUBBIN J.A. & FEINGLOS M.N. (1988). Diet-induced type II diabetes in C57BL/6J mice. *Diabetes.* **37.** 1163-1167.

SUTTON R.B., FASSHAUER D., JAHN R. & BRUNGER A.T. (1998). Crystal structure of a SNARE complex involved in synaptic exocytosis at 2.4 A resolution. *Nature.* **395.** 347-353.

TABORSKY G.J., Jr., AHREN B. & HAVEL P.J. (1998). Autonomic mediation of glucagon secretion during hypoglycemia: implications for impaired alpha-cell responses in type 1 diabetes. *Diabetes.* **47.** 995-1005.

TAKAHASHI N., MORISHIGE K., JAHANGIR A., YAMADA M., FINDLAY I., KOYAMA H. & KURACHI Y. (1994). Molecular cloning and functional expression of cDNA encoding a second class of inward rectifier potassium channels in the mouse brain. *J. Biol. Chem.* **269.** 23274-23279.

TAKATSU H., KATOH Y., SHIBA Y. & NAKAYAMA K. (2001). Golgi-localizing, gamma-adaptin ear homology domain, ADP-ribosylation factor-binding (GGA) proteins interact with acidic dileucine sequences within the cytoplasmic domains of sorting receptors through their Vps27p/Hrs/STAM (VHS) domains. *J. Biol. Chem.* **276.** 28541-28545.

TAN C.M., BRADY A.E., NICKOLS H.H., WANG Q. & LIMBIRD L.E. (2004). Membrane trafficking of G protein-coupled receptors. *Annu. Rev. Pharmacol. Toxicol.* **44.** 559-609.

TASCHENBERGER G., MOUGEY A., SHEN S., LESTER L.B., LAFRANCHI S. & SHYNG S.L. (2002). Identification of a familial hyperinsulinism-causing mutation in the sulfonylurea receptor 1 that prevents normal trafficking and function of K_{ATP} channels. *J. Biol. Chem.* **277.** 17139-17146.

TENG F.Y., WANG Y. & TANG B.L. (2001). The syntaxins. *Genome Biol.* **2.** REVIEWS3012.

TERZIC A., FINDLAY I., HOSOYA Y. & KURACHI Y. (1994). Dualistic behavior of ATP-sensitive K^+ channels toward intracellular nucleoside diphosphates. *Neuron.* **12.** 1049-1058.

TERZIC A., JAHANGIR A. & KURACHI Y. (1995). Cardiac ATP-sensitive K^+ channels: regulation by intracellular nucleotides and K+ channel-opening drugs. *Am. J. Physiol.* **269.** C525-C545.

THOMAS P., YE Y. & LIGHTNER E. (1996). Mutation of the pancreatic islet inward rectifier Kir6.2 also leads to familial persistent hyperinsulinemic hypoglycemia of infancy. *Hum. Mol. Genet.* **5.** 1809-1812.

THOMPSON K.S. & TOWLE H.C. (1991). Localization of the carbohydrate response element of the rat L-type pyruvate kinase gene. *J. Biol. Chem.* **266.** 8679-8682.

THOMSEN P., ROEPSTORFF K., STAHLHUT M. & VAN DEURS B. (2002). Caveolae are highly immobile plasma membrane microdomains, which are not involved in constitutive endocytic trafficking. *Mol. Biol. Cell.* **13.** 238-250.

THORNELOE K.S., MARUYAMA Y., MALCOLM A.T., LIGHT P.E., WALSH M.P. & COLE W.C. (2002). Protein kinase C modulation of recombinant ATP-sensitive K^+ channels composed of Kir6.1 and/or Kir6.2 expressed with SUR2B. *J. Physiol.* **541.** 65-80.

TIRONE T.A. & BRUNICARDI F.C. (2001). Overview of glucose regulation. *World J. Surg.* **25.** 461-467.

TORONOVSKY S., CRANE A., COSGROVE K.E., HUSSAINE K., LAVIE J., HEYMAN M., NESHER Y., KUCHINSKY N., BEN-SHUSHAN E., SHATZ O., NAHARI E., POTIKHA T., ZANGEN D., TENEMBAUM-RAKOVER Y., de VRIES L., ARGENTE J., GARCIA R., LANDAU H., ELIAKIM A., LINDLEY K., DUNNE M.J., AGUILAR-BRYAN L., GLASER B. (2004). Hyperinsulinism of infancy: novel ABCC8 and KCNJ11 mutations and evidence for additional locus heterogeneity. *J Clin Endocrinol Metab.* **89.** 6224-6234

TOKUYAMA Y., FAN Z., FURUTA H., MAKIELSKI J.C., POLONSKY K.S., BELL G.I. & YANO H. (1996). Rat inwardly rectifying potassium channel Kir6.2: cloning electrophysiological characterization, and decreased expression in pancreatic islets of male Zucker diabetic fatty rats. *Biochem. Biophys. Res. Commun.* **220.** 532-538.

TOOMRE D., STEYER J.A., KELLER P., ALMERS W. & SIMONS K. (2000). Fusion of constitutive membrane traffic with the cell surface observed by evanescent wave microscopy. *J. Cell Biol.* **149.** 33-40.

TOPERT C., DORING F., WISCHMEYER E., KARSCHIN C., BROCKHAUS J., BALLANYI K., DERST C. & KARSCHIN A. (1998). Kir2.4: a novel K^+ inward rectifier channel associated with motoneurons of cranial nerve nuclei. *J. Neurosci.* **18.** 4096-4105.

TORRES G.E., YAO W.D., MOHN A.R., QUAN H., KIM K.M., LEVEY A.I., STAUDINGER J. & CARON M.G. (2001). Functional interaction between monoamine plasma membrane transporters and the synaptic PDZ domain-containing protein PICK1. *Neuron.* **30.** 121-134.

TRAPP S., TUCKER S.J. & ASHCROFT F.M. (1997). Activation and inhibition of K-$_{ATP}$ currents by guanine nucleotides is mediated by different channel subunits. *Proc. Natl. Acad. Sci. U. S. A.* **94.** 8872-8877.

TRAPP S., HAIDER S., JONES P., SANSOM M.S. & ASHCROFT F.M. (2003). Identification of residues contributing to the ATP binding site of Kir6.2. *EMBO J.* **22.** 2903-2912.

TUCKER S.J., GRIBBLE F.M., ZHAO C., TRAPP S. & ASHCROFT F.M. (1997). Truncation of Kir6.2 produces ATP-sensitive K^+ channels in the absence of the sulphonylurea receptor. *Nature.* **387.** 179-183.

TUSNADY G.E., BAKOS E., VARADI A. & SARKADI B. (1997). Membrane topology distinguishes a subfamily of the ATP-binding cassette (ABC) transporters. *FEBS Lett.* **402.** 1-3.

UEDA K., KOMINE J., MATSUO M., SEINO S. & AMACHI T. (1999). Cooperative binding of ATP and MgADP in the sulfonylurea receptor is modulated by glibenclamide. *Proc. Natl. Acad. Sci. U. S. A.* **96.** 1268-1272.

UHDE I., TOMAN A., GROSS I., SCHWANSTECHER C. & SCHWANSTECHER M. (1999). Identification of the potassium channel opener site on sulfonylurea receptors. *J. Biol. Chem.* **274.** 28079-28082.

ULMSCHNEIDER M.B., SANSOM M.S. (2001). Amino acid distributions in integral membrane protein structures. *Biochim Biophys Acta.* **1512.** 1-14

UNGER R.H. (1981). The milieu interieur and the islets of Langerhans. *Diabetologia.* **20.** 1-11.

VAULONT S., MUNNICH A., DECAUX J.F. & KAHN A. (1986). Transcriptional and post-transcriptional regulation of L-type pyruvate kinase gene expression in rat liver. *J. Biol. Chem.* **261.** 7621-7625.

VAXILLAIRE M., POPULAIRE C., BUSIAH K., CAVE H., GLOYN A.L., HATTERSLEY A.T., CZERNICHOW P., FROGUEL P. & POLAK M. (2004). Kir6.2 mutations are a common cause of permanent neonatal diabetes in a large cohort of French patients. *Diabetes.* **53.** 2719-2722.

VOORHEES P., DEIGNAN E., VAN DONSELAAR E., HUMPHREY J., MARKS M.S., PETERS P.J. & BONIFACINO J.S. (1995). An acidic sequence within the cytoplasmic domain of furin functions as a determinant of *trans*-Golgi network localization and internalization from the cell surface. *EMBO J.* **14.** 4961-4975.

WAEBER G., THOMPSON N., HAEFLIGER J.A. & NICOD P. (1994). Characterization of the murine high Km glucose transporter GLUT2 gene and its transcriptional regulation by glucose in a differentiated insulin-secreting cell line. *J. Biol. Chem.* **269.** 26912-26919.

WAKATSUKI T., NAKAYA Y., MIYOSHI Y., ZENG X.R., NOMURA M., SAITO K. & INOUE I. (1992). Effects of vasopressin on ATP-sensitive and Ca^{2+}-activated K^{+} channels of coronary arterial smooth muscle cells. *Jpn. J. Pharmacol.* **58 Suppl 2.** 339P.

WALKER J.E., SARASTE M., RUNSWICK M.J. & GAY N.J. (1982). Distantly related sequences in the alpha- and beta-subunits of ATP synthase, myosin, kinases and other ATP-requiring enzymes and a common nucleotide binding fold. *EMBO J.* **1.** 945-951.

WAN L., MOLLOY S.S., THOMAS L., LIU G., XIANG Y., RYBAK S.L. & THOMAS G. (1998). PACS-1 defines a novel gene family of cytosolic sorting proteins required for *trans*-Golgi network localization. *Cell.* **94.** 205-216.

WAN Q.F., DONG Y., YANG H., LOU X., DING J., XU T. (2004). Protein kinase activation increases insulin secretion by sensitizing the secretory machinery to Ca^{2+}. *J Gen. Physiol.* **124.** 653-662.

WANG H., GAUTHIER B.R., HAGENFELDT-JOHANSSON K.A., IEZZI M. & WOLLHEIM C.B. (2002). Foxa2 (HNF3beta) controls multiple genes implicated in metabolism-secretion coupling of glucose-induced insulin release. *J. Biol. Chem.* **277.** 17564-17570.

WANG P.H., MOLLER D., FLIER J.S., NAYAK R.C. & SMITH R.J. (1989). Coordinate regulation of glucose transporter function, number, and gene expression by insulin and sulfonylureas in L6 rat skeletal muscle cells. *J. Clin. Invest.* **84.** 62-67.

WANG Z., ELDSTROM J.R., JANTZI J., MOORE E.D. & FEDIDA D. (2004). Increased focal Kv4.2 channel expression at the plasma membrane is the result of actin depolymerization. *Am. J. Physiol Heart Circ. Physiol.* **286.** H749-H759.

WARD E.S., MARTINEZ C., VACCARO C., ZHOU J., TANG Q. & OBER R.J. (2005). From Sorting Endosomes to Exocytosis: Association of Rab4 and Rab11 GTPases with the Fc Receptor, FcRn, during Recycling. *Mol. Biol. Cell.*

WATSON R.T., KANZAKI M. & PESSIN J.E. (2004). Regulated membrane trafficking of the insulin-responsive glucose transporter 4 in adipocytes. *Endocr. Rev.* **25.** 177-204.

WEIMBS T., LOW S.H., CHAPIN S.J., MOSTOV K.E., BUCHER P. & HOFMANN K. (1997). A conserved domain is present in different families of vesicular fusion proteins: a new superfamily. *Proc. Natl. Acad. Sci. U. S. A.* **94.** 3046-3051.

WHITE J., KELLER P. & STELZER E.H. (2001). Spatial partitioning of secretory cargo from Golgi resident proteins in live cells. *BMC. Cell Biol.* **2.** 19.

WILLIAMS M.A. & FUKUDA M. (1990). Accumulation of membrane glycoproteins in lysosomes requires a tyrosine residue at a particular position in the cytoplasmic tail. *J. Cell Biol.* **111.** 955-966.

WOODS A., AZZOUT-MARNICHE D., FORETZ M., STEIN S.C., LEMARCHAND P., FERRE P., FOUFELLE F. & CARLING D. (2000). Characterization of the role of AMP-activated protein kinase in the regulation of glucose-activated gene expression using constitutively active and dominant negative forms of the kinase. *Mol. Cell Biol.* **20.** 6704-6711.

XIA F., GAO X., KWAN E., LAM P.P., CHAN L., SY K., SHEU L., WHEELER M.B., GAISANO H.Y. & TSUSHIMA R.G. (2004). Disruption of pancreatic beta-cell lipid rafts modifies Kv2.1 channel gating and insulin exocytosis. *J. Biol. Chem.* **279.** 24685-24691.

YAMADA M., ISOMOTO S., MATSUMOTO S., KONDO C., SHINDO T., HORIO Y. & KURACHI Y. (1997). Sulphonylurea receptor 2B and Kir6.1 form a sulphonylurea-sensitive but ATP-insensitive K^+ channel. *J. Physiol.* **499 (Pt 3).** 715-720.

YAMASHIRO D.J. & MAXFIELD F.R. (1984). Acidification of endocytic compartments and the intracellular pathways of ligands and receptors. *J. Cell Biochem.* **26.** 231-246.

YAN F., LIN C.W., WEISIGER E., CARTIER E.A., TASCHEBERGER G., SHYNG S.L. (2004). Sulfonylureas correct trafficking defects of ATP-sensitive potassium channels caused by mutations in the sulfonylurea receptor. *J Biol Chem.* **279.** 11096-11105

YANEY G.C., FAIRBANKS J.M., DEENEY J.T., KORCHAK H.M., TORNHEIM K. & CORKEY B.E. (2002). Potentiation of insulin secretion by phorbol esters is mediated by PKC-alpha and nPKC isoforms. *Am. J Physiol. Endocrinol. Metab.* **283.** 880-888.

YANG W., HONG Y.H., SHEN X.Q., FRANKOWSKI C., CAMP H.S. & LEFF T. (2001). Regulation of transcription by AMP-activated protein kinase: phosphorylation of p300 blocks its interaction with nuclear receptors. *J. Biol. Chem.* **276.** 38341-38344.

YOSHIDA H., FEIG J.E., MORRISSEY A., GHIU I.A., ARTMAN M. & COETZEE W.A. (2004). K_{ATP} channels of primary human coronary artery endothelial cells consist of a heteromultimeric complex of Kir6.1, Kir6.2, and SUR2B subunits. *J. Mol. Cell Cardiol.* **37.** 857-869.

YUAN H., MICHELSEN K. & SCHWAPPACH B. (2003). 14-3-3 dimers probe the assembly status of multimeric membrane proteins. *Curr. Biol.* **13.** 638-646.

ZAWAR C., PLANT T.D., SCHIRRA C., KONNERTH A. & NEUMCKE B. (1999). Cell-type specific expression of ATP-sensitive potassium channels in the rat hippocampus. *J. Physiol.* **514 (Pt 2).** 327-341.

ZERANGUE N., SCHWAPPACH B., JAN Y.N. & JAN L.Y. (1999). A new ER trafficking signal regulates the subunit stoichiometry of plasma membrane K_{ATP} channels. *Neuron.* **22.** 537-548.

ZHOU G., MYERS R., LI Y., CHEN Y., SHEN X., FENYK-MELODY J., WU M., VENTRE J., DOEBBER T., FUJII N., MUSI N., HIRSHMAN M.F., GOODYEAR L.J. & MOLLER D.E. (2001). Role of AMP-activated protein kinase in mechanism of metformin action. *J. Clin. Invest.* **108.** 1167-1174.

ZHU Y., DORAY B., POUSSU A., LEHTO V.P. & KORNFELD S. (2001). Binding of GGA2 to the lysosomal enzyme sorting motif of the mannose 6-phosphate receptor. *Science.* **292.** 1716-1718.

Appendix

A.1 - Contents of the supplementary CD

The CD contains two video clips which are the result of the live cell imaging experiments described in chapter 5. The clips are in the .avi format.

Animation 1 - Visualising K_{ATP} channel movement

A HEK293 cell stably expressing HA-tagged Kir6.2 and SUR1 was viewed as described in chapter 5.2.7. An image was taken every 2 seconds for 6 minutes in a single focal plane. The images were then reconstituted into a video clip running at 15 frames sec^{-1}. Still images from this video clip were included in figure 5.2, figure 5.15 and figure 5.16.

Animation 2 - Control cells

A HEK293 cell which was not expressing HA-tagged K_{ATP} channels was imaged as described in chapter 5.2.7. An image was taken every 1 second for 6 minutes in a single focal plane. The images were then reconstituted into a video clip running at 15 frames sec-1. Still images from this video clip were included in figure 5.2.

A.2 - Plasmid maps

Shown in figure A.1, figure A.2 and figure A.3 are plasmid maps of the plasmid vectors used during the current investigations as well as maps of the Kir6.2-HA+11aa-HMKFLAG and SUR1 constructs used. These maps contain details of restriction enzyme sites and PCR primer sites which were required for the manipulation of these constructs during the investigations described in the main body of the thesis.

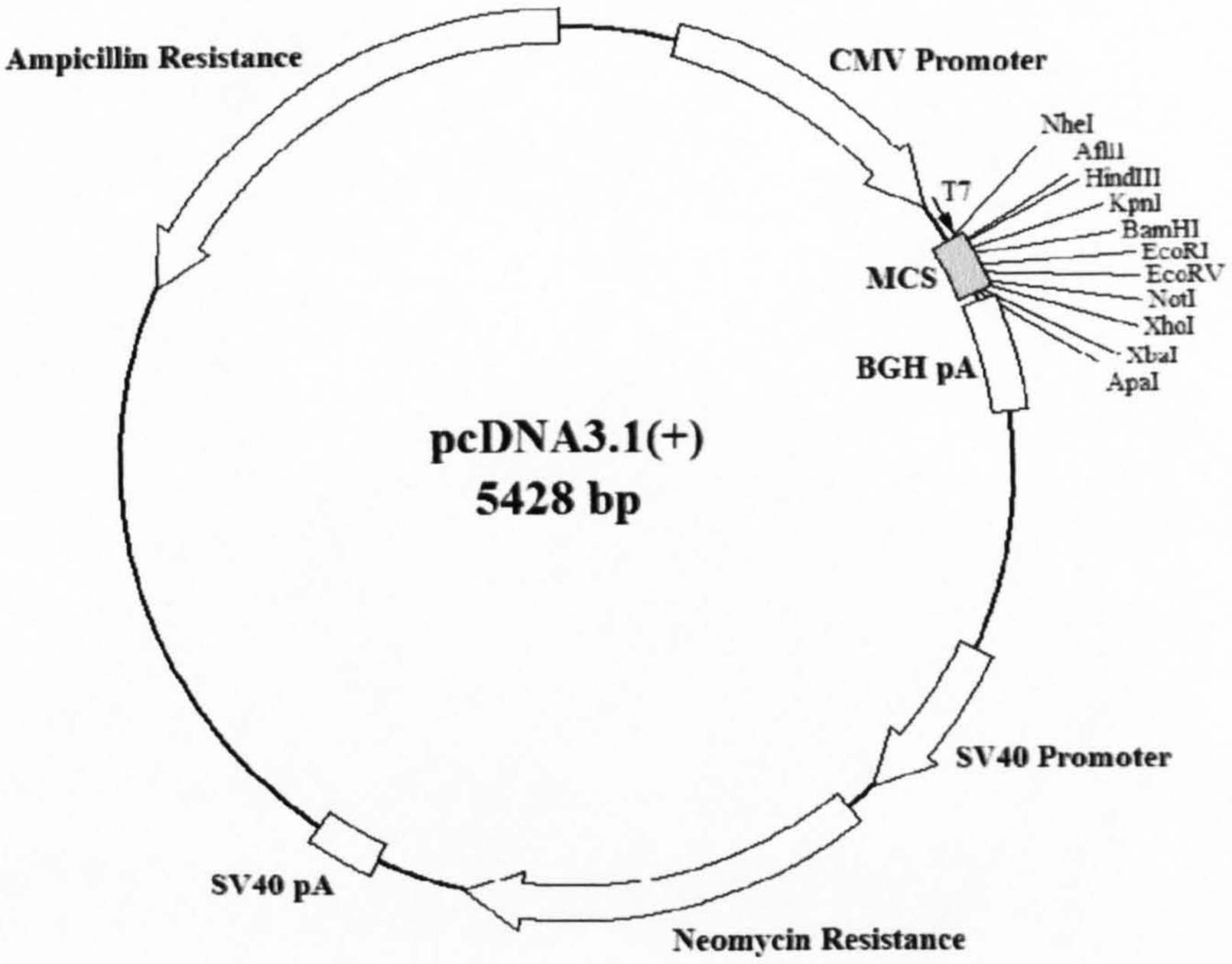

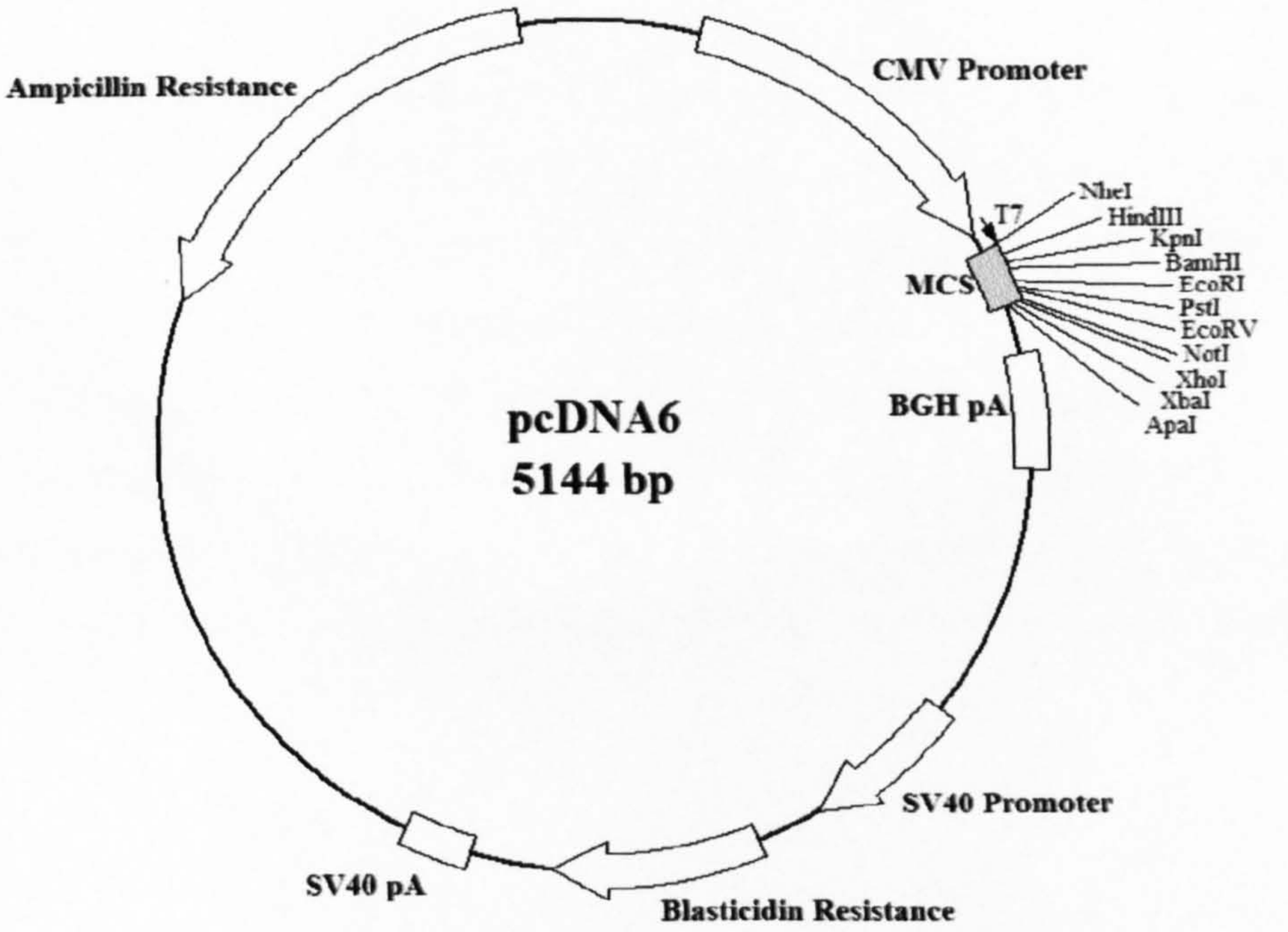

continued overleaf...

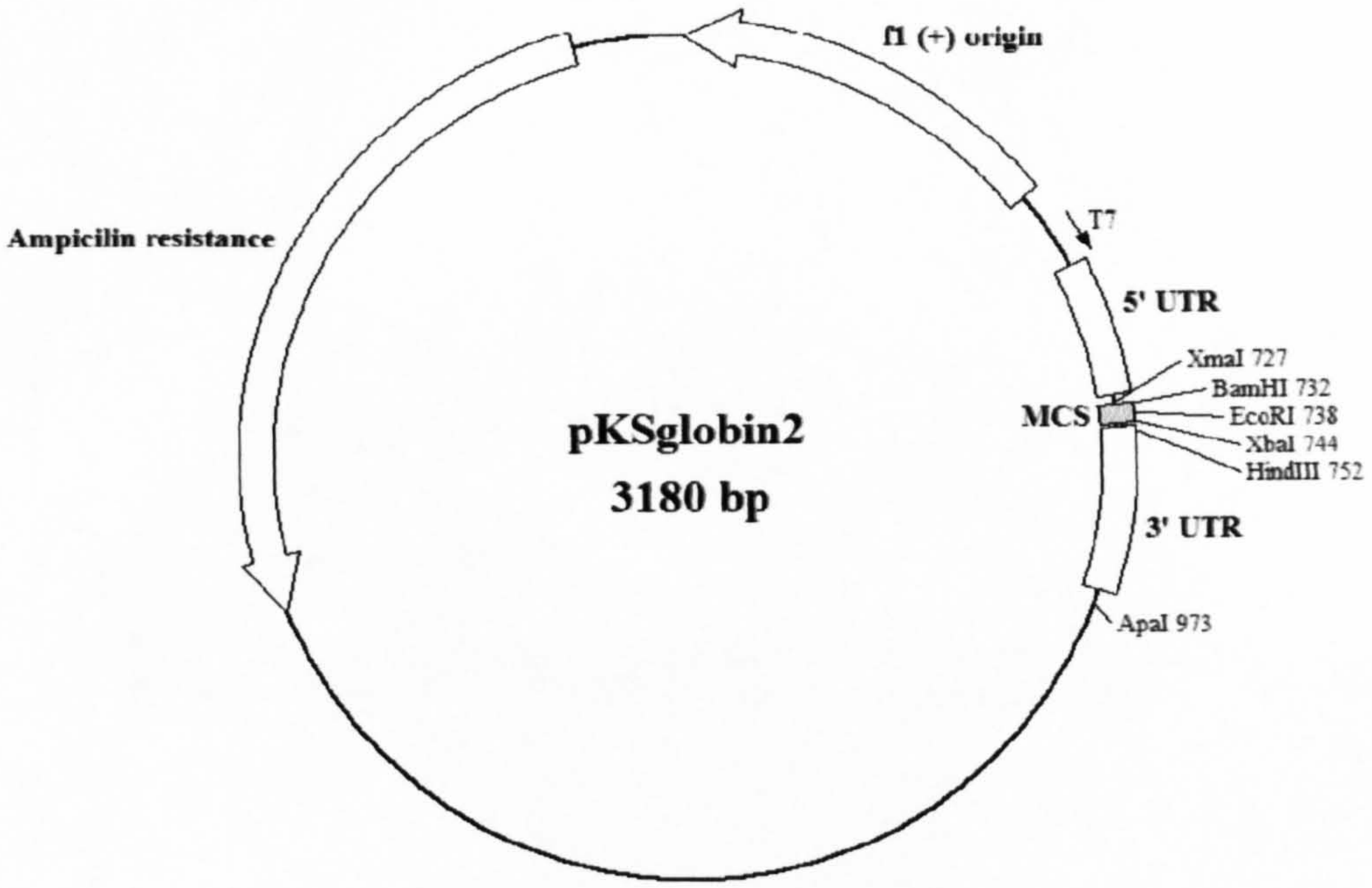

Figure A.1 - *Maps of the plasmids used for expression of the K_{ATP} channel subunits.* Both pcDNA3.1(+) and pcDNA6 allow expression in mammalian expression systems and were both obtained from Invitrogen life technologies. pKSglobin allows high efficiency expression in the *Xenopus laevis* oocyte expression system. This is due to the presence of the 5' and 3' untranslated regions (UTR) of the oocyte β-globin gene either side of the multiple cloning site (MCS). The unique restriction sites contained within the MCS of each plasmid vector are shown as well as the principal genes and associated promoter and polyadenylation sequences (pA) which have been used during cloning procedures.

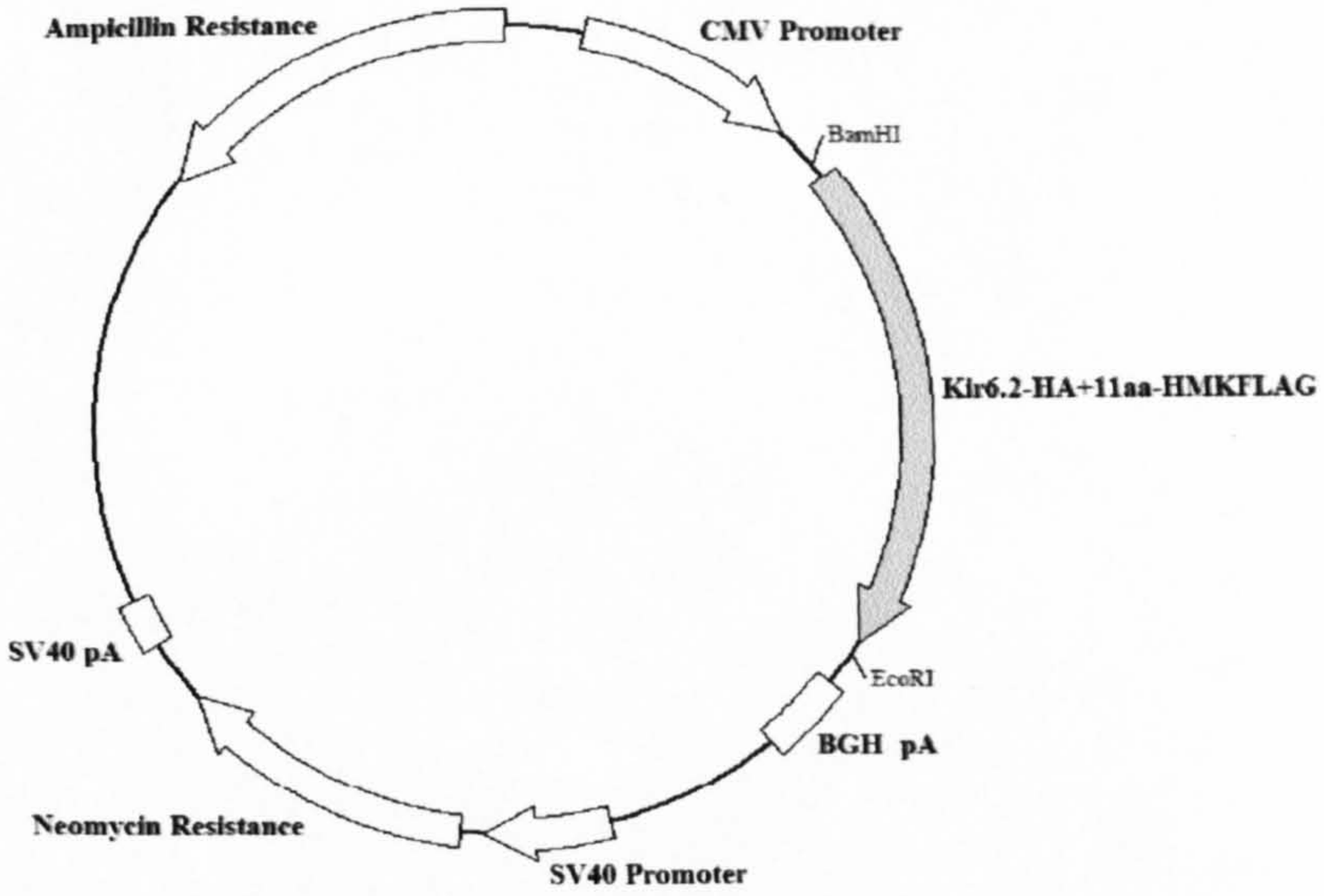

pcDNA3-Kir6.2-HA+11aa-HMKFLAG

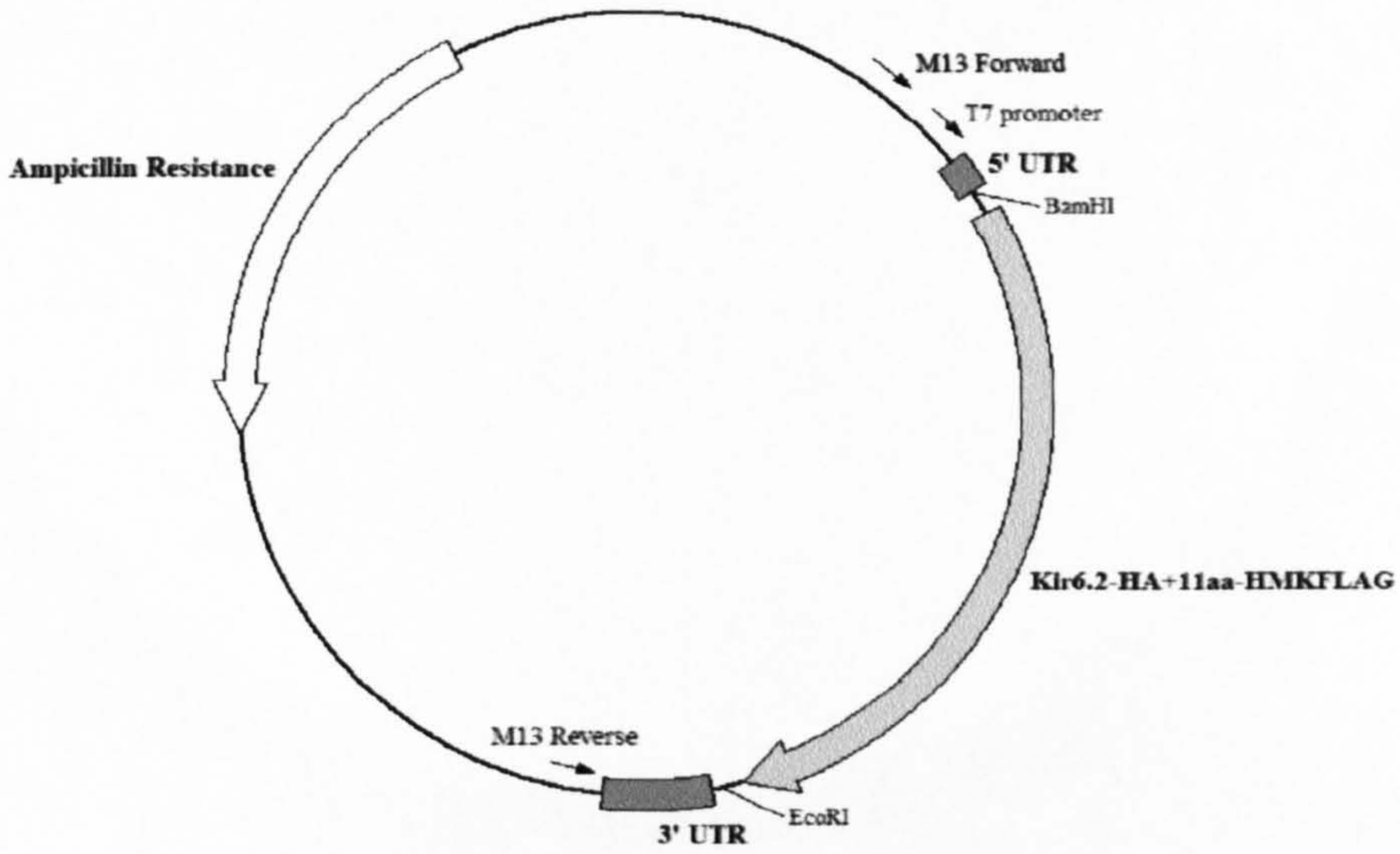

pKSglobin-Kir6.2-HA+11aa-HMKFLAG

Figure A.2 - *Plasmid maps of the Kir6.2-HA+11aa-HMKFLAG constructs.* Kir6.2-HA+11aa-HMKFLAG was subcloned into both pcDNA3.1(+) for mammalian expression and pKSglobin for *Xenopus* oocyte expression between the unique BamHI and EcoRI sites found in these vectors. For cRNA template production the M13 promoter sites in pKSglobin-Kir6.2-HA+11aa-HMKFLAG were used to isolate the construct via PCR.

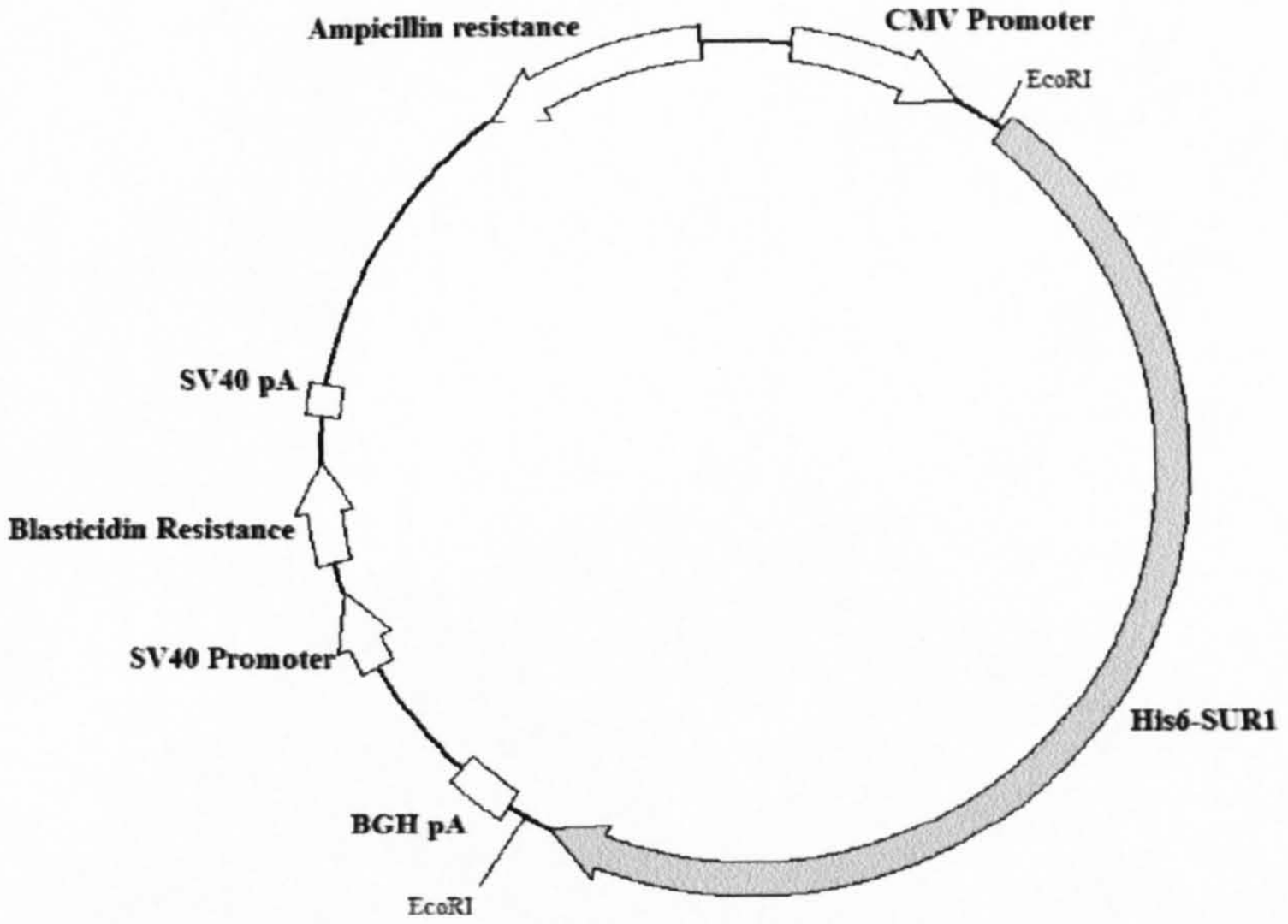

pcDNA6-His6-SUR1

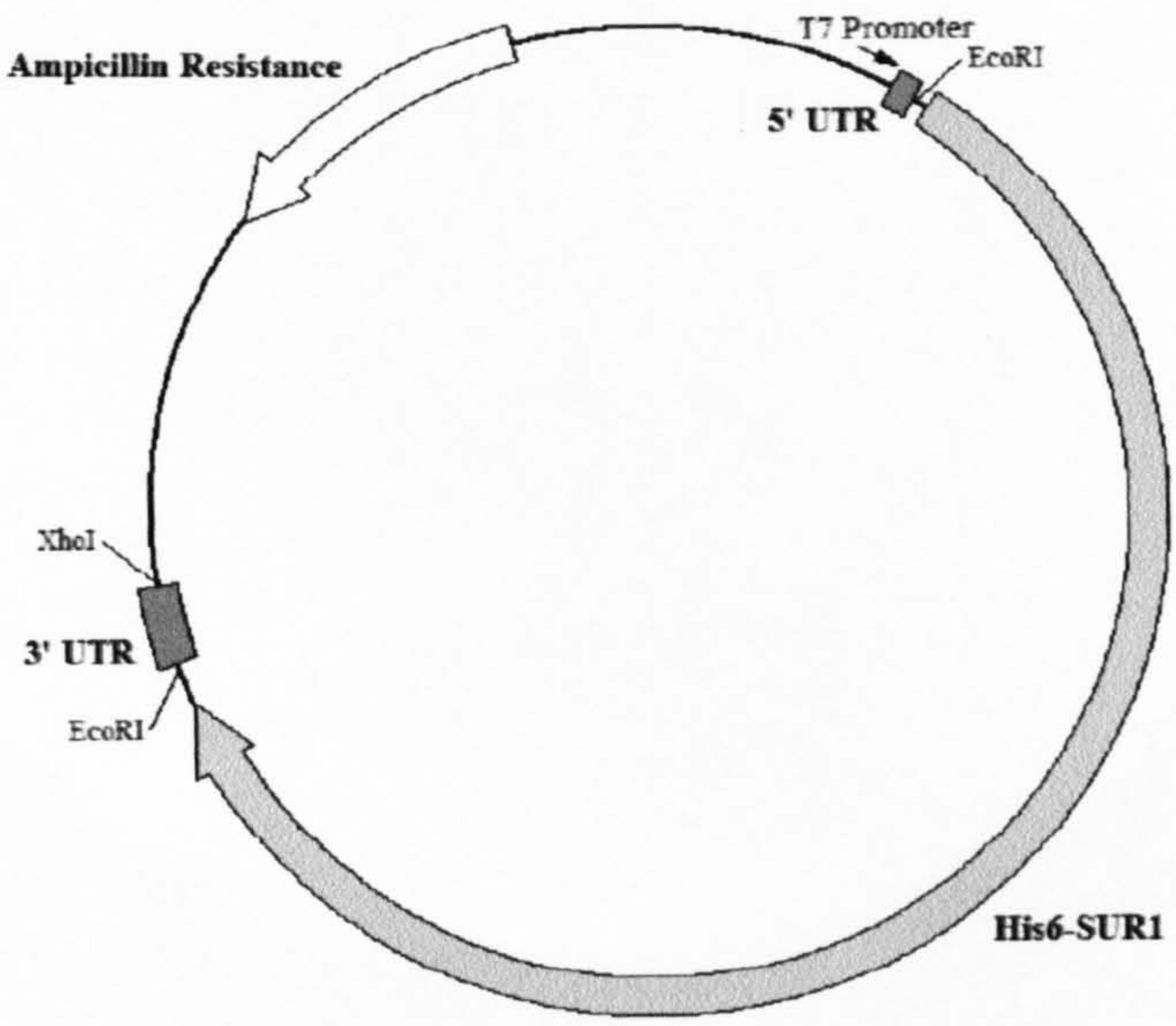

pKSglobin-His6-SUR1

Figure A.3 - *Plasmid maps of the His6-SUR1 constructs.* His6-SUR1 was subcloned into both pcDNA6 for mammalian expression and pKSglobin for *Xenopus* oocyte expression into the unique *EcoRI* site found in these vectors. For cRNA template production the pKSglobin-His6-SUR1 was linearised using *XhoI*.

THESIS CONTAINS CD ROM